ISSN 0021-9673

VOL. 504 NO. 1 MARCH 30, 1990

JOURNAL OF CHROMATOGRAPHY

INTERNATIONAL JOURNAL ON CHROMATOGRAPHY, ELECTROPHORESIS AND RELATED METHODS

ELSEVIER

JOURNAL OF CHROMATOGRAPHY

Scope. The *Journal of Chromatography* publishes papers on all aspects of chromatography, electrophoresis and related methods. Contributions consist mainly of research papers dealing with chromatographic theory, instrumental development and their applications. The section *Biomedical Applications*, which is under separate editorship, deals with the following aspects: developments in and applications of chromatographic and electrophoretic techniques related to clinical diagnosis or alterations during medical treatment; screening and profiling of body fluids or tissues with special reference to metabolic disorders; results from basic medical research with direct consequences in clinical practice; drug level monitoring and pharmacokinetic studies; clinical toxicology; analytical studies in occupational medicine.

Submission of Papers. Papers in English, French and German may be submitted, in three copies. Manuscripts should be submitted to: The Editor of *Journal of Chromatography*, P.O. Box 681, 1000 AR Amsterdam, The Netherlands, or to: The Editor of *Journal of Chromatography, Biomedical Applications*, P.O. Box 681, 1000 AR Amsterdam, The Netherlands. Review articles are invited or proposed by letter to the Editors. An outline of the proposed review should first be forwarded to the Editors for preliminary discussion prior to preparation. Submission of an article is understood to imply that the article is original and unpublished and is not being considered for publication elsewhere. For copyright regulations, see below.

Subscription Orders. Subscription orders should be sent to: Elsevier Science Publishers B.V., P.O. Box 211, 1000 AE Amsterdam, The Netherlands, Tel. 5803 911, Telex 18582 ESPA NL. The *Journal of Chromatography* and the *Biomedical Applications* section can be subscribed to separately.

Publication. The *Journal of Chromatography* (incl. *Biomedical Applications*) has 37 volumes in 1990. The subscription prices for 1990 are:

J. Chromatogr. (incl. *Cum. Indexes, Vols. 451–500*) + *Biomed. Appl.* (Vols. 498–534):
Dfl. 6734.00 plus Dfl. 1036.00 (p.p.h.) (total *ca.* US$ 3885.00)

J. Chromatogr. (incl. *Cum. Indexes, Vols. 451–500*) only (Vols. 498–524):
Dfl. 5616.00 plus Dfl. 756.00 (p.p.h.) (total *ca.* US$ 3186.00)

Biomed. Appl. only (Vols. 525–534):
Dfl. 2080.00 plus Dfl. 280.00 (p.p.h.) (total *ca.* US$ 1180.00).

Our p.p.h. (postage, package and handling) charge includes surface delivery of all issues, except to subscribers in Argentina, Australia, Brasil, Canada, China, Hong Kong, India, Israel, Malaysia, Mexico, New Zealand, Pakistan, Singapore, South Africa, South Korea, Taiwan, Thailand and the U.S.A. who receive all issues by air delivery (S.A.L. — Surface Air Lifted) at no extra cost. For Japan, air delivery requires 50% additional charge; for all other countries airmail and S.A.L. charges are available upon request. Back volumes of the *Journal of Chromatography* (Vols. 1–497) are available at Dfl. 195.00 (plus postage). Claims for missing issues will be honoured, free of charge, within three months after publication of the issue. Customers in the U.S.A. and Canada wishing information on this and other Elsevier journals, please contact Journal Information Center, Elsevier Science Publishing Co. Inc., 655 Avenue of the Americas, New York, NY 10010. Tel. (212) 633-3750.

Abstracts/Contents Lists published in Analytical Abstracts, ASCA, Biochemical Abstracts, Biological Abstracts, Chemical Abstracts, Chemical Titles, Chromatography Abstracts, Clinical Chemistry Lookout, Current Contents/Life Sciences, Current Contents/Physical, Chemical & Earth Sciences, Deep-Sea Research/Part B: Oceanographic Literature Review, Excerpta Medica, Index Medicus, Mass Spectrometry Bulletin, PASCAL-CNRS, Pharmaceutical Abstracts, Referativnyi Zhurnal, Science Citation Index and Trends in Biotechnology.

See inside back cover for Publication Schedule, Information for Authors and information on Advertisements.

0021-9673/90/$03.50

Printed in The Netherlands

CONTENTS

(*Abstracts/Contents Lists published in Analytical Abstracts, ASCA, Biochemical Abstracts, Biological Abstracts, Chemical Abstracts, Chemical Titles, Chromatography Abstracts, Current Contents/Life Sciences, Current Contents/Physical, Chemical & Earth Sciences, Deep-Sea Research/Part B: Oceanographic Literature Review, Excerpta Medica, Index Medicus, Mass Spectrometry Bulletin, PASCAL-CNRS, Referativnyi Zhurnal, Science Citation Index*)

(Continued overleaf)

In articles with more than one author, the name of the author to whom correspondence should be addressed is indicated in the article heading by a 6-pointed asterisk (*)

AQUEOUS SIZE-EXCLUSION CHROMATOGRAPHY

edited by **P.L. DUBIN,** *Indiana-Purdue University*

(Journal of Chromatography Library, 40)

The rapid development of new packings for aqueous size-exclusion chromatography has revolutionized this field. High resolution non-adsorptive columns now make possible the efficient separation of proteins and the rapid and precise determination of the molecular weight distribution of synthetic polymers. This technology is also being applied to the separation of small ions, the characterization of associating systems, and the measurement of branching. At the same time, fundamental studies are elucidating the mechanisms of the various chromatographic processes.

These developments in principles and applications are assembled for the first time in this book.

- Fundamental issues are dealt with: the roles of pore structure and macromolecular dimensions, hydrophobic and electrostatic effects, and the determination and control of column efficiency.
- High-performance packings based on derivatized silica are reviewed in detail.
- Special techniques are thoroughly described, including SEC/LALLS, inverse exclusion chromatography, and frontal zone chromatography.
- Attention is focussed on special applications of size-exclusion methods, such as the characterization of micelles, separations of inorganic ions, and Hummel-Dreyer and related methods for equilibrium systems.
- Protein chromatography is dealt with in both dedicated sections and throughout the book as a whole.

This is a particularly comprehensive and authoritative work - all the contributions review broad topics of general significance and the authors are of high repute.

The material will be of special value for the characterization of synthetic water-soluble polymers, especially polyelectrolytes. Biochemists will find fundamental and practical guidance on protein separations. Researchers confronted with solutes that exhibit complex chromatographic behavior, such as humic acids, aggregating proteins, and micelles should find the contents of this volume illuminating.

1988 xviii + 454 pages
US$ 144.75 / Dfl. 275.00
ISBN 0-444-42957-3

ELSEVIER SCIENCE PUBLISHERS

P.O. Box 211, 1000 AE Amsterdam, The Netherlands
P.O. Box 882, Madison Square Station, New York, NY 10159, USA

Analytical Artifacts

GC, MS, HPLC, TLC and PC

by **B.S. MIDDLEDITCH**, *Dept. of Biochemical and Biophysical Sciences, University of Houston, Houston, TX, USA*

(Journal of Chromatography Library, 44)

This encyclopaedic catalogue of the pitfalls and problems that all analysts encounter in their work is destined to spend more time on the analyst's workbench than on a library shelf. The author has dedicated the book to "the innumerable scientists who made mistakes, used impure chemicals and solvents, suffered the consequences of unanticipated side-reactions, and were otherwise exposed to mayhem yet were too embarrassed to publish their findings".

Traditionally, the mass spectroscopist or gas chromatographer learnt his trade by participating in a 4-6 year apprenticeship as graduate student and post-doctoral researcher. Generally, no formal training was provided on the things that go wrong, but this information was accumulated by sharing in the experiences of colleagues. Nowadays, many novice scientists simply purchase a computerized instrument, plug it in, and use it. Much time can be wasted in studying and resolving problems due to artifacts and there is also a strong possibility that artifacts will not be recognized as such. For example, most analysts realize that they should use glass rather than plastic containers; but few of them would anticipate the possibility of plasticizer residues on glassware washed using detergent from a plastic bottle.

This book is an easy-to-use compendium of problems encountered when using various commonly used analytical techniques. Emphasis is on impurities, by-products, contaminants and other artifacts. A separate entry is provided for each artifact. For specific chemicals, this entry provides the common name, mass spectrum, gas chromatographic data, CAS name and registry number, synonyms and a narrative discussion. More than 1100 entries are included. Mass spectral data are indexed in a 6-peak index (molecular ion, base peak, second peak, third peak) and there are also formula, author and subject indexes. An extensive bibliography contains complete literature citations.

The book is designed to be *used*. It will not only allow experienced analysts to profit from the mistakes of others, but it will also be invaluable to other scientists who use analytical instruments in their work.

1989 xxiv + 1028 pages
US$ 241.50 / Dfl. 495.00
ISBN 0-444-87158-6

ELSEVIER SCIENCE PUBLISHERS

P.O. Box 211, 1000 AE Amsterdam, The Netherlands
P.O. Box 882, Madison Square Station, New York, NY 10159, USA

Automatic Methods of Analysis

by **M. VALCÁRCEL** *and* **M.D. LUQUE DE CASTRO,**
Department of Analytical Chemistry, University of Córdoba, Córdoba, Spain

(Techniques and Instrumentation in Analytical Chemistry, 9)

This new book gives a comprehensive overview of the state of the art of the automation of laboratory processes in analytical chemistry. The topics have been chosen according to such criteria as the degree of consolidation, scope of application and most promising trends.

The book begins with the basic principles behind the automation of laboratory processes, then describes automatic systems for sampling and sample treatment. In the second part the principal types of analysers are discussed: continuous, batch and robotic. The third part is devoted to the automation of analytical instrumentation: spectroscopic, electroanalytical and chromatographic techniques and titrators. The last part presents examples of the application of automation to clinical chemistry, environmental pollution monitoring and industrial process control.

The text is supplemented by 290 figures and 800 literature references. It is written primarily for those directly involved in laboratory work or responsible for industrial planning and control, research centres, etc. It will also be useful to analytical chemists wishing to update their knowledge in this area, and will be of especial interest to scientists directly related to environmental sciences or clinical chemistry.

CONTENTS:

1988 xii + 560 pages
US$ 131.50 / Dfl.250.00
ISBN 0-444-43005-9

ELSEVIER SCIENCE PUBLISHERS

P.O. Box 211, 1000 AE Amsterdam, The Netherlands
P.O. Box 882, Madison Square Station, New York, NY 10159, USA

Determination of Beta-Blockers in Biological Material

edited by **V. Marko,** *Institute of Experimental Pharmacology, Centre of Physiological Sciences, Slovak Academy of Sciences, Bratislava, Czechoslovakia*

(Techniques and Instrumentation in Analytical Chemistry, 4C)

This is the third volume of a sub-series entitled *Evaluation of Analytical Methods in Biological Systems*. (The first two were *Analysis of Biogenic Amines* edited by G.B. Baker and R.T. Coutts and *Hazardous Metals in Human Toxicology* edited by A. Vercruysse). This new volume addresses beta-blockers - an area of research for which a Nobel Prize in Medicine was awarded in 1988. It provides an up-to-date and comprehensive coverage of the theory and practice of the determination of beta-blockers in biological material. Two main fields of research are dealt with in this book: analytical chemistry and pharmacology, and, as it deals with drugs used in clinical practice, it is also related to a third area: therapy. Thus, it offers relevant information to workers in all three fields.

Some 50 beta-blockers and nine methods of analysis are discussed. The methods are divided into three groups: optical, chromatographic, and saturation methods. In addition to the analytical methods themselves, sample handling problems are also covered in detail, as is the information content of the analytical results obtained. Special chapters are directed to those working in pharmacology and pharmacokinetics. Finally, as recent evidence points to the increased importance of distinguishing optical isomers of drugs, a chapter on the determination of optical isomers of beta-blockers in biological material is also included. An extensive subject index and two supplements giving retention indices and structures of beta-blockers complete the book.

This is the first book to treat beta-blockers from the point of view of their determination and to discuss in detail the use of analytical methods for beta-blockers. It will thus appeal to a wide-ranging readership.

1989 xiv + 334 pages
US$ 152.75 / Dfl. 290.00
ISBN 0-444-87305-8

ELSEVIER SCIENCE PUBLISHERS

P.O. Box 211, 1000 AE Amsterdam, The Netherlands
P.O. Box 882, Madison Square Station, New York, NY 10159, USA

Polymer Thermodynamics by Gas Chromatography

by **R. Vilcu** *and* **M. Leca,** *Polytechnic Institute, Bucharest, Romania*

(Studies in Polymer Science, 4)

This book presents direct and inverse gas chromatography as a powerful tool for determining a great number of thermodynamic properties and quantities for micro- and especially for macromolecular substances. In order to ensure the continuity and clarity of the presentation, the book first considers some frequently used concepts of chromatography with a mobile gas phase, i.e. the mechanism of separation, retention parameters and the theories of gas chromatography. The employment of this technique as an important method of studying solutions through the most representative statistical models is also discussed. The thermodynamics of direct gas chromatography, as applied to dissolution, adsorption and vaporization underlies the thermodynamic treatment of inverse gas chromatography.

The most extensive chapter of the book is devoted to the thermodynamics of inverse gas chromatography and deals with a number of important topics: phase transitions in crystalline-amorphous polymers and liquid crystals, glass transitions, other second order transitions in polymers, the determination of diffusion coefficients, the segregation of block copolymers and other applications.

This book is intended for those specialists in research and industry who are concerned with the modification and characterization of polymers, with establishing polymer applications, and with the processing of polymers. It will also be useful to students and specialists interested in the physicochemical basis of the phenomena involved in gas chromatography in general and its inverse variant in particular.

Contents:

1989 viii + 204 pages
Price: US$ 97.50 / Dfl. 190.00
ISBN 0-444-98857-2
Distributed in the East European Countries, China, N. Korea, Cuba, Vietnam and Mongolia by Editura Academiei Republicii Socialiste Romania, Bucharest

ELSEVIER SCIENCE PUBLISHERS

P.O. Box 211, 1000 AE Amsterdam,The Netherlands
P.O. Box 882, Madison Square Station, New York, NY 10159, USA

Also available in a paperback student edition

Contemporary Practice of Chromatography

by **C.F. Poole** *and* **S.A. Schuette,** *Dept. of Chemistry, Wayne State University, Detroit, MI, USA*

"A tremendous amount of work has gone into the writing of this book, and it may be considered to be one of the few volumes of its kind that could be used both as a text by senior students in the field and by analysts in many industries. All academic, research association and appropriate industrial laboratories should buy at least one copy (preferably more, as borrowers will probably wish to keep it on loan for some time)." (The Analyst)

Written for everyone who uses chromatography as an analytical tool, this book covers all areas of gas, liquid, and thin-layer chromatography; **no other book offers the same scope.** The authors have had considerable experience in teaching graduate-level courses and the material presented here has been tried and tested, having formed the basis for short courses taught to groups of industrial chemists. Emphasis is on the practice of chromatographic methods, including "how to" sections and numerous examples of calculation methods. Extensively illustrated, the book contains numerous tables of all useful constants, materials and formulas frequently used by chromatographers. Valuable features are the chapters on sample preparation for chromatographic analysis, on instrumental methods for sample identification, and the comprehensive literature review.

Contents: 1. Fundamental Relationships of Chromatography. 2. The Column in GC. 3. Instrumental Requirements for GC. 4. The Column in LC. 5. Instrumental Requirements for HPLC. 6. Preparative-Scale Chromatography. 7. Sample Preparation for Chromatographic Analysis. 8. Hyphenated Methods for Identification after Chromatographic Separation. 9. High Performance Thin-Layer Chromatography. Subject Index.

1984. 2nd repr. 1986 x + 708 pages

Hardcover edition:	*Paperback edition:*
US$92.00/Dfl.175.00	US$37.50/Dfl.110.00
ISBN 0-444-42410-5	ISBN 0-444-42506-3

ELSEVIER SCIENCE PUBLISHERS

P.O. Box 211, 1000 AE Amsterdam, The Netherlands
P.O. Box 882, Madison Square Station, New York, NY 10159, USA

JOURNAL OF CHROMATOGRAPHY

VOL. 504 (1990)

JOURNAL *of* CHROMATOGRAPHY

INTERNATIONAL JOURNAL ON CHROMATOGRAPHY,
ELECTROPHORESIS AND RELATED METHODS

ELSEVIER
AMSTERDAM — OXFORD — NEW YORK — TOKYO

J. Chromatogr., Vol. 504 (1990)

0021-9673/90/$03.50

Printed in The Netherlands

Journal of Chromatography, 504 (1990) 1–19
Elsevier Science Publishers B.V., Amsterdam — Printed in The Netherlands

CHROM. 22 178

Variance contributions to band spread in capillary zone electrophoresis

HARLAN K. JONES, NHUNG T. NGUYEN and RICHARD D. SMITH*
Chemical Methods and Separations Group, Chemical Sciences Department, Pacific Northwest Laboratory, Richland, WA 99352 (U.S.A.)
(First received July 4th, 1989; revised manuscript received November 22nd, 1989)

SUMMARY

A peak variance method is described and used to determine contributions to band spread in capillary zone electrophoresis (CZE) for model systems consisting of amino acids, peptides and proteins. A theoretical and experimental approach is proposed for isolating time-independent contributions to band spread from the time-dependent contributions to band spread in CZE. The significant time-independent contributions to CZE band spread include injection and detection, while important time-dependent contributions to band spread in CZE are due to molecular diffusion, Joule heating and deviation from ideal electroosmotic plug flow. The contribution of diffusion to band spread in CZE is experimentally determined by using a new approach involving multiple passes of the sample band past the detector, allowing measurement of the total variance of a sample band at periodically increasing residence times in the CZE column. Molecular diffusion is confirmed to be the major contributor to band spread under optimized CZE conditions. The experimental values for diffusion coefficients obtained in studies (without an externally applied electric field) are subsequently used to isolate the more subtle contributions to band spread which include Joule heating and the nature of electroosmotic (*i.e.*, flow deviation from plug). Important time-independent contributions, *i.e.*, injection, detection and voltage "on–off" switching are isolated for several analytes and compared to their total experimentally determined time-independent variance.

INTRODUCTION

Capillary zone electrophoresis (CZE) has been shown to be a fast, efficient separation method for mixtures of amino acids[1,2], polypeptides[3], proteins[4–6], bases, nucleosides and oligonucleotides[7], catechols[8] and a wide range of other biologically important molecules. Martin *et al.*[9] have studied some of the factors contributing to the loss of separation efficiency in CZE which include molecular diffusion, the nature of the fluid, effects due to flow in capillaries (*i.e.*, specifically the flow profile, deviation from plug flow), heating effects, injection volume, detection volume and sample

0021-9673/90/$03.50

specific contributions (*i.e.*, concentration effects and adsorption on capillary surfaces). Coxon and Binder[10] have previously addressed the problem of the radial temperature distribution for isotachophoresis in columns of circular cross-section. Martin and Guiochon[11] have studied longitudinal dispersion in liquid chromatography for the case of electroosmotic pumping. Most recently, Foret *et al.*[12] have described some of the dispersive processes relating to CZE separation efficiency, and Grushka *et al.*[13], have examined temperature gradients in CZE for capillary columns of varying diameters. Of considerable interest are non-ideal operating conditions, where compromises to sample size and electric field gradient may be necessary to allow collection, sample fractionation, enhanced sensitivity for detection, or greater separation speed.

Most workers in the area of CZE agree that the longitudinal contribution of molecular diffusion is the predominant contribution to the broadening of the solute band under "ideal" conditions. However, it has also been observed that Joule heating and deviation from ideal electroosmotic plug flow (resulting from additional effects due to heating, and other contributions due to inadvertent laminar flow) may also contribute substantially to loss of CZE separation efficiency since optimum CZE results are defined only by the relative rates of electrophoretic migration and molecular diffusion. The molecular diffusion coefficient is also an important physical property for molecules of biological importance, *i.e.*, proteins and smaller polypeptides. When combined with sedimentation-rate measurements, the diffusion coefficient can yield accurate molecular weight values for proteins[14]. More importantly, the ability to isolate the solute band broadening contribution due to molecular diffusion is the first step toward isolating other significant band broadening factors contributing to the loss of separation efficiency in CZE (*e.g.*, heating effects and deviations from "ideal" plug-flow). Our goal in this work is to first experimentally determine the contribution of diffusion to band spread in CZE, and to use this as a basis for attempting to experimentally isolate the other (more subtle) contributions. One aspect of our approach is to attempt to separate additional contributions (due directly or indirectly to heating) from any due inherently to electroosmotic flow.

The peak variance method used in this study for determining aqueous diffusion coefficients is based on a method first introduced by Giddings and Seager[15], and later modified by Knox and McLaren[16] for rapid determination of gaseous diffusion coefficients. The method was later extended to dense gases by Balenovic *et al.*[17], small solutes in liquid systems by Grushka and Kikta[18], and macromolecules in aqueous liquids by Walters *et al.*[19]. The CZE experiment provides a uniquely useful method for such studies. In contrast to the earlier studies which measured solute band spread after a single pass through the detector, the electromigration process allows one to manipulate the direction of analyte motion by reversing the polarity of the electric field, while having a nearly negligible effect on peak variance. This technique provides a simple means for moving the solute band back and forth, many times if desired, past the detector. This study also complements other recent experimental studies which have investigated various factors governing separation efficiency for CZE[20–22]. In this work we show that those CZE methods allow rapid and accurate measurement of diffusion coefficients, as well as isolation of variance contributions due to injection. We will also show that contributions due to heating effects and deviations from plug flow are largely interdependent and less easily resolved experimentally, and will suggest methods to determine their relative importance.

THEORY

Separation efficiency in CZE is most often measured in numbers of theoretical plates (N)[1,23]. Less often one will encounter plate height in discussions of how efficient one separation is from another[24]. In this work the peak variance, which is the link between plate height and number of theoretical plates, is the basic tool used for examining the important efficiency loss factors in CZE.

We have selected the total variance of the solute band as the starting point for isolation and determination of efficiency loss factors in CZE. By using the total variance of the solute band, which ideally assumes a gaussian distribution, we can say that all those processes which contribute to the total breadth of the solute band can be sunmed in terms of their individual variances as shown in the following expression:

$$\sigma^2 = \sigma_A^2 + \sigma_B^2 + \sigma_C^2 + \ldots \quad (1)$$

In this model, we have taken the total variance of the solute band and divided it into two categories, a constant or time-independent variance (due to discrete events during the separation), and a time-dependent variance, which varies with the residence time of the solute in the CZE column until reaching the detector. Table I lists the efficiency loss factors for CZE. The constant factors include injection volume, detection volume, and voltage switching (*i.e.* effects arising from turning the high voltage "on" or "off", which may be attributed primarily to initiation or cessation of electroosmotic flow). The importance of voltage switching to the experimental procedure will be discussed later in this paper. Time-dependent factors which appear to contribute significantly to the broadening of a solute band include longitudinal molecular diffusion, heating and deviation of the electroosmotic flow profile from idealized plug flow. The total variance in eqn. 1 can be expressed in terms of these contributions by

$$\sigma^2 = \sigma_a^2 + \sigma_b^2(t) \quad (2)$$

where σ_a^2 is the time-independent or constant variance and $\sigma_b^2(t)$ is the time-dependent variance contribution.

Detection and injection are considered to be the major components of the constant part of the total variance. Sternberg[25] has derived second moment or

TABLE I

TIME-INDEPENDENT AND TIME-DEPENDENT CZE EFFICIENCY LOSS FACTORS

Time-independent contributions to variance (σ_a^2)
Injection
Detection
Voltage switching (high voltage "on" or "off")
Time-dependent contributions to variance (σ_b^2)
Molecular diffusion
Joule heating
Flow profile (deviation from plug flow)
Sample specific contributions (local concentration effects and adsorption)

variance expressions for detection and injection. The variance contribution for a finite detector path length is

$$\sigma_{\text{det}}^2 = l_i^2/12 \tag{3}$$

where l_i is the path length of the detector cell. Since CZE detection generally occurs "on column" the detection process itself does not contribute to variance except in terms of the length (in the case of this study) of capillary corresponding to the detector cell volume. The assumption most workers make regarding the shape of the electroosmotic injection profile is that it can be approximated by a sufficiently narrow band which can gradually relax (under ideal conditions) to a gaussian shaped peak longitudinally[20,26]. This is, of course, an approximation since all the factors which contribute to variance during separation can contribute to injection when electromigration is used, as in this study. However, such contributions to variances can almost always be neglected; as an example, a recent study by Rose and Jorgenson[27] comparing electromigration and hydrostatic injection showed no significant differences in the measured efficiencies. For a plug sample injection profile, the contribution to variance is identical to that for detection and is given by

$$\sigma_{\text{inj}}^2 = l_j^2/12 \tag{4}$$

where l_j is sample injection migration distance.

The electromigration injection process in CZE is the combination of two functions. The injection process begins with the sample input function which carries with it the initial sample band width[25]. The electromigration injection plug profile is convoluted onto that input function during injection. In contrast to most chromatographic injection processes, the CZE input function and electromigration injection process occur simultaneously. The volume of the injection band for electromigration can be accurately approximated (for a specific analyte) given the elctroosmotic flow-rate, the analyte's electrophoretic mobility, sample buffer, injection time and voltage. However, the importance of other contributions leading to dispersion during injection may be dependent upon design of the spcific apparatus and procedures, and remain undetermined.

There are certain sample specific time-dependent contributions to CZE band broadening which include adsorption effects and local electric field effects due to excessive sample concentrations, which are much more complex and beyond the scope of the present work. Such effects are most significant in the early stages of the separation, immediately following injection. Fortunately, experimental conditions can be adjusted to minimize such specific contributions; we believe the conditions chosen for this work allow their effects to be neglected.

A requirement in our present study is isolating and determining the magnitude of the contribution due to longitudinal molecular diffusion as it relates to the total variance of the CZE solute band. The Einstein equation[28] relates variance due to molecular diffusion to the molecular diffusion coefficient D_{m}

$$\sigma^2 = 2D_{\text{m}}t \tag{5}$$

(where t is time in s and D_m has units of cm^2/s). Measurement of the variance due to molecular diffusion is ideally accomplished in the absence of Joule heating and, less generally, electroosmotic flow, both of which are inherent to CZE (although, in specific circumstances these effects *may* be made negligible—it is unclear at what point this is accomplished). Both heating and electroosmotic flow are induced by applying an electric field gradient across the length of the fused-silica glass capillary column, so such measurements would ideally be obtained in the absence of the applied field.

Our method is similar to Knox and McLaren's[16] gas chromatographic method. During the experiment, the applied potential is turned off, which stops electroosmotic flow, and then the analyte band is allowed to spread by diffusion only. Jorgenson and co-workers[20,26] have previously used a variation of Knox's method for measurement of molecular diffusion coefficients. A difficulty encountered in this approach is that one must assume or calculate contributions from detection, injection, and interruption of both electrophoretic migration and electroosmotic flow, or to choose conditions such that (one hopes) such contributions are negligible. A dual-detector approach like the one employed by Evans and McGuffin[29] for the elimination of extra column contributions to chromatographic peak variance would prove useful for the analysis of the CZE time-independent variance contributions, but would still require a "field on" condition for the measurement of diffusion coefficients. Rather than make one measurement of the solute band during an experiment or flow the analyte between two detectors, our method allows the analyte to diffuse freely during several "field off" time periods and diffusion is determined in a straightforward manner from the contribution to variance for two (or more) different measurements of the peak. The diffusion can occur in conjunction with normal CZE conditions (*i.e.*, field on) or with the field off, to obtain accurate measurements of diffusion coefficients. At the end of each free diffusion period the electroosmotic flow is reversed and the sample is moved immediately past the detector. Electroosmotic flow is discontinued immediately following detection of the solute band. At each pass, the peak width at half-height is measured which is converted to total peak variance by the following series of expressions which are related to column efficiency or number of theoretical plates N[30],

$$N = l_k^2/\sigma^2 \tag{6}$$

where l_k is the distance from injection to detector. The following expression relates peak width at half-height to N[30].

$$N = 5.545\ (l_k^2/w_{1/2}^2) \tag{7}$$

By combining eqns. 6 and 7, total peak variance σ^2 can be directly related to the square of $w_{1/2}$

$$\sigma^2 = w_{1/2}^2/5.545 \tag{8}$$

The peak integrator used for all experiments in this study calculates the area-to-height ratio (AR/HT) of an analyte peak in units of time which is equated to peak width at half-height. The width at half-height is used rather than width at baseline to reduce errors due to any adsorption[31]. The peak width at half-height must be

converted to column length units for peak variance. Once total peak variance is calculated, a plot of total variance *versus* column residence time is determined. According to eqn. 2, constant contributions to peak variance are found in the intercept σ_a^2 and the time-dependent variance contributions are contained in the slope. In our studies (where the high voltage is off except for the brief period required to move the band past the detector at relatively modest field strengths), we show that the time-dependent variance is due only to longitudinal molecular diffusion. We demonstrate that all other contributions may be neglected for diffusion rates typical of solutes in normal liquids. By applying the Einstein eqn. 5 to the slope of the variance *versus* time plot, one directly calculates the molecular diffusion coefficient D_m. Other voltage switching experiments have been done, which yield a slope containing the variance due to diffusion plus other significant contributions to the time-dependent variance. By subtracting the variance due to diffusion from the total time-dependent variance, one can begin to investigate the other factors contributing to the loss of separation efficiency in CZE.

EXPERIMENTAL

Apparatus

The apparatus used for all electrophoresis experiments was similar in design to that described by Jorgenson and Lukacs[1]. Fused-silica capillaries with inner diameter of 100 μm were obtained from Polymicro Technologies (Phoenix, AZ, U.S.A.), and used without any further treatment. The capillaries were all 150 cm in length and in all cases filled with 0.01 *M* phosphate buffer which was adjusted to pH 8.3. A Glassman High Voltage (Whitehouse Station, NJ, U.S.A.) Model LG60P2.5 0–60 kV d.c. power supply delivered the applied potential. The high-voltage lead is contained within a plastic insulating box equipped with electrical interlocks protecting the operator from the high-voltage region. Strips of platinum foil were used as electrodes. On-column UV detection was carried out by using a modified ISCO V[4] variable-wavelength high-performance liquid chromatography (HPLC) detector (Lincoln, NE, U.S.A.) at 215 or 280 nm. On-column fluorescence detection was carried out by using a McPherson FL-749 spectrofluorometer, Division of Schoeffel International (Acton, MA, U.S.A.). A 150 W Xenon short-arc lamp was used as the excitation source; fluorescence light was collected at 90° to the excitation beam through a 440-nm glass cut-off filter. Output signals from both absorbance and fluorescence detectors were connected to a 3390A Reporting Integrator, Hewlett Packard (Avondale, PA, U.S.A.). The window of the on-column detector cell was created by burning a small section of the polyimide coating off at the mid-point (75 cm) of the 150-cm capillary column. The on-column fluorescence cell length was 0.107 cm, and the on-column UV–VIS detector cell length was 0.104 cm.

Procedure

Sample was introduced by electromigration at the high-voltage end of the capillary column. Samples were prepared at the given concentration in the buffer used for CZE separation. For all cases except horse heart myoglobin, injection was done at 15 kV applied potential for 3 s with a current of 5.9 μA. In the case of myoglobin, injection was done at 10 kV applied potential for 5 s with a current of 4.1 μA. The

TABLE II

MOLECULAR WEIGHTS AND CONCENTRATIONS OF AMINO ACIDS, POLYPEPTIDES AND PROTEINS IN THIS STUDY

Sample	*Molecular weight*	*Sample concentration*
2-Naphthol	144	$5.80 \cdot 10^{-4}$
Dns-Ala	421	$1.92 \cdot 10^{-4}$
Dns-Ile	463	$1.88 \cdot 10^{-4}$
FL-methionine enkephalinamide[a]	868	$2.88 \cdot 10^{-5}$
FL-vacotocin[a]	2450	$5.10 \cdot 10^{-6}$
FL-insulin[a]	8220	$6.00 \cdot 10^{-5}$
Horse heart myoglobin	17 500	$3.57 \cdot 10^{-5}$

[a] FL corresponds to the fluorescamine labeled polypeptides and protein.

potential applied at the beginning of each experiment was 30 kV with a current of 12.5 μA. The high voltage remained on until the sample peak was detected. Immediately following detection, the applied potential was turned off for a period of approximately 60 min. At the end of 60 min, the ends of the capillary column were interchanged (reversing the electric field after voltage is reapplied), which caused a change in the direction of the elctroosmotic flow. The 30 kV potential was reapplied for as long as it took for the sample peak to be detected and then discontinued again for another 60-min period. This procedure was repeated a number of times. Any flow in the capillary due to a difference in reservoir heights was immediately apparent by a change in the amount of time required for detection when voltage was reapplied (ideally the time between detection of the peak maximum and turning the voltage off is precisely the same as the time between reapplying voltage and detection). A modification of the above experiment was done by keeping the voltage on throughout the entire experiment except during the 30-s periods when the column ends were interchanged to reverse the direction of electroosmotic flow. 2-Naphthol, dansyl-L-alanine (Dns-Ala) and dansyl-L-isoleucine (Dns-Ile) were studied by using the modified procedure at the following applied potentials: 30, 25, 20, 15, 10 and 5 kV.

Column maintenance

Buffer reservoirs were replenished with fresh buffer daily. The capillary column was flushed with 200 μl of fresh buffer each day before use. For separations of polypeptides and proteins the column was flushed with fresh buffer after each experiment.

Chemicals

Table II lists the amino acids, polypeptides, proteins and other molecules used in this work, their respective molecular weights and concentrations used for most studies. Fluorescamine was used to label the polypeptides and insulin for fluorescence detection. All of the polypeptides, proteins, dansylated amino acids, and fluorescamine used in this study were obtained from Sigma. Phosphate buffers were prepared from reagent-grade chemicals (NaH_2PO_4, Na_2HPO_4 and NaOH) and had an ionic strength of 0.01 *M* and a conductivity of 670 μS.

TABLE III

CONTRIBUTIONS TO THE TIME-INDEPENDENT VARIANCE

Sample	σ^2_{det} (cm^2)	σ^2_{inj} (cm^2)	$\sigma^2_{det} + \sigma^2_{inj}$ (cm^2)	σ^2_{exp} (cm^2)
2-Naphthol	0.000952	0.00608	0.00703	0.0510
Dns-Ala	0.000952	0.00396	0.00491	0.0348
Dns-Ile	0.000952	0.00378	0.00473	0.0365
FL-methionin enkephalinamide	0.000952	0.00456	0.00551	0.0190
FL-vacotocin	0.000952	0.00621	0.00716	0.0779
FL-insulin	0.000952	0.00059	0.00154	0.0268
Horse heart myoglobin	0.000906	0.00658	0.00749	0.0689

RESULTS AND DISCUSSION

The focus of this paper is measurement of the variance due to molecular diffusion, which we classify as a component of the time-dependent part of the total variance of the solute band (see Theory section). We then use these techniques to examine other contributions to variance. As a preface to the discussion of the molecular diffusion experiments, the time-independent part of the total variance requires a brief discussion.

Contributions due to injection and detection

Table III lists results for all the compounds used in the band spread study. The corresponding calculated time-independent variance values due to detection and injection and their respective sums are compared to the total experimental time-independent variance. Table IV shows the experimental contribution of voltage switching to the total time-independent variance for 2-naphthol and horse heart myoglobin. The voltage switching variance accounts for one cycle of turning the applied potential on and off.

The calculated variance due to detector path length will be the same for all molecules except horse heart myoglobin, where on-column UV absorbance detection was used. The detector variance, calculated from eqn. 3, is approximately 50 times smaller than the total experimental time-independent variance for each molecule.

The variance due to electromigration injection was calculated from eqn. 4. The

TABLE IV

VOLTAGE SWITCHING CORRECTION (σ^2_{vs}) TO THE TIME-INDEPENDENT VARIANCE

Sample	$\sigma^2_{det} + \sigma^2_{inj}$ (cm^2)	σ^2_{exp} (cm^2)	σ^2_{vs} (cm^2)	$\sigma^2_{correc.}$ (cm^2)
2-Naphthol	0.00703	0.0510	0.0012	0.0498
Horse heart myoglobin	0.00749	0.0689	0.0018	0.0671

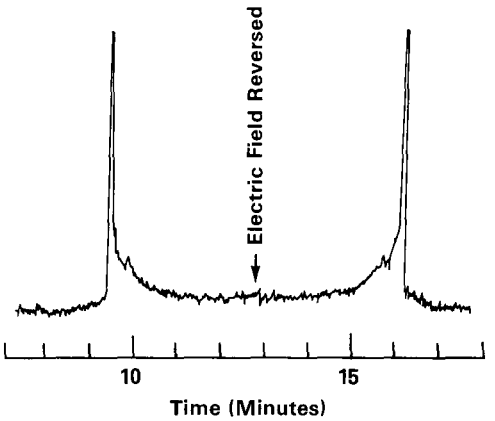

Fig. 1. Peak tailing due to poor manual electroosmotic injection, shown before and after reversing the polarity of the applied potential.

calculated variances for this mode of injection are all approximately an order of magnitude less than their respective total experimental variances. The summed variance due solely to detection and injection is approximately 7 times less than the total experimental variance for each sample molecule. While some of the difference may be due to voltage switching, the majority of the time-independent variance can be directly attributed to injection processes. An extreme case of poor manual electromigration injection is illustrated in Fig. 1. The tailing portion of the first 2-naphthol peak is the result of poor injection technique. Some experimental factors which can lead to band broadening during injection have been described by Grushka and McCormick[22]. Following reversal of the electric field, the same contribution to band spread due to injection is shown reflected as the leading portion of the 2-naphthol

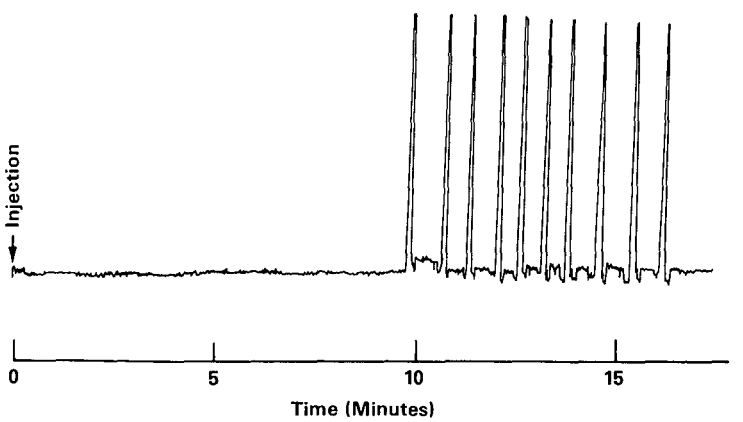

Fig. 2. Effect of reversing high-voltage polarity nine times to determine contributions to peak variance. The analyte was 2-naphthol (10^{-4} *M*), pH 8.3 phosphate buffer (10^{-2} *M*), 3-s/5-kV injection, 30 kV applied potential.

peak. Manual injection can be markedly improved by repetition and practice, and was utilized in all experiments. The important point relevant to the present study is that injection quality is verified by the initial passage through the detector at the start of each expriment, and any non-ideal effects due to injection or the early stages of electromigration are explicitly subtracted.

Contributions to peak variance from voltage switching

The voltage switching technique used in this study allows repetitive detection of sample bands during the CZE experiment by reversing the direction of electroosmotic flow. The peak width was independent of any additional delay after detection (before removing the high voltage) *i.e.*, subsequent detection did not indicate any effect of the time between between applying high voltage and peak width. These results indicate that electroosmotic flow is established very rapidly (or stopped very rapidly). In Table IV, experimental variance values for 2-naphthol and horse heart myoglobin are given for voltage switching (σ^2_{vs}). Fig. 2 shows an electropherogram illustrating the effect of voltage switching for 2-naphthol. The sample migrates through the column in response to the applied potential and passes through the detector. Following sample detection the voltage is turned off, the column ends are reversed and the voltage is turned back on (alternatively, the high-voltage polarity can be inverted). The variance due to voltage switching is assumed to be a constant for a given voltage, buffer and capillary diameter, but the contributions are cumulative and depend on the number of times the high voltage is switched off and on. Each time the voltage is switched off and on, a finite constant contribution to the variance of the sample band is added. If electromigration is the mode of injection, then such a situation applies at least once in a CZE separation. In the case of 2-naphthol, the experimental variance at experimental conditions due to one voltage off–on cycle is 0.0012 cm^2, and for horse heart myoglobin the voltage off–on variance is 0.0018 cm^2. Since these measurements neglect additional contributions to peak variance due to diffusion between measurements and any disruption due to the capillary manipulation, the values reported represent the maximum possible contribution from voltage switching. The electromigration injection procedure and its corresponding voltage off–on cycle is included in our time-independent variance contribution. In Table IV, the voltage off–on variance for 2-naphthol and horse heart myoglobin has been combined with their respective detection and injection variances and then subtracted from the total experimental time-independent variance. The time-independent variance, which has been corrected for voltage switching, is approximately 7 times greater in magnitude than the summed detection and injection variance for 2-naphthol and about 9 times the magnitude of $\sigma^2_{det+inj}$ for horse heart myoglobin. The remaining experimental time-independent variance is attributed to the injection input function discussed earlier.

The present results are also of practical interest since many situations exist where one may desire to stop or slow electromigration. For example, CZE fraction collection may require removal of high voltage for a brief period. Similarly, by dropping CZE voltage, or even stopping electromigration, the detector time constant can be increased, resulting in greater signal-to-noise or (at fixed detection time constant) often greater resolution. The present results show that the effects of such voltage changes will be small and will not, in general, significantly degrade separations.

Determination of molecular diffusion contributions to peak variance

Isolating the variance contribution due to molecular diffusion from other time-dependent broadening phenomena requires an approach which minimizes, or ideally eliminates, contributions due to Joule heating and the electroosmotic flow. The first step of our approach is the same as for a normal CZE experiment; the applied potential remains on until the sample peak is detected. Immediately following detection the power supply is turned off and the sample band is allowed to spread solely due to diffusion. The experiments included four free diffusion periods, with each free diffusion period lasting about 60 min. The variance for each peak detected in an experiment (corrected for voltage switching at each voltage on–off event) is calculated from peak width at half-height according to eqn. 8 and plotted against column residence time. The data show a linear relationship to residence time with the intercept corresponding to time-independent variance contributions and the slope directly

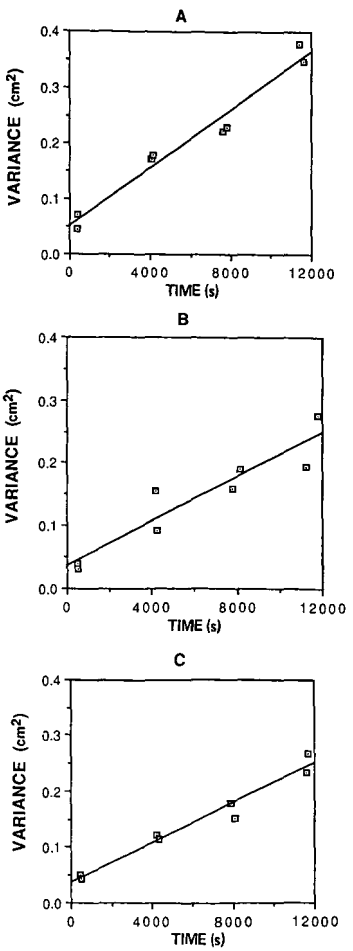

Fig. 3. Variance *versus* time plots for (A) 2-naphthol; (B) Dns-Ala; (C) Dns-Ile. Plots are used to isolate the variance contribution due to molecular diffusion.

TABLE V

MOLECULAR DIFFUSION COEFFICIENTS DETERMINED BY THE CAPILLARY ELECTROPHORESIS VARIANCE METHOD COMPARED TO VALUES DETERMINED BY OTHER METHODS

Sample	$D_m \cdot 10^6$ *by CZE variance method*[a]	$D_m \cdot 10^6$ *by other capillary electrophoresis methods*[b]	$D_m \cdot 10^6$ *by sedimentation-rate measurement*	$D_m \cdot 10^6$ *by laminar flow analysis*
2-Naphthol	13.0		12.1	
Dns-Ala	8.75	6.09		
Dns-Ile	8.77	5.37		
FL-methionine enkephalinamide	6.43			
FL-vacotocin	5.59			
FL-insulin	3.27		2.86	1.17
Horse heart myoglobin	2.06	1.15	1.13	1.03

[a] Determined without the presence of an applied electric field, at 25°C.
[b] Determined at an applied potential of 2.5 kV (ref. 20).

proportional to the molecular diffusion coefficient from eqn. 2. Fig. 3 shows a least-squares fit for three plots of total variance *versus* time for 2-naphthol, Dns-Ala and Dns-Ile. The diffusion coefficient can be calculated by applying the Einstein eqn. 5 to the slope of the line. The total variance due to molecular diffusion can then be determined for any CZE separation time.

Table V lists in order of increasing molecular weight molecular diffusion coefficients determined by the CZE variance method. Corrected molecular diffusion coefficients have been calculated for all the samples by subtracting the voltage switching variance from the uncorrected variance due to molecular diffusion. Diffusion coefficients determined by using other methods are also compared in Table V. As molecular weight increases, the molecular diffusion coefficient decreases, as expected. Our diffusion coefficients generally compare favorably with those values determined by other workers and methods, although slightly different temperatures and buffer compositions apply to each set of measurements. Somewhat surprisingly, the diffusion coefficient values determined by the present CZE variance method are slightly higher than the literature values. 2-Naphthol has a corrected diffusion coefficient (corrected for voltage switching) of $1.30 \cdot 10^{-5}$ cm^2/s compared to the literature value of $1.21 \cdot 10^{-5}$ cm^2/s, a difference of 6.9%. At the other end of the molecular weight range, horse heart myoglobin has a corrected diffusion coefficient of $2.06 \cdot 10^{-6}$ cm^2/s compared to $1.15 \cdot 10^{-6}$ cm^2/s as determined by Walbroehl and Jorgenson[20] using another capillary electrophoresis method (involving electrophoresis at low voltages where Joule heating effects should be small) and $1.13 \cdot 10^{-6}$ cm^2/s as determined by the sedimentation rate method. In the case of insulin, the percent deviation between our value and the literature value is approximately 15%, and for the dansylated amino acids the deviation is about 30%. No literature values were available for the two polypeptides. Rather than measuring peaks by AR/HT ratio which assumes a gaussian solute band distribution (and presumably valid for the symmetrical peaks generally obtained in this study), greater precision may be obtained by using

a moments analysis measurement of peak variance. The moments analysis of chromatographic peaks has been shown to yield more accurate peak variance values than the AR/HT method[31], but an evaluation of other peak measurement methods with respect to the CZE band spread study is needed prior to selecting a more accurate method. However, the ease, speed, reproducibility, and low instrumentation costs suggest that the present method has significant potential for routine measurements of diffusion coefficient. Our slightly higher values for molecular diffusion coefficients may be due to surface adsorption onto the untreated silica capillary walls, although the present methods would be expected to minimize any such effects. Surface adsorption can be best reduced by the appropriate choice of buffer pH (*i.e.*, choose a buffer pH that is above the isoelectric pH of the sample molecule, which will place a net negative charge on both the molecule and capillary wall), buffer ionic strength and sample concentration. Even when the net charge of the polypeptide or protein is the same as the capillary wall, therefore causing repulsion of the molecule from the wall, there may still be some surface adsorption due to interaction between hydrophobic sites on the molecule and the capillary wall. Sample concentration also needs to be at least two orders of magnitude less than the concentration of the buffer to avoid localized heating which could lead to measurable band spread (but not during the free diffusion period in the present study where no field is applied). Even lower molar concentrations are required for proteins which may carry numerous charges. One can sometimes minimize band spread due to surface adsorption by applying the lowest possible sample size. Since 2-naphthol, Dns-Ala and Dns-Ile were all near the upper concentration limit, band broadening due to concentration effects might be possible. By avoiding effects in the early stages of separation, the present methods should minimize such contributions. We tentatively conclude that our diffusion measurements are valid under the present experimental conditions, but additional studies are required to determine the origin of the differences obtained in comparison with other methods.

Variance contributions during CZE separations

Following determination of diffusion coefficients by the CZE variance method, the diffusion coefficient values were then used to examine the more subtle contributions of Joule heating and electroosmotic flow to sample band spread. The expriments were designed to investigate effects due to both heating and any potentially non-ideal contributions (*i.e.*, deviations from plug flow) due to the electroosmotic flow profile. The analyte migrated past the detector and was not stopped until it had almost electromigrated from the other end of the capillary. At that time the voltage was turned off and the polarity reversed. The sample was passed back and forth through the detector as in the measurements of diffusion coefficients; however, the only time the voltage was off was during 30-s periods when the ends of the column were reversed. The experiments were run at 6 different applied potentials; 30, 25, 20, 15, 10 and 5 kV. The three molecules used in the experiments were 2-naphthol, Dns-Ala and Dns-Ile. In contrast to the diffusion coefficient experiment, the voltage remains on throughout this experiment and analyte variance is due to the combined effects of diffusion, heating and electroosmotic flow.

Peak variance was measured as it was in the diffusion experiments and is given as plots of total variance *versus* time data. Fig. 4 shows electropherograms for the

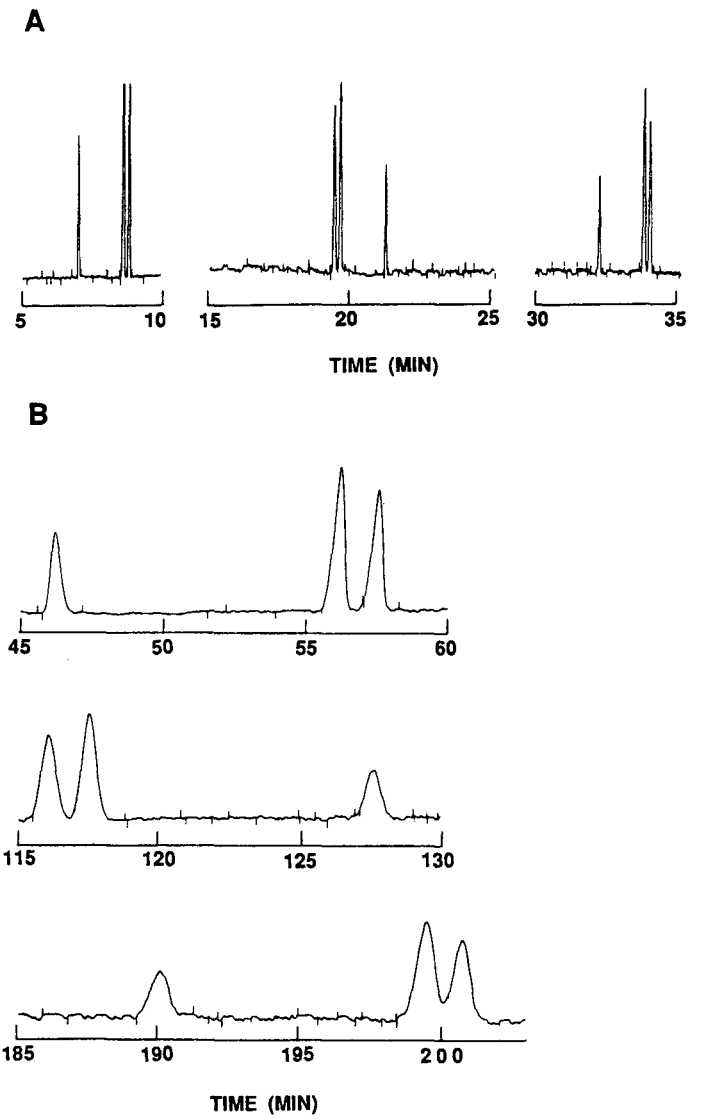

Fig. 4. Electropherograms at (A) 30 kV and at (B) 5 kV for a three-component mixture of (in order of retention times in first segment of the three segments shown) 2-naphthol, Dns-Ala and Dns-Ile. Band broadening is mainly due to molecular diffusion, heating and non-ideal flow effects.

three-component mixture for the first three measurements at 30 and 5 kV, the two extremes in applied potential. One can visually inspect the differences in band spread for each of the three components at 30 and 5 kV and observe the significant broadening of analyte peaks at the lower applied potential of 5 kV. The greater peak width obtained at 5 kV is due to slower migration through the detector, and does not effect variance measurements. Deconvolution of the relative magnitudes of the various time-dependent contributions to band spread requires a variance *versus* time plot for

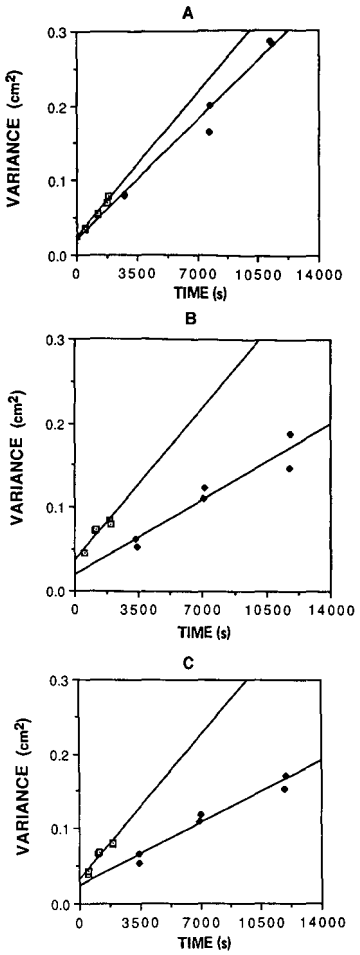

Fig. 5. CZE variable-voltage plots of total variance *versus* time for (A) 2-naphthol; (B) Dns-Ala; and (C) Dns-Ile at (⊡) 30 and (◆) 5 kV. These plots are generated from electropherograms similar to those shown in Fig. 4.

peaks which have undergone separations at different applied potentials. One can then isolate the time-independent contributions to band spread from the time-dependent contributions. Fig. 5 shows the plotted total variance *versus* time data for the peaks presented in Fig. 4. The time-independent contribution to peak variance is again denoted by the intercept on the variance axis. The time-independent variance includes detection, injection and voltage "on–off" contributions, the same as in the diffusion experiments. The difference between these experiments and the diffusion coefficient experiments is apparent in the slope or time-dependent variance contribution. The slope of the variance *versus* time plot contains not only variance due to molecular diffusion, but also other contributions resulting from the continuously applied potential. Joule heating and deviation from ideal plug flow are the most likely

significant contributions to time-dependent peak variance, assuming negligible surface adsorption and concentration effects.

One way to look at the combined effect of heating and non-ideal plug flow in terms of peak variance is to compare the slopes of the 30 and 5 kV experiments for 2-naphthol, a neutral molecule at pH 8.3, to the slopes of the two negatively charged amino acids Dns-Ile and Dns-Ala at the same applied potentials. Fig. 5A shows the 30 and 5 kV data plotted for 2-naphthol. The slopes of the two lines differ by approximately 16%. In the case of Dns-Ile, the slope of the 30 kV line is about 60% greater than the 5 kV slope and similarly, the 30 kV slope for Dns-Ala is 50% greater than its 5 kV slope. The neutral 2-naphthol band will not be directly influenced by *local* Joule heating (due to the presence of a higher conductivity band) since it does not carry a charge. Time-dependent band spread for 2-naphthol is therefore largely ascribed to molecular diffusion, non-ideal electroosmotic flow effects, and primary and secondary effects due to overall Joule heating of the capillary (which should be small due to the low currents utilized). Dns-Ile and Dns-Ala both carry a net negative charge and both will be influenced by local Joule heating, local changes in electric field strength (and resulting secondary effects), as well as any contribution due to deviation from plug flow and molecular diffusion. The comparison of total variance *versus* time plots for the 30 and 5 kV experiments in Fig. 5 suggests that the change in slope over the entire range of applied potentials may provide useful information regarding the isolation of ideal electroosmotic flow deviations from local effects due to Joule heating and field inhomogeneity.

Fig. 6 shows plots of slope *versus* applied potential for 2-naphthol, Dns-Ala and Dns-Ile. If disruptive effects were absent and ideal plug flow existed, the major contributor to time-dependent variance would be longitudinal molecular diffusion, and its slope would not change over the range of applied potentials. All total variance *versus* time plots would have the same slope, and slope *versus* applied potential would yield a horizontal line if molecular diffusion was the only contribution to time-dependent variance. The data shown in Figs. 5 and 6 confirm that molecular diffusion is not the only influence on time-dependent variance. Despite the scatter about the least squares fit for 2-naphthol in Fig. 6A, the data show a slight positive change in slope as voltage is increased from 5 to 30 kV, indicating other processes are contributing to the time-dependent variance. In the case of 2-naphthol, the additional effect contributing to band spread can be ascribed (with the assumption that effects of Joule heating to the buffer are minimal) to non-ideal plug flow and can be quantified over the 30 kV applied potential range in terms of cm^2/s^2-kV.

In Fig. 6B and C, Dns-Ala and Dns-Ile each show a more significant change in slope than 2-naphthol in Fig. 6A. For Dns-Ala and Dns-Ile, the change in slope over the 30 kV applied potential range provides preliminary quantitative evidence for the combined local heating and flow profile contributions to time-dependent peak variance. The total change in slope for 2-naphthol which contains these contributions is approximately $2 \cdot 10^{-7}$ cm^2/s^2-kV. The change in slope for each amino acid is about three times the change for 2-naphthol or $6 \cdot 10^{-7}$ cm^2/s^2-kV and contains the combined peak variance contributions of diffusion, non-ideal flow and Joule heating. One can readily isolate the molecular diffusion contribution from non-ideal flow in the case of 2-naphthol, but the combined effects of diffusion, Joule heating and non-ideal flow contributions to variance for Dns-Ala and Dns-Ile are not as easily separated.

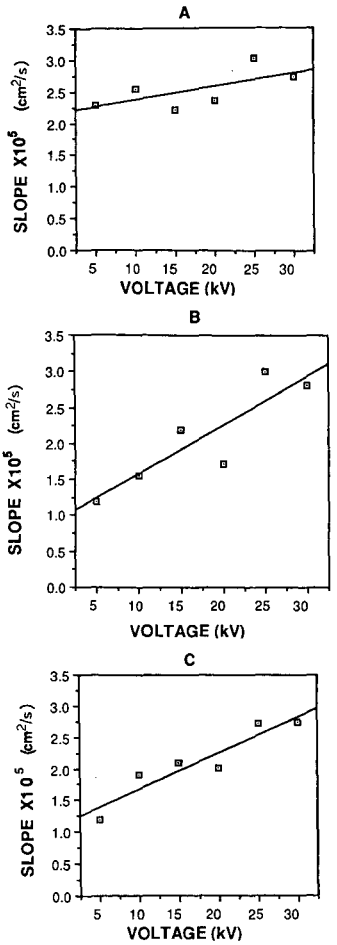

Fig. 6. CZE variable-voltage plots of slope (from variance *versus* time plots) *versus* applied potential for (A) 2-naphthol; (B) Dns-Ala; and (C) Dns-Ile. Plots are derived from a series of plots like those in Fig. 5 for the voltage range 0–30 kV, and experimentally confirm the presence of band spread due to effects other than molecular diffusion.

Subsequent studies are thus needed to isolate the contributions due to Joule heating from that due to non-ideal flow behavior.

CONCLUSIONS

Serial measurements of the total variance of a solute band during CZE separations show promise as a method for investigating the contributions to loss of efficiency. Time-independent contributions which include injection, detection and voltage switching can be calculated or determined experimentally. Injection and detection variances are often assumed to have plug flow profiles and calculated according to the equations of Sternberg[25]. Experimentally, however, injection can

result in additional variance contributions, which can be readily isolated using the methods described here. The variance due to voltage switching during separation was measured and determined to be small compared to the total time-independent peak variance. The results of these experiments indicate that effects due to voltage switching are generally negligible. This result is significant since it confirms that one can manipulate electric field strength during a separation to allow improved injection or detection (*i.e.*, slower peak passage through the detector region), or finer control of sample collection without significant degrading of the separation.

The time-dependent peak variance due to longitudinal molecular diffusion was determined experimentally for several molecules and their respective molecular diffusion coefficients were calculated from the Einstein equation. The diffusion coefficients determined by our CZE voltage switching experiments were higher than, but still compared favorably with, diffusion coefficients measured by other methods. The differences in diffusion coefficients obtained by CZE voltage switching and from other methods require further study, but the ease, quality and conceptual simplicity of the present method argues in its favor.

The CZE voltage switching method introduced in this work was extended and slightly modified for the study of Joule heating and non-ideal plug flow contributions to the time-dependent peak variance. This study was limited to three molecules: 2-naphthol, neutral at the experimental pH of 8.3, and Dns-Ile and Dns-Ala, which both carry net negative charges. In order to look at heating and flow effects, the applied potential was held constant throughout each experiment, and was turned off momentarily only to reverse the direction of electroosmotic flow.

As a result of the neutrality of 2-naphthol, both molecular diffusion and any non-ideal flow effects will contribute to its time-dependent peak variance, but not electrophoretic effects due to local heating of the solute band. It was observed that with increase of the applied potential, the slope of the peak variance *versus* time plot increased in magnitude. If only molecular diffusion was causing time-dependent variance, there should be negligible slope change over the experimental range of applied voltages since the calculated temperature increase was less than 1°C. To achieve improved quantitative values for the non-ideal flow contribution to time-dependent peak variance for 2-naphthol, the slope change from the variance *versus* time plot was plotted against applied potential. Over the 30 kV range of applied potential, the slope change increased by $6.6 \cdot 10^{-6}$ cm^2/s. Again, if only diffusion contributed to time-dependent peak variance, slope *versus* applied potential would yield a horizontal line. Our measurements show a positive increase in slope over the 30 kV range of applied potential. The increase in slope for compounds with zero electrophoretic mobility, such as neutral 2-naphthol, is the first step in isolating any non-ideal plug flow contribution to the time-dependent peak variance. Similar studies are required at a fixed voltage as a function of CZE current to determine the general contribution due to Joule heating. Similarly, the change in slope from the variance *versus* time plots of Dns-Ile and Dns-Ala was plotted against applied potential. Again, if only molecular diffusion contributed to time-dependent variance, the slope change over the range of applied potentials should be negligible for the two negatively charged dansylated amino acids. The two amino acids behaved like 2-naphthol in that they showed a positive change in slope over the 30 kV range, but the magnitude of the slope change for each amino acid was on the average a factor of 3 greater than that for

2-naphthol. The change in slope over the 30 kV applied potential range for Dns-Ala was $20 \cdot 10^{-6}$ cm^2/s and for Dns-Ile was $17 \cdot 10^{-6}$ cm^2/s.

For neutral molecules which are not directly affected by Joule heating, one can isolate the significant time-dependent band broadening factors, but for charged species one has to minimize heating effects to study non-ideal flow effects, and in turn minimize non-ideal flow effects to study the effects of Joule heating. If one makes the assumption that "non-ideal" flow effects are the same for all three analytes, then one can estimate that local Joule heating is approximately twice as significant under the experimental conditions chosen compared to any "non-ideal" flow contributions to solute band spread.

ACKNOWLEDGEMENTS

We thank the U.S. Department of Energy, Office of Health and Environmental Research, for support of this research under Contract DE-AC06-76RLO 1830. Pacific Northwest Laboratory is operated by Battelle Memorial Institute.

REFERENCES

1 J. W. Jorgenson and K. D. Lukacs, *Anal. Chem.*, 53 (1981) 1298.
2 E. Gassmann, J. E. Kuo and R. N. Zare, *Science (Washington, D.C.)*, 230 (1985) 813.
3 J. W. Jorgenson and K. D. Lukacs, *J. Chromatogr.*, 281 (1981) 209.
4 J. W. Jorgenson and K. D. Lukacs, *Science (Washington, D.C.)*, 222 (1983) 266.
5 H. H. Lauer and D. McManigill, *Anal. Chem.*, 58 (1986) 166.
6 R. M. McCormick, *Anal. Chem.*, 60 (1988) 2322.
7 A. S. Cohen, S. Terabe, J. A. Smith and B. L. Karger, *Anal. Chem.*, 59 (1987) 1021.
8 R. A. Wallingford and A. G. Ewing, *Anal. Chem.*, 60 (1988) 258.
9 M. Martin, G. Guiochon, Y. Walbroehl and J. W. Jorgenson, *Anal. Chem.*, 57 (1985) 559.
10 M. Coxon and M. J. Binder, *J. Chromatogr.*, 101 (1974) 1.
11 M. Martin and G. Guiochon, *Anal. Chem.*, 56 (1984) 614.
12 F. Foret, M. Deml and P. Boček, *J. Chromatogr.*, 452 (1988) 601.
13 E. Grushka, R. M. McCormick and J. J. Kirkland, *Anal. Chem.*, 61 (1989) 241.
14 A. L. Lehninger (Editor), *Biochemistry*, Worth Publishers, New York, 1975, Ch. 7.
15 J. C. Giddings and S. L. Seager, *J. Chem. Phys.*, 33 (1960) 1579.
16 J. H. Knox and L. McLaren, *Anal. Chem.*, 36 (1964) 1477.
17 Z. Balenovic, M. N. Myers and J. C. Giddings, *J. Chem. Phys.*, 52 (1970) 915.
18 E. Grushka and J. Kikta, *J. Phys. Chem.*, 78 (1974) 2297.
19 R. R. Walters, J. F. Graham, R. M. Moore and D. J. Anderson, *Anal. Biochem.*, 140 (1984) 190.
20 Y. Walbroehl and J. W. Jorgenson, *J. Microcolumn Sep.*, 1 (1989) 41.
21 A. E. Jones and E. Grushka, *J. Chromatogr.*, 466 (1989) 219.
22 E. Grushka and R. M. McCormick, *J. Chromatogr.*, 471 (1989) 421.
23 J. S. Green and J. W. Jorgenson, *J. High Resolut. Chromatogr. Chromatogr. Commun.*, 7 (1984) 529.
24 T. Tsuda, K. Nomura and G. Nakagawa, *J. Chromatogr.*, 248 (1982) 241.
25 J. C. Sternberg, *Adv. Chromatogr. (NY)*, 2 (1966) 205.
26 Y. Walbroehl, *Ph.D. Dissertation*, University of North Carolina, Chapel Hill, NC, 1986.
27 D. J. Rose, Jr., and J. W. Jorgenson, *Anal. Chem.*, 60 (1988) 642.
28 J. C. Giddings, *Dynamics of Chromatography, Part I, Principles and Theory*, Marcel Dekker, New York, 1965, Ch. 2.
29 C. E. Evans and V. L. McGuffin, *Anal. Chem.*, 60 (1988) 573.
30 B. L. Karger, L. R. Snyder and C. Horvath (Editors), *An Introduction to Separation Science*, Wiley, New York, 1973, Ch. 5.
31 E. L. Johnson and R. Stevenson, *Basic Liquid Chromatography*, Varian Associates, Palo Alto, CA, 1978, Ch. 9.
32 B. A. Bidlingmeyer and F. V. Warren, Jr., *Anal. Chem.*, 56 (1984) 1583A.

Journal of Chromatography, 504 (1990) 21–43
Elsevier Science Publishers B.V., Amsterdam — Printed in The Netherlands

CHROM. 22 190

High-precision sampling of trace gas-borne volatiles by the dynamic solvent effect with a comparative review of alternative techniques

PETER J. APPS[a]
Institute for Chromatography, University of Pretoria, Pretoria 0002 (South Africa)
(First received September 6th, 1989; revised manuscript received December 4th, 1989)

SUMMARY

The precise determination of traces of organic volatiles is particularly challenging in semiochemistry and clinical chemistry, where specimen sizes are intrinsically limited and amounts of trace components correspondingly very small. This demands a sampling technique that is fully compatible with the ability of capillary columns and gas chromatographic detectors to separate and quantify nanogram and sub-nanogram amounts from complex mixtures.

The quantitative precision of dynamic solvent-effect sampling of low parts per billion (10^9) aqueous carbonyl compounds, high ppb and low parts per million aqueous phenols, low ppb and high parts per trillion (10^{12}) airborne hydrocarbons and the volatiles from wine, human urine and a slow-release pesticide was tested with specimen sizes that yielded amounts of volatiles down to the sub-nanogram level.

Provided that sources of variability, such as temperature changes, adsorption on containers, incomplete peak resolution and changes in the specimens themselves, were adequately controlled, dynamic solvent-effect sampling consistently provided coefficients of variation in peak areas, peak percentage areas and peak-area ratios of less than 10% at nanogram and sub-nanogram levels. The literature was surveyed for data on the performance of other sampling systems. None of them have been demonstrated to match the precision of the dynamic solvent effect with such small amounts from such a wide range of materials.

INTRODUCTION

The use of films of liquid to extract volatiles from gases for chromatographic analysis extends back to at least 1964 when Pavelka[1] used a film of solvent spread on glass beads to trap airborne volatiles. Grob[2] demonstrated focusing by the solvent effect, on a 2-μl film of hexane on a capillary column, of low-boiling volatiles from 1

[a] Present address: Food Hygiene, Veterinary Research Institute, Onderstepoort 0110, South Africa.

0021-9673/90/$03.50

cm^3 of the headspace of a spice. Jennings[3] trapped food headspace volatiles on a refluxing film of Freon 12. Roerade and Blomberg[4] mentioned the possibility of using the solvent effect to focus gas-phase volatiles, but presented no experimental results. Pretorius and Bertsch[5] provided a theoretical treatment but their requirement that the carrier gas be saturated with solvent to prevent evaporation of the solvent film is impractical, and imcompatible with sampling from live animals and any specimen that cannot be enclosed and pressurized. Pretorius and Lawson[6] considered theoretically a more versatile method in which the solvent film is allowed to evaporate during sampling. Neither of these theoretical papers included any experimental findings.

The dynamic solvent effect accumulates gas-phase volatiles by trapping them on the evaporating edge of a film of pure solvent held in dynamic equilibrium between evaporation and capillary rise in an axially perforated, porous, packed bed[7]. The resulting sample consists of the trapped volatiles and approximately 20 μl of solvent; it can be transferred directly to a capillary column by carrying out static solvent-effect focusing with the bed in an inlet to which the column is connected[8,9].

The dynamic solvent effect was developed specifically to provide a sampling technique that allows full exploitation of the ability of capillary columns and gas chromatographic detectors to separate and quantify low- and sub-nanogram amounts of solutes in complex mixtures, a need which is keenly felt in work on semiochemicals[10] and clinical chemistry[11].

The quantitative precision of dynamic solvent-effect sampling of gas-borne volatiles from a range of specimens is reported here. The specimens were chosen to represent types of material commonly analysed by capillary gas chromatography and to provide a test of the performance of the dynamic solvent effect with small specimens and samples.

EXPERIMENTAL

Separations were carried out in a Varian 3700 gas chromatograph fitted with a dynamic solvent-effect inlet[8] and a 25 m × 0.3 mm I.D. capillary column coated with a 0.4-μm film of methylsilicone. The initial temperature of the inlet and column was 40°C, the inlet was heated ballistically to 220°C after a solvent evaporation time determined for each concentrator[8], and the column temperature was programmed at 10°C min^{-1} after 6 min for synthetic specimens, or at 5°C min^{-1} for natural specimens. The carrier gas was hydrogen with a linear velocity of 50 cm s^{-1}. A flame ionization detector was used at a sensitivity of 10^{-11} A mV^{-1} and chromatograms were recorded on a Varian 4270 integrator with a full-scale deflection of 2 or 4 mV. Eight dynamic solvent effect concentrators were used for the various specimens.

Attempts to make up standard specimens with low parts per billion (10^9) concentrations, which were accurate to within the 1–2% limits needed to test the accuracy of dynamic solvent-effect sampling, proved unproductive. Adsorption, the effects of temperature on density, limited volumetric accuracy and evaporation of volatile solvents all contribute to uncertainty in the concentration of standards[12–15]. Nor was it possible to measure the concentration of a standard independently because even the best of the alternative methods yield sampling variations as large as or larger than that provided by the dynamic solvent effect (see Table XIII and Discussion). Consequently, only the precision of dynamic solvent-effect sampling was investigated; the

concentrations of the specimens are presented only as guide to the levels at which the performance was obtained.

Similarly, the masses of each compound represented by a given peak are based on calibrations of detector response from split injections of relatively concentrated solutions. When the identity of component was unknown, as in the wine and urine samples, its quantification was based on the response of the detector to *n*-alkanes, so the amounts given are probably slightly higher than the true values. The figures for the mass of each component are offered only as a guide to the level of sensitivity at which the reported precision was obtained. As standard deviations were calculated from raw peak areas, these approximations do not affect the reported precision of the dynamic solvent effect.

The test specimens were prepared as follows.

Aqueous aldehydes and ketones

The standard solution contained (concentrations in ppb) 2-heptanone (40), heptanal (16), 2,6-dimethyl-4-heptanone (16), nonanal (48), decanal (16), undecanal (24) and dodecanal (8) in distilled water, which had been purged of organic volatiles by vigorous boiling and sparging with charcoal-filtered nitrogen.

Each specimen was a 5-cm^3 aliquot of the stock standard solution measured into a 10-cm^3 borosilicate glass bubbler (Fig. 1) using a borosilicate glass pipette. Both the pipette and bubbler were rinsed with 5 cm^3 of standard solution immediately before each specimen was measured. The test compounds were purged from the water with a 10 cm^3 min^{-1} flow of palladium-purified hydrogen for 10 min, and trapped by the dynamic solvent effect using *n*-hexane as solvent at 30-30.6°C. A series of five samples were run on each of three concentrators.

A further series of five samples, for which the pipette and bubbler were not rinsed, were run on one concentrator.

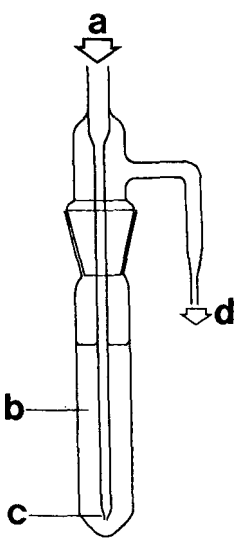

Fig. 1. Bubbler used to sparge volatiles from up to 10 cm^3 of liquid when sampling by the dynamic solvent effect. a = pure gas; b = liquid specimen; c = fine tip; d = to dynamic solvent effect concentrator.

Aqueous phenols

Precisely weighed portions (*ca.* 140–250 mg) of phenol, *p*-cresol and 2,4-dichlorophenol were each dissolved in 2 cm^3 of 5 *M* sodium hydroxide solution. Interfering impurities were extracted from the solutions with 5 × 100 μl of *n*-hexane. Sufficient of each solution was added to 1 l of water in a borosilicate glas flask to give concentrations of $1.67{:}10^6$ of phenol, $0.42{:}10^6$ of *p*-cresol and $0.13{:}10^6$ of 2,4-dichlorophenol. The water had been distilled three times from alkaline permanganate and percolated through activated charcoal.

Each sample was obtained by bubbling palladium-cell-purified hydrogen through the 1 l of solution at a flow-rate of 5 $cm^3\ min^{-1}$ for 10 min. The temperature was held at 29.6°C. Five samples were taken on each of three concentrators using *n*-hexane as solvent.

Airborne hydrocarbons

Low concentrations of a complex mixture of hydrocarbons in air were generated by passing a 10 $cm^3\ min^{-1}$ flow of charcoal-filtered air over the surface of *ca.* 10 cm^3 of white petroleum jelly in a 20-cm^3 tube (Fig. 2) at room temperature (26–27°C). The air flow was maintained for 1 week, with hydrocarbon concentrations monitored daily, to allow the system to stabilize before serial sampling was carried out. Sampling

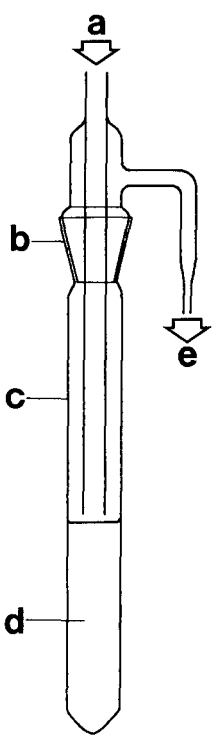

Fig. 2. Apparatus used to generate ppb concentrations of complex mixtures of airborne hydrocarbons. a = 10 $cm^3\ min^{-1}$ of charcoal-purified air; b = 14/23 joint; c = 20-cm^3 tube; d = 10 cm^3 white petroleum jelly; e = to dynamic solvent effect concentrator.

was carried out by passing the hydrocarbon-loaded air through a dynamic solvent-effect concentrator, with *n*-hexane as solvent, for 10 min. A series of five samples were taken on each of three concentrators.

Wine

Each specimen was 10 cm^3 of a red table wine (Tassenberg, Stellenbosch Farmers Winery, Oude Libertas, Stellenbosch, South Africa) dispensed directly from its commercial, laminated foil container into a graduated, borosilicate glass bubbler that had been rinsed with the same wine. Palladium-purified hydrogen was bubbled through the wine for 10 min at a flow-rate of 10 $cm^3\ min^{-1}$ at 29.6°C for each of a series of five samples on one concentrator.

Urine

Approximately 250 cm^3 of human urine were collected and kept at 0°C until analysis. Portions of 10 cm^3 were measured with a borosilicate glass pipette into a 50-cm^3 borosilicate pear-shaped flask. The urine specimen was allowed 10 min to warm to the sampling temperature of 29.6°C, then 10 $cm^3\ min^{-1}$ of palladium-purified hydrogen were bubbled through it for 10 min. Five samples were taken on one concentrator.

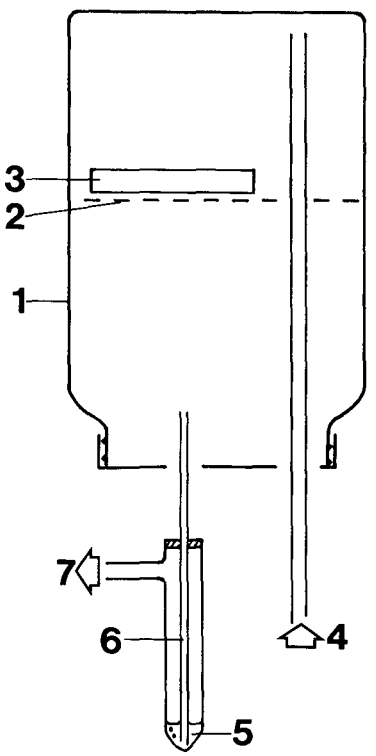

Fig. 3. Apparatus used for sampling volatiles from a slow-release pesticide strip by the dynamic solvent effect. 1 = 500-cm^3 jar; 2 = wire grid; 3 = pesticide strip; 4 = 1 l min^{-1} charcoal-filtered air; 5 = *n*-hexane; 6 = dynamic solvent-effect concentrator; 7 = 5 $cm^3\ min^{-1}$ gas flow to vacuum.

Dichlorvinphos

A commercial, slow-release pesticide strip, designed for small spaces and containing 19.5% of dichlorvinphos (Vapona Cupboard Exterminator, Shell Chemicals) was aged for 8 days in the open air and for a further 9 days in a glass container flushed with 1 l min^{-1} of charcoal-filtered air. On the 18th day eight samples were taken on one concentrator by sucking air from the container at 5 cm^3 min^{-1} for 5 min (Fig. 3). Over the sampling period the temperature varied between 23.6 and 24.1°C. The identity of the dichlorvinphos peak was confirmed by gas chromatography–mass spectrometry.

Chromatograms of the volatiles from each type of specimen are shown to illustrate the general quality of the separations achieved.

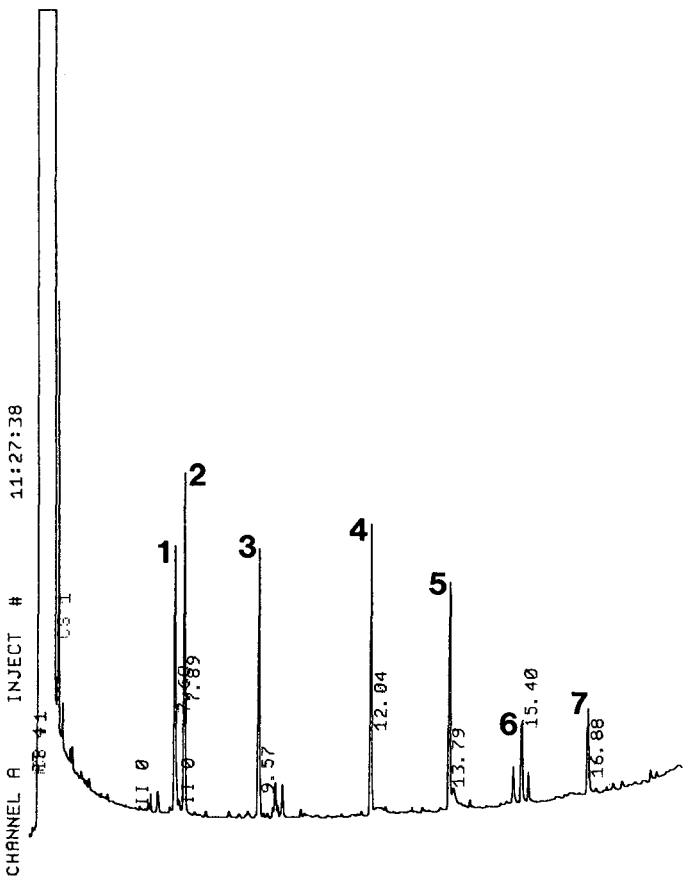

Fig. 4. Chromatogram of carbonyl compounds sampled from 5 cm^3 of aqueous solution by gas sparging at 10 cm^3 min^{-1} for 10 min at 30–30.6°C and trapping by the dynamic solvent effect using *n*-hexane as solvent. Peaks: 1 = *n*-heptan-2-one; 2 = *n*-heptanal; 3 = 2,6-dimethylheptan-4-one; 4 = *n*-nonanal; 5 = *n*-decanal; 6 = *n*-undecanal; 7 = *n*-dodecanal. Computer-printed values at peaks are retention times in min.

TABLE I

COEFFICIENTS OF VARIATION OF PEAK AREAS AND PERCENTAGE AREAS, OVER FIVE REPLICATES ON EACH OF THREE CONCENTRATORS, FOR AN AQUEOUS SOLUTION OF CARBONYL COMPOUNDS SAMPLED BY THE DYNAMIC SOLVENT EFFECT

Glassware rinsed with specimen solution

Compound	*Approx. mass (ng)*	*Coefficient of variation (%)*					
		Concentrator Q2		*Concentrator Q3*		*Concentrator H7*	
		Area	*% Area*	*Area*	*% Area*	*Area*	*% Area*
n-Heptanone	2.5	3.87	4.02	3.94	2.79	6.25	3.20
n-Heptanal	3.5	3.22	2.83	2.43	1.79	7.63	7.17
Dimethylheptanone	3.1	4.30	5.66	3.88	2.83	6.14	2.96
n-Nonanal	3.0	3.92	1.27	5.29	2.31	8.84	3.02
n-Decanal	2.6	10.51	7.96	5.22	2.05	16.18	8.70
n-Undecanal	0.9	9.68	6.25	8.48	6.53	10.14	8.99
n-Dodecanal	1.5	10.88	8.06	9.61	7.58	12.94	11.44

Statistical analysis

Means, standard deviations and coefficients of variation [(S.D./mean) · 100] were calculated for peak areas, peak percentage areas and peak-area ratios from sets of five consecutive runs.

RESULTS

Aqueous aldehydes and ketones

For all the test components the peaks were sharp and symmetrical (Fig. 4). The coefficients of variation of the various statistics are given in Tables I–III.

Omitting the rinsing of the pipette and bubbler with specimen solution seriously degraded the precision of the peak areas (Table IV).

TABLE II

COEFFICIENTS OF VARIATION OF PEAK-AREA RATIOS, OVER FIVE REPLICATES ON EACH OF THREE CONCENTRATORS, FOR AQUEOUS CARBONYL COMPOUNDS SAMPLED BY THE DYNAMIC SOLVENT EFFECT

Glassware rinsed with specimen solution.

Compound	*Coefficient of variation (%)*		
	Concentrator Q2	*Concentrator Q3*	*Concentrator H7*
Heptanone:heptanal	3.68	2.96	2.17
Heptanal:dimethylheptanone	5.83	2.92	2.34
Dimethylheptanone:nonanal	5.67	3.75	5.55
Nonanal:decanal	7.71	1.09	6.73
Decanal:undecanal	9.69	7.10	15.82
Undecanal:dodecanal	3.35	3.46	3.63

TABLE III

COEFFICIENTS OF VARIATION, POOLED FOR FIVE REPLICATES ON EACH OF THREE CONCENTRATORS, OF PEAK AREAS, PERCENTAGE AREAS AND PEAK-AREA RATIOS FOR DYNAMIC SOLVENT-EFFECT SAMPLING FROM AN AQUEOUS SOLUTION OF CARBONYL COMPOUNDS

Glassware rinsed with specimen solution.

Compound	*Coefficient of variation (%)*		
	Area	*% Area*	*Ratio*
n-Heptanone	8.09	17.04	
n-Heptanal	4.99	12.42	
Dimethylheptanone	12.06	4.18	
n-Nonanal	12.32	2.81	
n-Decanal	24.48	15.06	
n-Undecanal	14.83	7.33	
n-Dodecanal	38.11	31.93	
Heptanone:heptanal			5.64
Heptanal:dimethylheptanone			13.63
Dimethylheptanone:nonanal			4.70
Nonanal:decanal			14.69
Decanal:undecanal			15.45
Undecanal:dodecanal			34.50

Aqueous phenols

The phenols were eluted as sharp, symmetrical peaks (Fig. 5). All three concentrators yielded coefficients of variation of better than 10% for all three peak measurements (Tables V and VI). Analysis of the pooled data also produced coefficients of variation of less than 10% (Table VII).

Airborne hydrocarbons

Despite the complexity of the mixture of hydrocarbons (Fig. 6) and the small

TABLE IV

COEFFICIENTS OF VARIATION OF PEAK AREAS, OVER FIVE REPLICATES ON ONE CONCENTRATOR (Q2), FOR AN AQUEOUS SOLUTION OF CARBONYL COMPOUNDS SAMPLED BY THE DYNAMIC SOLVENT EFFECT

Glassware not rinsed with specimen solution.

Compound	*Coefficient of variation (%)*
n-Heptanone	6.36
n-Heptanal	11.55
Dimethylheptanone	6.70
n-Nonanal	17.93
n-Decanal	28.65
n-Undecanal	27.02
n-Dodecanal	43.25

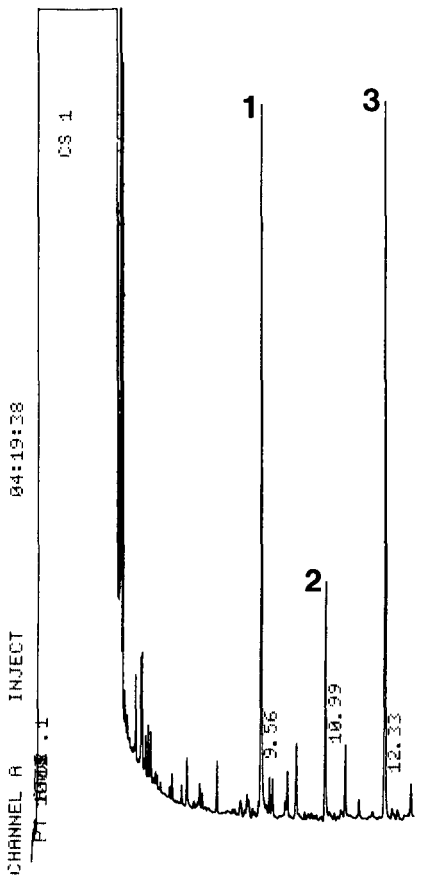

Fig. 5. Chromatogram of phenols sampled from an aqueous solution by gas sparging and the dynamic solvent effect with a flow-rate of 5 cm^3 min^{-1} for 10 min. Peaks: 1 = phenol (2.2 ng); 2 = *p*-cresol (0.8 ng); 3 = 2,4-dichlorophenol (2.5 ng).

amounts involved (0.6–2.0 ng), the coefficients of variation were below 10% in all instances (Tables VIII–X).

Wine

The wine samples yielded moderately complex chromatograms (Fig. 7). The coefficients of variation for the peaks which were above the integration threshold (0.5 ng) in all five runs are given in Table XI.

Urine

A chromatogram of the volatiles from the urine samples is shown in Fig. 8 and the coefficients of variation are given in Table XII.

Dichlorvinphos

In addition to its major pesticide component, the Vapona strip emitted a mix-

TABLE V

COEFFICIENTS OF VARIATION OF PEAK AREAS AND PERCENTAGE AREAS FOR FIVE REPLICATE SAMPLES, ON EACH OF THREE DYNAMIC SOLVENT-EFFECT CONCENTRATORS, FROM AN AQUEOUS STANDARD CONTAINING PHENOL AT $1.67{:}10^6$, *p*-CRESOL AT $0.42{:}10^6$ AND 2,4-DICHLOROPHENOL AT $0.13{:}10^6$

Compound	*Approx. mass (ng)*	*Coefficient of variation (%)*					
		Concentrator 4		*Concentrator 5*		*Concentrator 7*	
		Area	*% Area*	*Area*	*% Area*	*Area*	*% Area*
Phenol	2.2	3.5	2.3	1.3	1.3	4.3	4.6
p-Cresol	0.8	4.0	2.0	2.8	1.6	4.2	1.2
2,4-Dichlorophenol	2.5	2.8	2.2	1.7	0.9	7.6	4.7

TABLE VI

COEFFICIENTS OF VARIATION OF PEAK-AREA RATIOS FOR FIVE REPLICATE SAMPLES, ON EACH OF THREE DYNAMIC SOLVENT-EFFECT CONCENTRATORS, FROM AN AQUEOUS STANDARD CONTAINING PHENOL AT $1.67{:}10^6$, *p*-CRESOL AT $0.42{:}10^6$ AND 2,4-DICHLOROPHENOL AT $0.13{:}10^6$

Ratio	*Coefficient of variation (%)*		
	Concentrator 4	*Concentrator 5*	*Concentrator 7*
Phenol:*p*-cresol	3.0	4.8	2.6
Phenol:2,4-dichlorophenol	4.6	9.1	2.1
p-Cresol:2,4-dichlorophenol	3.6	4.8	2.1

TABLE VII

COEFFICIENTS OF VARIATION OF PEAK AREAS, PERCENTAGE AREAS AND PEAK-AREA RATIOS FROM AN AQUEOUS STANDARD CONTAINING PHENOL AT $1.67{:}10^6$, *p*-CRESOL AT $0.42{:}10^6$ AND 2,4-DICHLOROPHENOL AT $0.13{:}10^6$, FOR DATA POOLED FROM THREE SERIES OF FIVE REPLICATES ON THREE CONCENTRATORS

Compound	*Coefficient of variation (%)*		
	Area	*% Area*	*Ratio*
Phenol	7.94	4.62	
p-Cresol	7.97	2.00	
2,4-Dichlorophenol	7.50	4.32	
Phenol:*p*-cresol			5.08
Phenol:2,4-dichlorophenol			9.34
p-Cresol:2,4-dichlorophenol			5.16

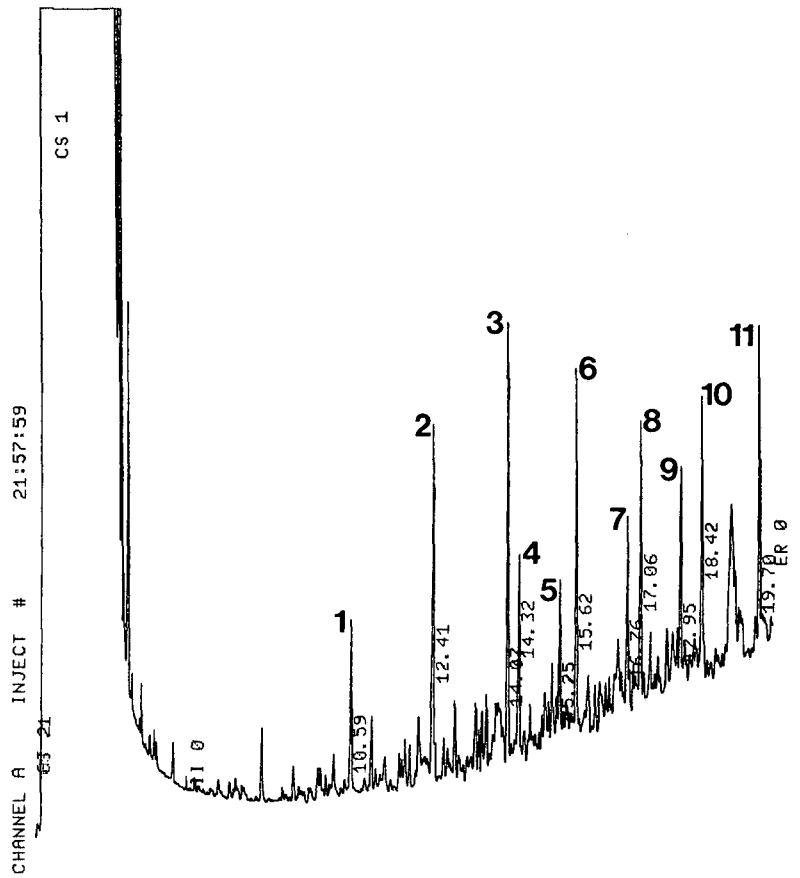

Fig. 6. Chromatogram of airborne hydrocarbons sampled by the dynamic solvent effect for 10 min with an air flow-rate of 10 cm^3 min^{-1}, using *n*-hexane as solvent at 26–27°C. Peaks: 1 = *n*-decane; 2 = *n*-undecane; 3 = *n*-dodecane; 6 = *n*-tridecane; 8 = *n*-tetradecane; 10 = *n*-pentadecane; 11 = *n*-hexadecane.

ture of hydrocarbons, presumably solvents (Fig. 9). Each sample contained *ca.* 90 ng of dichlorvinphos, giving a rate of emission from the strip of 60 ng s^{-1}. The coefficients of variation of the area and percentage area of the dichlorvinphos peak were both 1.61%. The ratio of the dichlorvinphos peak area to that of the largest hydrocarbon peak had a coefficient of variation of 2.46%.

DISCUSSION

The generation of accurately known concentrations of gas-phase volatiles in the ppb range presents considerable problems. Of the techniques available, the use of diffusion/permeation tubes appears to be the most accurate[12]. However, even at 50 ppm the calibration, by weight loss, of such a device is "tedious and time consuming"[16]. At ppb levels it would be almost impossible; an emission rate yielding 1 ng in a 100-cm^3 specimen sampled at 10 cm^3 min^{-1} would give a weight loss of 1 mg over a

TABLE VIII

COEFFICIENTS OF VARIATION OF PEAK AREAS AND PEAK PERCENTAGE AREAS OVER A SERIES OF FIVE REPLICATES ON EACH OF THREE CONCENTRATORS FOR A MIXTURE OF AIRBORNE HYDROCARBONS SAMPLED BY THE DYNAMIC SOLVENT EFFECT

Peak[a]	*Concentration (ppb, v/v)*[b]	*Coefficient of variation (%)*					
		Concentrator Q2		*Concentrator H5*		*Concentrator H7*	
		Area	*% Area*	*Area*	*% Area*	*Area*	*% Area*
1	1.3	4.69	1.79	2.46	2.12	0.63	2.77
2	2.9	4.14	2.00	2.44	1.56	1.07	2.66
3	2.6	3.48	1.74	2.40	1.74	0.95	2.23
4	1.3	3.60	1.58	1.92	1.87	0.67	2.80
5	0.7	2.70	3.26	2.07	1.70	1.34	4.08
6	1.8	4.24	1.89	1.96	1.73	1.84	1.69
7	0.9	3.17	2.19	1.58	2.59	1.63	1.89
8	1.4	4.57	2.19	2.70	1.23	9.26	7.38
9	1.8	3.23	3.06	3.13	1.78	1.39	1.85
10	1.5	3.72	1.96	3.12	1.68	1.39	3.18
11	1.4	6.30	4.07	7.21	6.33	3.10	3.32

[a] Peak numbers correspond to Fig. 6.
[b] Approximate, based on assumption of no sampling losses.

period of 19 years! Serial dilution of a more concentrated vapour provides a solution to the weighing problem, but the accuracy with which the final concentration is known will be limited by the cumulative inaccuracies of gas flow measurement and regulation at each dilution step[17]. Crisp[18] suggested that diffusion standards be cali-

TABLE IX

COEFFICIENTS OF VARIATION OF PEAK-AREA RATIOS OVER FIVE REPLICATES ON EACH OF THREE CONCENTRATORS FOR DYNAMIC SOLVENT-EFFECT SAMPLING OF A MIXTURE OF AIRBORNE HYDROCARBONS

Peak[a]	*Coefficient of variation (%)*		
	Concentrator Q2	*Concentrator H5*	*Concentrator H7*
1:2	1.26	2.82	0.51
2:3	1.42	1.94	0.70
3:4	0.62	0.66	0.69
4:5	2.13	2.60	1.40
5:6	2.38	2.47	2.67
6:7	1.13	1.40	0.47
7:8	1.66	3.13	6.91
8:9	2.44	2.65	7.91
9:10	1.24	1.14	3.18
10:11	3.23	4.58	6.54

[a] Peak numbers correspond to Fig. 6.

TABLE X

COEFFICIENTS OF VARIATION, POOLED FOR FIVE REPLICATES ON EACH OF THREE CONCENTRATORS, OF PEAK AREAS, PERCENTAGE AREAS AND PEAK-AREA RATIOS FOR DYNAMIC SOLVENT-EFFECT SAMPLING OF AIRBORNE HYDROCARBONS

Peak[a]	*Coefficient of variation (%)*		
	Area	*% Area*	*Ratio*
1	2.85	2.62	
2	2.99	3.65	
3	2.30	2.10	
4	2.25	2.43	
5	3.25	3.74	
6	2.87	1.75	
7	2.77	2.08	
8	6.25	4.49	
9	3.14	2.18	
10	4.80	2.66	
11	7.30	5.48	
1:2			2.24
2:3			2.33
3:4			0.64
4:5			3.02
5:6			3.27
6:7			1.28
7:8			4.29
8:9			4.81
9:10			2.43
10:11			4.89

[a] Peak numbers correspond to Fig. 6.

brated analytically, a procedure which is neatly circular. Lieber and Berk[19] generated ppb "gas-phase" standards by injecting a calculated volume of liquid onto adsorbent traps, but still obtained accuracies of no better than 6% above the calculated levels.

Hence it appears that measurement of the accuracy of dynamic solvent-effect sampling of airborne volatiles will have to await the development of more accurate methods of generating such specimens.

The external standard method of quantitation involves dividing the area of an experimental peak by the area of a peak obtained from an independently estimated amount of the same compound[20]. Therefore, the coefficient of variation of the calculated mass will be an additive combination of that for the peak area (Tables I, III, V, VII, VIII, X, XI and XII) and for the standard amount. Internal standardization involves comparison of the areas of two peaks on the same chromatogram[21], in this instance the coefficients of variation of peak-area ratios (Tables II, III, VI, IX, X and XI) provide a direct measure of the highest available precision. The high precision of the dynamic solvent effect means that, in practice, the precision of both standardizations will probably be limited by errors in the estimates of the standard amounts rather than by variation in sampling.

Dynamic solvent-effect sampling from solvent specimens has been shown to be

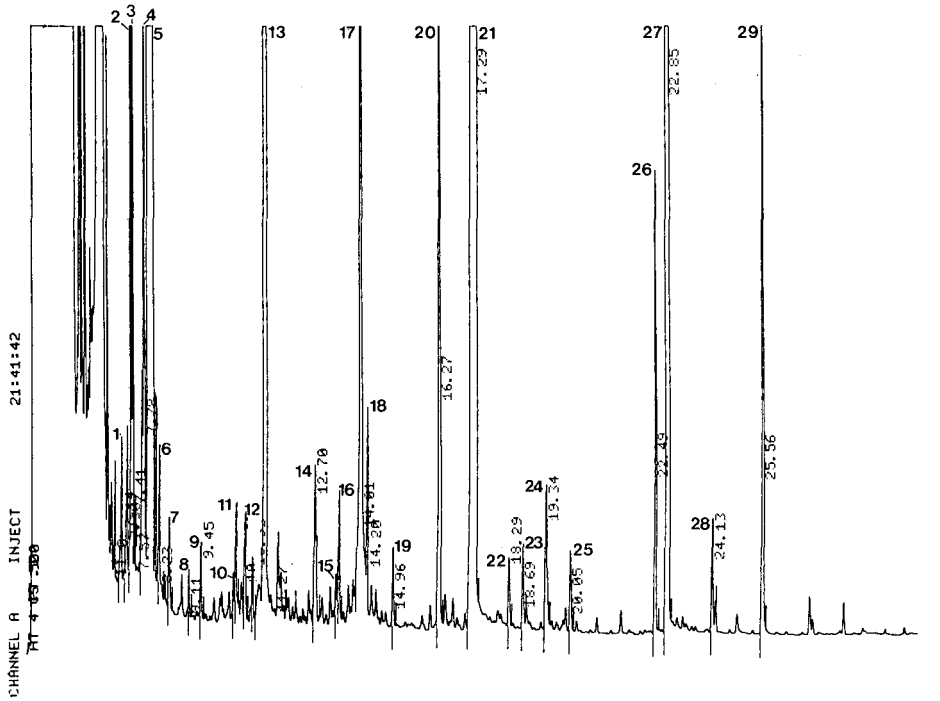

Fig. 7. Chromatogram of volatiles from 10 cm^3 of red wine sampled by the dynamic solvent effect for 10 min with a gas flow-rate of 10 cm^3 min^{-1} using *n*-hexane as solvent at 29.6°C. Peak numbers correspond to Table XI.

extremely precise for sub-nanogram amounts of a wide range of solutes[22]. Transfer of the sample from the concentrator to the column is identical for samples from solvents and from gas-borne specimens. It can be expected, therefore, that the contribution of this step to the quantitative variation will be the same for both types of specimen. From this it follows that differences in precision between the two types of specimen are due to either or both of the entrainment of volatiles from the specimen by the sampling gas and their subsequent focusing on the dynamic solvent film. The focusing mechanism is independent of the source of the volatiles (although the route by which they reach the evaporating edge of the film is different in the two cases)[7,23], so that variations in entrainment are the most likely source of variation in quantitative results.

The entrainment step is probably also why the relative sizes of the peaks in chromatograms from the solutions of carbonyl compounds and phenols (Figs. 4 and 5) do not closely reflect the relative calculated concentrations of the components of each mixture. This is most likely to be due to differences in partition coefficients between water and the hydrogen purge gas, and to differential adsorption on glass surfaces, but small differences in the purities of the standard materials may also have contributed.

The importance of precise temperature control during the sampling of gas-borne volatiles has been stressed by Jennings and Rapp[24] and by Ioffe and Viten-

TABLE XI

COEFFICIENTS OF VARIATION OF PEAK AREAS AND PERCENTAGE AREAS FOR FIVE REPLICATE SAMPLES OF WINE VOLATILES SAMPLED BY THE DYNAMIC SOLVENT EFFECT

Peak[a]	*Approx. mass (ng)*	*Coefficient of variation (%)*		
		Area	*% Area*	*Ratio*
1	1.7	30.8	31.5	8: 9 5.9
2	2.4	21.9	21.5	11:12 4.7
3	22.0	3.0	2.9	13:27 2.3
4	8.4	36.5	37.3	19:22 3.0
5	52.0	2.7	1.0	21:27 1.1
6	1.4	34.4	35.4	23:25 1.8
7	1.4	51.2	51.1	24:28 4.7
8	0.5	5.3	3.8	26:29 9.5
9	1.0	7.9	7.7	
10	0.4	6.4	7.1	
11	1.5	9.8	8.4	
12	1.6	6.4	5.0	
13	228.0	2.7	1.1	
14	3.2	5.4	6.1	
15	0.6	18.8	19.7	
16	2.0	8.1	7.6	
17	24.5	12.9	13.4	
18	3.6	22.8	23.3	
19	1.2	3.4	2.6	
20	14.7	7.4	5.9	
21	630.0	1.4	0.4	
22	1.1	5.8	4.6	
23	1.1	1.6	1.4	
24	2.9	7.1	6.4	
25	2.3	2.2	1.4	
26	7.7	3.0	2.8	
27	112.1	0.6	1.4	
28	1.5	3.6	2.3	
29	11.2	6.8	6.2	

[a] Peak numbers correspond to Fig. 7.

berg[25], who recommend thermostating to ± 0.1°C. Slight variations in temperature may well account for some of the variability reported here. Etievant *et al.*[26] found that temperature fluctuations degraded the precision of sampling from wine.

The role of peak resolution in determining precision[27] is illustrated by the series of samples from wine (Fig. 7, Table XI). The coefficients of variation of peak areas vary from 0.63 to 51.2%. Every peak which was reported by the integrator as baseline resolved on every run had a coefficient of variation of its area of less than 8%. All peaks with coefficients of variation of their areas of more than 12% were reported as incompletely resolved in some runs. In any complex sample there are likely to be some instances of incompletely resolved peaks; if these represent significant components the chromatographic conditions may need to be adjusted to obtain precise quantitation.

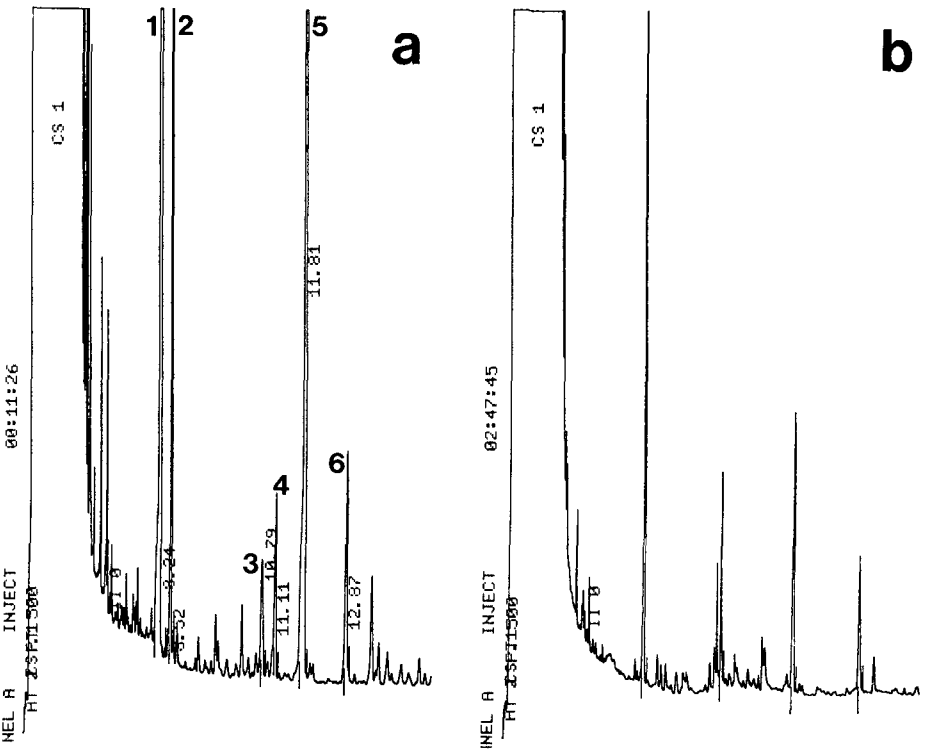

Fig. 8. Chromatograms of volatiles sampled from 10 cm^3 of human urine by the dynamic solvent effect for 10 min with a gas flow-rate of 10 cm^3 min^{-1} using *n*-hexane as solvent at 29.6°C. (a) Previous meal spiced lamb with wine; (b) previous meal sausage, egg and beans. Peak numbers correspond to Table XII.

TABLE XII

COEFFICIENTS OF VARIATION OF PEAK AREAS AND PERCENTAGE AREAS FOR FIVE REPLICATE SAMPLES OF HUMAN URINE VOLATILES SAMPLED BY THE DYNAMIC SOLVENT EFFECT

Peak[a]	*Approx. mass (ng)*	*Coefficient of variation (%)*	
		Area	*% Area*
1	92.0	3.6	1.69
2[b]	5.5	29.6	30.63
3	1.0	17.2	15.71
4	1.2	7.2	6.36
5	11.7	0.6	2.19
6	1.7	6.9	5.46

[a] Peak numbers correspond to Fig. 8.
[b] See Fig. 10.

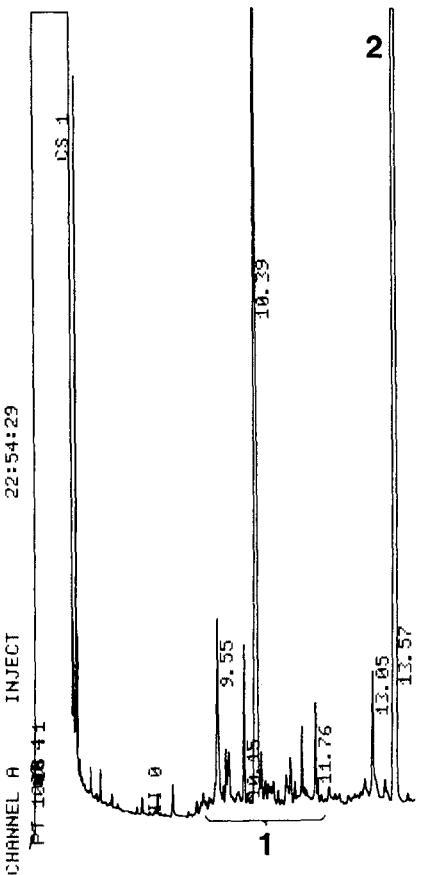

Fig. 9. Chromatogram of volatiles emitted by a Vapona Cupboard Exterminator pesticide strip, sampled by the dynamic solvent effect for 5 min with a sampling flow-rate of 5 cm^3 min^{-1} from a flow of 1 l min^{-1} over the strip. The group of peaks at 1 are hydrocarbons; peak 2 is dichlorvinphos.

The sharp, symmetrical peaks in Figs. 4–9 demonstrate that dynamic solvent-effect concentrators deactivated with silicon and ethene[28] are effectively free of adsorptive activity[22]. This contributes to high-precision analyses by preserving the resolving power of the column (above) and by simplifying the sampling procedure; for example, the test-mixture phenols were eluted as sharp, symmetrical peaks (Fig. 5) without the need for the derivatization that forms part of alternative methods[29, 30].

An additional source of variation may be the foaming which some liquids undergo during gas purging. The urine specimens in particular produced very stable foams. About 40 cm^3 of foam were produced when 100 cm^3 of gas were used for sampling, so almost half the volatiles purged from the liquid remained trapped in bubbles from which they were released only erratically when, and if, the bubbles burst. It should be mentioned that at the sensitivity levels considered here the use of silicone anti-foam agents gives rise to unacceptable levels of contamination. Differen-

ces in bubble size during purging have been identitified as a source of variability in sampling from wine[26].

Highly reproducible results cannot (indeed should not) be obtained if the specimens themselves change from sample to sample. Such variability is difficult to recognize unless its contribution to the overall variation shows some bias away from the random noise to be expected from analytical errors. A consistent trend is one such recognizable bias. Among the cases considered here, trends occurred in the area of peak 2 of the urine samples and in the emission rate of all the volatiles from the Vapona strip (Fig. 10). These trends can be confidently ascribed to changes in the specimens rather than, for example, a progressive conditioning of the apparatus, because they occurred only with these two materials whereas conditioning would have been expected to affect at least some of the others. The trend in the areas of the peaks from the Vapona strip was accompanied by a rise in the temperature of sampling. With the urine specimens the occurrence of the trend inflated the estimate of the coefficient of variation for peak 2.

The role of adsorption onto sampling glassware in degrading quantitative performance is clear from the improvement in precision achieved by simply rinsing the glassware used for the carbonyl standard (Tables I and IV). Adsorption is also indicated by the tendency of the precision to be better for lower molecular weight carbonyl compounds and for compounds present in higher concentrations. The extent to which the variability seen when the glassware had been rinsed was due to residual adsorptive activity is uncertain. When variable adsorption was eliminated, as with the hydrocarbon and phenol standards, the precision was higher, even though phenols are less tractable, and the hydrocarbon standard was more complex, than the carbonyls. The

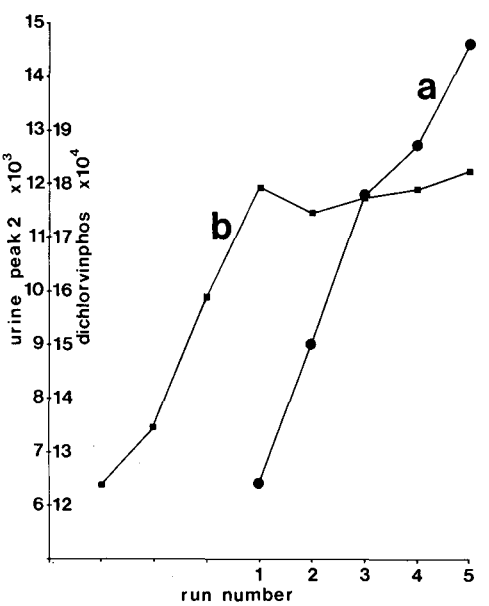

Fig. 10. Trends in peak area with sample number (and time) for (a) peak 2 from the urine sample (Fig. 8), (b) the dichlorvinphos peak in Fig. 9. Precision was calculated from the numbered samples.

TABLE XIII

QUANTITATIVE PERFORMANCE OF A VARIETY OF SAMPLING METHODS FOR GAS CHROMATOGRAPHIC ANALYSIS OF GAS-BORNE VOLATILES

Techniques are abbreviated as follows: ads = adsorption; ct = cold-trapping; d = derivatization; di = distillation; e = extraction; ECD = electron-capture detection; FID = flame ionization detection; hs = headspace; HPLC = high-performance liquid chromatography; MS = mass spectral detection; Nafion = water subtraction by porous polymer; NPD = nitrogen–phosphorus detection; oc = on-column injection; p = purging; ptv = programmed-temperature vaporizer; SIM = specific-ion monitoring; sl = splitless injection; sp = splitting; TEA = thermal energy analyser detection; TIM = total ion monitoring; vi = valve inlet.

No.	*Matrix*	*Solute*	*Technique*	*Concentration*	*Coefficient of variation (%)*	*Ref.*
1	Air	C_{14}–C_{16} acetate	hs ads e sl FID	4.8 ± 3.5 ng/600 cm^3	10–19	34
2	Air	Solvents	vi FID	7–529 ppm, 28 μl	2.2–11.3	35
3	Air	Hydrocarbons	ct FID	32–6680 ppt, 300 cm^3	1.5–8.4	36
4	Air	Pesticides	ads NPD/ECD	0.5 ng/5 l	3.4–12.4	37
		Amphetamine	ads/d SIM	50 ng	13.3	37
5	Air	Halocarbons	ads[a] e sp ECD	0.5–0.05 ng	0.4–3.9	19
6	Aqueous	Wine flavour	p ct sp FID	400 ppm	2–12	26
			p e sp FID	400 ppm	4–14	26
			hs sp FID	400 ppm	1–35	26
7	Water	Hydrocarbons	hs ct sl FID	0.1–15 μg/50 cm^3	8.6–27	38
8	Water	Alcohols/ carbonyls	e ads ct FID	0.13 ng/100 μl	4.5–9.8	39
9	Water	Pollutants	p ads[a] FID	640 ng/40 cm^3	1.4–18	40
10	Water	Aromatics	p Nafion ct FID	27–100 ng/5 cm^3	0.4–2.6	41
			p Nafion ct FID	260–500 ng/5 cm^3	2–2.6	41
11	Water	Chlorophenols	d e sl ECD	1–100 ng/100 cm^3	1–8.9	30
			d e sl ECD	0.1–0.5 ng/100 cm^3	10–20	30
12	Water	Halocarbons	hs sp ECD	0.5–3.0 μg/l	5.5–7.1	42
13	Water	Wide range	ads e FID	100 μg/l	2–22	43
14	Water	Phenols	di/e sp FID	20 ppb	2.4–12	44
15	Water	Pesticides	HPLC vi ECD	0.1 ng/1 cm^3	1.9–32	45
			HPLC vi ECD	2.5 ng/1 cm^3	1.1–48	45
16	Water	Range	p Nafion ct FID	100 ng/8 cm^3	1.3–26	46
17	Water	Non-polar	p ads[a] ct FID	100 ng/l	3–250	15
18	Water	Pyridines	di e SIM	1 μg/500 cm^3	2–3.9	47
19	Water	Halomethanes	p ads[a] FID	100–120 ng/20 cm^3	4–23	48
20	Water	Hydrocarbons	p ads[a] FID	0.15–15 μg/15 cm^3	6.4–14.3	49
21	Urine/ plasma	Drugs	e d spl SIM	2–500 ng/1 cm^3	2–5	50
22	Water	Pollutants	p ads SIM	200 ng/5 cm^3	0.8–31	51
23	Water	Flavour test	p ads[a] ct FID	100 ng	1.7–6.8	31
24	Solid	Aromatics	p ads[a] ct FID	800–935 ng	0.8–2.8	52
25	Sediment	PCBs	e oc/sl ECD	250–375 μg/l	1.8–9	53
26	Meat	Nitrosamines	di/e TEA	5–20 ppb	3.3–25	54

[a] The adsorbent used was Tenax.

adsorptive activity of containers can be neutralized by rinsing until the surface is in equilibrium with the specimen solution but then, during sampling, adsorbed material will bleed back into the specimen when its concentration falls as volatiles are purged from it.

When the coefficients of variation from pooled data and from individual concentrators are compared (Tables I and II *vs.* Table III, Tables V and VI *vs.* Table VII and Tables VIII and IX *vs.* Table X), it can be seen that using a single concentrator for replicate samples provides higher precision than if three are used. If the highest precision is required, the serial use of one concentrator is the method of choice; failing this it may be possible to select matched sets of concentrators.

Sampling was carried out at room temperature (26–27°C) or just above (29.6–30.6°C). This is in contrast to the elevated temperatures in some other sampling techniques. For example, Werkhoff and Bretschneider[31] heated their standard to 80°C, Belkin and Eposito[32] to 70°C and Kolb *et al.*[33] to 150°C. Elevated temperatures distort the volatile profile in ways which may be unacceptable in investigations of semiochemicals or flavours and may hasten the degradation of the specimen.

The literature was surveyed for reports on the precision of various methods of sampling from specimens similar to those investigated here. Table XIII is a compilation of those reports which included sufficient information on the composition, concentration and size of their test specimens for a meaningful comparison with the results for the dynamic solvent effect.

During the compilation of Table XIII, it became apparent that quantitative precision is not an aspect of analytical performance that has received general attention[55]. Indeed, it was the exception, rather than the rule, that data on quantitative performance accompanied, or even followed, descriptions of sampling techniques. For example, the series of papers by Grob and co-workers[56–59] on their closed-loop stripping apparatus contains no figures for precision. Neither Reece and Scott[27] nor Jennings and Rapp[11] provided any figures for the precision of the sampling and separation systems which they discussed. Even where precision was reported, its interpretation was confounded by a lack of information on the composition of the test specimens. The works by Schomburg *et al.*[60], Haynes and Steimie[61], Grob[62] and Yang *et al.*[63] are examples of (otherwise detailed) reports of high-precision results from which the quantitative compositions of the test specimens were omitted, and which, as a consequence, have had to be omitted from the present discussion.

Of the five studies of airborne volatiles in Table XIII, four were as precise as dynamic solvent-effect sampling. Two of these four used specific detectors. Schmidbauer and Oehme[36] (3) cold-trapped light hydrocarbons, to which their method's range of application is limited by the use of a potassium carbonate drying tube which would remove fatty acids and phenols as well as water. Radell and Rea[35] (2) sampled difficult solvent vapours in a process-monitoring application, but their method is restricted to small sample volumes, and therefore high concentrations, by the use of a valve inlet with no focusing step.

The figures obtained here for the precision of the dynamic solvent effect are similar to those from the eighteen investigations of sampling from aqueous specimens in Table XIII. Eleven of these studies (Nos. 6, 7, 9, 10, 12, 16, 17, 19, 20, 22 and 23) can be directly compared with the performance of the dynamic solvent effect in that they employed a purging or headspace step, which would be necessary if the techniques were to be used for quantitative semiochemistry or work on flavours. Two of these eleven (10 and 16) included cold trapping, and a drying step which removed medium-polarity solutes and hydrocarbons above *n*-decane[46]. A further five used only hydrocarbon and halocarbon test compounds, which throw little light on the performance to be expected with less tractable substances.

Etievant *et al.*[26] (6) tested five different sampling techniques, four of which involved gas-phase volatiles, with synthetic wine flavour specimens. Unfortunately, the concentration of their specimens ($400:10^6$) was 2–3 orders of magnitude higher than that of the phenol standard, and four orders higher than that of the aqueous solution of carbonyls used in this study, making meaningful comparisons difficult.

Gas purging and trapping on Tenax were used for sampling an aqueous mixture of pollutants, including some ketones and an alcohol, by Otson and Williams[40] (9). Although their test mixture covered a wide range of volatilities and included some difficult compounds, each component was present in amounts too large to provide a realistically challenging test for a technique as sensitive as capillary gas chromatography.

From 5-cm^3 specimens, Lopez-Avila *et al.*[51] (22) purged and trapped 250 ng of pollutant test compounds, including some ketones. The precision of their method was good, although variable, but its dependence on single-ion mass spectrometric monitoring is likely to restrict its applicability.

Werkhoff and Bretschneider[31] (23) investigated a purge–adsorb–thermally desorb–cold trap system for flavour compounds in water. Their adsorbent was Tenax and cold trapping was at an elevated flow-rate to overcome the incompatability between analytical and desorption flow-rates. The high precisions reported, and the quality of the chromatograms presented, suggest that a similar system might be useful for some types of semiochemical and clinical analysis, provided that the precision could be maintained if the specimen size and solute abundance were to be reduced by two orders of magnitude.

Of the three studies on sampling from solids, only that by Venema[52] (24) involved a non-specific detector, and the amounts and types of solutes do not suggest that the method would be particularly versatile.

Surprisingly few workers have tested their methods with standards that take advantage of the sensitivity of capillary column analyses. For example, Liebich and Al-Babbili[64] employed 150 ng per component in a urine test mixture and Schomburg *et al.*[60] injected micrograms of some of their test compounds. Bertsch *et al.*[29] used 500 ng of pure compounds or 2.8 μg of gasoline per sample. In only eight of the 26 studies in Table XIII (Nos. 1, 3, 4, 5, 8, 11, 15 and 26) were the amounts of solute as small as, or smaller than, those used to test the dynamic solvent effect. In four of these cases (4, 5, 11 and 15) an electron-capture detector, which is both selective and two to three orders of magnitude more sensitive than a flame ionization detector, was used.

The work by Du *et al.*[34] (1) on acetate moth pheromones closely approaches the performance of the dynamic solvent effect in terms of high precision with small amounts of test compounds. If their method of adsorption on glass-wool is adaptable to a wider range of compounds, it will probably prove to be more than adequately precise for most work.

Lee *et al.*[39] (8) are the only group in Table XIII to report coefficients of variation from a sampling system designed, like the dynamic solvent effect, to handle small amounts of biological materials. Their transevaporator operates in two stages. First the lighter volatiles are purged from the specimen and collected on Tenax, then the less volatile and more polar solutes are collected on glass beads by an extraction–readsorption process. It is a pity that precision was not reported for the Tenax mode, as this would be the more useful for work on semiochemicals and flavours. The

adsorption mode yielded excellent results with very small amounts of intractable solutes. Even to elute 0.13 ng of butanol as a recognizable peak requires, apart from anything else, an uncommonly well deactivated column. In view of the use of very active silica adsorbents and a dynamically coated stainless-steel capillary column, this performance must be regarded as extremely good.

No single study in Table XIII covers such a diversity of specimen types as the present one on the dynamic solvent effect. Only adsorption–desorption appears to match the dynamic solvent effect in terms of demonstrated versatility.

The high precision of dynamic solvent-effect sampling has already found application in semiochemical analyses[65–68] and, as an example, changes in human urine volatiles due to a change in diet are readily detectable (Fig. 8).

CONCLUSION

Provided that other potential sources of variation are adequately controlled, dynamic solvent-effect sampling allows low- and sub-nanogram amounts of a wide range of solutes to be determined with coefficients of variation of less than 10%. In terms of precision, the dynamic solvent effect is at least as good as other sampling techniques and in terms of the amounts with which the precision is achieved it is substantially better than most.

ACKNOWLEDGEMENTS

This work was funded by grants to professor V. Pretorius, Director of the Institute for Chromatography. The author also thanks Egmont Rohwer, Willie Viljoen and Tony Hasset, and Amanda de Klerk and David Masemula who made the column.

REFERENCES

1 F. Pavelka, *Mikrochim. Acta*, 6 (1964) 1121.
2 K. Grob, *Chromatographia*, 8 (1975) 423.
3 W. G. Jennings, *J. High. Resolut. Chromatogr. Chromatogr. Commun.*, 2 (1979) 221.
4 J. Roerade and S. Blomberg, *Chromatographia*, 17 (1983) 387.
5 V. Pretorius and W. Bertsch, *J. High Resolut. Chromatogr. Commun.*, 6 (1983) 567.
6 V. Pretorius and K. Lawson, *S. Afr. J. Chem.*, 40 (1987) 169.
7 P. J. Apps and V. Pretorius, *J. Chromatogr.*, 471 (1989) 81.
8 P. J. Apps, V. Pretorius, K. H. Lawson, E. R. Rohwer, M. R. Centner, H. W. Viljoen and G. Hulse, *J. High Resolut. Chromatogr. Chromatogr. Commun.*, 10 (1987) 122.
9 P. J. Apps, *Ph.D. Thesis*, University of Pretoria, Pretoria, 1988, pp. 98–108.
10 P. J. Apps, *Ph.D. Thesis*, University of Pretoria, Pretoria, 1988, p. 18.
11 W. G. Jennings and A. Rapp, *Sample Preparation for Gas Chromatographic Analysis*, Hüthig, Heidelberg, 1983.
12 R. S. Barret, *Analyst (London)*, 106 (1981) 817.
13 B. V. Ioffe and A. G. Vitenberg, *Head Space Analysis and Related Methods in Gas Chromatography*, Wiley, New York, 1983, p. 234.
14 C. K. Huynh and T. Vu Duc, *J. High Resolut. Chromatogr. Chromatogr. Commun.*, 8 (1985) 198.
15 W. E. Hammers and H. F. P. M. Bosman, *J. Chromatogr.*, 360 (1986) 425.
16 J. Namiesnik, L. Torres, E. Kozlowski and J. Mathieu, *J. Chromatogr.*, 208 (1981) 239.
17 G. Bertoni, F. Bruner, A. Liberti and C. Perrino, *J. Chromatogr.*, 203 (1981) 263.
18 S. Crisp, in E. Reid (Editor), *Trace Organic Sample Handling*, Ellis Horwood, Chichester, 1980, pp. 39–42.

19 M. A. Leiber and H. C. Berk, *Anal. Chem.*, 56 (1984) 2134.
20 M. L. Lee, F. J. Yang and K. D. Bartle, *Open Tubular Column Gas Chromatography: Theory and Practice*, Wiley, New York, 1984, p. 224.
21 M. L. Lee, F. J. Yang and K. D. Bartle, *Open Tubular Column Gas Chromatography: Theory and Practice*, Wiley, New York, 1984, pp. 222–223.
22 P. J. Apps, *J. Chromatogr.*, submitted for publication.
23 P. J. Apps, *Ph.D. Thesis*, University of Pretoria, Pretoria, 1988, p. 147.
24 W. G. Jennings and A. Rapp, *Sample Preparation for Gas Chromatographic Analysis*, Hüthig, Heidelberg, 1983, pp. 19–21.
25 B. V. Ioffe and A. G. Vitenberg, *Head Space Analysis and Related Methods in Gas Chromatography*, Wiley, New York, 1983, p. 15.
26 P. Etievant, H. Maarse and F. Van den Berg, *Chromatographia*, 21 (1986) 379.
27 C. E. Reece and R. P. W. Scott, in E. Katz (Editor), *Quantitative Analysis Using Chromatographic Techniques*, Wiley, Chichester, 1987, pp. 157–191.
28 P. J. Apps, *Ph.D. Thesis*, University of Pretoria, Pretoria, 1988, pp. 75–76.
29 W. Bertsch, E. Anderson and G. Holzer, *J. Chromatogr.*, 112 (1975) 701.
30 K. Abrahamson and T. M. Xie, *J. Chromatogr.*, 279 (1983) 199.
31 P. Werkhoff and W. Bretschneider, *J. Chromatogr.*, 405 (1987) 99.
32 F. Belkin and G. G. Eposito, *J. Chromatogr. Sci.*, 24 (1986) 216.
33 B. Kolb, B. Liebhardt and L. S. Ettre, *Chromatographia*, 21 (1986) 305.
34 J.-W. Du, C. Löfstedt and J. Löfqvist, *J. Chem. Ecol.*, 13 (1983) 1431.
35 E. A. Radell and D. F. Rea, *J. High Resolut. Chromatogr. Chromatogr. Commun.*, 6 (1983) 189.
36 N. Schmidbauer and M. Oehme, *J. High Resolut. Chromatogr. Chromatogr. Commun.*, 9 (1986) 502.
37 A. H. Lawrence, *J. Chromatogr.*, 395 (1987) 531.
38 J. Drozd, J. Novak and J. A. Rijks, *J. Chromatogr.*, 158 (1978) 471.
39 K. Y. Lee, D. Nurok and A. Zlatkis, *J. Chromatogr.*, 158 (1978) 377.
40 R. Otson and D. Y. Williams, *Anal. Chem.*, 54 (1982) 942.
41 J. W. Cochran, *J. High Resolut. Chromatogr. Chromatogr. Commun.*, 6 (1983) 573.
42 B. Kolb, M. Auer and P. Pospisil, *J. Chromatogr.*, 279 (1983) 341.
43 M. Giabbai, L. Roland, M. Ghosal, J. H. Reuter and E. S. K. Chian, *J. Chromatogr.*, 279 (1983) 373.
44 J. Rijks, J. Carvers, T. Noy and C. Cramers, *J. Chromatogr.*, 279 (1983) 395.
45 E. Noroozian, F. A. Maris, M. W. F. Nielen, R. W. Frei, G. J. De Jong and U. A. T. Brinkman, *J. High Resolut. Chromatogr. Chromatogr. Commun.*, 10 (1987) 17.
46 T. Noij, A. van Es, C. Cramers, J. Rijks and R. Dooper, *J. High Resolut. Chromatogr. Chromatogr. Commun.*, 10 (1987) 60.
47 T. Tsukioka and T. Murakami, *J. Chromatogr.*, 396 (1987) 319.
48 A. Cailleux, A. Turcant, P. Allain, D. Toussaint, J. Gaste and A. Roux, *J. Chromatogr.*, 391 (1987) 280
49 F. Belkin and G. G. Eposito, *J. Chromatogr. Sci.*, 24 (1986) 216.
50 T. Marunaka, Y. Umeno, Y. Minami, E. Matsushima, M. Maniwa, K. Yoshida and M. Nagamachi, *J. Chromatogr.*, 420 (1987) 43.
51 V. Lopez-Avila, R. Wood, M. Flanagan and R. Scott, *J. Chromatogr. Sci.*, 25 (1987) 286.
52 A. Venema, *J. High Resolut. Chromatogr. Chromatogr. Commun.*, 9 (1986) 637.
53 F. I. Onuska, K. J. Kominar and K. A. Terry, *J. Chromatogr.*, 279 (1983) 111.
54 M. Gavinelli, L. Airoldi and R. Fanelli, *J. High Resolut. Chromatogr. Chromatogr. Commun.*, 9 (1986) 257.
55 P. Werkhoff and W. Bretschneider, *J. Chromatogr.*, 405 (1987) 87.
56 K. Grob, *J. Chromatogr.*, 84 (1973) 255.
57 K. Grob and G. Grob, *J. Chromatogr.*, 90 (1974) 303.
58 K. Grob, K. Grob and G. Grob, *J. Chromatogr.*, 106 (1975) 299.
59 K. Grob and F. Zürcher, *J. Chromatogr.*, 117 (1976) 285.
60 G. Schomburg, H. Husmann and R. Rittmann, *J. Chromatogr.*, 204 (1981) 85.
61 L. V. Haynes and A. R. Steimie, *J. High Resolut. Chromatogr. Chromatogr. Commun.*, 10 (1987) 441.
62 K. Grob, *Classical Split and Splitless Injection in Capillary Gas Chromatography*, Hüthig, Heidelberg, 1985, pp. 206 and 249.
63 F. J. Yang, A. C. Brown and S. P. Cram, *J. Chromatogr.*, 158 (1978) 91.
64 H. M. Liebich and O. Al-Babbili, *J. Chromatogr.*, 112 (1975) 539.
65 P. J. Apps, H. W. Viljoen and V. Pretorius, *Onderstepoort J. Vet. Res.*, 55 (1988) 135.
66 P. J. Apps, A. Rasa and H. W. Viljoen, *Aggress. Behav.*, 14 (1988) 451.
67 D. Jacobs, P. J. Apps and H. W. Viljoen, *Comp. Biochem. Physiol. B*, 93 (1989) 459.
68 P. J. Apps, *Ph.D. Thesis*, University of Pretoria, Pretoria, 1988, pp. 186–297.

Journal of Chromatography, 504 (1990) 45–53
Elsevier Science Publishers B.V., Amsterdam — Printed in The Netherlands

CHROM. 22 211

Regression against temperature of gas chromatographic retention data

REYNALDO CÉSAR CASTELLS*
CIDEPINT, 52 e/121 y 122, 1900 La Plata, and División Química Analítica, Facultad de Ciencias Exactas, Universidad Nacional de La Plata, 1900 La Plata (Argentina)
ELEUTERIO LUIS ARANCIBIA
Instituto de Ingeniería Química, Facultad de Ciencias Exactas y Tecnología, Universidad Nacional de Tucumán, 4000 Tucumán (Argentina)
and
ANGEL MIGUEL NARDILLO
CIDEPINT, 52 e/121 y 122, 1900 La Plata, and División Química Analítica, Facultad de Ciencias Exactas, Universidad Nacional de la Plata, 1900 La Plata (Argentina)
(First received August 23rd, 1989; revised manuscript received December 8th, 1989)

SUMMARY

Specific retention volumes were measured in the range 25–75°C for benzene + squalane, benzene + triethylene glycol and *n*-hexane + squalane and in the range 15–55°C for benzene + tetraethylene glycol dimethyl ether, each in steps of 5°C. Values for the solution thermodynamic properties and their errors were obtained by fitting the experimental data to equations with two or more constant by using the method of Clarke and Glew. The best thermodynamic results were obtained by means of the three-constant equation; adding a fourth constant did not improve the adjustment. However, when the objective is interpolation, the results obtained with the classical, two-constant equation, are of adequate accuracy.

INTRODUCTION

Gas chromatography (GC) has been widely used to measure the free energy change associated with the solution process. There is a high degree of agreement between activity coefficients measured by GC and those derived by extrapolating values obtained by means of static techniques at finite concentrations[1–3]. Values thus obtained can be correlated with the molecular or macroscopic properties of the solutes and of the stationary phases; the predictions of theoretical models have in many instances been successfully tested against chromatographic results[4,5].

The dependence on temperature of the specific retention volume, V_g, can in principle be employed to determine first-order (enthalpy) and second-order (heat capacity) partial molar quantities. However, with the exception of a small number of

0021-9673/90/$03.50

workers, a linear relationship between ln V_g and $1/T$ has been assumed, this implying a zero partial molar heat capacity. The exceptions are the papers by Meyer and Baiochi[6–8], Hammers and de Ligny[9] and Roth and Novák[10]; the systems they studied were composed of hydrocarbon solutes and stationary phases that were either another hydrocarbon or a poly(dimethylsiloxane). The reproducibility of the results was tested in only one instance[7] where, unfortunately, an equation without a sound theoretical basis was employed.

In this work, the specific retention volumes of benzene were measured using three stationary phases with major chemical differences: squalane (SQ), triethylene glycol (TEG) and tetraethylene glycol dimethyl ether (TEGDME); data for the system *n*-hexane + SQ are also reported. Duplicate runs were performed over relatively broad temperature ranges; measurements were carefully made, using conventional equipment. Data were processed by the method of Clarke and Glew[11], which furnishes values both for the standard thermodynamic functions and for their standard deviations.

The system benzene + TEG was chosen on the assumption that, TEG being a self-associating liquid, the dissolution of a non-polar solute could be decreasingly exothermic as the temperature increases[12]. Whereas it can be demonstrated that retention in chromatographic columns packed with TEG on Chromosorb W is due exclusively to gas–liquid partitioning[13], important contributions from adsorption at the gas–liquid interface can be expected when more strongly associated liquids (such as formamide, glycerol or ethylene glycol) are used as stationary phases. Small temperature effects on the heats of solution were expected for the systems benzene + SQ and *n*-hexane + SQ, and an intermediate behaviour for the solutions of benzene in TEGDME. The system *n*-hexane + TEG could not be studied because of significant adsorption effects[13].

The number of calorimetric studies on excess heats of solution and heat capacities has grown in recent years as a consequence of the introduction of very precise instruments[14–16], and it is improbable that chromatographic data could compete in quality against them. A comparison between both sets of data is difficult because calorimetric measurements are regularly performed at finite concentrations and on mixtures with limited chromatographic interest; the two types of information can thus be complementary.

THEORY

It can be proved[17] that the change in the partial molar free energy of a solute on its transfer from the pure ideal vapour phase at $p = 1$ atm to a hypothetical solution at unit molar fraction and obeying Henry's law is related to the specific retention volume, V_g, by the equation

$$\Delta\bar{G}_1^0 = -RT\ln(V_g M_2/273.15R) + (2B_{13} - v_1)p_o J_3^4/41.303 \qquad (1)$$

where M_2 is the molecular weight of the stationary phase, B_{13} is the second virial coefficient for the interactions between the solute and the carrier gas, v_1 is the solute molar volume and J_3^4 is a function of the outlet (p_o) and inlet (p_i) pressures. Using the definition of Gibbs free energy, eqn. 1 becomes

$$\ln V_g = -(\Delta\bar{H}_1^0/RT) + (\Delta\bar{S}_1^0/R) - \ln(M_2/273.15R) + (2B_{13} - v_1)p_o J_3^4/41.303RT \quad (2)$$

If it is assumed that $\Delta\bar{H}_1^0$ and $\Delta\bar{S}_1^0$ are independent of temperature and that effects of non-ideality of the vapour phase are negligible, eqn. 2 can be simplified to

$$\ln V_g = A + (B/T) \quad (3)$$

where $B = -\Delta\bar{H}_1^0/R$ and $A = (\Delta\bar{S}_1^0/R) - \ln(M_2/273.15R)$. In the usual GC practice, experimental V_g values are fitted to eqn. 3 by the least-squares method, thus obtaining the best estimates for $\Delta\bar{H}_1^0$ and $\Delta\bar{S}_1^0$ and their standard errors. This approach is justified over short temperature ranges or with retention volumes of limited accuracy.

When accurate V_g values are obtained over a broad temperature range, non-linearity in the plots of $\ln V_g$ against $1/T$ can sometimes be detected. This effect, which cannot be ascribed to experimental error, can in principle be attributed to changes in $\Delta\bar{H}_1^0$ and $\Delta\bar{S}_1^0$ with temperature. According to eqn. 1, the problem of improving the regression of chromatographic retention data against temperature pertains to the more general problem of obtaining ΔH, ΔS and ΔC_p values by fitting ΔG data (obtained through measurements of equilibrium constants, solubilities, vapour pressures, etc.) to some reasonable function of T. With this objective, and although there are some other options available[18], the method of Clarke and Glew[11], or some variant of it, is still one of the preferred choices.

Clarke and Glew begin with the very plausible assumption that the standard enthalpy change in a given process, ΔH_T^0, can be expressed as a perturbation on the value ΔH_θ^0 at some reference temperature θ by means of Taylor's series expansion. Then, using formal thermodynamic equations, they deduced the following expression for the standard free energy change:

$$-\Delta G_T^0/T = -\Delta G_\theta^0/\theta + \Delta H_\theta^0[(1/\theta) - (1/T)] + \Delta C_{p_\theta}^0[(\theta/T) + \ln(T/\theta) - 1] + \\ + (\theta/2)(\partial\Delta C_p^0/\partial T)_\theta[(T/\theta) - (\theta/T) - 2\ln(T/\theta)] + \ldots \quad (4)$$

By introducing the temperature variable $x = (T - \theta)/\theta$, eqn. 4 can be written as

$$-\Delta G_T^0/T = -\Delta G_\theta^0/\theta + \sum_{j=0}^{q} \frac{\theta^{j-1}}{j!}\left(\frac{\partial^j \Delta H^0}{\partial T^j}\right)_\theta \left[x^{j+1}\sum_{n=0}^{\infty}(n/n+j)(-x)^{n-1}\right] \quad (5)$$

In order to fit this equation to a set of experimental values by the method of least squares, the following definitions are adopted:

$$b_0 = -\Delta G_\theta^0/\theta \quad (6)$$

$$b_{j+1} = (\theta^{j-1}/j!)(\partial^j \Delta H^0/\partial T^j)_\theta \quad (7)$$

$$u_{j+1} = x^{j+1}\sum_{n=0}^{\infty}(n/n+j)(-x)^{n-1} \quad (8)$$

In this way eqn. 5 is reduced to a linear function in the variables $u_1, u_2, \ldots, u_{q+1}$:

$$-\Delta G^0_T/T = b_0 + b_1u_1 + b_2u_2 + \ldots b_{q+1}u_{q+1} \tag{9}$$

The number of terms in the series is based on the application of the t-test: q is taken as the highest value of j for which b_{j+1} is significantly different from zero. Alternatively, the results obtained by applying successive polynomials may be compared by means of the F-test, in order to determine if the inclusion of an additional term produces a meaningful improvement in the regression[19].

Eqn. 5 can be applied to the distribution of a volatile solute between a solution and a vapour phase. Thus, when $q = 0$, eqn. 5 reduces to

$$-\Delta \bar{G}^0_{1,T}/T = -\Delta \bar{G}^0_{1,\theta}/\theta + \Delta \bar{H}^0_{1,\theta}[(1/\theta) - (1/T)] = \Delta \bar{S}^0_{1,\theta} - \Delta \bar{H}^0_{1,\theta}/T \tag{10}$$

The combination of eqns. 10 and 1 under the assumption of an ideal vapour phase results in eqn. 3. The same calculation, but for $q = 1$, gives

$$\ln V_g = A' + (B'/T) + C' \ln T \tag{11}$$

where

$$A' = (1/R)\{\Delta \bar{S}^0_{1,\theta} - \Delta \bar{C}^0_{p_{1,\theta}} \ln(1 + \theta)\} - \ln(M_2/273.15R)$$

$$B' = -(1/R)(\Delta \bar{H}^0_{1,\theta} - \theta \Delta C^0_{p_{1,\theta}})$$

$$C' = \Delta \bar{C}^0_{p_{1,\theta}}/R$$

Infinite dilution activity coefficients measured at several temperatures have been fitted by Roth and Novák[10] to an equation similar in form to eqn. 11.

EXPERIMENTAL

Apparatus

Measurements were carried out in a modified Perkin-Elmer Sigma 300 gas chromatograph, equipped with a thermal conductivity detector and an LCI-100 computing integrator. Hydrogen, dried by passing it through a trap containing molecular sieve 5A, was used as the carrier gas. The instrument flow controller was connected by means of an 1 m × 1/8 in. copper coil (immersed in the same bath as the column) with a stainless-steel H, the other arms of which were connected to a mercury manometer, to a silicone gum septum and to the analytical column. A Haake N3B water-bath, constant to ±0.01°C, was used as a column thermostat. A short stainless-steel tube, 0.51 mm I.D., wrapped with heating tape, was used to connect the column outlet to the detector. The inlet and outlet pressures were measured to ±0.5 Torr by means of a mercury manometer and a barometer, respectively; a soap-bubble flow meter with an air jacket was used to measure the flow-rates. Temperatures were measured to ±0.05°C by means of a mercury thermometer with 0.1°C graduations that had been calibrated against two certified thermometers (Cannon, for ASTM kinematic viscosity, 28.5–31.5°C and 58.5 to 61.5°C, respectively).

Columns and reagents

The columns were stainless-steel tubes of 0.53 cm I.D.; Chromosorb W (60–80 mesh) was used as the solid support. The following columns were used: 9.29% (w/w) SQ (Hewlett-Packard), 1 m in length; 8.18% (w/w) TEGDME (Aldrich), 0.6 m in length; and 10.82% (w/w) TEG (Carlo Erba, RPE), 1 m in length. Packings were prepared in a rotary evaporator under a flow of dry nitrogen using *n*-hexane as the solvent for SQ and dry methanol for TEG and TEGDME. A 25-cm precolumn, containing the same packing as the analytical column and immersed in the same water-bath, was intercalated in the runs with TEGDME and TEG. The solutes were of 99+% purity (Aldrich) and were used as received.

Procedure

The columns were preconditioned before each run by heating for 4 h at the maximum operating temperature under a flow of hydrogen. All measurements were made in quadruplicate over a temperature range from 25 to 75°C for SQ and TEG and from 15 to 55°C for TEGDME, each in steps of about 5°C. After each run the V_g of the solute was measured at the lower temperature and compared with the value initially obtained; no significant loss of stationary phase could be detected. On-column injection of the solutes in the vapour form were made with 100- and 250-μl Hamilton syringes. Carrier gas flow-rate measurements (about 30 ml/min) were started as soon as the solute was injected, and repeated as many times as was possible during the time required for its elution.

Data treatment

Specific retention volumes were calculated from corrected peak retention times and operating conditions using the expression derived by Littlewood *et al.*[20]. $\Delta\bar{G}_1^0$ values were calculated by means of eqn. 1 using mixed second virial coefficients computed from the corresponding states equation of McGlashan and Potter[21]. Critical constants for the pure compounds were taken from the compilation by Kudchadker *et al.*[22]; critical volumes and temperatures for the mixtures were calculated by means of the Lorentz rule and the equation proposed by Hudson and McCoubrey[23], respectively.

Temperatures, which were measured with greater accuracy than the retention volumes, were considered to be error free. The coefficients of variation, C.V. = $[s(V_g)/\overline{V_g}] \cdot 100$, where $\overline{V_g}$ represents the mean and $s(V_g)$ the standard deviation for the sample of data obtained at a given temperature, ranged between 0.05 and 0.25%. As the influence of temperature on the C.V. values calculated for a given run was erratic, it was assumed that the retention volumes were affected by the same percentage random error over all the temperature range. In other words, it was assumed that the experimental data resulting from a run can be considered as a set of ln V_g values with constant precision, measured at exactly known temperatures. On the basis of this simplifying hypothesis, $\Delta\bar{G}_1^0/T$ data were fitted to eqn. 9 by means of least-squares multiple linear regression[19]. Best estimates of the b_j coefficients and their standard deviations were thus obtained; these, in turn, were transformed into thermodynamic functions by means of eqns. 6 and 7.

RESULTS AND DISCUSSION

The results of the regression analysis for $q = 0$, 1 and 2 are given in Tables I–III. The values for runs A and B in Tables I and II correspond to regressions performed with experimental data obtained in this work (eleven points per run), whereas those for run W correspond to regressions performed on the seven data points reported by Wicarová *et al.*[24]. Values for runs TEG A, TEG B and TEGDME in Table III correspond to the fitting of the experimental data obtained using TEG (eleven points per run) or TEGDME (nine points) as the stationary phase. The s values are the residual standard deviations, *i.e.*, the square root of the quotient between the residual sum of squares for the N observed values about the corresponding regression equation (as defined by q) and the number of degrees of freedom, $N-q-2$; s is an estimator of the standard error in the measurement of $\Delta\bar{G}^0_1/T$. Numbers preceded by $\pm$ are the standard deviations of the thermodynamic properties, calculated from s and from the elements of the inverse matrix. Values for the thermodynamic properties and for their standard deviations at the reference temperature are given in the tables; however, values at any other temperature within the experimental range are easily calculated by means of the computer program, and are independent of the chosen reference temperature. Figures in parentheses are the percentage significance level for the values of the thermodynamic functions; they were calculated by the t-test and represent estimates of the probability that the value of the function calculated in the last place for a given value of q differs from zero by chance.

The value of s suffers a considerable decrease on passing from $q = 0$ to $q = 1$, and the values obtained for $\Delta\bar{C}^0_{p_{1,\theta}}$ are significantly different from zero in all instances;

TABLE I

STANDARD PARTIAL MOLAR THERMODYNAMIC PROPERTIES FOR SOLUTIONS OF BENZENE IN SQUALANE AT $\theta = 323.15$ K

Run[a]	*Parameter*	*q = 0*	*q = 1*	*q = 2*
A	$s \times 10^3$	11.725	4.852	5.089
B		11.766	8.181	7.701
W		12.796	7.428	8.567
A	$\Delta\bar{G}^0_{1,\theta}$	−944.3 ± 1.18	−940.8 ± 0.71	−940.7 ± 0.78
B		−947.9 ± 1.15	−944.9 ± 1.22	−945.0 ± 1.16
W		−935.9 ± 1.57	−932.9 ± 1.27	−932.9 ± 1.56
A	$\Delta\bar{H}^0_{1,\theta}$	−7250 ± 24	−7276 ± 11	−7264 ± 26
B		−7283 ± 24	−7273 ± 17	−7218 ± 42
W		−7320 ± 44	−7274 ± 29	−7280 ± 77
A	$\Delta\bar{C}^0_{p_{1,\theta}}$		9.42 ± 1.412 (<0.1%)	9.94 ± 1.781
B			8.19 ± 2.514 (1.2%)	7.57 ± 2.408
W			15.46 ± 4.695 (3.4%)	15.92 ± 7.699
A	$\left(\frac{\partial\Delta\bar{C}^0_{p_1}}{\partial T}\right)_\theta$			−0.177 ± 0.342 (63%)
B				−0.798 ± 0.560 (10%)
W				0.159 ± 1.870 (>80%)

[a] Runs A and B, experimental data obtained in this work; run W, experimental data from ref. 26.

TABLE II

STANDARD PARTIAL MOLAR THERMODYNAMIC PROPERTIES FOR SOLUTIONS OF *n*-HEXANE IN SQUALANE AT θ = 323.15 K

Run[a]	*Parameter*	*q* = 0	*q* = 1	*q* = 2
A	$s \times 10^3$	15.085	9.089	8.410
B		12.989	4.345	3.890
W		10.138	4.911	4.747
A	$\Delta\bar{G}^0_{1,\theta}$	−711.7 ± 1.47	−707.4 ± 1.36	−707.6 ± 1.26
B		−711.6 ± 1.27	−707.4 ± 0.65	−707.5 ± 0.59
W		−693.9 ± 1.24	−691.5 ± 0.84	−691.1 ± 0.86
A	$\Delta\bar{H}^0_{1,\theta}$	−7390 ± 31	−7377 ± 19	−7312 ± 45
B		−7393 ± 26	−7376 ± 9	−7343 ± 21
W		−7393 ± 35	−7355 ± 19	−7398 ± 43
A	$\Delta\bar{C}^0_{p_{1,\theta}}$		11.45 ± 2.793 (0.4%)	10.71 ± 2.269
B			11.35 ± 1.334 (<0.1%)	10.74 ± 1.247
W			12.91 ± 3.104 (1.5%)	16.35 ± 4.266
A	$\left(\frac{\partial\Delta\bar{C}^0_{p_1}}{\partial T}\right)_\theta$			−0.936 ± 0.612 (18%)
B				−0.484 ± 0.281 (14%)
W				1.173 ± 1.036 (37%)

[a] See Table I.

TABLE III

STANDARD PARTIAL MOLAR THERMODYNAMIC PROPERTIES FOR SOLUTIONS OF BENZENE IN TEG AND TEGDME AT θ = 323.15 K

Run	*Parameter*	*q* = 0	*q* = 1	*q* = 2
TEG A	$s \times 10^3$	15.298	6.732	6.064
TEG B		14.489	5.164	5.521
TEGDME		12.354	4.564	4.959
TEG A	$\Delta\bar{G}^0_{1,\theta}$	168.9 ± 1.49	173.7 ± 1.01	173.9 ± 0.92
TEG B		172.5 ± 1.41	177.1 ± 0.77	177.1 ± 0.83
TEGDME		−846.8 ± 2.01	−848.2 ± 0.77	−848.1 ± 0.90
TEG A	$\Delta\bar{H}^0_{1,\theta}$	−7621 ± 32	−7604 ± 14	−7655 ± 33
TEG B		−7603 ± 30	−7581 ± 11	−7581 ± 30
TEGDME		−8228 ± 30	−8017 ± 33	−8006 ± 55
TEG A	$\Delta\bar{C}^0_{p_{1,\theta}}$		13.43 ± 2.165 (<0.1%)	14.24 ± 2.009
TEG B			12.84 ± 1.620 (<0.1%)	12.85 ± 1.840
TEGDME			13.50 ± 2.005 (<0.1%)	16.08 ± 9.594
TEG A	$\left(\frac{\partial\Delta C^0_{p_1}}{\partial T}\right)_\theta$			0.794 ± 0.469 (14%)
TEG B				0.002 ± 0.411 (>80%)
TEGDME				0.169 ± 0.612 (70%)

the s values for $q = 2$ are not very different from those for $q = 1$, and all the results for $(\partial \Delta \bar{C}^0_{p_1}/\partial T)_\theta$ are of poor significance. On the other side, the smallest standard errors for the heat of solution are obtained with the three-constant equation; it can be concluded that this equation gives a better fit to the experimental data than the two- or four-constant equation.

The results show a very good reproducibility between runs. In Tables I and II they are compared with those obtained by applying the same regression technique to the experimental data reported by Wicarová *et al.*[24]. They measured the specific retention volumes for benzene and *n*-hexane in SQ in a high-precision instrument; even though their measurements were performed at only seven different temperatures, over a temperature range narrower than ours, each V_g value represents the arithmetic mean of 15–20 measurements. With the exception of the $\Delta \bar{C}^0_{p_{1,\theta}}$ value for benzene in SQ, the comparison with our results is very encouraging. Unfortunately, there are no calorimetric data available for the systems studied in this work.

Corrections for non-ideality of the vapour phase are hardly justifiable when hydrogen is used as the carrier gas: corrected and uncorrected values for the heats of solution of *n*-hexane and benzene differ by less than 5 cal/mol when the equation of McGlashan and Potter[21] is used to calculate second virial coefficients and their dependence on temperature. However, when nitrogen is the carrier gas this difference can amount to 30 cal/mol, and the correction cannot be neglected.

Differences between experimental V_g values and the values calculated by means of the two-constant equation can amount to a maximum of about 1%, and this at the extremes of a broad temperature range. When the objective is interpolation, the use of more sophisticated regression techniques is not justified, at least for the heat capacity values of the systems studied here.

To summarize, the application of Clarke and Glew's regression method to chromatographic data leads to an improvement in the measurement of thermodynamic solution properties, but not in the interpolation of retention volumes.

ACKNOWLEDGEMENTS

This work was sponsored by the Consejo Nacional de Investigaciones Científicas y Técnicas (CONICET) and by the Comisión de Investigaciones Científicas de la Provincia de Buenos Aires (CIC).

REFERENCES

1 A. J. Ashworth, *J. Chem. Soc., Faraday Trans. I*, 69 (1973) 459.
2 D. C. Locke, *Adv. Chromatogr.*, 14 (1976) 87.
3 G. L. Vogel, G. L., M. A. Hamzavi-Abedi and D. E. Martire, *J. Chem. Thermodyn.*, 15 (1983) 739.
4 R. J. Laub and R. L. Pecsok, *Physicochemical Applications of Gas Chromatography*, Wiley-Interscience, New York, 1978.
5 J. R. Conder and C. L. Young, *Physicochemical Measurement by Gas Chromatography*, Wiley, New York, 1979.
6 E. F. Meyer and F. A. Baiochi, *J. Chem. Thermodyn.*, 9 (1977) 1051.
7 E. F. Meyer and F. A. Baiochi, *Anal. Chem.*, 49 (1977) 1029.
8 E. F. Meyer and F. A. Baiochi, *J. Chem. Thermodyn.*, 10 (1978) 823.
9 W. E. Hammers and C. L. de Ligny, *J. Polym. Sci., Polym. Phys. Ed.*, 12 (1974) 2065.
10 M. Roth and J. Novák, *Macromoles*, 19 (1986) 364.

11 E. C. Clarke and D. N. Glew, *Trans. Faraday Soc.*, 62 (1966) 539.
12 E. Grunwald, *J. Am. Chem. Soc.*, 106 (1984) 5414; and references cited therein.
13 E. L. Arancibia and J. A. Catoggio, *J. Chromatogr.*, 197 (1980) 135.
14 J. L. Fortier, G. C. Benson and P. Picker, *J. Chem. Thermodyn.*, 8 (1976) 289.
15 M. J. Costigan, L. J. Hodges, K. N. Marsh, R. H. Stokes and C. W. Tuxford, *Aust. J. Chem.*, 33 (1980) 2103.
16 K. N. Marsh, *Pure Appl. Chem.*, 55 (1983) 467.
17 R. C. Castells, *J. Chromatogr.*, 350 (1985) 339.
18 E. Wilhelm, *Thermochim. Acta*, 119 (1987) 17.
19 N. R. Draper and H. Smith, *Applied Regression Analysis*, Wiley, New York, 2nd ed., 1981.
20 A. B. Littlewood, C. S. G. Phillips, and D. T. Price, *J. Chem. Soc.*, (1955) 1480.
21 M. L. McGlashan and D. J. B. Potter, *Proc. R. Soc. London, Ser. A*, 267 (1962) 478.
22 A. P. Kudchadker, G. H. Alani and B. J. Zwolinski, *Chem. Rev.*, 68 (1968) 659.
23 G. H. Hudson and J. C. McCoubrey, *Trans. Faraday Soc.*, 56 (1960) 761.
24 O. Wicarová, J. Novák and J. Janák, *J. Chromatogr.*, 51 (1970) 3.

Journal of Chromatography, 504 (1990) 55–67
Elsevier Science Publishers B.V., Amsterdam — Printed in The Netherlands

CHROM. 22 184

Effects of isotherm non-linearity on the determination of the binding constant in affinity chromatography

WEN-CHIEN LEE*,[a], GOW JEN TSAI and GEORGE T. TSAO
Laboratory of Renewable Resource Engineering, Purdue University, West Lafayette, IN 47907 (U.S.A.)
(First received August 29th, 1989; revised manuscript received November 30th, 1989)

SUMMARY

A systematic study was made of non-linear effects on the determination of the binding constant in affinity chromatography. The criteria for the applicable range of linear theory are derived for both frontal and zonal analysis. The difference in the criteria between zonal and frontal analysis indicates that the latter may not be preferred in some instances. Investigation of experimental data from the literature showed that the effect of isotherm non-linearity on elution volume is not small in affinity chromatography, where the binding constant is very large and the experimental design does not permit work in the linear region. A universal function $\Phi(a)$ for zonal analysis has been derived. The strong correlation of experimental and calculated $\Phi(a)$ demonstrates that the equations derived in this work are valuable. In applying these equations, one can determine both the binding constant and the maximum binding capacity from experiments by evaluating the capacity factor at various sample concentrations with or without an inhibitor in the mobile phase.

INTRODUCTION

Affinity chromatography is widely used in the investigation of specific interactions between biomolecules. Both zonal and frontal elution approaches have been developed in order to determine quantitatively the interaction constant[1]. Differences have been found when two methods are applied to evaluate the inhibitory constant of the complex of an enzyme and its soluble or immobilized inhibitor[2]. Whichever method is used, a working equation for the elution volume has to be used to interpret the experimental data. The observation of elution volume depending on the sample concentration or inhibitor concentration is essentially a result of a non-linear equilibrium isotherm, which is conventionally of the Langmuir type. Hence affinity chromatography in the case of a Langmuir isotherm is non-linear chromatography.

Arnold *et al.*[3] pointed out some inconsistencies in the theoretical treatments of

[a] Present address: Department of Chemical Engineering, Chung Yuan Christian University, Chung Li 32023, Taiwan.

0021-9673/90/$03.50

analytical affinity chromatography and identified these as the sources of erroneous results. Recently, Golshan-Shirazi and Guiochon[4–6] derived analytical solutions of elution time as a function of sample volume and sample concentration for the ideal (equilibrium) model of non-linear chromatography. However, the elution time they obtained was the retention time of the shock front. A thorough examination of the non-linear problem in affinity chromatography was made by Muller and Carr[7]. No theory was available in their work to interpret the effects of isotherm non-linearity on the capacity factor and desorption rate constant. Recent work on non-linear affinity chromatography includes that of Anderson and co-workers[8–10].

In this paper, a systematic approach is presented by first introducing a more realistic model to describe the chromatographic behavior; the equations relating elution volume and capacity factor to concentrations of immobilized and soluble ligand, inhibitor, etc., are derived by following the clarified definitions and a correlation is given to demonstrate the effects of isotherm non-linearity. By using the equations derived in this work, a proper determination of the binding constant, the interaction constant between the soluble solute and its immobilized ligand, can be achieved in affinity chromatography.

MATHEMATICAL MODEL AND DEFINITIONS OF THE FIRST MOMENT

The governing equation of affinity chromatography can be derived from a material balance. For a simple system contaning one single solute, it is given as

$$\varepsilon \frac{\partial C}{\partial t} = - u_0 \frac{\partial C}{\partial z} + \varepsilon D \frac{\partial^2 C}{\partial z^2} + r'' \tag{1}$$

where r'' denotes the net mass transfer rate from the bulk fluid to the adsorbed phase and can be expanded as shown in Table I. The model, including eqn. 1 and Table I, may be the most sophisticated and realistic one for the description of affinity chromatography. In this model, a uniform diameter d_p is assumed for monodisperse porous media, an imaginary external film separating the bulk fluid and solid phase is present and an effective diffusion coefficient D_i based on the entire particle volume is used to describe the diffusion of solute into the pores. The concentrations, in pores and in the bulk liquid surrounding the particle, c and C, are coupled by the mass-transfer rate through the film, which is accounted by k_f. The parameter k_a accounts for the desorption rate; q is the concentration on the inner surface of the solid. The equilibrium isotherm describes the relationship between concentrations c and q. It represents a plot of amount adsorbed in equilibrium with the concentration of free solute in the pores. To account for the possibility that all sites can be filled with the adsorbent, many workers considered the equilibrium relation to be of the Langmuir type:

$$q^* = \frac{q_s K_L c}{1 + K_L c} \tag{2}$$

The model presented above has been reported elsewhere by Arnold *et al.*[11] and

TABLE I

MODEL OF FLUID-TO-PARTICLE DIFFUSION AND BIO-SPECIFIC ADSORPTION

Pore diffusion with external film resistance (spherical particles).

$$-r'' = \frac{6\,(1 - \varepsilon)}{d_p} \cdot D_i \frac{\partial c}{\partial r}\bigg|_{r=d_p/2}$$

$$D_i\left(\frac{\partial^2 c}{\partial r^2} + \frac{2}{r} \cdot \frac{\partial c}{\partial r}\right) - \varepsilon_p \cdot \frac{\partial c}{\partial t} - \rho_p \cdot \frac{\partial q}{\partial t} = 0$$

$$k_f\,(C - c\,|_{r=d_p/2}) = D_i \cdot \frac{\partial c}{\partial r}\bigg|_{r=d_p/2}$$

$$\frac{\partial c}{\partial r}\bigg|_{r=0} = 0$$

$$\frac{\partial q}{\partial t} = k_a\,(q^* - q)$$

$$q^* = \frac{q_s\,K_L\,c}{1 + K_L\,c}$$

McCoy[12]. It could also be reduced to the model of Horváth and Lin[13] by defining the film mass transfer coefficient as a linear function of $u_0^{1/3}$.

The use of the statistical moments to characterize chromatographic processes is well known, but some inconsistencies may be frequently found in the literature. Mathematically, the moments for each distribution function can be evaluated as soon as the function is well defined. In zonal elution chromatography, the effluent concentration profile can be regarded as a distribution function, by which the expressions of the moments are derived. For frontal elution chromatography, the effluent concentration profile, which is called a breakthrough curve, is no longer a distribution function. In general, the breakthrough curve can be treated as the integral of the distribution function of the quantity t. Therefore, the function $\partial c/\partial t$ can be treated as the distribution function of this quantity. The definition of the first moment for frontal elution is then given by

$$\mu_1^{\mathrm{F}} = \frac{\int_0^\infty t \frac{\partial C^{\mathrm{F}}}{\partial t}\,\mathrm{d}t}{\int_0^\infty \frac{\partial C^{\mathrm{F}}}{\partial t}\,\mathrm{d}t} \tag{3}$$

and that for zonal elution by

$$\mu_1^{\mathrm{Z}} = \frac{\int_0^\infty t\,C^{\mathrm{Z}}\,\mathrm{d}t}{\int_0^\infty C^{\mathrm{Z}}\,\mathrm{d}t} \tag{4}$$

TABLE II

RESULTS OF THE FIRST MOMENT

Isotherm	$\mu_1^F = \dfrac{\int_0^\infty t \cdot \dfrac{\partial C^F}{\partial t} \cdot dt}{\int_0^\infty \dfrac{\partial C^F}{\partial t} \cdot dt}$	$\mu_1^Z = \dfrac{\int_0^\infty t\, C^Z\, dt}{\int_0^\infty C^Z\, dt}$
Linear isotherm	$\dfrac{L}{u_0}[\varepsilon + (1-\varepsilon)\varepsilon_p + (1-\varepsilon)\rho_p q_s K_L]$	$\dfrac{L}{u_0}[\varepsilon + (1-\varepsilon)\varepsilon_p + (1-\varepsilon)\rho_p q_s K_L]$
Rectangular isotherm	$\dfrac{L}{u_0}\left[\varepsilon + (1-\varepsilon)\varepsilon_p + \dfrac{(1-\varepsilon)\rho_p q_s}{C_0}\right]$	$\dfrac{L}{u_0}\left\{\varepsilon + (1-\varepsilon)\varepsilon_p + \dfrac{\varepsilon + (1-\varepsilon)\varepsilon_p}{\mu_0}\cdot\left(\dfrac{L}{u_0}\right)\cdot\dfrac{(1-\varepsilon)\rho_p q_s}{C_0}\left[\dfrac{1}{2} - \dfrac{\varepsilon D}{L u_0}\right] - \dfrac{(1-\varepsilon)\rho_p q_s}{\mu_0 C_0}\left[\dfrac{R\,\varepsilon_p}{3k_f} + \dfrac{1}{k_a} + \dfrac{1}{15}\cdot\dfrac{R^2\varepsilon_p}{D_i}\right]\right\}$ where $\mu_0 = \int_0^\infty C^Z\, dt = 1 - \dfrac{L}{u_0}\cdot\dfrac{(1-\varepsilon)\rho_p q_s}{C_0}$
Langmuir isotherm:		
Equilibrium	$\dfrac{L}{u_0}\left[\varepsilon + (1-\varepsilon)\varepsilon_p + \dfrac{(1-\varepsilon)\rho_p q_s K_L}{1+K_L C_0}\right]$	$\dfrac{L}{u_0}[\varepsilon + (1-\varepsilon)\varepsilon_p + (1-\varepsilon)\rho_p q_s K_L \Phi(a)]$
Finite mass-transfer rate	$\dfrac{\varepsilon L}{u_0}(1 + k'')$ with $k'' = \mathrm{f}(v, v_i, Bi, K_a, K_L^+, q_s^+, \varepsilon_p^+)$ (numerical value)	$\dfrac{\varepsilon L}{u_0}(1 + k'')$ with $k'' = \mathrm{f}(t_0^+, v, v_i, Bi, K_a, K_L^+, q_s^+, \varepsilon_p^+)$ (numerical value)

where $t_0^+ = \dfrac{u_0 t_0}{\varepsilon L}$, $v = \dfrac{u_0 L}{2\,\varepsilon D}$, $v_i = \dfrac{\varepsilon_p R^2 u_0}{\varepsilon L D_i}$, $Bi = \dfrac{R k_f}{D_i}$, $K_a = \dfrac{\varepsilon k_a L}{u_0}$, $K_L^+ = K_L C_0$, $\varepsilon_p^+ = \left(\dfrac{1-\varepsilon}{\varepsilon}\right)\varepsilon_p$, $q_s^+ = \dfrac{\rho_p q_s}{\varepsilon_p C_0}$

In eqns. 3 and 4, the superscripts F and Z represent frontal and zonal elutions (analyses), respectively. In frontal analysis, the concentration C^F is the effluent concentration normalized by dividing by sample concentration, *i.e.*, $C^F = C/C_0$.

Solving eqn. 1, along with proper initial/boundary conditions gives the concentration profiles in either zonal or frontal analysis. After substituting the profiles into eqns. 3 and 4, we can obtain the predicted values of the first moments. The results are summarized in Table II for various isotherm cases. It is noted that with the Langmuir isotherm, analytical solutions are not available when the mass transfer effects are considered. In the following sections, the results in Table II will be discussed in detail.

It has been proved that eqn. 3 is equivalent to the following equation:

$$\mu_1^F = \int_0^\infty (1 - C^F)dt \tag{5}$$

Eqn. 5 has been used in the literature to evaluate the first moment from experimental data[14]. The quantity in eqn. 5 is the area behind the breakthrough curve and represents the dynamic capacity of the affinity column in frontal elution. The equality between eqns. 3 and 5 indicates that eqn. 3 is a proper definition of the retention time. The resulting expressions of the first moments derived from eqns. 3 and 4 and are not identical except for the case of a linear isotherm. We have proved that the equality between eqns. 3 and 4 exists only when the mathematical model is linear. In this instance, the equilibrium isotherm will be linear.

ELUTION VOLUME AND BINDING CONSTANT DETERMINATION

Basically, all the equations of elution volume used in affinity chromatography are related to the expressions of the first moment. We usually call the first moment μ_1 the average retention time. The elution volume, V_t, also called retention volume, is simply the product of μ_1 and volumetric flow-rate, *i.e.*,

$$V_t = \mu_1 Q \tag{6}$$

Typical elution volume equations can be found in ref. 15 for frontal elution and in ref. 16 for zonal elution. Both analyses were used by Malanikova and Turkova[2] for the determination of binding (or association) constants, K_L, of complexes of trypsin and its low-molecular-weight inhibitors.

The elution volume is a measure of the extent to which the soluble component is retained in the packing bed of a chromatographic system or, in other words, the degree of retardation of the component in a matrix. The retardation of a solute in a matrix certainly depends on the intensity of interaction between the solute and its immobilized ligand. In a physical sense, an increase in the association constant between the solute and the ligand (or binding site) increases the capacity of the bio-adsorption, and hence increases the elution volume.

The elution volume is widely used to determine the binding constants in affinity chromatography because it is assumed to be independent of the mass-transfer rate and

the column dispersity. Actually, this common belief is not completely correct. Many factors may affect the value of the first moment or elution volume. For example, different initial/boundary conditions that come from different methods of sample injection and system considerations may result in different expressions for the first moment. Table III lists four sets of commonly used initial/boundary conditions for zonal analysis in the literature: (1) Kucera[17], (2) Aust[18], (3) Horváth and Lin[19] and (4) Chung and Hsu[20]. A comparison of the solutions of μ_1 in Table III shows that all four sets will lead to the same solution when the sample size t_0 and column dispersion $\varepsilon D/\mu_0 L$ are sufficiently small. Horváth and Lin's initial/boundary conditions can be regarded as an ideal case of Chung and Hsu's. In this work, the last set of initial/boundary conditions with $t_0 \to 0$ is used. A dependence of elution time on flow-rate was also reported by Heathcote and DeLisi[21]. It is believed that the dispersive effect of the boundary conditions can be made trivial by a reasonable design of the experiment.

It should be noted that the solutions in Table III are true only for linear isotherms, *i.e.*, in the range $K_L c \ll 1$ in eqn. 2. Under this assumption, μ_1 value is directly related to the total void fraction, $\varepsilon + (1-\varepsilon)\varepsilon_p$, and a product of the two quantities, $(1-\varepsilon)\rho_p q_s$ and K_L. The quantity $(1-\varepsilon)\rho_p q_s$ represents the maximum

TABLE III

EFFECTS OF INITIAL/BOUNDARY CONDITIONS ON THE FIRST MOMENT IN ZONAL ANALYSIS

Initial/boundary conditions[a]	μ_1^z
(1) Kucera[17]: $C = q = c = 0;\ t < 0$ and $z = \pm\infty$ $t = 0;\ q = c = 0;\ -\infty < z < \infty;\ 0 < r < \frac{d_p}{2}$ $C = M\delta(z);\ 0 < z < L$	$\left(1 + \frac{2\varepsilon D}{u_0 L}\right)\left[1 + \frac{(1-\varepsilon)}{\varepsilon}\cdot\varepsilon_p + \left(\frac{1-\varepsilon}{\varepsilon}\right)\rho_p q_s K_L\right]\varepsilon\cdot\frac{L}{u_0}$
(2) Aust[18]: $C = q = c = 0;\ t = 0$ $\varepsilon D\left.\frac{\partial C}{\partial z}\right\|_{z=0^+} = u_0\,[C(z=0^+) - C(z=0^-)]$ $\left.\frac{\partial C}{\partial z}\right\|_{z=L} = 1;\ C(z=0^-) = \delta(t)M$	$\left[1 + \frac{(1-\varepsilon)}{\varepsilon}\cdot\varepsilon_p + \left(\frac{1-\varepsilon}{\varepsilon}\right)\rho_p q_s K_L\right]\varepsilon\cdot\frac{L}{u_0}$
(3) Horvath and Lin[19]: $C = q = c = 0;\ t = 0$ $C = 0;\ z = \infty$ $C = \delta(t)M;\ z = 0$	$\left[1 + \frac{(1-\varepsilon)}{\varepsilon}\cdot\varepsilon_p + \left(\frac{1-\varepsilon}{\varepsilon}\right)\rho_p q_s K_L\right]\varepsilon\cdot\frac{L}{u_0}$
(4) Chung and Hsu[20]: $C = q = c = 0;\ t = 0$ $C = C_0\,[u(t) - u(t-t_0)];\ z = 0$ $C = 0;\ z = \infty$	$\left[1 + \frac{(1-\varepsilon)}{\varepsilon}\cdot\varepsilon_p + \left(\frac{1-\varepsilon}{\varepsilon}\right)\rho_p q_s K_L\right]\varepsilon\cdot\frac{L}{u_0} + \frac{t_0}{2}$

[a] $\int_a^b f(z)\,\delta(z-z')\,dz = \begin{cases} f(z') & \text{if } a < z' < b \\ 0 & \text{otherwise} \end{cases}$

number of moles of solute that can be adsorbed per unit volume of packing bed. In other words, it is the concentration of accessible binding sites. In an affinity chromatographic system, the K_L value could be as large as 10^6 l mol^{-1}. By the linear theory, K_L is determined from the plot of elution volume *vs.* $(1-\varepsilon)\rho_p q_s$.

Elution volume can also be expressed in terms of the total penetrable volume of the colum, $V_0\{=[\varepsilon+(1-\varepsilon)\varepsilon_p]V_B\}$, which is measured by the elution of an unretained component having the same degree of penetration as a desired component but no specific affinity for the immobilized ligand. The ratio, which is referred to as the capacity factor (retention factor), k', is given by the following expression:

$$k' = \frac{V_t - V_0}{V_0} \tag{7}$$

The quantity k' is related to the thermodynamics of distribution between the mobile phase and stationary phase in chromatography. As one of the most important chromatographic parameters, its value is characteristic of individual solutes and the selection of the chromatographic system. For example, the ratio of the capacity factors is directly related to the resolution, which is the selectivity of two components in chromatography.

EFFECT OF ISOTHERM NON-LINEARITY

As shown in Table II, $\mu_1^F = \mu_1^Z$ when the isotherm is linear. Another idealized model was proposed[22] for which the absorbate is bound irreversibly, and other species are totally unadsorbed. The equilibrium isotherm is considered to be irreversible and is of the rectangular type, *i.e.*,

$$\begin{aligned} q^* &= q_s;\ c > 0 \\ q^* &= 0;\ c = 0 \end{aligned} \tag{8}$$

For the first two types of isotherm, Laplace transformation has been used to solve the governing equation and hence to derive the expressions of μ_1^F and μ_1^Z. The effects of column dispersion and fluid-to-particle mass transfer are accounted for in these cases. As expected, these expressions are independent of dispersion and mass transfer except the rectangular isotherm in zonal analysis, where the parameters accounting for dispersion and mass transfer appear. The effect of dispersion and mass transfer will be small if we take the values $R/k_f \to 0$, $R^2/D_i \to 0$ and $\mu_0 L/D \to \infty$. When the parameters values are in the above range, the system is in local equilibrium. Even for the equilibrium case, $\mu_1^F \neq \mu_1^Z$.

Both a linear isotherm and a rectangular isotherm can be regarded as special cases of the Langmuir isotherm. When all mass-transfer resistances are negligible, the method of the particle-volume average can reduce the governing equations to being analytically solvable[12]. Therefore, the method of characteristics serves to provide solutions of eqn. 1[23]. The expressions of the first moment were derived by substituting the resulting concentration profiles into eqns. 4 and 5. As shown in Table II, the deviation of the Langmuir from the linear isotherm is due to the effect of sample inlet concentration, C_0. In frontal analysis, the factor is $1/(1+K_L C_0)$. In zonal analysis, we

derived a universal function $\Phi(a)$. This function results from the method of characteristics and can be represented as

$$\Phi = \frac{1}{4} + \frac{\frac{1-a}{2}(2a-a^2)^{3/2}}{\frac{\pi}{2} - \sin^{-1}|1-a| - (1-a)(2a-a^2)^{1/2}}; \qquad a \leqslant 1 \tag{9}$$

$$\Phi = \frac{\frac{\pi}{8}}{a^2 - 1 + \frac{\pi}{2}}; \qquad a \geqslant 1 \tag{10}$$

where

$$a = \sqrt{\left(\frac{u_0 t_0}{L}\right)} \frac{C_0}{(1-\varepsilon)\rho_p q_s} \tag{11}$$

The function can also be represented as in Fig. 1. It is tedious to obtain the results, *i.e.*, eqns. 9–11; we ignore the mathematical details here. Fig. 1 shows that the effect of isotherm non-linearity is relatively small (1% deviation), provided that the value of a is less than 0.01. The a value reflects the amounts of relative feed concentration and sample size. The smaller the feed concentration, the smaller is a and hence the smaller is the effect of non-linearity. The contribution of sample size to elution time was also examined by Golshan-Shirazi and Guiochon[4–6], but the retention time they derived is the retention time of the shock front, not the true one as defined in eqn. 4.

If we take a 10% deviation from linear theory as an acceptable figure, then the criteria for the applicable range of linear theory can be derived as $a \ll 0.09$ for zonal analysis and $K_L C_0 \ll 0.11$ for frontal analysis. In addition to the sample concentration C_0, the a value also depends on the sample size and the quantity $(1-\varepsilon)\rho_p q_s$. For an affinity chromatographic system with large K_L and $(1-\varepsilon)\rho_p q_s$, zonal elution could be preferable, *i.e.*, it could be operated with a linear behavior over a wide range of sample concentrations, as shown in Fig. 2. The system in the linear region may take advantage

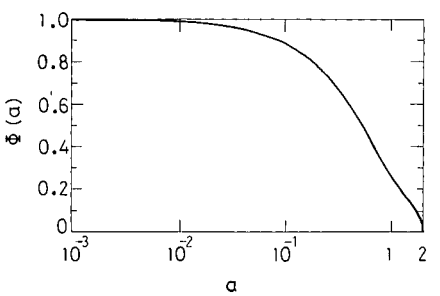

Fig. 1. Universal function of isotherm non-linearity effects in zonal analysis.

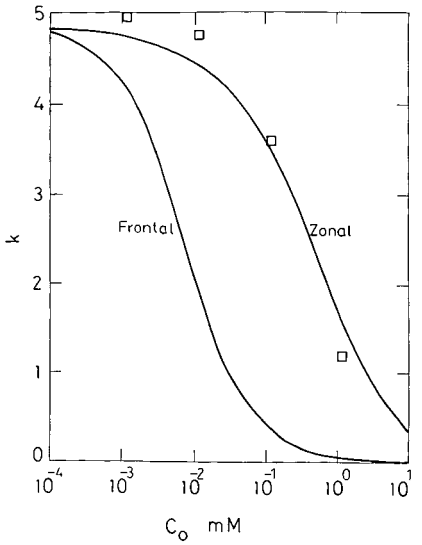

Fig. 2. Effects of sample concentration on the capacity factor. Data after Anderson and Walters[9] in their Fig. 1; binding of 4-methylumbelliferyl α-D-mannopyranoside on concanavalin A in a column using Hypersil 300 as support. $t_0 = 0.01$ min, $V_B = 0.66$ ml, $\varepsilon = 0.35$, $\varepsilon_p = 0.44$, $L = 5$ cm, flow-rate = 1 ml min^{-1}; $(1-\varepsilon)\rho_p q_s K_L = 3.1$ and $K_L = 1.17 \cdot 10^5$ l mol^{-1} are estimated from inhibition experiments (Fig. 2 in Anderson and Walters'[9] paper).

of using the theories in linear chromatography, for example, the height equivalent to a theoretical plate (HETP). The difference in the criteria between zonal and frontal analysis indicates that frontal analysis may not be preferable in some instances. Also, these criteria are different from that in the work of Arnold *et al.*[3].

For the Langmuir isotherm, the expression of μ_1^F in Table II is the same as that given by Arnold *et al.*[3], which was obtained from a local equilibrium approach. This elution volume equation with different nomenclature was also derived by Kasei and Oda[15]. Arnold *et al.* pointed out that the elution volume equation derived by Dunn[24] and Chaiken[16] is similar to this expression of μ_1^F. However, Dunn and Chaiken[25,26] used the equation to estimate the K_L value with zonal elution data.

The effects of concentration on the capacity factor in affinity chromatography are show in Fig. 2. Both predicted values and experimental data from the literature[9] are shown. The predicted values were calculated with the equations in Table II for a Langmuir isotherm at equilibrium, *i.e.*,

$$k' \text{ (zonal)} = \frac{(1-\varepsilon)\rho_p q_s K_L}{\varepsilon + (1-\varepsilon)\varepsilon_p} \cdot \Phi(a) \tag{12}$$

$$k' \text{ (frontal)} = \frac{(1-\varepsilon)\rho_p q_s K_L}{[\varepsilon + (1-\varepsilon)\varepsilon_p](1 + K_L C_0)} \tag{13}$$

TABLE IV

EXPRESSIONS OF THE FIRST MOMENT AND CAPACITY FACTOR IN INHIBITION EXPERIMENTS

Inhibitor	*Frontal analysis, μ_1^F and k'*		*Zonal analysis, μ_1^Z and k'*	
Competing free (soluble) inhibitor:				
$P + L = PL: K_L = \dfrac{[PL]}{[L]C_p}$	$\mu_1^F = \dfrac{L}{u_0}\left[\varepsilon + (1-\varepsilon)\varepsilon_p + \dfrac{(1-\varepsilon)\rho_p q_s K_L}{(1+K_I C_I)(1+K_L C_0)}\right]^a$	(F1)	$\mu_1^Z = \dfrac{L}{u_0}\left[\varepsilon + (1-\varepsilon)\varepsilon_p + \dfrac{(1-\varepsilon)\rho_p q_s K_L}{(1+K_I C_I)} \cdot \Phi(a)\right]$	(Z1)
$P + I = PI: K_I = \dfrac{C_{PI}}{C_I C_p}$	$k' = \dfrac{(1-\varepsilon)\rho_p q_s K_L}{[\varepsilon+(1-\varepsilon)\varepsilon_p](1+K_I C_I)(1+K_L C_0)}$	(F2)	$k' = \dfrac{(1-\varepsilon)\rho_p q_s K_L}{[\varepsilon+(1-\varepsilon)\varepsilon_p](1+K_I C_I)} \cdot \Phi(a)$	(Z2)
			$a = \sqrt{\left(\dfrac{u_0\ t_0}{L}\right)\dfrac{C_0\ (1+K_I C_I)}{(1-\varepsilon)\rho_p q_s}}$	(Z3)
Competing binding inhibitor:				
$P + L = PL: K_L = \dfrac{[PL]}{[L]C_p}$	$\mu_1^F = \dfrac{L}{u_0}\left[\varepsilon + (1-\varepsilon)\varepsilon_p + \dfrac{(1-\varepsilon)\rho_p q_s K_L}{(1+K_I C_I+K_L C_0)}\right]$	(F3)	$\mu_1^Z = \dfrac{L}{u_0}\left[\varepsilon + (1-\varepsilon)\varepsilon_p + \dfrac{(1-\varepsilon)\rho_p q_s K_L}{(1+K_I C_I)} \cdot \Phi(a)\right]$	(Z1)
$I + L = IL: K_I = \dfrac{[IL]}{[L]C_I}$	$k' = \dfrac{(1-\varepsilon)\rho_p q_s K_L}{[\varepsilon+(1-\varepsilon)\varepsilon_p](1+K_I C_I+K_L C_0)}$	(F4)	$k' = \dfrac{(1-\varepsilon)\rho_p q_s K_L}{[\varepsilon+(1-\varepsilon)\varepsilon_p](1+K_I C_I)} \cdot \Phi(a)$	(Z2)
			$a = \sqrt{\left(\dfrac{u_0\ t_0}{L}\right)\dfrac{C_0}{(1-\varepsilon)\rho_p q_s}}$	(Z4)

[a] Where C_0 is the concentration C_p in the influent solution.

It is obvious that the theoretical results fit very well the data for zonal elution experiments with high-performance affinity chromatography. The linearity of the capacity factor no longer exists in either zonal or frontal analysis.

Eqns. 12 and 13 provide a means of estimating the values of K_L and $(1-\varepsilon)\rho_p q_s$ from the experimental data for concentration C_0 *vs.* capacity factor. Note that the dependence of the capacity factor on the binding site concentration, $(1-\varepsilon)\rho_p q_s$, is different from that of linear theory. As shown in Table II, K_L cannot be distinguished from $(1-\varepsilon)\rho_p q_s$ in the expression of the first moment for a linear isotherm. On the contrary, K_L and $(1-\varepsilon)\rho_p q_s$ can be determined simulaneously from a reciprocal plot or from a non-linear regression of C_0 *vs.* capacity factor for a Langmuir isotherm.

Sometimes the K_L and $(1-\varepsilon)\rho_p q_s$ values were obtained from other independent experiments, *e.g.*, batch isotherm measurement or inhibition experiments. In this case, a correlation can be drawn between the calculated and experimental values of Φ. The calculated values of Φ are obtained directly from eqns. 9–11, and the experimental values are from the capacity factors obtained by experiments with various C_0. Fig. 3 shows the correlation with data from the literature[7,9]. The strong correlation demonstrates that the equations in Table II are valuable.

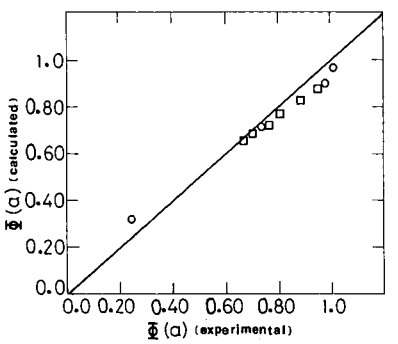

Fig. 3. Correlation of the universal function $\Phi(a)$ in zonal analysis. (○) Data after Anderson and Walters[9], same source as in Fig. 2; (□) data after Muller and Carr[7] in their Fig. 4; binding of *p*-nitrophenyl α-D-mannopyranoside on concanavalin A immobilized in 50-μm silica particle. $t_0 = 0.025$ min, $V_B = 1.06$ ml, $V_0 = 0.85$ ml, $\varepsilon = 0.5$, $\varepsilon_p = 0.6$, $Q = 1$ ml min^{-1}, $L = 15$ cm, $K_L = 1.5 \cdot 10^4$ l mol^{-1} and $(1-\varepsilon)\rho_p q_s = 6.39 \cdot 10^{-4}$ M are estimated with eqns. Z2 and Z4 using the data in Muller and Carr's Fig. 3.

INHIBITION EXPERIMENTS AND FINITE MASS-TRANSFER EFFECTS

As the K_L value in a common affinity chromatographic system is very large, the volume needed to saturate the packing bed (in the frontal mode) or to elute isocratically the desired component (in the zonal mode) is large. The use of a competing inhibitor will reduce the elution volume to a manageable level. Two types of inhibitor for inhibition experiments have been used, namely competing free (soluble) inhibitor and competing binding inhibitor, as in this work. In the former instance, a soluble inhibitor (I), which competes with an immobilized ligand (L) for the desired macromolecular compound (P), is present in the sample solution and pre-equilibrated buffer[16]. In the latter a macromolecular compound (L) is im-

mobilized and is saturated with sample containing a solute (P) and a competing inhibitor (I), or a solute (P) is isocratically eluted using a competing inhibitor (I) in the mobile phase. The latter case may also be called reversed-role affinity chromatography[9]. As shown in Table IV, expressions of the first moment and capacity factor for both zonal and frontal analyses have been derived. It should be noted that there is a small mistake in the paper by Arnold *et al.*[3]. They used the equation for the second type of inhibition, *i.e.*, eqn. F3 in Table IV, to calculate the association constant from the first type of inhibition experiment. A correction should replace eqn. 11 in their paper by eqn. F1 in Table IV.

As an example of using inhibition experiments for determining binding constants, we consider the work of Dunn and Chaiken[26] in which nuclease was adsorbed on pdTpAp-Sepharose with soluble pdTp as competing soluble inhibitor. Fig. 1 in that paper gives a plot of elution volume *vs.* concentration of immobilized ligand, $(1-\varepsilon)\rho_p q_s$, from a zonal elution experiment. They used an equation similar to eqn. F2 in Table IV (for frontal analysis) to estimate the constant K_L to be $3.85 \cdot 10^5$ M. If we use eqns. Z2 and Z3 to calculate the binding constant, it will be $K_L = 2.5 \cdot 10^5$ M by non-linear regression. They overestimated the K_L value by 54%.

In applying the equations in this work to determine the binding constant, one may test first whether the experiment can be performed in the linear region by running it at various sample concentrations C_0 with or without inhibitors. If the resulting capacity factor k' is independent of C_0, then linear theory is required to calculate K_L. In contrast, if a dependence of k' on C_0 is obvious, eqn. 12 or 13 or the equation in Table IV is required to determine K_L and also $(1-\varepsilon)\rho_p q_s$ from the experimental data for k' *vs.* C_0.

Previous investigators have reported that the major effect of column dispersion and mass-transfer resistances is zone spreading. Their effect on elution volume is believed to be relatively small. Numerical calculations were made for frontal analysis and it was observed that the μ_1 values are nearly independent of parameters that characterize the dispersion and mass-transfer resistances. If we consider the column for μ_1^F in Table II, it will be no surprise that the effect of column dispersion and mass transfer on frontal elution is negligible. Although no results are reported at this stage for zonal analysis, it is believed that the effect of dispersion and mass transfer on elution volume is relatively small compared with that of concentration, *i.e.*, the isotherm non-linearity.

SYMBOLS

c concentration of solute in pores, M
C concentration of solute in bulk fluid phase, M
C_0 sample concentration, M
C_p concentration of component P, M
C_I concentration of inhibitor I, M
d_p diameter of particle, cm
D dispersion coefficient in column, $cm^2\ s^{-1}$
D_i pore diffusivity of solute, $cm^2\ s^{-1}$
k' capacity factor
k_a desorption rate constant, s^{-1}

k_f fluid film mass transfer coefficient of solute, cm s^{-1}
K_I inhibition constant, l mol^{-1}
K_L binding constant, l mol^{-1}
L length of the column, cm
q sorbate concentration, mmol (g particle)$^{-1}$
q^* equilibrium value of q
q_s maximum number of available binding sites, mmol (g particle)$^{-1}$
Q volumetric flow-rate, cm^3 s^{-1}
R radius of particle, cm
r radial distance in particle, cm
t time, s
t_0 time interval of sample injection, s
u_0 liquid superficial velocity, cm s^{-1}
V_0 unretarded void volume, cm^3
V_B total bed volume, *i.e.*, the empty column volume, cm^3
V_t retention (elution) volume, cm^3
z linear coordinate along the packed bed, cm

ε void fraction of the packed bed, equal to the volume outside the particles divided by the empty column volume
ε_p porosity of particle
ρ_p particle density, the density of packed stationary phase in column, g (cm^3 particle)$^{-1}$
μ_1 first moment, s

REFERENCES

1 P. D. G. Dean, W. S. Johnson and F. A. Middle (Editors), *Affinity Chromatography —A Practical Approach*, IRL Press, Washington, DC, 1985.
2 M. Malanikova and J. Turkova, *J. Solid-Phase Biochem.*, 2 (1977) 237.
3 F. H. Arnold, S. A. Schofield and H. W. Blanch, *J. Chromatogr.*, 355 (1986) 1.
4 S. Golshan-Shirazi and G. Guiochon, *Anal. Chem.*, 60 (1988) 2364.
5 S. Golshan-Shirazi and G. Guiochon, *Anal. Chem.*, 61 (1989) 462.
6 S. Golshan-Shirazi and G. Guiochon, *J. Phys. Chem.*, 93 (1989) 4143.
7 A. J. Muller and P. W. Carr, *J. Chromatogr.*, 284 (1984) 33.
8 D. J. Anderson and R. R. Walters, *J. Chromatogr.*, 331 (1985) 1.
9 D. J. Anderson and R. R. Walters, *J. Chromatogr.*, 376 (1986) 69.
10 D. J. Anderson, J. S. Anhalt and R. R. Walters, *J. Chromatogr.*, 359 (1986) 369.
11 F. H. Arnold, H. W. Blanch and C. R. Wilke, *J. Chromatogr.*, 330 (1985) 159.
12 B. J. McCoy, *AIChE Symp. Ser.*, 82 (1986) 115.
13 Cs. Horváth and H.-J. Lin, *J. Chromatogr.*, 149 (1978) 43.
14 C. Ho, C. B. Ching and D. M. Ruthven, *Ind. Eng. Chem. Res.*, 26 (1987) 1407.
15 K.-I. Kasai and Y. Oda, *J. Chromatogr.*, 376 (1986) 33.
16 I. M. Chaiken, *J. Chromatogr.*, 376 (1986) 11.
17 E. Kucera, *J. Chromatogr.*, 19 (1965) 237.
18 E. Aust, *Chem. Eng. J.*, 35 (1987) 179.
19 Cs. Horváth and H.-J. Lin, *J. Chromatogr.*, 126 (1976) 401.
20 I.-J. Chung and H.-W. Hsu, *J. Chromatogr.*, 110 (1975) 1.
21 H. W. Heathcote and C. DeLisi, *J. Chromatogr.*, 248 (1982) 183.
22 B. J. McCoy, *Biotechnol. Bioeng.*, 27 (1985) 1477.
23 R. Aris and N. R. Amundson, in *Mathematical Methods in Chemical Engineering*, Vol. 2, Prentice-Hall, Englewood Cliffs, NJ, 1973.
24 B. M. Dunn, *Appl. Biochem. Biotechnol.*, 9 (1984) 261.
25 B. M. Dunn and I. M. Chaiken, *Proc. Natl. Acad. Sci. U.S.A.*, 171 (1974) 2382.
26 B. M. Dunn and I. M. Chaiken, *Biochemistry*, 14 (1975) 2343.

Journal of Chromatography, 504 (1990) 69–78
Elsevier Science Publishers B.V., Amsterdam — Printed in The Netherlands

CHROM. 22 218

Surface affinity chromatographic separation of blood cells

VII. Relationship between capacity factors of human peripheral blood cells and the rate of penetration of liquids into xerogel column packings

USHIHO MATSUMOTO, YŌICHI SHIBUSAWA* and MASAAKI YAMASHITA
Division of Analytical Chemistry, Tokyo College of Pharmacy, 1432-1, Horinouchi, Hachioji, Tokyo 192-03 (Japan)
(Received October 2nd, 1989)

SUMMARY

Eleven kinds of column packing gels which bonded poly(ethylene glycol) (PEG) to Sepharose 6B (PEG–C_{10}–Sepharose) were prepared. Human peripheral blood cells were chromatographed on these gel columns by eluting with 0.09 *M* phosphate-buffered 2% (w/w) dextran T40 solution at the pH of the respective isoelectric points of the blood cells. The rate of penetration of water or the mobile phases into the PEG–C_{10}–Sepharose xerogels as a measure of the hydrophobicity of the gels depended on both the oxyethylene residue content and the number of oxyethylene units of the packing gels. The capacity factors of granulocytes and lymphocytes were increased on the columns packed with gels having a slower rate of penetration of the liquids into the xerogels.

INTRODUCTION

In previous papers[1–6], the chromatographic behaviour of human peripheral blood cells was studied by the use of bisoxirane-coupled poly(ethylene glycol) 400, 4000, 6000 and 20 000 (PEG 400, 4000, 6000 and 20M)–Sepharose 6B (PEG–C_{10}–Sepharose) columns and poly(propylene glycol) 200, 400 and 950 (PPG 200, 400 and 950)-coupled agarose (PPG–C_3–Chromagel A4) columns. Sodium phosphate-buffered solutions containing dextran T40 or T500 were used as the mobile phase at pH 7.4 or the pH of the respective isoelectric point of blood cells ($pH_{c.p.}$). The retention behaviour of blood cells on PEG 20M–C_{10}–Sepharose columns depended on the molecular weight and concentration of dextrans and on the neutral salts, such as sodium chloride, in the mobile phase at pH 7.4[1,2].

Further, the retention volumes of granulocytes and lymphocytes increased with increasing number of oxyethylene units in the range of 9–450 on PEG 400–, 4000–,

0021-9673/90/$03.50

6000– and 20M-C_{10}–Sepharose columns eluted with 0.09 *M* sodium phosphate-buffered solution containing 2% (w/w) dextran T40[3].

The hydrophobicities ($\Delta\log K$) of four kinds of blood cells were determined by the hydrophobic affinity partition method[7] using PEG 6000 monopalmitate as a hydrophobic ligand. A linear correlation between the retention volumes of platelets, granulocytes and lymphocytes on a PEG 20M–C_{10}–Sepharose column and the $\Delta\log K$ values of these cells was observed[4]. Similarly, an approximately linear relationship was found between the $\Delta\log K$ values of platelets granulocytes and lymphocytes and the retention volumes of these cells on PPG 200–, 400– and 950–C_3–, PPG 400–C_{10}– and PEG 20M–C_{10}–agarose columns[5].

In the preceding study[6], the $\Delta\log K$ values of four kinds of blood cells and the PPG 200–, 400– and 950–C_3–Chromagel beads were determined by the hydrophobic affinity partition method using Pluronic P84, a block polymer of PEG and PPG, as a hydrophobic ligand. The $\Delta\log K$ values of blood cells increased in the order erythrocytes, platelets, granulocytes and lymphocytes, which coincided with the elution order of these cells from PPG–C_3–Chromagel columns, except in a few instances. A linear relationship was found between the capacity factors [$k' = (V_R - V_m)/V_m$, where V_R is the retention volume of the cells and V_m the interstitial volume of the column determined from the elution volume of native dextran] of granulocytes on the various PPG–C_3–Chromagel columns and the $\Delta\log K$ values of the PPG-bonded gel beads. The packing beads with $\Delta\log K > 0.5$ caused a considerable increase in the retention of lymphocytes. The k' values of platelets increased slightly on the PPG-bonded gel beads that have the highest $\Delta\log K$ values. On the other hand, the retention of erythrocytes on the columns was not dependent on the $\Delta\log K$ values of the gel beads. The $\Delta\log K$ values of the column packing beads determined by the hydrophobic affinity partition method merely indicate the affinity between the hydrophobic ligand, such as PEG monopalmitate or Pluronic P84, and the gel beads. It is necessary to measure the affinity between the column packing beads and a liquid, such as water or aqueous mobile phase, and to evaluate the degree of hydrophobicity of the gel beads.

The affinity between a solid and a liquid is determined by the wettability of the solid as the contact angle. However, in order to measure the contact angle of powder particles, the particles must be moulded into the plate and the liquid dropped on it for measurement. The other method for measurement of wettability is known as the ascending capillary method[8], that is, the liquid rises in a column which is packed with powder particles, the ascending rate of penetration of the liquids is measured and the affinity between the powder particles and liquid is determined.

In this study, we measured the rate of penetration of water or the mobile phase used for chromatography of blood cells into PEG–C_{10}–Sepharose xerogels with different oxyethylene residue contents and with different numbers of oxyethylene units for the determination of the hydrophobicity of the packing gel beads. The relationship between the k' values of four kinds of human peripheral blood cells and the rate of penetration of the liquid into the column packing xerogels is discussed.

EXPERIMENTAL

Materials

Epoxy-activated Sepharose 6B and dextran T40 (weight-average molecular weight $M_w = 40\,000$) were obtained from Pharmacia LKB (Uppsala, Sweden). PEG 400 (number-average molecular weight $M_n = 400$), 4000 ($M_n = 3000$), 6000 ($M_n =$ 6000-7500) and 20M ($M_n = 15\,000$–$20\,000$) were purchased from Wako Junyaku (Osaka, Japan). Other reagents were of analytical-reagent grade.

Instruments

A JNM-FX 200 NMR spectrometer (JEOL, Tokyo, Japan) operating at 199.5 MHz in the pulsed Fourier transform mode was used for the determination of oxyethylene residue content of PEG–C_{10}–Sepharose 6B. A Model 5100C osmometer (Wescor, Logan, UT, U.S.A.) was used for the measurement of the osmotic pressure of the mobile phase. An ISCO Model UA-5 absorbance monitor (Instrumentation Specialties, Lincoln, NE, U.S.A.) was used for detecting the absorbance of eluates at 254 and 405 nm simultaneously. An LKB 2112 Varioperpex II or 2132 Microperpex peristaltic pump and a RediRac fraction collector (LKB, Bromma, Sweden) were employed for chromatographing blood cells and for fractionation of the eluates. A Coulter counter Model D (Coulter Electronics, Harpenden, U.K.) was used for counting the number of blood cells. A FACE type PHW immersion wetting measurement apparatus (Kyowa Kaimenkagaku, Tokyo, Japan) was used for the determination of the rate of penetration of both water and mobile phase into PEG–C_{10}–Sepharose 6B xerogels.

Preparation of PEG–C_{10}–Sepharose 6B

Oxirane coupling of PEG 400, 4000, 6000 and 20M to epoxy-activated Sepharose 6B was performed at 40°C for 16 h in a solution of pH 12.0 as described previously[1]. PEG–C_{10}–Sepharose 6B gels having lower oxyethylene residue contents were prepared by oxiran coupling of PEG to epoxy-activated Sepharose 6B for shorter times. The residual epoxy groups on the PEG–C_{10}–Sepharose 6B were hydrolysed with 0.1 *M* perchloric acid for 1 h at room temperature[3].

Oxyethylene residue content in PEG–C_{10}–Sepharose 6B

Visible absorbance photometric determination. PEG–C_{10}–Sepharose 6B column packings were carefully washed with acetone on a glass filter-funnel (G3) and about 5 g of the packings were lyophilized. A 20-ml volume of 88% (v/v) formic acid was added to about 100 mg of the PEG–C_{10}–Sepharose xerogels and was heated for about 4 h on a boiling water-bath for hydrolysis and then evaporated to dryness under reduced pressure at 70°C. The hydrolysed product was dissolved in 10 ml of water. To 1-ml volume of this solution, 1 ml of dilute hydrochloric acid (1:4), 1 ml of 10% (w/v) barium chloride and 1 ml of 10% (w/v) phosphomolybdic acid were added. This mixture was allowed to stand for at least 1 h, during which a flocculent greenish precipitate formed from the phosphomolybdic acid and any PEG present. The precipitate was washed with 3 ml of 0.1 *M* hydrochloric acid and then with 7 ml of water. After centrifugation, the precipitate was dissolved in 3 ml of sulphuric acid, then 1 ml each of nitric acid and 70% (v/v) perchloric acid were added. The oxyethylene

residue content in the solution was determined according to the method of Shaffer and Critchfield[9] as follows. The solution was diluted with water, neutralized with sodium hydroxide and then diluted to 100 ml. To a 10-ml aliquot, phenylhydrazine in dilute sulphuric acid was added and the mixture was heated on water-bath. The absorbance was measured at 490 nm.

Determination by ^1H NMR. In a similar manner to the above, PEG–C_{10}–Sepharose 6B was hydrolysed with formic acid and the PEG present in this product was precipitated with phosphomolybdic acid. The precipitate was dissolved in 0.5 ml of [$^2H_2$]sulphuric acid for ^{1}H NMR measurements. A signal from the PEG–phosphomolybdic acid complex was observed at about 8.5 ppm as a single peak. The content of oxyethylene residues in the PEG-bonded gels (mg/g dry powder) was obtained from the integrated peak intensity originating from the PEG complex using calibration graphs (0–0.5 mg PEG/ml). The mean values of the oxyethylene residue contents (mg/g dry gel) in PEG 400–, 4000–, 6000– and 20M–C_{10}–Sepharose 6B column gels are given in Table I. The values obtained by ^{1}H NMR are in good agreement with those determined by visible absorbance photometry. The procedure for the determination of the oxyethylene residue content by ^{1}H NMR is simpler than that by absorbance photometry. The quantitative values obtained by the NMR method were used as the oxyethylene residue contents of PEG–C_{10}–Sepharose column packings.

Determination of rate of penetration of water or mobile phase solution into PEG–C_{10}–Sepharose xerogels

About 100 mg of PEG–C_{10}–Sepharose 6B xerogels were packed into a Teflon column (10 × 0.6 cm I.D.) by vertical tapping 200 times with the aid of a mechanical packer. The column was hung vertically with its lower end dipping into a liquid. The increase in weight of the packed column as a result of penetration of water or mobile phase solution into the xerogel was recorded automatically for the weight–time curve using the FACE immersion wetting measurement apparatus. The rate of penetration [l^2/t(cm^2/s)] was obtained using the following equation, which is same in principle as Washburn's equation[8]:

$$l^2/t(\mathrm{cm}^2/\mathrm{s}) = \{[L/(SL - W_s/\varphi_2)\varphi_1](Wt_2 - W_0)\}^2/t_2$$
$$W_0 = (\sqrt{t_2}Wt_1 - \sqrt{t_2}Wt_2)/(\sqrt{t_2} - \sqrt{t_1})$$

TABLE I

OXYETHYLENE RESIDUE CONTENT (mg/g DRY GEL) IN PEG–C_{10}–SEPHAROSE 6B COLUMN PACKING GELS

The values are averages of 3–15 determinations.

Bonded phase	*Absorbance photometry*	*^1H NMR*
PEG 400	13.3	13.5
PEG 4000	27.3	26.8
PEG 6000	46.1	46.3
PEG 20M	158.7	157.4

where L is the height of xerogel packed in the column, W_s is the cross-sectional area of the column [$(0.3 \times 0.3 \times \pi)$ cm^2], φ_1 is the specific gravity of water or mobile phase solution, φ_2 is the specific gravity of the xerogel, t_1 and t_2 (s) are the times of the start and end of measurement and w_1 and w_2 are the weight of liquid penetrated into the xerogel at t_1 and t_2 s, respectively.

Collection and isolation of blood cells

Human blood was drawn from normal male adult donors by venous puncture and heparin was added (0.05 ml of a 1000 U/ml solution per 10 ml of blood). A 1-ml volume of 3.8% (w/v) sodium citrate solution was added to 10 ml of blood for collection of platelets. Siliconized glassware was used in all procedures. Centrifugal isolation was used for erythrocytes. The isolation technique based on that of Leeksma and Cohen[10] was employed. For granulocytes, the sodium metrizoate–dextran sedimentation technique of Bøyum[11] was used. The sodium metrizoate–Ficoll sedimentation technique of Thorsby and Bratlie[12] was employed for the collection of lymphocytes. These isolation procedures for blood cells have been described in detail in previous papers[1,2].

Chromatography of blood cells

Sodium phosphate-buffered solution (0.09 *M*) containing 2% (w/w) dextran T40 at the isoelectric points ($pH_{c.p.}$) of the respective blood cells, which were determined previously[3] by the cross-partition method[13], was used as the mobile phase. These $pH_{c.p.}$ values for lymphocytes, erythrocytes and platelets are 5.2, 5.5 and 6.8, respectively. The $pH_{c.p.}$ value for granulocytes is the same as that of platelets. A 0.2-ml volume of the respective cell suspensions containing *ca.* $3 \cdot 10^4$ erythrocytes, *ca.* 10^6 platelets, *ca.* $2 \cdot 10^5$ granulocytes or *ca.* 10^5 lymphocytes was loaded separately onto the PEG–C_{10}–Sepharose 6B (45–165 μm wet particle diameter) column (25 × 0.9 cm I.D.) and eluted at a flow-rate of 10.0–12.0 ml/h by use of a peristaltic pump. The eluate was monitored at 254 and 405 nm. The fractions were collected in volumes of about 1.0 ml. Each fraction was diluted with Isoton and the number of blood cells was counted on a Coulter counter.

RESULTS

Correlations between oxyethylene residue content or number of these units and the rate of penetration

The rates of penetration of water or 0.09 *M* sodium phosphate-buffered solution containing 2% (w/w) dextran T40 (pH 6.8) into eleven kinds of PEG–C_{10}–Sepharose 6B xerogels are given in Table II.

There are four groups of column packing gels, PEG 400–, 4000–, 6000–and 20M–C_{10}–Sepharose 6B, corresponding to Nos. 1, 2–3, 4–5 and 6–11, respectively. Each group has the same number of oxyethylene units but a different oxyethylene residue content. It was observed that the rate of penetration of the liquids into these xerogels having nearly the same oxyethylene residue contents (Nos. 1, 2, 4 and 6) was slower as the number of these units increased from 9 (No. 1) to 470 (No. 6). It can be seen in Table II that the rate of penetration of water or the mobile phase is slower with increasing oxyethylene residue content in each group.

TABLE II

RATES OF PENETRATION OF DIFFERENT PEG-C_{10}–SEPHAROSE 6B XEROGELS

Bonded phase		*Oxyethylene residue content (mg/g dry gel)*	*Rate of penetration (10^{-2} cm^2/s)*	
No.	*Component*		*Water*	*Mobile phase*[a]
1	PEG 400	13.5	34.0	15.0
2	PEG 4000	12.5	24.0	8.8
3	PEG 4000	26.8	18.0	1.2
4	PEG 6000	12.2	15.0	6.9
5	PEG 6000	46.3	3.9	5.1
6	PEG 20M	13.0	8.3	6.3
7	PEG 20M	27.4	5.9	5.9
8	PEG 20M	45.5	5.3	4.8
9	PEG 20M	63.0	4.8	3.4
10	PEG 20M	80.0	3.7	3.4
11	PEG 20M	157.4	3.0	1.4

[a] Contained 2% (w/w) of dextran T40–0.09 *M* NaH_2PO_4–Na_2HPO_4 (pH 6.8).

Plots of the rate of penetration of the liquids into xerogels *versus* oxyethylene residue content for eleven kinds of packings are shown in Fig. 1. In spite of the number of oxyethylene units, the rate increased with decrease in the oxyethylene residue content of the xerogels. The rate of penetration of water into the xerogels having less than 50 mg oxyethylene residues/g dry gel increased considerably (Fig. 1A). The rate of penetration of the mobile phase into xerogels increased linearly with decreasing oxyethylene residue content (Fig. 1B). This suggests that the influence of the oxyethylene residue content on the rate of penetration is greater than that of the number of oxyethylene units. The rate of penetration obtained by use of the mobile phase at pH 5.2 and 5.5, the $pH_{c.p.}$ values of erythrocytes and lymphocytes respectively, was the same as that obtained with the mobile phase at pH 6.8 (data not shown).

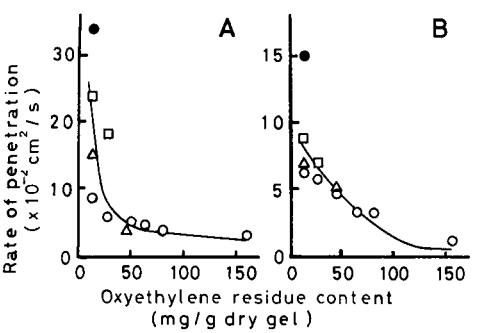

Fig. 1. Relationship between oxyethylene residue content and the rate of penetration of (A) water or (B) the mobile phase into PEG–C_{10}–Sepharose 6B xerogels. ● = PEG 400; □ = PEG 4000; △ = PEG 6000; ○ = PEG 20M.

Capacity factors of blood cells on PEG–C_{10}–Sepharose 6B columns

Table III shows the capacity factors (k') of human blood cells determined by elution from PEG–C_{10}–Sepharose 6B columns (25 × 0.9 cm I.D.) with 0.09 *M* sodium phosphate buffer ($pH_{c.p.}$) containing 2% (w/w) dextran T40 together with the oxyethylene residue contents of the packing gels. These k' values of four kinds of blood cells were calculated by combining the retention volumes of these cells with the interstitial volumes (V_m) of the column determined by the elution volume of native dextran as described previously[6]. The k' values of erythrocytes and platelets were less than 1.0 but not zero, and it was clear that these cells were retained slightly on the PEG–C_{10}–Sepharose 6B columns. The maximum k' values of 0.49 for erythrocytes and 0.71 for platelets were obtained on the column with 80.0 and 157.4 mg/g dry gel oxyethylene residue contents (Nos. 10 and 11), respectively.

On the other hand, the k' values of granulocytes and lymphocytes were higher than 1.0 for every column used. The increase in the oxyethylene residue contents in the groups which bonded the same number of oxyethylene units (Nos. 2–3, 4–5 and 6–11) resulted in an increase in the k' values of granulocytes and lymphocytes, except in a few instances. It found that the k' values of granulocytes were above 2.0 by use of PEG–C_{10}–Sepharose 6B columns having oxyethylene residue contents of more than 63.0 mg/g dry gel. The k' values of lymphocytes were greater than those of granulocytes on every PEG–C_{10}–Sepharose column. The column packings with oxyethylene residues bonded more than 26.5 mg/g dry gel gave the k' values above *ca.* 2.5 for lymphocytes. As the oxyethylene residue content increased above 45.5 mg/g dry gel, the k' values became greater than *ca.* 3.0 (Nos. 8–11).

TABLE III

CAPACITY FACTORS OF HUMAN ERYTHROCYTES (E), PLATELETS (P), GRANULOCYTES (G) AND LYMPHOCYTES (L)

Columns: PEG–C_{10}–Sepharose 6B (25 × 0.9 cm I.D.). The mobile phase contained 2% (w/w) of dextran T40–0.09 *M* NaH_2PO_4–Na_2HPO_4 ($pH_{c.p.}$).

Bonded phase[a]	V_m *(ml)*[b]	*Capacity factors (k')*			
		E	*P*	*G*	*L*
1	3.6	0.19	0.17	1.14	1.56
2	3.6	0.36	0.44	1.47	1.89
3	3.6	0.31	0.53	1.83	2.75
4	3.6	0.39	0.47	1.52	1.89
5	3.9	0.38	0.41	1.90	2.97
6	3.6	0.16	0.44	1.78	1.92
7	4.1	0.17	0.42	1.71	2.49
8	3.8	0.39	0.45	1.97	3.08
9	3.8	0.42	0.50	2.00	3.08
10	3.7	0.49	0.57	2.08	3.22
11	3.8	0.47	0.71	2.00	3.21

[a] See Table II.

[b] V_m: elution volume of native dextran.

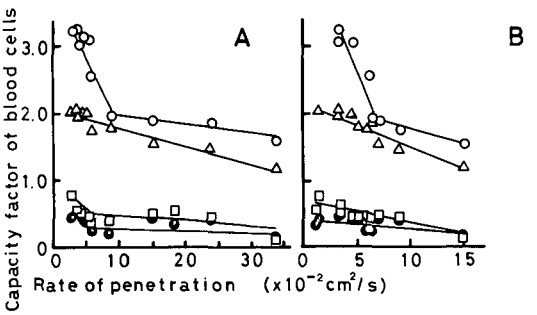

Fig. 2. Relationship between capacity factors of human (●) erythrocytes, (□) platelets, (△) granulocytes and (○) lymphocytes and the rate of penetration of (A) water or (B) the mobile phase into PEG–C_{10}–Sepharose 6B xerogels.

Correlation between the capacity factors of blood cells and the rate of penetration

The rate of penetration of both water and the mobile phase into eleven kinds of PEG–C_{10}–Sepharose 6B xerogels is plotted in Fig. 2 as a function of the k' values of erythrocytes, platelets, granulocytes and lymphocytes obtained on these PEG–C_{10}–Sepharose 6B columns by use of phosphate-buffered mobile phase at the respective $pH_{c.p.}$ values. The packing gel with a rate of penetration of water of less than $10 \cdot 10^{-2}$ cm^2/s and of the mobile phase of less than $7.0 \cdot 10^{-2}$ cm^2/s gave a substantial increase in the k' values of lymphocytes. For granulocytes, linear relationships were found between k' and the rate of penetration of both water and the mobile phase into these xerogels. The k' values of platelets increased slightly when using packing gels with a slower rate of penetration of both water and the mobile phase. The k' values of erythrocytes were almost unchanged even when the PEG–C_{10}–Sepharose 6B packing beads having the slowest rate of penetration were used.

DISCUSSION

It has been shown that the hydrophobic interactions between peripheral blood cells and the bonded PEG or PPG phase of column packing gels play an important role in retaining the cells on these columns in our chromatographic system[4–6]. It has also been shown that the retention of the blood cells depends on the difference in the hydrophobicity of the packing beads based on the oxyethylene or oxypropylene residue content and on the number of these units[4,5].

In previous papers[5,6], the hydrophobicity ($\Delta\log K$ values) of PEG–C_{10}–Sepharose, PPG–C_3–Chromagel beads and blood cells were determined by hydrophobic affinity partition[7] using PEG 6000 monopalmitate or Pluronic P84, a block polymer of PEG and PPG, as the hydrophobic ligand. A linear relationship was found between the capacity factors (k') of granulocytes on PPG–C_3–Chromagel columns and the $\Delta\log K$ values of the gel beads. The retention of lymphocytes increased gradually on the columns of packing gel beads with $\Delta\log K$ values <0.5, but increased considerably on the gel beads with values >0.5.

In general, the hydrophobic affinity partition method has been applied to the measurement of the hydrophobicities of soluble proteins, insoluble suspended materials such as cell particles, subcellular organelles and cell membranes[14]. Partition

of the particles such as the blood cells and the packing gel beads was characterized by the partition coefficient (K) calculated as the ratio of the particle concentration in the upper PEG-rich phase to that in the bottom dextran-rich phase. In this method, the number of particles attached to the interface is calculated as the difference between the total number added and the number in the upper or the bottom phase. Half of the number in the interface fraction add to each number in the upper and bottom phases[4]. The partition experiments for the particles are tedious because the separation of the two immiscible aqueous phases is particularly slow and many particles such as blood cells and gel beads become attached to the interface of the two PEG and dextran phases. In addition, the $\Delta\log K$ values determined by the partition method are dominated by chemical species of the hydrophobic ligand, such as PEG palmitate or Pluronic.

It is well known that the wetting of powder particles is of great importance for the measurement of the affinity between particles and a liquid. In general, the wettablity is determined as the contact angle of a liquid droplet which forms on the compressed powder particles. The other method for determining the wetting of powder particles by a liquid is the immersion wetting method[8], in which the wettability is determined as the rate of penetration of the liquid which rises in a column packed with the particles.

In this paper, we determined the rate of penetration of water or the mobile phase used in our chromatographic systems for the separation of blood cells into eleven kinds of PEG–C_{10}–Sepharose 6B xerogels. The rate was considered as a measure of hydrophobicity of these column packing gels. It was found that the hydrophobicity of the packing gels increases with decrease in the rate of penetration of water or the mobile phase (Fig. 1). The rate of penetration of these liquids into PEG–C_{10}–Sepharose xerogels was slow as the oxyethylene residue content increased. It was also found that the rate decreased with increase in the number of oxyethylene units. This suggests that the oxyethylene residue content rather than the number of oxyethylene units affects the hydrophobicity of PEG–C_{10}–Sepharose beads (Table II).

The capacity factors (k') of four kinds of human blood cells were calculated by combining the retention volumes of the cells with the elution volume of the native dextran by using a PEG–C_{10}–Sepharose 6B column and a 0.09 M phosphate-buffered solution containing 2% (w/w) dextran T40 at the respective isoelectric points ($pH_{c.p.}$) of the cells. The relationship between the rate of penetration of water or the mobile phase into PEG–C_{10}–Sepharose xerogels and the k' values of the blood cells was examined (Fig. 2). It is clear that the k' values of lymphocytes on a PEG–C_{10}–Sepharose column increase considerably when the rate of penetration of water is $> 10 \cdot 10^{-2}$ cm^2/s and that of the mobile phase is $> 7 \cdot 10^{-2}$ cm^2/s. A linear correlation was found between the k' values of granulocytes and the rate of penetration of both water and the mobile phase. The k' values of granulocytes and lymphocytes increase with decrease in the rate of penetration. These results are in fair agreement with the preceding study[6] in which the k' values of the granulocytes increased linearly with increasing the hydrophobicity ($\Delta\log K$) of PPG–C_3–Chromagel beads and the retention of lymphocytes increased considerably on PPG-bonded gels with $\Delta\log K > 0.5$. Platelets were retained on the PEG–C_{10}–Sepharose column having the slowest rate of penetration. On the other hand, no change was found for the k' values of erythrocytes even if we used the PEG–C_{10}–Sepharose column with the highest oxyethylene residue content (Fig. 2).

In conclusion, it is clear that hydrophobic interactions play an important role in the retention and separation of granulocytes and lymphocytes on PEG–C_{10}–Sepharose 6B columns. The use of PEG-bonded gels with higher oxyethylene residue contents with a slower rate of penetration of the liquids is necessary for separating erythrocytes and platelets on the chromatographic columns.

REFERENCES

1 U. Matsumoto and Y. Shibusawa, *J. Chromatogr.*, 187 (1980) 351.
2 U. Matsumoto and Y. Shibusawa, *J. Chromatogr.*, 206 (1981) 17.
3 U. Matsumoto, Y. Shibusawa and Y. Tanaka, *J. Chromatogr.*, 268 (1983) 375.
4 U. Matsumoto, M. Ban and Y. Shibusawa, *J. Chromatogr.*, 285 (1984) 69.
5 U. Matsumoto and Y. Shibusawa, *J. Chromatogr.*, 356 (1986) 27.
6 Y. Shibusawa, U. Matsumoto and M. Takatori, *J. Chromatogr.*, 398 (1987) 153.
7 V. P. Shanbhag and C.-G. Axelson, *Eur. J. Biochem.*, 60 (1975) 17.
8 E. W. Washburn, *Phys. Rev.*, 17 (1921) 273.
9 C. B. Shaffer and F. H. Critchfield, *Anal. Chem.*, 19 (1947) 90.
10 C. H. W. Leeksma and J. A. Cohen, *J. Clin. Invest.*, 35 (1956) 964.
11 A. Bøyum, *Nature (London)*, 204 (1964) 793.
12 E. Thorsby and A. Bratlie, in P. I. Terasaki (Editor), *Histocompatibility Testing*, Munksgaard, Copenhagen, 1970, p. 655.
13 P.-Å. Albertsson, S. Sasakawa and H. Walter, *Nature (London)*, 228 (1970) 1329.
14 H. Westrin, P.-Å. Albertsson and G. Johansson, *Biochim. Biophys. Acta*, 436 (1976) 696.

Journal of Chromatography, 504 (1990) 79–88
Elsevier Science Publishers B.V., Amsterdam — Printed in The Netherlands

CHROM. 22 167

Settling-time dependence of rat bone marrow cell partition and counter-current distribution in charge-sensitive aqueous two-phase systems

Relationship with the cell partitioning mechanism

ANA-ISABEL GARCÍA-PÉREZ, PILAR SANCHO and JOSÉ LUQUE*
Departamento de Bioquímica y Biología Molecular, Campus Universitario, Universidad de Alcalá, 28871 Alcala de Henares, Madrid (Spain)
(First received July 17th, 1989; revised manuscript received November 21st, 1989)

SUMMARY

Differences in the settling-time dependence of single and multiple cell partitions have been found between heterogeneous (bone marrow cells) and homogeneous (erythrocytes) populations when using charge-sensitive dextran–poly(ethylene glycol) aqueous two-phase systems. The cell populations were partitioned using both single test-tube experiments and multiple thin-layer counter-current distribution. Lengthening the settling time, to favour phase separation, and decreasing the upper phase volume are more effective in fractionation by the counter-current distribution of heterogeneous cell populations than increasing the interfacial tension, although all three were employed to speed phase settling. On the basis of these results, the original cell partitioning mechanism proposed for non-charge-sensitive systems has been extended to charge-sensitive systems.

INTRODUCTION

Aqueous two-phase systems are formed when buffered and isotonic mixtures of dextran (D) and poly(ethylene glycol) (PEG) are allowed to separate over time. Mixtures of D and PEG near the critical point (low interfacial tension systems) need a relatively long settling time for phase separation. The higher the interfacial tension (far away from the critical point), the faster is the speed of phase separation. A partition ratio, P, between the total amount of cells in the PEG-rich upper phase and the cells adsorbed at the interface is obtained in single-tube experiments. Cell partitioning, which is based on differences in cell surface properties and their interaction with the phases, can be altered in various ways. Ions of some salts affect the physical

0021-9673/90/$03.50

properties of the systems. The affinity of phosphate for the D-rich bottom phase results in charge-sensitive systems, with a positive upper phase[1–4].

To increase the resolution of cells with close P values, multiple partitions can be carried out using a thin-layer counter-current distribution (CCD) procedure[1,4]. To produce a shorter time of phase separation, and thus increase the speed of phase settling, the height of the phase column of the CCD unit was reduced by Albertsson[1] in the thin-layer rotor. Other conditions of the CCD procedure can be varied to facilitate phase separation. A direct correlation between length of settling time and efficiency of fractionation was observed in charge-sensitive two-phase systems for heterogeneous cell populations from rat and human bone marrow[5–7] and from developing chicken erythrocytes[8–11]. As erythrocytes with very close P values are present in the blood of adult animals (rats and chickens), the settling time does not affect cell age fractionation in these homogeneous erythrocyte populations. This paper confirms that settling time is a determinant parameter for partitioning in single-tube experiments and for bone marrow cell fractionation by CCD in charge-sensitive two-phase systems.

Increasing system interfacial tension is an additional condition that can determine a shorter time of phase separation and thus affect the dependence of P on time[4,12]. Increasing polymer concentrations were then used in charge-sensitive systems to increase their interfacial tension. However, a higher interfacial tension did not affect the improved CCD fractionation observed with the lengthened settling time in the heterogeneous cells.

It has been reported recently that the decrease in time of phase separation, which can be produced by reducing the height of the phase column in the thin-layer CCD rotor, may result in a lower cell fractionation efficiency[13]. In our experience, shortening the height of the phase column (by reducing the volume of the upper phase in the cavities of the CCD rotor) and simultaneous lengthening of settling time are required for more efficient fractionation of heterogeneous cells[6], even when systems with higher interfacial tension were used, as shown here.

Finally, the results presented in this paper are interpreted in the light of the cell partitioning mechanism proposed for erythrocytes in non-charge-sensitive systems[12,14,15]. Taking into account the charge of the system and the lower surface charge of bone marrow cells with respect to erythrocytes[16], this mechanisms may serve to explain the higher efficiency of bone marrow cell fractionation by CCD with lengthened settling time[6].

EXPERIMENTAL

Preparation of cells

Male Wistar rats (150–250 g) were anaesthetized with diethyl ether and killed by exsanguination. Bone marrow cell suspensions were prepared from the femur and tibia of at least five rats using a phosphate buffer (pH 6.8) saline solution (SSP) as previously described[17]. Bone marrow cells were resuspended in SSP, usually 1:1 (v/v). The total number of cells in the bone marrow cell suspensions was $9.48 \pm 3.61 \cdot 10^8$ cells/ml ($n = 36$). Blood was collected into heparinized tubes and, after centrifugation (400 g for 10 min), erythrocytes were washed three times with SSP.

Preparation of two-phase systems

Charge-sensitive two-phase systems, containing 0.03 mol/l sodium chloride and 0.09 mol/l sodium phosphate buffer (pH 6.8), were prepared and equilibrated as previously described[6,16]. The increasing polymer concentrations, expressed as % (w/w) dextran T-500 (D) (Pharmacia)–% (w/w) polyethylene glycol 6000 (PEG) (Serva), were 5.0–4.0, 5.2–4.2, 5.3–4.3 and 5.6–4.6.

Single partition experiments

Either 100 μl of bone marrow cell suspension or 5 μl of packed erythocytes were added to the phase systems formed by 2 g of bottom phase and 2 g of top phase from the above equilibrated phase systems. As equal volumes of both phases (phases density *ca.* 1)[4] are then being used, the top-to-bottom phase-volume ratio at equilibrium is $L = 1$, which is the normal phase-volume ratio used for cells in single partition experiments[3,12]. Systems were mixed by 60 inversions and allowed time to separate at 4°C. Duplicate aliquots were removed from the top phase at different times (10, 20, 40, 60 or 80 min). Haemoglobin[18] and protein[19] concentrations were measured and cells were counted in a Model ZBI Coulter counter. The partition ratio, P, is the amount of haemoglobin, protein or cells in the top phase given as a percentage of the total cells added to the system. P values were calculated by taking into account phase dilution from sample addition and top phase volume[3,4]

Counter-current distribution (multiple partitions)

An automatic thin-layer CCD apparatus (Bioshef TLCCD, MK3) with two 60-cavity circular rotors was used[4,20]. Each of five adjacent cavities of the rotor received a mixture of 0.6 ml of D-rich bottom phase and 0.1 ml of bone marrow cell suspension, while the other 55 cavities each received 0.7 ml of the bottom phase. Two different volumes (0.9 or 0.4 ml) of the top PEG-rich phase were then added to all sixty cavities to reach two different heights of phase columns. These are given by the top-to-bottom phase-volume ration, L, which was 1.3 (*i.e.*, 0.9/0.7 ml) or 0.6 (0.4/0.7 ml). The normal phase-volume ratio at phase equilibrium used for red cells on CCD is $L = 1.3$[3,21]. A partition step is formed by a 20-s shaking time, settling time (5 or 20 min) and a twist of the top rotor plate to transfer the top phase cavity to the next bottom phase cavity on the lower rotor plate. With each transfer the cells in the top phase are carried forward and re-extracted with the fresh bottom phase. Cavities of the lower (stator) plate contained 88% of their total capacity, thus allowing enough space for the cells to be adsorbed at the interface during each partition step. Fifty-five transfers were repeated at 4°C. More details are given in ref. 6.

The distribution of cells in the different cavities along the extraction train (*i.e.*, the CCD profile) is given in terms of absorbance at 410 nm (Uvikon 810 spectrophotometer; Kontron) and haemoglobin concentration[18]. Cells with affinity for the top phase (high P values) are distributed as fast-moving cells and migrate to the higher numbered fractions (*i.e.*, towards the right-hand side of the CCD profile). Cells with affinity for the interface (lower P values), and as slow moving cells, tend to remain in the fraction with a lower number (*i.e.*, towards the left-hand side of the CCD profile).

RESULTS AND DISCUSSION

Cell partition in single test-tube experiments

The partitioning of erythrocytes[3,12,16] and bone marrow cells[16], as a function of the increase in polymer concentration used to increase the interfacial tension, is mainly determined by hydrophobicity, in non-charge-sensitive systems, or charge, in charge-sensitive systems, of the cell surface. In all these studies a standard settling time (usually 20 min) was used. However, partitioning depends on the specific interaction between cells and microscopic D droplets suspended in the PEG-rich upper phase and the settling speed of cell–D droplet complexes to the bulk interface as phase separation proceeds[12]. This means that cellular P values are a function of the sampling time, *i.e.*, the phase settling time. Our objective was to study the dependence of P values on settling time (up to 80 min) with increase in interfacial tension, for both homogeneous (erythrocytes) and heterogeneous (bone marrow) cell populations in charge-sensitive systems. Low, intermediate and high interfacial tension systems, formed by concentrations that were very close [5.0% (w/w) D–4.0% (w/w) PEG], close [5.3% (w/w) D–4.3% (w/w) PEG] and at some distance [5.6% (w/w) D–4.6% (w/w) PEG] from the critical point[4] were used here.

Erythrocyte partition

Low and intermediate interfacial tension systems. The dependence of P values on settling time with increase in interfacial tension has only been studied for erythrocytes in non-charge-sensitive systems[12,15]. The marked decrease with time of P values (60% at 80 min) observed in a low interfacial tension system [5.0% (w/w) D–4.0% (w/w) PEG] is a consequence of almost all the erythrocytes being associated with D droplets in the PEG-rich top phase and the fact that cell–D droplet complexes settle to the interface more rapidly than do free cells[12,14]. The interaction of cells with D droplets is reduced in charge-sensitive systems with a low interfacial tension[3,12] and, therefore, more free cells should be present in the upper phase. The high P values shown by erythrocytes in these systems[3,12,16,22] could therefore be due to slow sedimentation by the abundant free cells in the upper phase.

The decrease with time of P values in charge-sensitive systems with a low [5.0% (w/w) D–4.0% (w/w) PEG; Fig. 1A] or intermediate [5.3% (w/w) D–4.3% (w/w) PEG; Fig. 1B] interfacial tension seems not to be very pronounced (*ca.* 10% decrease at 20 min and 20–25% decrease at 80 min in both instances). It may be that erythrocytes (negatively charged at pH 6.8) tend to remain in the positive PEG-rich upper phase as free cells. The upper phase is positive with respect to the D-rich bottom phase, because phosphate partition towards this phase is asymmetric. Another contribution to the increase in the number of free cells in the upper phase may be electrostatic repulsion between cells and the phosphate-rich negative D droplets in the upper phase. As a consequence, interaction between cells and D droplets would be weaker in charge-sensitive systems than in non-charge-sensitive systems and a larger number of free cells would be present in the upper phase of charge-sensitive systems[12]. As free cells settle more slowly than cell–D droplet complexes, a smaller number of total cells are adsorbed at the interface at any given settling time and the decrease over time of the high P values is slow at both interfacial tensions (Fig. 1A and B).

The fact that erythrocytes are mainly free in the upper phase was supported by

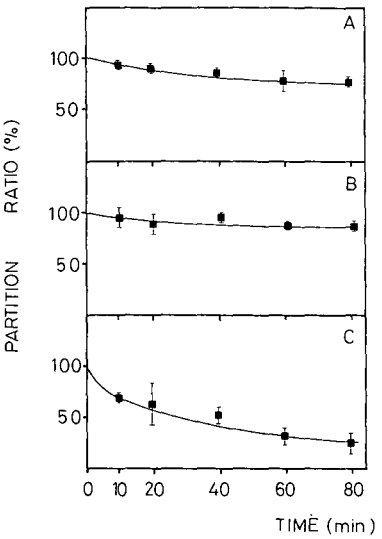

Fig. 1. Partitioning behaviour of erythrocytes with increase in phase settling time and interfacial tension in charge-sensitive systems. Partition values, *P*, in (A) 5.0% (w/w) D–4.0% (w/w) PEG, (B) 5.3% (w/w) D–4.3% (w/w) PEG and (C) 5.6% (w/w) D–4.6% (w/w) PEG two-phase systems are given in terms of haemoglobin content in the top phase as a percentage of that present in the total cells added. Points represent the means (± S.D.) at least of four separate partition experiments, each samples and measured in duplicate.

the results of additional cell partitioning experiments. A mixture of erythrocytes and the upper phase of a charge-sensitive system was carefully added to an equal volume of bottom phase from a similar system (thus forming a D droplet-free two-phase system). The proportion of cells remaining unsedimented after an 80-min settling time (higher than 80%; results not shown) is similar to *P* values obtained by mixing the two-phase system (Fig. 1A).

High interfacial tension systems. Increasing interfacial tension leaves a higher proportion of cell–D droplet complexes in the upper phase of non-charge-sensitive systems and results in a more pronounced decrease in *P* values with time than that found in low interfacial tension systems[12] The partition of erythrocytes in charge-sensitive systems of 5.6% (w/w) D–4.6% (w/w) PEG (far away from the critical point) also shows a marked decrease with time (50% at 20 min; 75% at 80 min) (Fig. 1C). This means that, in comparison with the data in Fig. 1A and B, a smaller number of free cells (*i.e.*, a larger proportion of cell–D droplet complexes) are present in the upper phase at any given settling time. The larger proportion of cell–D droplet complexes and their faster settling at the interface can explain the marked decrease in partition values over time (Fig. 1C). The effect of the large potential difference between the phases of charge-sensitive systems is then overcome by the effect of the high interfacial tension. This agrees with the decrease in sensitivity by charge-sensitive systems to the surface charge of erythrocytes with increase in polymer concentration[16].

Bone marrow cell partition

Low and intermediate interfacial tension systems. Variations with time of P values are shown in Fig. 2 for low [5.0% (w/w) D–4.0% (w/w) PEG; Fig. 2A] and intermediate [5.3% (w/w) D–4.3% (w/w) PEG; Fig. 2B] interfacial tension systems. Because of bone marrow cell heterogeneity, P values are expressed in terms of cell number, protein content and haemoglobin levels (as an index of erythroid cells). No significant differences were found between these parameters.

A small decrease in P values with time (*ca.* 20–25% at 20 min and 30–40% at 80 min) is observed in charge-sensitive systems with low interfacial tension (Fig. 2A). This decrease is slightly higher than that shown by erythrocytes in a similar system (10% at 20 min and 20–25% at 80 min; Fig. 1A). The surface-charge dependence of P values on the electrical potential difference between the phases is lower for bone marrow cells (as a reflection of their lower surface charge at pH 6.8) than for erythrocytes[16]. Interaction with the positive PEG-rich upper phase will then be weaker for bone marrow cells, implying that a smaller number of free cells (and a larger amount of cell–D droplet complexes) are present in the upper phase at any settling time. The larger proportion and the higher mobility of cell–D droplet complexes at the interface serve to explain the small decrease in P values over time in Fig. 2A.

The fact that a smaller number of free bone marrow cells are present in the upper phase is also supported by additional experiments carried out as for erythrocytes. A mixture of bone marrow cells and upper phase was carefully added to the bottom phases. The proportion of unsedimented cells after 80 min (*ca.* 80%; results not shown) is higher than P values obtained by mixing the two-phase system (60–70%; Fig. 1A).

The decrease with time of P values in intermediate interfacial tension systems is clearly higher for bone marrow cells (45–50% at 20 min and 75–80% at 80 min; Fig. 2B) than for erythrocytes (10% at 20 min and 20–25% at 80 min; Fig. 1B). Both the low negative surface charge of the bone marrow cells[16] and the increase in interfacial

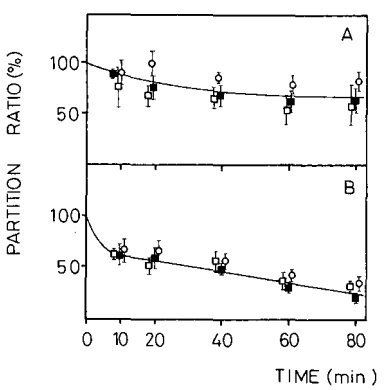

Fig. 2. Partitioning behaviour of bone marrow cells with increase in phase settling time and interfacial tension in charge-sensitive systems. Partition values, P, in (A) 5.0% (w/w) D–4.0% (w/w) PEG and (B) 5.3% (w/w) D–4.3% (w/w) PEG two-phase systems are given in terms of (■) haemoglobin, (□) protein content and (○) cell number in the top phase as a percentage of that present in the total cells added. Points represents the means (± S.D.) of at least four separate partition experiments, each sampled and measured in duplicate.

tension favour a decrease in P values over time. The proportion of rapidly moving cell–D droplet complexes is higher in the upper phase. Therefore, the tendency for bone marrow cells to remain as free cells in the upper phase can be assumed to be lower.

High interfacial tension systems. Experiments were also carried out at a 5.6% (w/w) D–6.6% (w/w) PEG polymer concentration (results not shown). The decrease in P values over time was nearly total (75% at 20 min and >90% at 80 min), indicating that this cell population moves quickly (in the form of cell–D droplet complexes) to the interface. The effect of this high interfacial tension again overcomes the effect of the potential difference on the partitioning of bone marrow cells. The number of cell–D droplet complexes formed increases progressively from low to high interfacial tension values. The increase in interfacial tension then favours the adsorption of cell–D droplet complexes at the interface more in bone marrow cells than in erythrocytes.

Bone marrow cell fractionation by counter-current distribution

Improved fractionation of heterogeneous cell populations has been observed previously when the settling times are longer (20 min) than those usually employed (5–7 min) during thin-layer CCD in low-interfacial charge-sensitive systems. CCD profiles with at least two or three peaks (due to the presence of different cell subpopulations) were always obtained. The increase in settling time did not improve the fractionation of homogenous erythrocyte populations where single-peak profiles were observed[5,6,8–11].

These observations were studied in this work using higher interfacial tension-systems, which facilitate phase separation and therefore sedimentation of the cell–D droplet complexes. As P values for bone marrow cells decrease with increase in interfacial tension (Fig. 2A and ref. 16), the possibility exists of employing a shorter settling time during the fractionation and so improve cell resolution.

Another factor determining the speed of phase settling is the height of the phase column. The more rapid settling of phases produced by reducing the height of the phase column in the thin-layer CCD rotor seems to decrease the interaction of cells with D droplets, thereby interfering with the cell partitioning mechanism, which, in turn, may result in a lower efficiency of cell fractionation[13]. As weak interaction between cells and D droplets in charge-sensitive systems has already been shown (preceding section), reducing the height of the phase column in the CCD rotor should not affect the cell partitioning mechanism in these systems significantly. In fact, fractionation of heterogeneous bone marrow cells is not improved by just shortening the height of the phase column (for instance, reducing the volume of the upper phase) in the cavities of the CCD rotor. A longer settling time (20 min) than that usually employed (5–7 min) was simultaneously required to improve cell fractionation[6]. Therefore, experiments were carried out at both a short (5 min; Fig. 3) and a long (20 min; Fig. 4) settling time, using three systems with a range of low and intermediate interfacial tension values [5.0% (w/w) D–4.0% (w/w) PEG; 5.2% (w/w) D–4.2% (w/w) PEG; 5.3% (w/w) D–4.3% (w/w) PEG]. Bone marrow cells are totally adsorbed at the interface of systems with higher interfacial tension (preceding section), and therefore they cannot be used.

Fractionation at short settling times. Representative CCD profiles for the fractionation of bone marrow cells, at a short settling time (5 min), are shown in charge-sensitive systems with low (Fig. 3A) and intermediate (Fig. 3B and C) interfacial tensions. A high (L = 0.9/0.7 = 1.3) and a low (L = 0.4/0.7 = 0.6) phase column were employed. Results are given for a high phase column (L = 1.3; Fig. 3) as similar single-peak profiles, located in the earlier cavities of the rotor, were also obtained for a low-phase column (L = 0.6; results not shown).

Assuming that a high proportion of free bone marrow cells is present in the upper phase of low interfacial tension systems (high P values; see discussion for Fig. 2A) and that free cells settle slowly towards the interface[12], a displacement of free cells in the top phase of each cavity towards the next one may take place during the CCD procedure. A low fractionation efficiency (single-peak profile) is obtained as a consequence of free cell displacement towards the high-numbered cavities of the CCD rotor (Fig. 3A and ref. 6). In contrast, the fractionation of bone marrow cells in non-charge-sensitive systems, at both a similar interfacial tension value and a short settling time, gave rise to two broad subpopulations[23,24], as a result of the small proportion of free bone marrow cells in the upper phase of low interfacial tension systems (low p values; ref. 16) and the fact that cells bound to D droplets settle rapidly towards the interface[12].

Owing to the rising affinity of bone marrow cells for D droplets with increase in interfacial tension, the P values decrease (Fig. 2 and ref. 16). However, improved fractionation was not achieved by increasing the interfacial tension of the systems. As shown, a single-peak profile was also obtained in intermediate interfacial tension

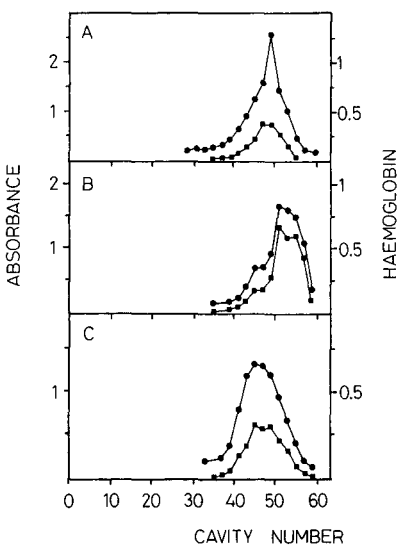

Fig. 3. Influence of interfacial tension on the fractionation by thin-layer CCD of rat bone marrow cells, at a short settling time (5 min). Two-phase systems contained (A) 5.0% (w/w) D–4.0% (w/w) PEG, (B) 5.2% (w/w) D–4.2% (w/w) PEG and (C) 5.3% (w/w) D–4.3% (w/w) PEG polymer concentrations. Distribution of cells is given in terms of (●) absorbance (410 nm) and (■) haemoglobin (mg/ml) present in each cavity of the distribution rotor. See text for details.

systems [5.2% (w/w) D–4.2% (w/w) PEG, Fig. 3B, 5.3% (w/w) D–4.3% (w/w) PEG, Fig. 3C]. In summary, a short settling time (5 min) was not long enough to improve the fractionation of bone marrow cells at any suitable polymer concentration.

Fractionation at long settling times. Representative CCD profiles for bone marrow cell fractionations at a long (20 min) settling time, in charge-sensitive systems with low and intermediate interfacial tension values, are shown in Fig. 4A–C. When using a low phase column (upper phase 0.4 ml; $L = 0.6$), fractionation into two broad subpopulations at any polymer concentration is observed (Fig. 4). However, when using a higher phase column (upper phase 0.9 ml; $L = 1.3$) only single-peak profiles were obtained (ref. 6 and results not shown). This means that settling time combined with the decrease in the height of the phase column affects the fractionation of heterogeneous bone marrow cells more significantly than does the increase in polymer concentration. Similar conclusions have been reached in experiments with heterogeneous avian red cell populations during animal development. CCD fractionation in two subpopulations was obtained, in this instance, by using a slightly higher volume of upper phase (0.7 ml) and a 20-min settling time[9–11].

A comment must be made in relation to the improvement in fractionation using a low phase column, *i.e.*, those made using a lower volume (0.4 ml) of upper phase. As free cells predominate in the upper phase of charge-sensitive systems, the more rapid settling of phases produced by reducing the height of the phase column should not, by itself, affect the partitioning behaviour of cells during CCD fractionation. However, the shorter distance between the cells ad the interface, and the longer settling time, are both parameters that favour free cell sedimentation and therefore influence CCD separation. It can then be suggested that most of the free cells (those with a high surface charge in the bone marrow cell population) would be those located in the high-numbered cavities of the CCD profile (around cavities 30–50, Fig. 4), whereas

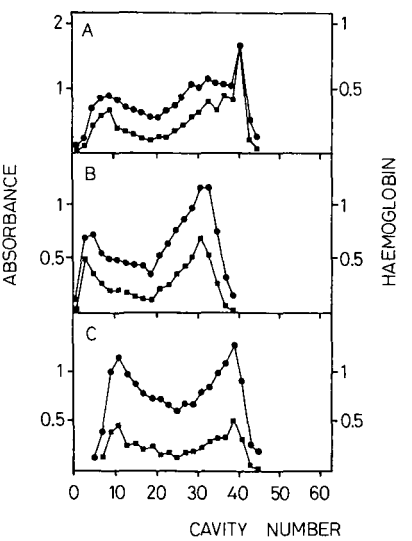

Fig. 4. Influence of interfacial tension on the fractionation by thin-layer CCD of rat bone marrow cells, at a long settling time (20 min). Two-phase systems and symbols as in Fig. 3. See text for details.

cell–D droplet complexes, because of their faster sedimentation, would be located in the low-numbered cavities (between 5 and 20, Fig. 4).

In summary, more efficient CCD fractionation of bone marrow cells is achieved when a long settling time (20 min) and a short phase column ($L = 0.6$) are used. Changes in interfacial tension then seem not to be as important as variations in settling time and phase column height to improve the efficiency of bone marrow fractionation. The above results support the necessity of taking these two parameters into account when attempting the CCD fractionation of heterogeneous cell populations in charge-sensitive systems.

ACKNOWLEDGEMENTS

This work was supported by a grant from the Comisión Internacional de Ciencia y Tecnologia (PBT85-0048), Spain. We thank the Excma. Diputación Provincial de Guadalajara, Spain, for a fellowship to A.-I. G.-P., and C. F. Warren of the Instituto de Ciencias de la Educación de la Universidad de Alcalá de Henares for editorial assistance.

REFERENCES

1 P. A. Albertsson, *Anal. Biochem.*, 11 (1965) 121.
2 D. Fisher, *Biochem. J.*, 196 (1981) 1.
3 H. Walter, in H. Walter, D. E. Brooks and D. Fisher (Editors), *Partitioning in Aqueous Two-Phase Systems: Theory, Methods, Uses and Applications to Biotechnology*, Academic Press, New York, 1985, p. 328.
4 P. A. Albertsson, *Partition of Cell Particles and Macromolecules*, 3rd ed., Wiley, New York, 1986.
5 M. D. Delgado, A. I. Garcia-Perez, M. Pinilla, M. N. Recio, P. Sancho and J. Luque, *An. R. Acad. Farm.*, 50 (1984) 145.
6 P. Sancho, M. D. Delgado, A. I. Garcia-Perez and J. Luque, *J. Chromatogr.*, 380 (1986) 339.
7 J. Luque, M. D. Delgado, E. Ferrer, M. Moreno, M. Pinilla and P. Sancho, in I. N. Rich (Editor), *Molecular and Cellular Aspects of Erythropoietin and Erythropoiesis (NATO Science Series*, Vol. H8), Springer, Berlin, 1987, p. 353.
8 A. Ruiz-Ruano, M. Martín and J. Luque, *Cell Biochem. Funct.*, 2 (1984) 257.
9 M. Martin and J. Luque, *Br. Poult. Sci.*, 26 (1985) 163.
10 E. Ferrer, M. Martin, R. Alonso and J. Luque, *J. Chromatogr.*, 411 (1987) 167.
11 E. Ferrer, M. Martin, R. Alonso and J. Luque, *J. Chromatogr.*, 455 (1988) 327.
12 F. D. Raymond and D. Fischer, *Biochim. Biophys. Acta*, 596 (1980) 445.
13 H. Walter and E. J. Krob, *Biochim. Biophys. Acta*, 966 (1988) 65.
14 D. Fisher and H. Walter, *Biochim. Biophys. Acta*, 801 (1984) 106.
15 D. E. Brooks, K. Sharpe and D. Fisher, in H. Walter, D. E. Brooks and D. Fisher (Editors), *Partitioning in Aqueous Two-Phase Systems: Theory, Methods, Uses and Applications to Biotechnology*, Academic Press, New York, 1985, p. 11.
16 A. I. Garcia-Perez, M. N. Recio, P. Sancho and J. Luque, *J. Chromatogr.*, 403 (1987) 131.
17 M. Pineda, M. Pinilla and J. Luque, *Cell Biochem. Funct.*, 2 (1984) 254.
18 W. G. Zijlstra and E. J. Van Kampen, *J. Clin. Chem. Clin. Biochem.*, 19 (1981) 521.
19 O. H. Lowry, N. J. Rosebroug, A. L. Farr and R. L. Randal, *J. Biol. Chem.*, 193 (1951) 265.
20 T. Treffry, P. T. Sharpe, J. Walter and D. E. Brooks, in H. Walter, D. E. Brooks and D. Fisher (Editors), *Partitioning in Aqueous Two-Phase Systems: Theory, Methods, Uses and Applications to Biotechnology*, Academic Press, New York, 1985, p. 132.
21 H. Walter, *Methods Cell Biol.*, 9 (1975) 25.
22 P. S. Gascoine and D. Fisher, *Biochem. Soc. Trans.*, 12 (1984) 1084.
23 O. M. Smith, E. S. Green, G. E. Francis and D. Fisher, *Biochem. Soc. Trans.*, 14 (1986) 752.
24 A. I. García-Pérez, J. Mendieta, P. Sancho and J. Luque, in preparation.

Journal of Chromatography, 504 (1990) 89–95
Elsevier Science Publishers B.V., Amsterdam — Printed in The Netherlands

CHROM. 22 172

Study of the dynamic binding capacity of two anion exchangers using bovine serum albumin as a model protein

AMOS M. TSAI* and DAVID ENGLERT
Pharmacia–LKB Biotechnology, 800 Centennial Avenue, Piscataway, NJ 08854 (U.S.A.)
and
EARL E. GRAHAM
Department of Chemical Engineering, Cleveland State University, Cleveland, OH 44115 (U.S.A.)
(First received April 4th, 1989; revised manuscript received September 12th, 1989)

SUMMARY

The dynamic binding capacity (DBC) of two anion exchangers (particle sizes 30 and 90 μm) were evaluated using bovine serum albumin as a model protein. The DBC showed a Langmuirian dependence on protein concentration. In general, the DBC decreased with increased loading flow-rate, but this dependence was insignificant with long (10- and 20-cm) columns. The DBC of the 30-μm anion exchanger was only slightly dependent on flow-rate even in short (5-cm) columns. The breakthrough curves were generally steeper with narrow columns and with the 30-μm material.

INTRODUCTION

In preparative chromatography, the maximum throughput is important for economic reasons; one would like to load as much protein in as little time as possible. As suggested by Chase[1], frontal analysis can be used to evaluate the dynamic binding capacity (DBC) of a chromatographic matrix. The protein is continuously loaded onto the column at a particular flow-rate until breakthrough of the feed stream occurs. The amount of protein that has been applied at this point is the DBC. If one continues to feed the protein through the column, a breakthrough curve is generated, its slope representing the rate of increase in protein concentration in the effluent. The sharpness of such a curve provides a measure of the binding efficiency and a clue to the kinetics involved. This approach is far better than performing batch studies, as it represents real operating conditions.

The DBC for a particular protein is dependent on many factors[2]: the nature of the gel matrix[3,4], the flow-rate at which the protein is applied to the column, the column dimensions (*i.e.*, column diameter and bed height), protein size, film, pore and overall diffusion constants of the protein and the nature of the adsorption isotherm of the protein. Regnier and co-workers[4–6] have collected extensive data on various parameters that affect the intrinsic loading capacity of silica-based materials

0021-9673/90/$03.50

for both reversed-phase and anion-exchange chromatography of proteins. Protein binding depended on the accessible surface binding sites rather than the total surface area, and the pore size affected not only the loading capacity but also the resolution of the proteins. An extensive review on ion-exchange chromatography was published by Helfferich[7]. Despite recent advances in the theoretical understanding of chromatographic processes[8–13], protein chromatography still remains largely empirical. Recently, Kopaciewicz *et al.*[14] studied the effects of particle, pore and protein sizes on the binding capacity of silica-based media. In their study, both static and dynamic experiments were carried out. They found that the DBC was inversely proportional to flow-rate and particle size, and the magnitude of these relationships depended strongly on the pore size of the media. The purpose of this work was to study experimentally the effect of loading flow-rate, column dimensions, gel particle size and initial concentration on the DBC of two agarose-based media for a protein.

EXPERIMENTAL

Materials

Bovine serum albumin (BSA) (fraction V) was purchased from Miles Diagnostics. The two anion exchangers tested were Q Sepharose Fast Flow (FF) and Q Sepharose High Performance (HP) (Pharmacia). Both of these gels are 6% cross-linked agarose-based media with similar pore-size distributions (they both have exclusion limit of 4×10^6 daltons). Their average bead sizes are 90 and 30 μm, respectively. In addition, they share similar chemical properties with $-CH_2N^+(CH_3)_3$ as the ion exchange group. Analytical-reagent grade Tris–HCl was obtained from Sigma, and the fast protein liquid chromatographic (FPLC) system and HR columns (Pharmacia) were used throughout this study.

Methods

The DBC of Q Sepharose Fast Flow and Q Sepharose High Performance were evaluated using BSA as a model protein. The DBC is defined as the sample load at which the sample concentration of the effluent, monitored by UV absorbance at 280 nm, is 10% of the input stream. This is expressed as milligrams of BSA per millilitre of packed gel. The slopes of the breakthrough curves are approximated by the straight line connecting 10% and 90% of maximum deflection of the UV trace. Columns of I.D. 5 and 10 mm were packed at bed heights of 5, 10 and 20 cm under a linear flow-rate of 5 cm/min. BSA, dissolved in 50 m*M* Tris–HCl, pH 7.0 at 10 mg/ml, was fed through the gel matrices at linear flow-rates from 0.25 to 4.0 cm/min. The DBC was determined as a function of four parameters: the linear sample loading flow-rate (F), the column diameter (D), the packed bed height (H) and the average particle size of the gel. Experiments were performed according to the combinations of F, H and D listed in Table I, and two data points were collected for each combination.

The DBC was also determined as a function of initial protein concentration according to Table II. A 5 mm I.D. column packed with 90 μm FF material to a height of 10 cm was used for this study. BSA at concentrations from 1 to 10 mg/ml was loaded onto the column at 1.0 or 4.0 cm/min.

All experiments were performed at room temperature. To avoid systematic effects due to uncontrolled variables such as small temperature fluctuations, the order of the experiments was randomized.

TABLE I

AVERAGE VALUES OF DBC FOR ALL EXPERIMENTAL COMBINATIONS OF *F*, *H*, *D*, AND PARTICLE SIZE

Linear velocity, F (cm/min)	*Bed height, H (cm)*	*Column diameter, D (mm)*	*DBC (mg BSA/ml packed gel)*	
			30 μm	*90 μm*
0.25	5	5	86.3	68.7
0.50	5	5	86.7	68.0
1.00	5	5	85.6	66.3
2.00	5	5	84.6	64.7
4.00	5	5	84.6	56.2
0.25	5	10	59.6	66.5
0.50	5	10	57.2	65.3
1.00	5	10	60.0	63.2
2.00	5	10	50.0	59.6
4.00	5	10	57.3	45.6
0.25	10	5	77.1	72.1
0.50	10	5	77.7	71.4
1.00	10	5	78.0	70.3
2.00	10	5	76.4	69.1
4.00	10	5	76.0	66.0
0.25	10	10	71.6	61.1
0.50	10	10	70.7	58.8
1.00	10	10	71.3	60.0
2.00	10	10	69.1	56.8
4.00	10	10	68.1	56.7
0.25	20	5	72.2	67.4
0.50	20	5	72.9	67.3
1.00	20	5	72.4	66.3
2.00	20	5	71.7	66.8
4.00	20	5	72.2	66.5
0.25	20	10	64.7	62.9
0.50	20	10	63.6	62.2
1.00	20	10	63.2	61.8
2.00	20	10	61.5	61.8
4.00	20	10	62.0	60.9

RESULTS AND DISCUSSION

Effect of gel particle size

In Fig. 1, DBC is plotted against linear flow-rate. Each line is associated with a particular column dimension. The DBC of both media are similar. The 30-μm HP material showed only a very small dependence on flow-rate even in the 5-cm column. The 90-μm material showed a substantial decrease in the DBC with flow-rate only in the 5-cm column.

TABLE II

DBC VALUES AS A FUNCTION OF INITIAL PROTEIN CONCENTRATION TESTED WITH A 10 cm × 5 mm I.D. COLUMN USING THE 90-μm BEADS

Initial concentration (mg/ml)	*DBC (mg BSA/ml packed gel)*	
	0.2 ml/min	*0.8 ml/min*
1	50.5	53.0
2	55.6	56.2
4	61.4	59.8
6	71.3	65.8
8	72.0	69.1
10	74.4	72.4

The sharpness of the breakthrough curves is presented in Fig. 2 in the same manner as in Fig. 1. This is expressed as the rate of increase in the effluent concentration with respect to the amount of BSA applied. The 30-μm material achieves a steeper breakthrough slope, and hence a more efficient binding of protein, than the

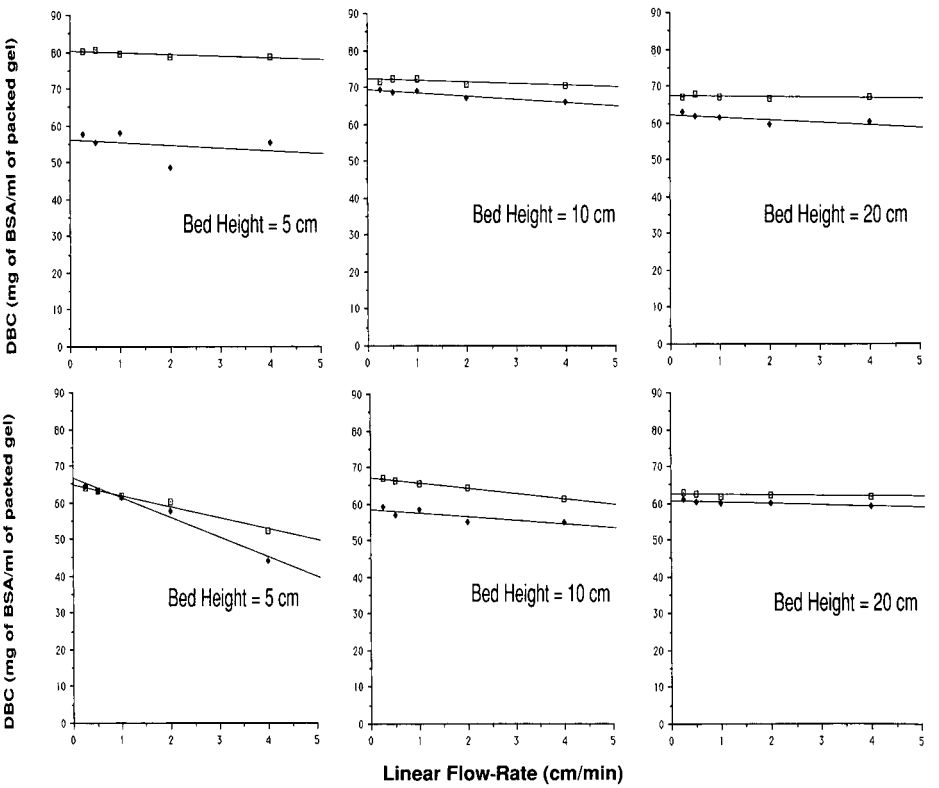

Fig. 1. DBC *vs.* linear flow-rate for (top) the 30-μm gel and (bottom) the 90-μm gel. □ = 5 mm I.D.; ◆ = 10 mm I.D.

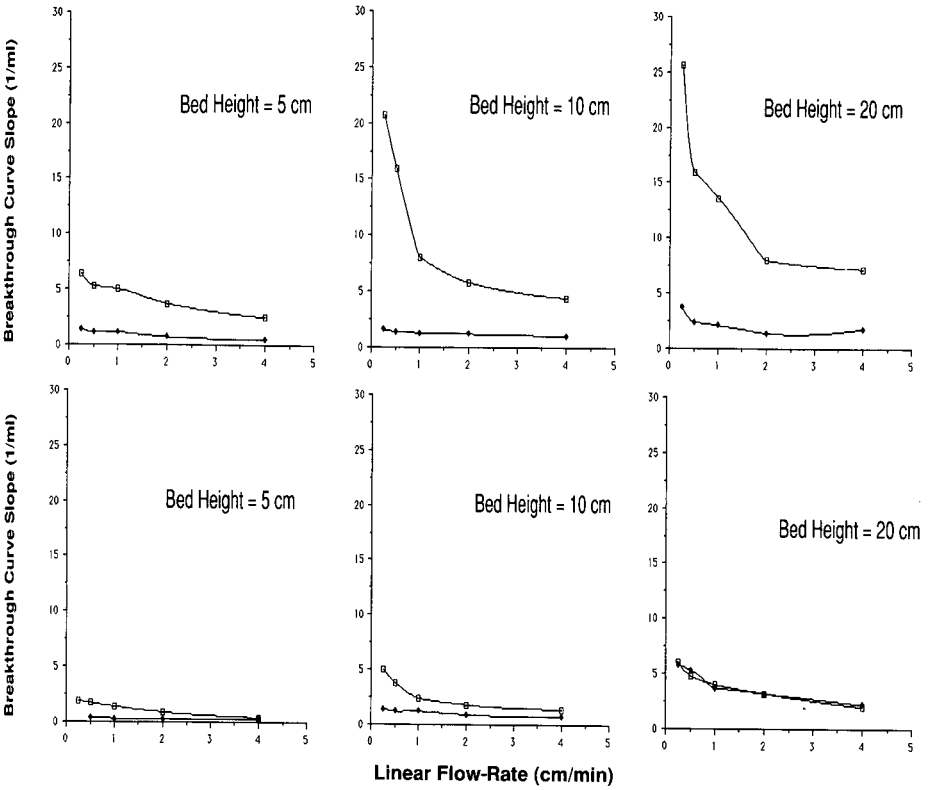

Fig. 2. Breakthrough curve slope *vs.* linear flow-rate for (top) the 30-μm gel and (bottom) the 90-μm gel. □ = 5 mm I.D.; ◆ = 10 mm I.D.

90-μm beads. The rate of protein adsorption, particularly for large proteins, is improved when small gel particles are used[15]. This is due to the increase in surface area and shorter intraparticle diffusion path. Assuming a two-phase model, the increase in surface area facilitates film diffusion and results in a higher DBC. The shorter pore diffusion path allows a faster adsorption of protein and thus a higher adsorption efficiency.

Coupling effect of bed height and linear flow-rate

In Fig. 1, the DBC of the 90-μm material becomes less dependent on the flow-rate as the bed height increases from 5 to 20 cm. When the bed height reaches 20 cm, one can increase the loading flow-rate 16-fold (from 0.25 to 4.0 cm/min) with only a slight decrease in the DBC. As for the 30-μm material, the DBC has very little dependence on the flow-rate at all the bed heights tested. In addition, steeper breakthroughs are associated with a lower loading flow-rate for both media, as shown in Fig. 2.

In general, an increase in linear flow-rate corresponds to a decrease in the DBC. This is largely due to the mass-transfer resistance experienced by the protein. At high loading flow-rates, not enough time is allowed for pore diffusion, and poor utilization

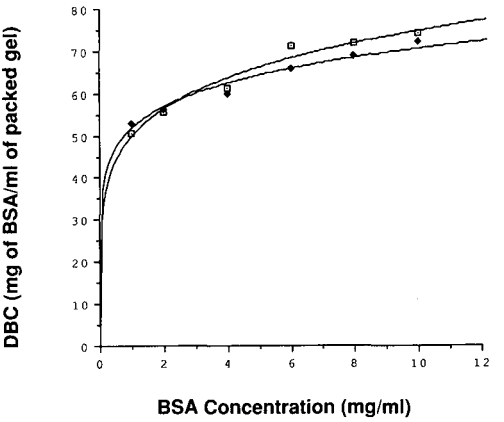

Fig. 3. DBC *vs.* initial BSA concentration at different flow-rates. □ = 1.0 cm/min; ◆ = 4.0 cm/min.

of the gel bed results. For the 90-μm FF material, we found that the effect of linear flow-rate on the DBC decreases with increasing bed height. A longer gel bed allows for a longer residence time, and therefore more time for pore diffusion to be completed. When using larger gel particles, a long gel bed is recommended to maximize throughput in the sample loading stage. Naturally, when using a long column, the tradeoffs are a higher operating back-pressure and an increased separation time.

Effect of protein concentration

In Fig. 3, the DBC of the 90-μm FF material is plotted against protein concentration for two loading flow-rates. These two curves are Langmuirian. If batch adsorption of BSA on an ion exchanger is of the Langmuir type, the dynamic adsorption of this protein may exhibit a deviation from Langmuirian behavior owing to the kinetic effect[16]. In this instance, a 10-cm bed was used to guarantee efficient gel utilization, which explains the similarity of the curves at two different flow-rates.

Effect of column diameter

A higher DBC and a steeper breakthrough are associated with the 5-mm I.D. columns. We attribute this effect of column diameter to an uneven radial distribution of protein during sample loading.

CONCLUSIONS

When using smaller particles (HP medium, 30 μm), the DBC hardly depends on the loading flow-rate even in a short column. Also, steeper breakthroughs are associated with smaller particles. The tradeoff here is a higher operating pressure.

A long gel bed can compensate for the effect of flow-rate on the DBC when larger gel particles (FF medium, 90 μm) are used. The tradeoffs here are a higher operating pressure and a longer separation time owing to the long column.

Dynamic adsorptions at different flow-rates display similar Langmuirian behavior if efficient mass transfer is maintained.

ACKNOWLEDGEMENTS

We thank Mr. Charlie Mason for his important suggestions in formulating this study and Phil Roberts, John Mural and Carl Brown for performing the experiments.

REFERENCES

1 H. Chase, *J. Chromatogr.*, 297 (1984) 179.
2 J. C. Janson and P. Hedman, *Biotechnol. Prog.*, 3 (1987) 9.
3 M. Schmuck, D. Gooding and K. Gooding, *J. Chromatogr.*, 359 (1986) 323.
4 M. Rounds, W. Kopaciewicz and F. Regnier, *J. Chromatogr.*, 362 (1986) 187.
5 G. Vanecek and F. Regnier, *J. Chromatogr.*, 121 (1982) 156.
6 J. Pearson, N. Lin and F. Regnier, *J. Chromatogr.*, 124 (1982) 217.
7 F. Helfferich, *Ion Exchange*, McGraw-Hill, New York, 1962.
8 J. Knox and H. Pyper, *J. Chromatogr.*, 363 (1986) 1.
9 S. Ghodbane and G. Guiochon, *J. Chromatogr.*, 452 (1988) 209.
10 S. Ghodbane and G. Quiochon, *J. Chromatogr.*, 444 (1988) 275.
11 L. Snyder, G. Cox and P. Antle, *J. Chromatogr.*, 444 (1988) 303.
12 F. Arnold, S. Schofield and H. Blanch, *J. Chromatogr.*, 355 (1986) 1.
13 P. Lövkvist and J. Å. Jönsson, *J. Chromatogr.*, 356 (1986) 1.
14 W. Kopaciewicz, S. Fulton and S. Lee, *J. Chromatogr.*, 409 (1987) 111.
15 M. W. Phillips, G. Subramanian and S. Cramer, *J. Chromatogr.*, 454 (1988) 1.
16 D. M. Ruthven, *Principles of Adsorption and Adsorption Processes*, Wiley, New York, 1984.

Journal of Chromatography, 504 (1990) 97–112
Elsevier Science Publishers B.V., Amsterdam — Printed in The Netherlands

CHROM. 22 222

High-performance liquid chromatography separation media based on functional polymers containing phenolic hydroxyls

WESLEY A. ROLLS
Department of Chemistry, University of Ottawa, Ottawa, Ontario (Canada)
and
JEAN M. J. FRÉCHET*
Department of Chemistry, Baker Laboratory, Cornell University, Ithaca, NY 14853-1301 (U.S.A.)
(First received August 29th, 1989; revised manuscript received December 15th, 1989)

SUMMARY

New separation media based on highly cross-linked porous-bead polymers containing pendant phenolic groups have been prepared. The steric environment and acidity of the phenolic groups have been varied systematically to provide access to a new family of separation media useful in the separation of aromatic as well as aliphatic amines. The bead polymers with 10 μm average size are prepared by suspension polymerization of 4-*tert.*-butyloxycarbonyl (t-BOC) derivatives of 4-hydroxystyrene or analogues with alkyl substituents in positions 3 and 5, with divinylbenzene under conditions which afford polymers with surface areas of more than 200 m^2/g. The t-BOC groups are removed from the bead polymers by a thermolysis process which greatly facilitates bead processing. The unclassified polymers gave high-performance liquid chromatography columns with approximately 18 000 plates per meter and were found to be very effective in the separation of amines.

INTRODUCTION

In the last decade there has been a large increase in the number of polymer-based high-performance liquid chromatography (HPLC) columns available for difficult separations. This increase has come about even though the plate counts of the best of these materials cannot match those of most of the silica-based separation media. The latter have enjoyed immense popularity because silica-based separation media can be produced inexpensively with small particle sizes, narrow particle size distributions, very uniform pore structures and with enough mechanical stability to easily withstand the high pressures of modern HPLC[1]. These properties result in columns which have high plate counts and very high resolution. In addition, the reactive silanol groups on the silica surface can be reacted with a variety of organic moieties to give separation media with a wide range of polarities[1], some of which may, for example, be useful in the resolution of stereoisomers[2]. A significant draw-

0021-9673/90/$03.50

back of the silica columns is their lack of stability in basic media[3]. Their use under basic conditions leads to dissolution of the silica matrix with formation of large void volumes, which limits the kinds of separations that can be performed. In spite of recent efforts to shield the silica with bulky silanizing reagents[4] or thick layers of polymer[5], none of the currently available silica-based materials is truly stable over the entire pH range.

This pH instability has sparked interest in new materials such as polymeric HPLC resins because many of these offer pH stability over the entire pH range, which places fewer limitations on the kinds of separations that can be performed. The first resins prepared by suspension polymerization were rather large particles, 50–100 μm, which were not very useful for HPLC[6]. Gradual improvements in reactor design and suspension polymerization methodology[7] have allowed the reproducible large-scale preparation of resins with an average particle size of 5 μm. One of the first high-resolution polymeric HPLC columns was packed with the PRP-1 resin, introduced in 1980 by the Hamilton company[8]. This spherical, 10-μm macroporous resin is a copolymer of styrene and divinylbenzene, which is stable from pH 0 to 14 and can be used for the separation of a wide variety of organic molecules. Many other unique polymeric HPLC columns have since been introduced, including ion exchangers[9], unique reversed-phase columns[10] and a new graphitized carbon column[11]. Other developments in this field include the seeded polymerization technique introduced by Ugelstad and co-workers[12,13], which allows the production of monodisperse polymeric resins, thereby avoiding the time-consuming size classification which is necessary with conventional suspension polymerized resins. The newest innovation has been the pellicular polymeric resins[14], which have efficiencies approaching those of the silica-based materials in certain applications and are likely to see further advances in the near future.

This paper describes the chromatographic properties of a series of macroporous polymeric resins containing reactive phenolic functionalities. The design and synthesis of the monomers and polymers used in this study is described in detail elsewhere[15–17]. Substituted phenol resins were selected since the phenol moiety contains an acidic hydrogen atom that can form strong hydrogen bonds to basic compounds such as amines, as demonstrated previously[18] in the removal of ε-caprolactam from aqueous solutions by using large particles of a cross-linked poly(hydroxystyrene) resin. In our research, a series of 10-μm, rigid, spherical, macroporous beads (Fig. 1, structures **1–3**) were prepared, in which the acidity of the phenolic hydrogen and the steric environment around the phenolic hydrogen was changed systematically in order to observe the influence of structure on separation ability.

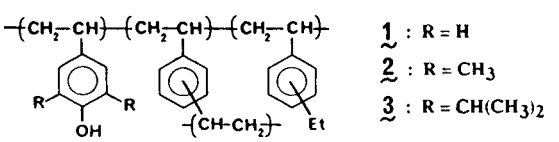

Fig. 1. Structure of the cross-linked bead polymers **1–3**. Et = Ethyl.

EXPERIMENTAL

Polymer beads were packed into HPLC columns with a Chromatem slurry packing machine for HPLC columns purchased from Touzart and Matignon. For a typical experiment, 1,5 g of polymer beads were suspended in 15 ml of slurry solvent (a balanced-density mixture as described in the section below) with the aid of sonication. This suspension was poured into the column packing tube and packed for 1 h at 3000 p.s.i. by using methanol as the packing solvent. The analytical HPLC equipment used included a Perkin-Elmer Sigma 15 chromatography data station, a Perkin-Elmer Series 10 liquid chromatograph, a Perkin-Elmer LC-25 refractive index (RI) detector, and a Rheodyne 7125 sample injector equipped with a 6-μl sample loop. Stainless steel columns (15 cm × 0.46 cm I.D.) were purchased from Mandel Scientific, and all stainless-steel frits were purchased from P.M. Instruments (Toronto, Canada). Plate/meter efficiencies of the columns were calculated from the half-width height of a pentane peak by using methanol as the mobile phase at a flow-rate of 0.5 ml/min. All solvents used were HPLC grade and all of the solutes injected on the columns were purchased from Aldrich. Thermogravimetric analyses were done with a Mettler TA 3000 at a heating rate of 10°C/min and under a nitrogen atmosphere. Detailed experimental procedures for monomer synthesis and suspension polymerizations, as well as procedures for porosity and particle size analysis, can be found elsewhere[15,16].

Determination of the balanced-density slurry

A balanced-density solvent mixture is a mixture of two solvents, one having a higher density and the other a lower density than the polymer beads[19], and the overall density matching that of the polymer beads. The quantities of the two solvents are adjusted so that the beads do not rise or fall in the slurry solvent mixture. This helps to give a more homogeneously packed column because the larger and heavier polymer beads will not tend to settle to the bottom of the column while the slurry is in the column packing apparatus; this is especially important for an unsized sample of polymer beads. In order to determine the balanced-density slurry, a small amount of polymer beads (enough to fit on the tip of a spatula) was placed in a 10-ml vial and 2 ml of carbon tetrachloride (density = 1.594 g/ml) were added. In this solvent the polymer beads float up to the top of the vial. Methanol (density = 0.791 g/ml) was then added to the vial from a buret in 0.1-ml increments, and the direction of travel of the polymer beads was observed after the addition of each increment. The addition of methanol was stopped when the particles began to sink towards the bottom of the vial because the balanced density of the slurry was reached at this point. For polymers **1** and **2**, the balanced-density slurry composition was methanol–carbon tetrachloride (1.2:1.0, v/v), while for polymer **3** it was methanol–carbon tetrachloride (1.4:1.0, v/v).

*Thermal cleavage of the t-BOC groups of **9**, **10** and **11***

These reactions were done in 100-ml round-bottom flasks equipped with adapters connecting the flasks to a high-vacuum pump. The flask containing the polymer beads were immersed in an oil bath preheated to 220–230°C and left for time periods adjusted according to the sample size. Our previous work with t-BOC-protected phenolic polymers[17,20] has shown that deprotection times can be reduced drastically to a few minutes by decreasing the size of the polymer sample or by using a slowly rotating

system for which heat transfer is greatly improved. Fourier transfrom infrared (FT-IR) spectra confirmed the complete removal of the t-BOC groups after the thermolysis reaction (loss of strong t-BOC carbonyl band centered near 1760 cm^{-1}).

RESULTS AND DISCUSSION

Design and synthesis of the resins

The conditions used in the synthesis of our series of substituted phenolic resins are outlined schematically in Fig. 2. Suspension copolymerization of the appropriate alkyl-substituted *p*-t-BOC styrene monomer (**4–6**) with commercial "divinylbenzene" (55% of **7** and 45% of **8**) at 80°C in the presence of a porogen gave a series of rigid, spherical, macroporous substituted phenolic resins (**9–11**). High stirring speeds (800 rpm) and high concentrations of suspension stabilizer [2% poly(vinyl alcohol) in water] were used as these conditions favor the formation of small beads. Cyclohexanol (60% of the total organic phase) was used as the porogen as it gave resins with high surface areas and porosities. Monomers **4–6**, containing the t-BOC protecting group, were chosen because the t-BOC group can easily be thermolyzed once the polymer beads have been prepared to yield the desired phenolic functionality[17].

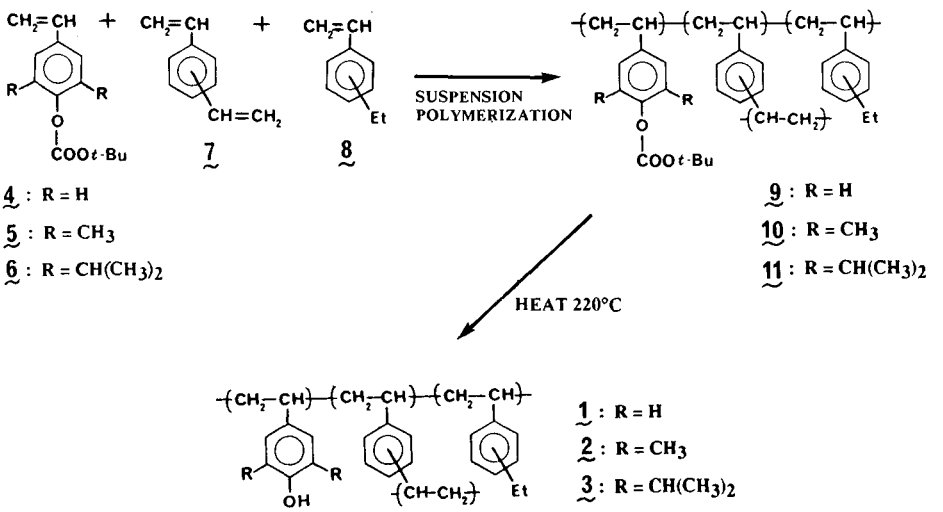

Fig. 2. Preparation of polymers **1–3**. Et = Ethyl; *t*-Bu = *tert.*-butyl.

Because of the small scale of the polymerization reaction no attempts were made to size the resin beads, but instead, conditions were optimized to produce batches with relatively narrow size distributions. Fig. 3 shows an example of a batch with an average particle size of about 10 μm, which was best suited for our study as distributions with a smaller average particle size led to high column back pressures because of the large percentages of fines in these samples. The physical data for polymers **9–11** are reported in Table I, which shows that we were successful in pro-

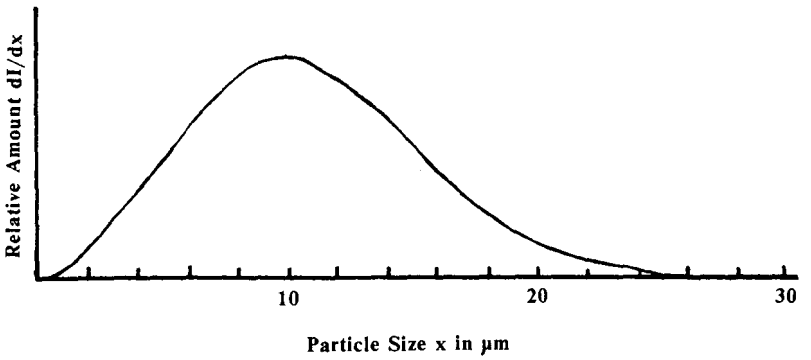

Fig. 3. Particle size distribution for polymer **9** prepared by suspension polymerization.

ducing a series of resins having small average particle sizes (10–12 μm) and high surface areas (200–300 m^2/g). This table also shows the thermolysis temperature for the t-BOC group of each polymer and the percentage weight loss upon heating from 50 to 300°C. In all cases, loss of the t-BOC groups upon thermolysis was confirmed by FT-IR monitoring as the strong carbonyl band near 1760 cm^{-1}, which is characteristic of the t-BOC groups, was absent after thermolysis. The mole fraction of protected phenolic units incorporated in each sample could be calculated from these weight losses. Fig. 4 contains the thermogravimetric analysis trace for **9**, demonstrating that the t-BOC protecting group can be removed cleanly and quantitatively simply by heating the resin to the appropriate temperature; similar curves were obtained in the thermolysis of polymers **10** and **11**. Fig. 5 shows the cumulative mercury porosimetry curve for polymer **9**. Most of the porosity can be found in pores below 1000 Å, which accounts for the high surface area of this polymer. The rise of this curve above 5000 Å is an artifact of the mercury porosimetry technique and represents the filling of the spaces between the beads by mercury; similar curves were obtained for **10** and **11**.

TABLE I

PHYSICAL DATA FOR POLYMERS **9**, **10** AND **11**

Parameter	*Polymer*		
	9	***10***	***11***
Mean particle size (μm)	10.20	10.42	12.00
(Standard deviation)	(4.4)	(4.3)	(5.7)
Surface area (m^2/g)	232	313	262
Thermolysis temperature (°C)	191	211	216
% Weight loss	23.4	23.6	21.6
Mole fraction of phenolic units	0.39	0.43	0.45

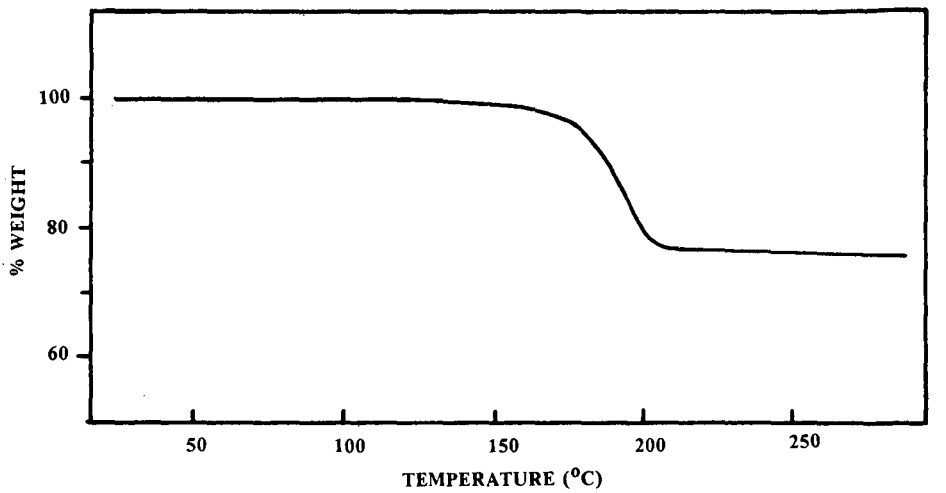

Fig. 4. Thermogravimetric analysis data recording the loss of t-BOC protecting group upon heating of polymer **9**.

Ease of processing of the bead products resulting from the thermal cleavage of the t-BOC group

The cleavage of protecting groups in HPLC-size polymer beads though easily conceived in terms of chemistry, is in fact a demanding and time-consuming operation due to the physical form of the polymer beads, which presents a special problem. While excess reagents, solvents and reaction by-products are usually removed from insoluble polymer beads by filtration, it is extremely difficult to filter very small polymer beads as small-size particles can easily clog filtration media leading to exceedingly long filtration times. To avoid these problems, it is convenient to wash the small beads through a series of decantations with appropriate solvents. This is a lengthy procedure that may typically require up to four weeks because one must allow the solvent to fully penetrate the beads and the impurities to diffuse out of the highly porous beads.

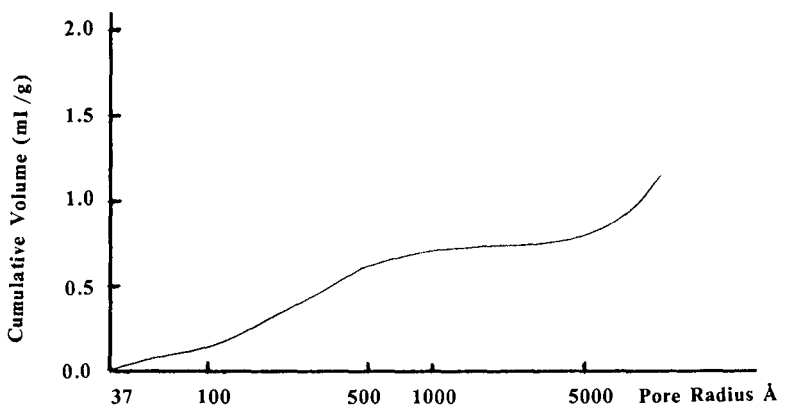

Fig. 5. Cumulative pore volume for polymer **9**.

The t-BOC protecting group was used in this research because it is easily and cleanly removed by thermolysis in a process which affords only gaseous by-products; therefore, it can be removed in a solid-state reaction that does not require any subsequent tedious washing procedures to isolate the purified beads. In our process, the polymer beads containing the t-BOC-protected phenolic groups were placed in a round-bottom flask and heated to the appropriate temperature under a flow of inert gas or under high vacuum. The by-products of this reaction — carbon dioxide and isobutylene[17] — are gases at the temperatures used for the cleavage reaction and are therefore easily removed. Once the cleavage reaction is complete, the beads are ready to be packed into HPLC columns without further work-up or washing. It is interesting to note that the thermolysis of the t-BOC groups of polymer **9** results in an apparent decrease in the surface area of the beads (from *ca.* 230 to *ca.* 150 m^2/g) as the flexibility of the more lightly cross-linked portions of the beads increase during the heating process and some temporary collapse is observed. However, the original surface area of the beads is regained (to *ca.* 225 m^2/g) after deprotection if the beads are again suspended in hexane, allowed to equilibrate and dried *in vacuo*.

Another advantage of the thermal reaction is that it is free from the steric inhibition effects which may be observed in the deprotection of the more hindered phenolic polymers used in this study. For example, we have found that the t-BOC group of **9** could be cleaved easily and quantitatively by heating to 65°C overnight a suspension of the polymer beads in a 5% solution of sodium hydroxide in methanol. In contrast, the t-BOC group of **11** proved much more resistant to cleavage under these conditions because the bulky isopropyl groups shield the carbonate group from attack by chemical reagents. Even after seven days of reaction at 65°C a significant amount of the t-BOC group remained. In contrast, the t-BOC group of **11** can be removed thermolytically in a few minutes by heating **11** at 200–230°C; accessibility of reactive sites is clearly not a factor with the thermolysis reaction.

Chromatographic properties of the resins

The polymer beads prepared above were packed *without prior sizing* into 15 cm × 0.46 cm I.D. stainless-steel HPLC columns at a solvent pressure of 3000 p.s.i. by using methanol as the mobile phase and a balanced-density slurry[19] of methanol and carbon tetrachloride. Polymers **1** and **2** gave columns with approximately 18 000

TABLE II

CALCULATION OF HEIGHT EQUIVALENT TO A THEORETICAL PLATE (HETP) FOR HPLC COLUMNS

Calculated from: $N = (t_{R_p}/W_{1/2})^2 \cdot 5.545$ and HETP = L/N, where N = number of plates, t_{R_p} = retention time for pentane (min), $W_{1/2}$ = width of pentane peak at half-height (min) and L = length of HPLC column (150 mm). HETP is measured by injection of 6 μl of a 2% solution of pentane in methanol by using 0.5 ml/min methanol as the mobile phase.

Polymer	t_{R_p}	$W_{1/2}$	N	N/m	*HETP (μm)*
1	4.85	0.220	2690	17 900	55.6
2	5.06	0.225	2800	18 700	53.5
3	5.51	0.330	1550	10 300	97.0

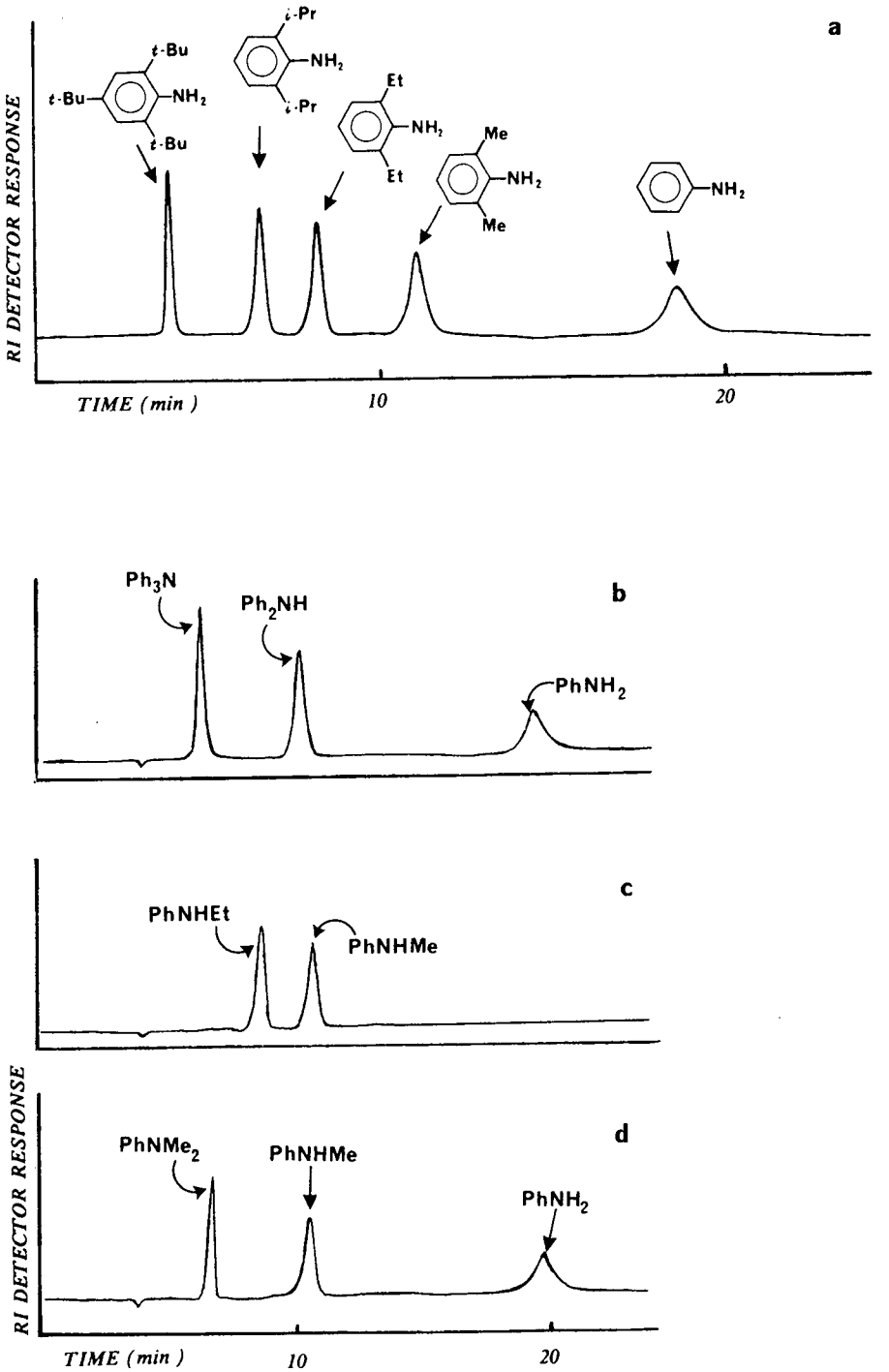
a
t-Bu
t-Bu
NH2
t-Bu
i-Pr
NH2
i-Pr
Et
NH2
Et
Me
NH2
Me
NH2
RI DETECTOR RESPONSE
TIME (min)
10
20
b
Ph3N
Ph2NH
PhNH2
c
PhNHEt
PhNHMe
d
PhNMe2
PhNHMe
PhNH2
RI DETECTOR RESPONSE
TIME (min)
10
20

Fig. 6.

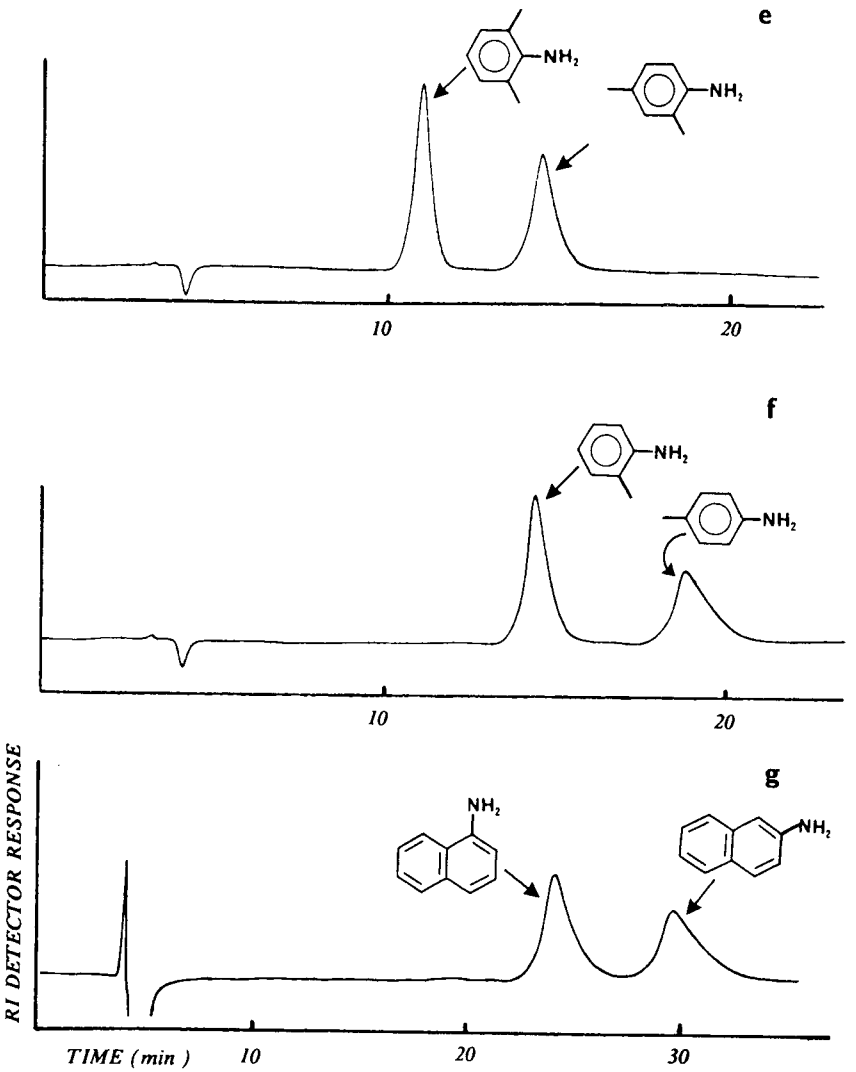

Fig. 6. Separation of aromatic amines on a 15-cm column of polymer **1** by using ethyl acetate–hexane (10:90, v/v) at 0.5 ml/min. Et = Ethyl; *i*-Pr = isopropyl; Me = methyl; Ph = phenyl; *t*-Bu = *tert.*-butyl. See text and Table III.

plates/m, as seen in Table II, while polymer **3** gave a column with approximately 10 000 plates/m; these values are considered to be very good for *unsized* polymer samples. Mobile phases ranging in polarity from methanol to hexane could be used with these columns without appreciable back pressure (about 1000 p.s.i.) and with retention of column efficiency as long as the flow-rates were not raised above 1.5 ml/min. Column dead volume times, t_0, were taken as the retention time for a heptane peak by using ethyl acetate–hexane (1:10, v/v) as the mobile phase.

A number of separations of a variety of aromatic amines performed by using polymer **1**, the unhindered phenol, are displayed in Fig. 6a–g; the corresponding

TABLE III

CHROMATOGRAPHIC DATA FOR SEPARATIONS DONE WITH **1**

$k' = (t_R - t_0)/t_0$, t_R = retention time, t_0 = retention time of an unretained component (heptane) and $\alpha = k'_2/k'_1$. Both t_R and t_0 are in min.

Compound	t_R	t_0	k'	α
2,4,6-Tri-*tert.*-butylaniline	3.9	3.5	0.1	–
2,6-Diisopropylaniline	6.6	3.5	0.8	8.1
2,6-Diethylaniline	8.3	3.5	1.4	12.7
2,6-Dimethylaniline	11.2	3.5	2.2	20
Aniline	18.9	3.5	4.4	40
Triphenylamine	6.1	3.5	0.7	–
Diphenylamine	9.8	3.5	1.8	2.6
Aniline	18.9	3.5	4.4	6.3
N-Ethylaniline	8.2	3.5	1.3	–
N-Methylaniline	10.3	3.5	1.9	1.5
N,N-Dimethylaniline	6.4	3.5	0.8	–
N-Methylaniline	10.3	3.5	1.9	2.4
Aniline	19.0	3.5	4.4	5.5
2,6-Dimethylaniline	11.3	3.5	2.2	–
2,4-Dimethylaniline	14.3	3.5	3.1	1.4
2-Methylaniline	14.8	3.5	3.2	–
4-Methylaniline	18.7	3.5	4.3	1.3
2-Methylpyridine	12.1	3.5	2.4	–
4-Methylpyridine	14.7	3.5	3.2	1.3
2,6-Dimethylpyridine	10.9	3.5	2.1	–
2,5-Dimethylpyridine	13.6	3.5	2.9	1.4
2,4-Dimethylpyridine	15.6	3.5	3.4	1.6
1-Aminonaphthalene	23.7	3.5	5.7	–
2-Aminonaphthalene	29.5	3.5	7.4	1.3

chromatographic data are given in Table III. The term "α", which is the relative retention of one solute with respect to another, is obtained by dividing the capacity factors (k') of the solutes; the larger the value of α, the better the separation[21]. All of the values of α reported in Table III are determined relative to the first component of each mixture. Elution of these aromatic amines was possible by using a small percentage (10%) of a polar solvent, ethyl acetate, mixed with a non-polar solvent, hexane. The various amines could not be eluted from this column by using pure hexane as the mobile phase because of the relatively strong hydrogen bonds which are formed between the amines and the phenolic hydroxyl. Low flow-rates were used with the columns of unsized beads since higher flow-rates (>1.5 ml/min) caused excessive pressure drops.

Fig. 6a shows that aniline, 2,6-dimethylaniline, 2,6.diethylaniline, 2,6-diisopropylaniline and 2,4,6-tri-*tert.*-butylaniline are all easily separated from one another by polymer **1**. The most hindered molecule, 2,4,6-tri-*tert.*-butylaniline, elutes with the

column dead volume because it is too hindered to form hydrogen bonds with the phenol, while the least hindered molecule, aniline, shows the most retention because it can most easily form hydrogen bonds with the phenol. Fig. 6b illustrates the separation of triphenylamine, diphenylamine and aniline; Fig. 6c shows a good separation of N-methylaniline and N-ethylaniline, while Fig. 6d confirms that this column can easily separate primary, secondary and tertiary amines. Fig. 6e–g shows good separations for aromatic amine isomers, namely 2,6- and 2,4-dimethylaniline, 2- and 4-methylaniline and 1- and 2-aminonaphthalene. In each case, the least sterically hindered amine shows the greatest retention on the column.

Fig. 7a and b shows that excellent separations are obtained on resin **1** with some alkyl pyridine isomers, 2- and 4-methylpyridine, as well as 2,4-, 2,5- and 2,6-dimethylpyridine. For the separation of pyridines, which are generally more basic than anilines[22], a more polar mobile phase, ethyl acetate–hexane (90:10, v/v), was required to achieve retention times similar to those of the aromatic amines. At this point, it should be pointed out that these types of separations are normally very difficult to carry out on *any type* of silica-based separation media because of the severe hydrogen bonding and the ion-exchange type of interactions which occur between the amines and the residual silanol groups on the silica surface[23]; such interactions generally lead to badly shaped chromatographic peaks.

The separations discussed above were then performed on polymers **2** and **3**

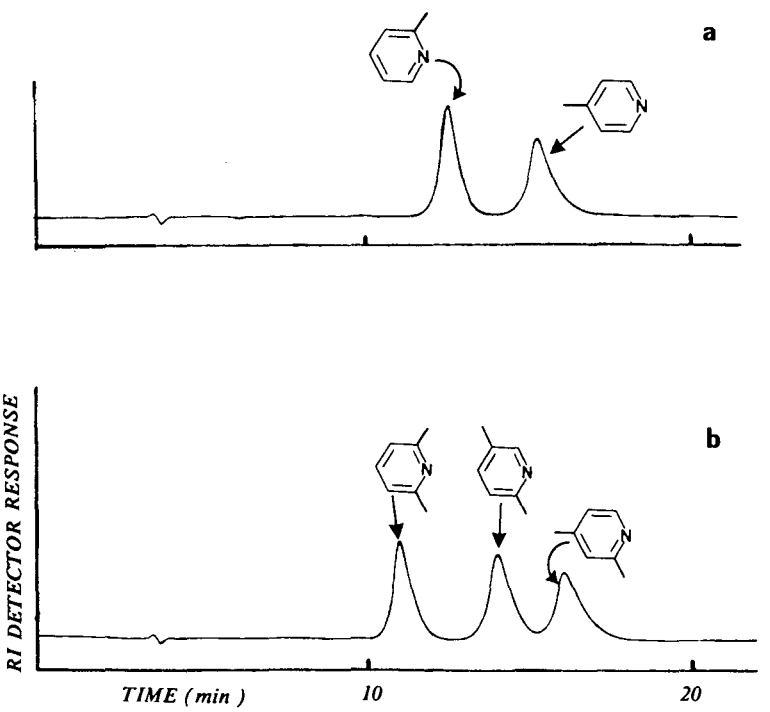

Fig. 7. Separation of substituted pyridines by using polymer **1**. A 15-cm column was eluted with ethyl acetate–hexane (90:10, v/v) at 0.5 ml/min.

under the conditions used with **1**; typical results are shown in Fig. 8. While baseline resolution of 2,6- 2,5- and 2,4-dimethylpyridine can be achieved by using the unhindered phenol polymer, **1**, the separation becomes progressively worse as the steric hindrance around the phenolic hydroxyl is increased. It is not surprising to see that the pyridines have less retention on the hindered phenol columns because the hindered phenols are less acidic than the unhindered phenol[24] and would be expected to form weaker hydrogen bonds with nitrogen containing compounds. In these cases, the decreased acidity and increased steric hindrance in **2** and **3** do not help to improve the selectivity of the separations. An aditional example of the differences which are observed in the separation of substituted pyridines with columns packed with polymers **1–3** is shown in Fig. 9. It is seen in this figure that some advantage may be taken of the differences in retention between the three types of packing materials. The

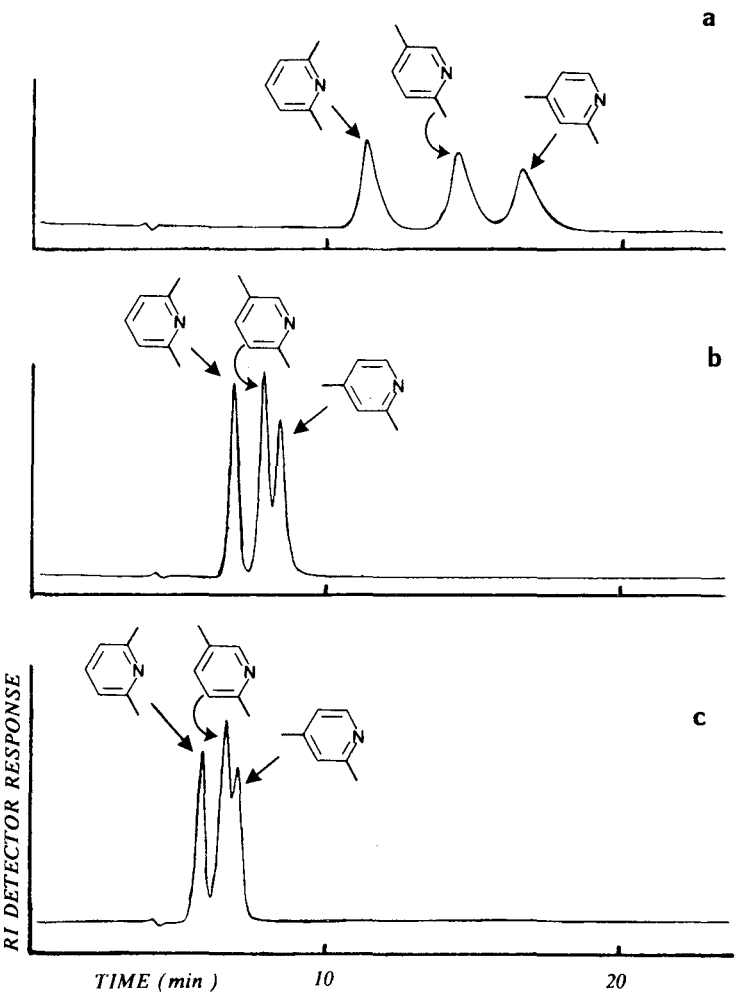

Fig. 8. Separation of substituted pyridines on 15-cm columns of (a) polymer **1**, (b) polymer **2**, and (c) polymer **3**, by using ethyl acetate–hexane (90:10, v/v) at 0.5 ml/min.

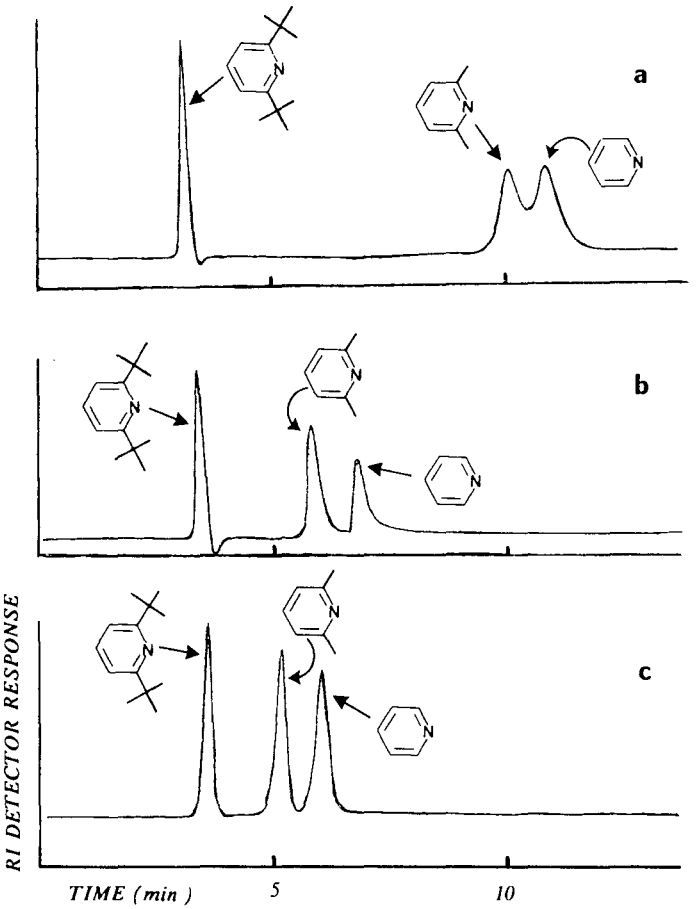

Fig. 9. Separation of substituted pyridines on 15-cm columns of (a) polymer **1** (Fig. 9a), (b) polymer **2**, and (c) polymer **3**, by using ethyl acetate–hexane (90:10, v/v) at 0.5 ml/min.

improved separation characteristics observed with columns packed with **2** or **3** likely result from the increased steric demands of these two polymers; it is noteworthy that columns packed with **2** or **3** also provide faster elution times.

It was expected that the hindered phenolic polymers **2** and **3** might prove even more versatile for the separation of aliphatic amines, which are much more basic than pyridines and anilines. As can be seen in Fig. 10a it is virtually impossible to achieve any meaningful separation of aliphatic amines by using polymer **1**. The phenol moiety of **1** has a pK_a of approximately 10 (in aqueous solution), while the pK_a of the conjugate acid of most aliphatic amines lies between 9 and 10 (ref. 24). In this region of pK_a values, proton exchange can occur between a phenol and an amine in addition to very strong hydrogen bonding. The separation attempted in Fig. 10a involved 1-phenylethylamine and 2-phenylethylamine on a column packed with polymer **1**; in this separation a very polar solvent, methanol, was required to achieve elution of the aliphatic amines. It can be seen that both of these amines adsorb so strongly onto **1**

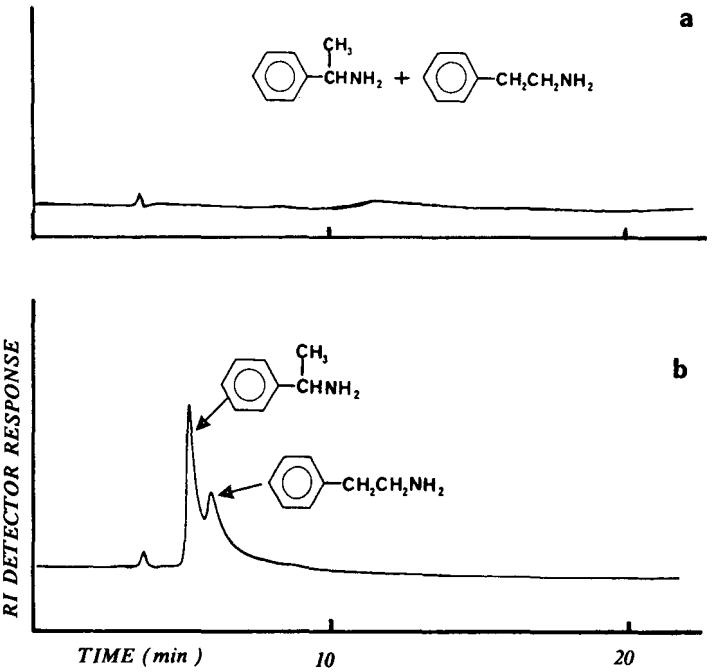

Fig. 10. Attempted separation of isomeric aliphatic amines by using 15-cm columns packed with (a) polymer **1**, and (b) polymer **3**, by using methanol at 0.5 ml/min.

that the resulting chromatographic peaks are so broad as to virtually disappear in the baseline.

2,6-Dimethylphenol and 2,6-diisopropylphenol are reported to have pK_a values of 10.6 and 11.1 respectively[24], which means that they are significantly less acidic than the unhindered phenol moiety and therefore should form weaker hydrogen bonds with aliphatic amines. Fig. 10b shows that more "normal" chromatographic peaks can be obtained with polymer **3** for a mixture of 1- and 2-phenylethylamine. Both the reduced acidity of **3** and the sterically congested environment of its phenolic group contribute to weaken the strength of the hydrogen bonds to the amino groups. This effect has been quantified previously with low molecular weight analogues[25]. Fig. 11a shows that the separation of these two compounds can be further improved by using methanol–water (80:20, v/v) as the mobile phase; Fig. 11b shows a similar separation of benzylamine, 2-phenylethylamine and 4-phenylbutylamine by using **3** as the separation medium and methanol–water (80:20, v/v) as the mobile phase.

Here again the ability of **3** to separate aliphatic amines is important in terms of potential practical applications since silica-based adsorbents are generally not suitable for the separation of such systems. In a recent article[26], procainamide, which contains a tertiary aliphatic amine group, showed very bad tailing on an octadecyl silica gel because of interactions, with residual silanol groups, which have been reported to have pK_a's ranging from 5 to 10 (ref. 27). In addition, our columns can operate both with aqueous as well as non-aqueous mobile phases, while bonded silica columns tend to be unstable[3] above pH 7.

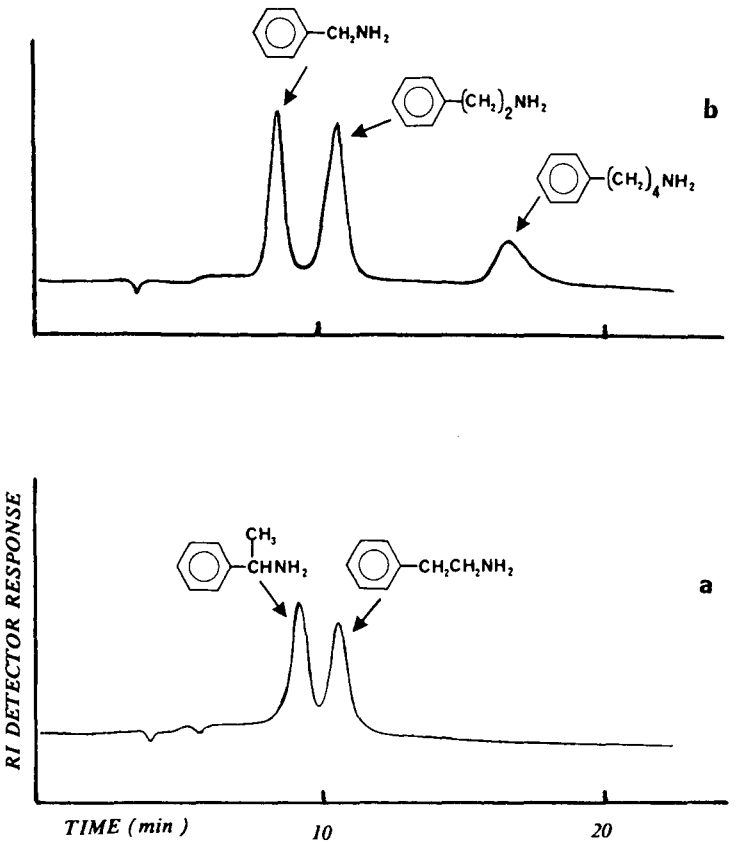

Fig. 11. Separation of aliphatic amines on a 15-cm column of polymer **3** by using methanol–water (80:20, v/v) at 0.5 ml/min.

CONCLUSION

This work demonstrates that the versatility of functionalized polymers can be applied to the preparation of HPLC separation media. The porous polymers can be used in both organic and aqueous media and their adsorption properties can be tuned to accommodate a variety of organic separations. In the case of our poly(hydroxystyrene) resins, both the steric environment and the pK_a of the phenolic groups are important variables which control the ultimate HPLC properties of the polymers. While suspension polymerization may be used effectively to prepare highly porous high-surface area resins, other techniques which can be used to produce porous but uniformly sized resins may provide another dimension to the approach. Our current work is also directed towards novel, monodispersed, non-porous, small-diameter beads with a high density of surface functionalities.

ACKNOWLEDGEMENTS

Financial assistance of this research on novel polymeric materials by IBM Corporation (Materials and Processing Sciences Program) and by the Natural Sciences and Engineering Research Council of Canada, is gratefully acknowledged.

REFERENCES

1 R. E. Majors, *J. Chromatogr. Sci.*, 18 (1980) 488.
2 D. Johns, *Am. Lab. (Fairfield, Conn.)*, 19 (1987) 72.
3 J. R. Benson and D. J. Woo, *J. Chromatogr. Sci.*, 22 (1984) 386.
4 J. J. Kirkland, J. L. Glajch and R. D. Farlee, *Anal. Chem.*, 61 (1989) 2.
5 G. Heinemann, J. Kohler and G. Schomburg, *Chromatographia*, 23 (1987) 435.
6 C. Chu and D. J. Pietrzyk, *Anal. Chem.*, 46 (1974) 330.
7 D. Horak, Z. Pelzbauer, F. Svec and J. Kalal, *J. Appl. Polym. Sci.*, 26 (1981) 3205.
8 D. P. Lee and J. H. Kindsvater, *Anal. Chem.*, 52 (1980) 2425.
9 D. P. Lee, *J. Chromatogr. Sci.*, 22 (1984) 327.
10 D. MacBlane, N. Kitagawa and J. R. Benson, *Am. Lab. (Fairfield, Conn.)*, 19 (1987) 134.
11 R. E. Majors, *LC · GC, Mag. Liq. Gas Chromatogr.*, 7 (1989) 212.
12 J. Ugelstad and P. C. Mork, *Adv. Colloid Interface Sci.*, 13 (1980) 101.
13 J. Ugelstad, L. Soderberg, A. Berge and J. Bergstrom, *Nature (London)*, 303 (1983) 95.
14 D. J. Burke, J. K. Duncan, L. C. Dunn, L. Cummings, C. J. Siebert and G. S. Ott, *J. Chromatogr.*, 353 (1986) 425.
15 W. Rolls and J. M. J. Fréchet, *Am. Chem. Soc. Polym. Mat. Sci. Eng.*, 56 (1987) 745.
16 W. Rolls, F. Svec and J. M. J. Fréchet, *Polymer*, 31 (1990) 165.
17 J. M. J. Fréchet, E. Eichler, H. Ito and C. G. Willson, *Polymer*, 24 (1983) 995.
18 N. Kawabata and Y. Taketani, *Bull. Chem. Soc. Jpn.*, 53 (1980) 2986.
19 B. Coq, C. Gonnet and J. Rocca, *J. Chromatogr.*, 106 (1975) 249.
20 H. Ito, C. G. Willson, J. M. J. Fréchet and E. Eichler, *Macromolecules*, 16 (1983) 510.
21 R. J. Hamilton and P. A. Sewell, *Introduction to High Performance Liquid Chromatography*, Chapman & Hall, London, 1982, p. 31.
22 D. D. Perrin, *Dissociation Constants of Organic Bases in Aqueous Solution*, Butterworths, London, 1965, pp. 13–451.
23 A. Wehrli, J. C. Hildebrand, H. P. Keller, R. Stampfli and R. W. Frei, *J. Chromatogr.*, 149 (1978) 199.
24 E. P. Serjeant and B. Dempsey, *Ionisation Constants of Organic Acids in Aqueous Solution*, Permagon Press, New York, 1979, pp. 9–765.
25 L. Lamberts, *J. Chim. Phys.*, 62 (1965) 1404.
26 H. Wada, *Chromatographia*, 22 (1986) 194.
27 J. Nawrocki and B. Buszewski, *J. Chromatogr.*, 449 (1988) 1.

Journal of Chromatography, 504 (1990) 113–128
Elsevier Science Publishers B.V., Amsterdam — Printed in The Netherlands

CHROM. 22 176

Adduct formation identification between phenyl glycidyl ether and 2′-deoxyadenosine and thymidine by chromatography, mass spectrometry and nuclear magnetic resonance spectroscopy

E. VAN DEN EECKHOUT*
University of Ghent, College of Pharmacy, Harelbekestraat 72, B-9000 Ghent (Belgium)
A. DE BRUYN
University of Ghent, Laboratory for Organic Chemistry, Krijgslaan 281, B-9000 Ghent (Belgium)
H. PEPERMANS
Unilever Research Laboratorium Vlaardingen, O. van Noortlaan 120, 3133 AT Vlaardingen (The Netherlands)
E. L. ESMANS and I. VRYENS
University of Antwerp (RUCA), Laboratory for Organic Chemistry, Groenenborgerlaan 171, B-2020 Antwerp (Belgium)
J. CLAEREBOUDT and M. CLAEYS
University of Antwerp (U.I.A.), Department of Pharmacy, Universiteitsplein 1, B-2610 Wilrijk (Belgium)
and
J. E. SINSHEIMER
University of Michigan, College of Pharmacy, Ann Arbor, MI 48109 (U.S.A.)
(First received June 15th, 1989; revised manuscript received October 13th, 1989)

SUMMARY

Thymidine and 2′-deoxyadenosine were reacted with phenyl glycidyl ether in order to study the formation of the corresponding 2′-deoxynucleoside adducts. Separation methods were elaborated using either reversed-phase high-performance liquid chromatography with photodiode-array detection, or centrifugal circular thin-layer chromatography. The adducts were isolated on a preparative scale and were fully characterized by UV spectroscopy, desorption chemical ionization and fast atom bombardment mass spectrometry and 270- and 360-MHz ^{1}H NMR spectrometry. For thymidine the main adduct was characterized as N-3-(2-hydroxy-3-phenoxypropyl)thymidine. With 2′-deoxyadenosine, predominantly N-1-(2-hydroxy-3-phenoxypropyl)-2′-deoxyadenosine was formed. With longer reaction times, the formation of a minor amount of dialkylated 2′-deoxyadenosine was observed. These nucleoside adducts will be used as marker compounds for studies of DNA adduct formation.

0021-9673/90/$03.50

INTRODUCTION

Mono- and bifunctional glycidyl ethers are widely used for the production of epoxy resins and to improve the processing and stability of industrial polymers. Therefore, their structure–mutagenicity and structure–genotoxicity relationships have been the subject of *in vitro*[1–13] and *in vivo* studies[2,14–17] in order to assess the genotoxic potential of these particular chemicals.

From a review published by Hopkins[18], it could be concluded that although these compounds were mutagenic, *in vitro* and *in vivo* studies needed more emphasis. Further, as it has been reported that workers exposed to glycidyl ethers suffered skin and eye irritation and allergic reactions[19] and that even adverse testicular and haemopoietic effects have been described[20], a thorough study of the biological action of these compounds is warranted. The effects described above led in 1978 to recommendations for limiting the occupational exposure to these compounds[19]. It is generally believed that reactions of electrophilic reactants with sites in DNA, RNA or protein are fundamental to the induction of mutations. Our interest in the structure–mutagenicity relationships for aliphatic epoxides[12,13,21–25] and in the reactivity of some of these epoxides with 2′-deoxynucleosides and DNA[26–28] prompted us to extend the limited literature[9,29] on the reactivity and identification of adduct formation between phenylglycidyl ethers and 2′-deoxynucleosides.

In this paper we report the separation and structure elucidation of the nucleoside adducts formed between 2′-deoxyadenosine and thymidine with phenyl glycidyl ether. For this purpose, preparative centrifugal circular thin-layer chromatography (TLC) and both analytical and preparative reversed-phase high-performance liquid chromatography (HPLC) were used. On-line identification during HPLC analysis was done by means of a photodiode-array detector, which proved to be a powerful approach for the assignment of the alkylation site. The main adducts isolated were confirmed by means of mass spectrometry (MS) and nuclear magnetic resonance (NMR) spectrometry.

EXPERIMENTAL

Materials

All solvents were of analytical-reagent grade. Phenyl glycidyl ether (2,3-epoxypropyl phenyl ether) was obtained from Janssen Chimica (Beerse, Belgium), and was distilled *in vacuo* before use. 2′-Deoxyadenosine (dAdo) and thymidine (Thy) were purchased from Sigma (St. Louis, MO, U.S.A.). 3-Phenoxypropane-1,2-diol was synthesized as reported[30].

Reaction of 2′-deoxynucleosides with phenyl glycidyl ether

Thymidine or 2′-deoxyadenosine (2 mg) was dissolved in 2 ml of methanol and 1 ml of 1 *M* phenyl glycidyl ether in methanol was added. The compounds were allowed to react for 24 or 48 h at 37°C in tightly sealed test-tubes equipped with a PTFE-lined screw-cap. For preparative purposes 50 mg of 2′-deoxynucleoside in methanol were used.

Thin-layer chromatography

TLC was performed on silica gel 60 G F_{254}, thickness 0.25 mm (10 cm × 10 cm plates) (E. Merck, Darmstadt, F.R.G.). The following solvent systems were used as mobile phases: (I) dichloromethane–methanol (90:10); (II) dichloromethane–methanol (60:20); (III) butanol–acetone–acetic acid–water (10:10:2:5); (IV) dichloromethane–tetrahydrofuran (THF) (20:80); and (V) isopropanol–ammonia–water (70:10:20).

A 10-μl volume of the reaction mixture was applied to the plate, together with Thy, dAdo (1 mg/ml), phenyl glycidyl ether (1 mg/ml) and phenoxypropane-1,2-diol (1 mg/ml) (synthesized[30]) as reference compounds.

Preparative centrifugal circular thin-layer chromatography

Centrifugal circular TLC was performed on a Chromatotron instrument (Harrison Research, Palo Alto, CA, U.S.A.). Silica gel plates were used with a layer thickness of 2 mm, prepared by suspending 65 g of Kieselgel 60 P F_{254} (E. Merck) in 130 ml of distilled water.

Analysis of the thymidine–phenyl glycidyl ether reaction mixture. The mobile phase was dichloromethane–THF (30:70) at a flow-rate of 7 ml/min. For samples preparation, after reaction 24 or 48 h (see above), the methanol was removed under reduced pressure and the residue was dissolved in 1.1 ml of THF containing 3 drops of methanol. The amount injected was 1.0 ml.

Under these conditions and with both reaction times, three compounds eluted, with R_F values from analytical TLC on silica gel of 0.95, 0.80 and 0.70. The first band, identified as phenyl glycidyl ether, was discarded. The other two compounds were collected, the solvent was removed under reduced pressure and the residues were analysed by NMR and MS. The compound with R_F 0.70 was identified as thymidine and that with R_F 0.80 as an adduct.

Analysis of the 2'-deoxyadenosine–phenyl glycidyl ether reaction mixture. The mobile phase was dichloromethane–THF (20:80) at a flow-rate of 7 ml/min. Samples and amounts injected were as for thymidine.

When the reaction was performed for 24 h, four compounds were separated, with R_F values from analytical TLC on silicagel of 0.10, 0.36, 0.80 and 0.95. However, when the reaction was performed for 48 h, five compounds were detected, with R_F values from analytical TLC on silica gel of 0.10, 0.20, 0.36, 0.80 and 0.95.

The bands with R_F 0.36 (AD-1) and 0.20 (AD-2) were collected. After removal of the solvent under reduced pressure, AD-1 (main compound) was subjected to NMR and desorption chemical ionization (DCI) MS. AD-2 was subjected only to DCI and fast atom bombardment (FAB) MS, as the amount recovered was insufficient for NMR analysis.

Analytical reversed-phase HPLC

Analytical reversed-phase HPLC was done on a chromatograph equipped with a Waters Assoc. M-45 pump and a 20-μl six-way Valco valve external loop. Detection was effected with a Hewlett-Packard Model 1040A photodiode-array detector equipped with a Hewlett-Packard Model 8290M flexible disk drive and Hewlett-Packard 85 computer.

For the analysis of the thymidine–phenyl glycidyl ether and the deoxyaden-

osine–phenyl glycidyl ether reaction mixtures, a 10 RP-18 column (25 cm × 4.6 mm I.D.) (Bio-Rad, Ghent, Belgium) was used. The eluent for the thymidine–phenyl glycidyl ether mixture was 0.01 *M* ammonium formate (adjusted with formic acid to pH 5.1)–methanol (95:5) at a flow-rate of 2 ml/min. For deoxyadenosine–phenyl glycidyl ether the same eluent was used but in the proportions 90:10, at a flow-rate of 1.8 ml/min. The detection wavelength was 260 nm.

Preparative reversed-phase HPLC

Preparative reversed-phase HPLC was used for the isolation of the main 2′-deoxyadenosine adduct. This was done on the same apparatus as for the analytical separations but with a 10 RP-18 (25 cm × 2.2 cm I.D.) column (Alltech). The mobile phase was 0.01 *M* ammonium formate (pH 5.1)–methanol (80:20) at a flow-rate of 7.2 ml/min. The mixtures after reaction for 24 and 48 h were injected separately using a six-way Valco valve with a 100-μl loop. The detection wavelength was 260 nm.

NMR spectrometry

One-dimensional (1D) ^{1}H NMR spectra were run on a Bruker WH 360 apparatus at 18°C with 2% solutions. A pulse of 2 μs, quadrature detection and a resolution of 0.208 Hz per point were used.

A spin-lock experiment[31,32] was performed on 3 mg of dAdo adduct in 0.4 ml of methanol–water (1:1, v/v) at 30°C on a Bruker AM 270 spectrometer. The experiment was recorded with the pulse sequence PS–90°–t_1–SL–t_2, SL being a 100-ms spin-lock pulse with 4.0-kHz field strength and PS a 1-s presaturation period on the water signal. The phase of the first pulse was incremented with t_1 to obtain pure absorption spectra [Time Proportional Phase Increment (TPPI) method][33]. In a total time of 15 h, 256 interferograms of 1K data points were recorded. These were multiplied by a $\pi/3$ shifted sine-bell, Fourier transformed and phase-corrected. The t_1 interferograms were multiplied by a $\pi/3$ sine-bell, zero-filled to 1K, Fourier transformed and phase-corrected. The digital resolution in both dimensions was 5.8 Hz per point.

Desorption chemical ionization mass spectrometry

DCI mass spectra were recorded on a Ribermag 10-10B quadrupole mass spectrometer (Nermag, Paris, France) equipped with a Sidar data system. Primary ionization of the reagent gas (ammonia) was done with the aid of 70-eV electrons. The ionizaton current was 0.08 mA and the source temperature was 100°C. The ion source pressure was 0.1 mmHg. The compounds were brought onto the DCI probe with a microsyringe. After evaporation of the solvent, the DCI probe was heated at a rate of 9 mA/s. Spectra were recorded over a mass range of 100–600 u using an integration time of 2 ms/u. The ion current profile generated during DCI was reconstructed from the total ion current associated with each of the consecutively recorded mass spectra and the mass spectra which were associated with the scan numbers corresponding to the maximum intensity in the reconstructed total ion current profile were plotted for interpretation.

Fast atom bombardment mass spectrometry

FAB-MS and tandem MS (MS–MS) were carried out on a VG 70 SEQ hybrid mass spectrometer (VG Analytical, Winsford, U.K.), controlled through a VG

11-250 data system. The instrument is equipped with an Ion Tech saddle field atom gun and consists of a high-resolution double-focusing mass spectrometer (MS-I) with EB configuration followed by an radiofrequency (RF)-only quadrupole collision gas cell and a high-performance quadrupole mass analyser, which is used as MS-II. Samples were dissolved in the minimum amount of methanol and a 1-μl aliquot was added to the matrix (*e.g.*, glycerol). Fast atom bombardment by a 1-mA beam of 8-keV xenon atoms was used to desorb ions from the matrix. Spectra were recorded by repetitive scanning over the range 20–600 u using a scan time of 2 s/decade.

MS–MS or daughter ion spectra were obtained by collisionally activated decomposition (CAD) using argon as collision gas in the third field-free region (RF-only quadrupole collision gas cell) and by scanning MS-II. The FAB-MS–CAD-MS spectra were obtained by averaging ten scans.

Ultraviolet spectroscopy

UV spectra were recorded on-line during HPLC analysis in the HPLC solvent system with the aid of the photodiode-array detector.

UV spectra from preparatively isolated samples such as AD-1 and Th-1 were taken off-line on a Perkin-Elmer Lambda 15 UV–VIS spectrophotometer equipped with a Perkin-Elmer EX-800 printer.

Dried samples were diluted in water to obtain absorbance values between 0.5 and 1.0. UV spectra were recorded at acidic pH by mixing the aqueous samples with an equal volume of 0.1 *M* hydrochloric acid or at alkaline pH by mixing with an equal volume of 0.1 *M* sodium hydroxide solution. Aliquots of preparatively collected fractions were mixed with an equal volume of 12 *M* hydrochloric acid to observe any changes in the UV spectrum 18 h after addition of the acid.

RESULTS AND DISCUSSION

Thymidine and 2′-deoxyadenosine were reacted with phenyl glycidyl ether in methanol. After 24 and 48 h at 37°C, the resulting reaction mixtures were analysed and the structures of the resulting 2′-deoxynucleoside adducts were elucidated. Phenoxypropane-1,2-diol was formed in minor amounts as a hydrolysis product of phenyl glycidyl ether in some of the reactions.

HPLC–UV spectroscopy

As it has been shown that nucleoside mixtures are excellent candidates for HPLC analysis, the adduct formation described above was investigated by reversed-phase HPLC using 0.01 *M* ammonium formate (pH 5.1)–methanol mixtures as eluents.

The eluted compounds were detected by a photodiode-array detector, which is particularly useful in these analyses as the recording of detailed UV spectra of the compounds in the mixture indicates the location of the alkylated 2′-deoxynucleosides on the HPLC trace. Further, these UV data give a strong indication of the alkylation site on the heterocyclic base moiety, as supported by the work of Singer[34], who published a large amount of UV spectral data for nucleosides. She showed that the UV spectra of nucleosides obtained at different pH values, together with the calculation of the absorbance ratio measured at 254 and 280 nm, provide information on the alkylation site on the heterocyclic base moiety. Our group has used this approach for

TABLE I

COMPARATIVE TABLE OF UV SPECTRAL DATA OF ADDUCTS OF THYMIDINE AND DEOXYADENOSINE

Adduct	*Solvent*	λ_{max} *(nm)*	*Ratio, 254/280 nm*
N-3-Ethylthymidine[a]	H_2O	269	0.95
	pH 1	269	
N-3-Epichlorohydrin–thymidine[b]	H_2O	269	1.00
	pH 1	269	
N-3-Phenyl glycidyl ether–thymidine[c]	H_2O,	269	1.00
	pH 1	269	
Thymidine[c]	H_2O,	267	1.20
	pH 1	267	
N-1-Propylene oxide–deoxyadenosine[b]	H_2O,	259	2.8
	pH 1	259	3.1
N-1-Glycidoldeoxyadenosine[b]	H_2O,	258	2.5
	pH 1	258	2.5
N-1-Phenyl glycidyl ether–deoxyadenosine[c]	H_2O	261	2.4

[a] Ref. 34.
[b] Ref. 27.
[c] Our results.

the identification of N-3-alkylated thymidines formed by the reaction between thymidine and several propylene oxides[27]. The results obtained in these studies, as they pertain to the present study, are summarized in Table I. Comparison with the UV results given by photodiode-array detection coupled with HPLC as summarized in Table II led to the suggestion of N-1 alkylation for 2′-deoxyadenosine and N-3 alkylation for thymidine, as the 254/280 nm ratios of the isolated peaks corresponded to the ratios found by either Singer or our group.

TABLE II

HPLC CAPACITY FACTORS, UV PEAK MAXIMA AND 254/280 nm ABSORBANCE RATIOS FOR PEAKS FROM THYMIDINE AND DEOXYADENOSINE REACTIONS AS SHOWN IN FIG. 2

Peak	k'[a]	λ_{max} *(nm) (ratio)*[c]		
		0.05 M HCl[b]	*pH 5.1*	*0.05 M NaOH*[b]
dAdo	8.5	257 (4.4)	260 (5.9)	260 (6.0)
AD-1	19.5	261 (2.4)	261 (2.4)	263 (2.1)
Phenyl glycidyl ether-diol	23.5[d]		269 (1.0)	
Phenyl glycidyl ether	33.0[d]		269 (1.0)	
Th-1	0.65	269 (1.0)	269 (1.0)	270 (1.0)
Thy	3.53	267 (1.2)	267 (1.2)	

[a] Capacity factors by reversed-phase HPLC, $k' = (t - t_0)/t_0$.
[b] Reagents (0.1 *M* HCl or 0.1 *M* NaOH) added to an equal volume of sample in water, so that the absorbance is between 0.5 and 1.0.
[c] Peak maxima in nm and 254/280 nm absorbance ratios in parentheses.
[d] Capacity factor in the solvent system 0.01 *M* ammonium formate (pH 5.1)–methanol (90:10); flow-rate 1.8 ml/min.

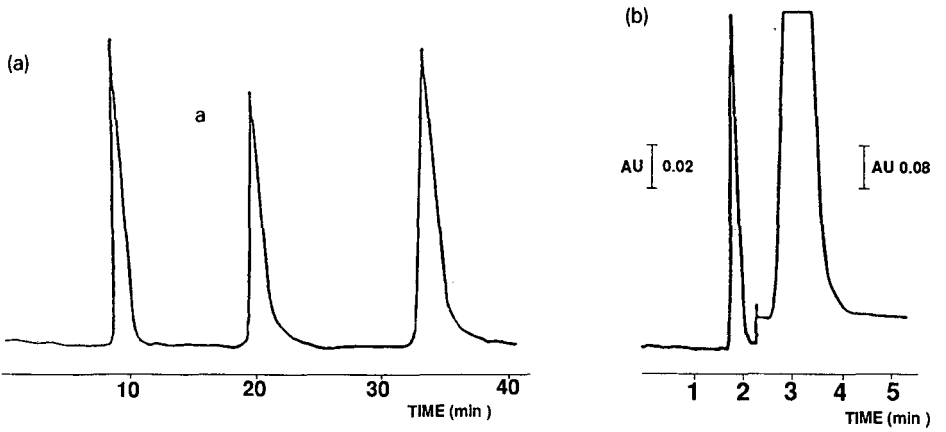

Fig. 1. (a) Analytical reversed-phase HPLC of dAdo–phenyl glycidyl ether reaction mixture. Column, 10 RP-18 (25 cm × 4.6 mm I.D.); eluent, 0.01 *M* ammonium formate (pH 5.1)–methanol, 90:10) flow-rate, 1.8 ml/min, (b) Analytical reversed-phase HPLC of Thy–phenyl glycidyl ether reaction mixture. Column, 10 RP-18 (25 cm × 4.6 mm I.D.); eluent, 0.01 *M* ammonium formate (pH 5.1)–methanol, (95:5); flow-rate, 2.0 ml/min.

For both the 2′-deoxyadenosine–phenyl glycidyl ether mixture and the thymidine–phenyl glycidyl ether mixture, the eluents used separated the reaction product from the other components, *i.e.*, unreacted base, phenyl glycidyl ether and phenyl glycidyl ether-diol, which is sometimes formed in minor amounts. The results obtained for the reaction mixtures after 24 and 48 h are given in Fig. 1a and b and Table II. Adduct formation in the thymidine reaction mixture after 24 and 48 h was identical. For deoxyadenosine, however, although the analytical HPLC traces of the 24- and 48-h reaction mixtures were identical, preparative isolation of the adduct peak (t_R = 27.6 min) (Fig. 2) revealed that in the 24-h mixture only a monoalkylated adduct was formed (see mass spectra), whereas in the 48-h mixture mono- and dialkylated adducts were formed and not separated in the present system.

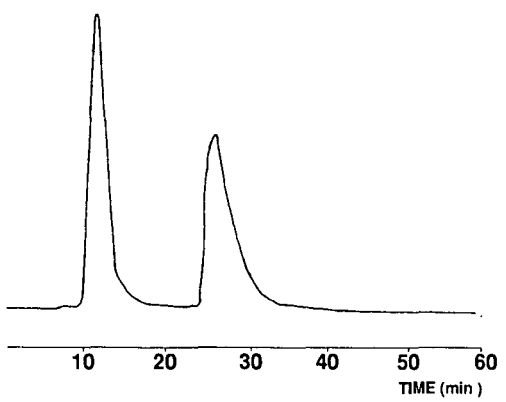

Fig. 2. Preparative reversed-phase HPLC of dAdo–phenyl glycidyl ether reaction mixture. Column, 10 RP-18 (25 cm × 2.2 cm I.D.); eluent, 0.01 *M* ammonium formate (pH 5.1)–methanol, (80:20); flow-rate, 7.2 ml/min.

Thin-layer chromatography and preparative circular thin-layer chromatography

As a preliminar screening technique and to establish conditions for circular TLC, regular TLC in several solvent systems was tried. The results for the 48-h thymidine and deoxyadenosine reaction mixtures are given in Table III. In the thymidine reaction mixture only one reaction product is detected in all the systems used; in the 24-h 2′-deoxyadenosine reaction mixture one product is formed and in the 48-h mixture in solvent systems II and IV two products are separated.

TABLE III

R_F VALUES OF 48-h THYMIDINE AND 2′-DEOXYADENOSINE REACTION MIXTURES

Solvent	*dThy*	*TH-1*	*dAdo*	*AD-2*	*AD-1*	*Phenyl glycidyl ether-diol*	*Phenyl glycidyl ether*
I	0.38	0.67	0.33	0.16	0.16	0.80	0.95
II	0.82	0.90	0.61	0.32	0.21	0.88	1.00
III	0.79	0.79	0.69	0.60	0.60	0.79	1.00
IV	0.70	0.80	0.10	0.20	0.36	0.80	0.95
V			0.87	0.92	0.92	0.95	1.00

As TLC gave a good separation of the reaction products the technique of centrifugal circular TLC on a Chromatotron instrument was evaluated to obtain pure 2′-deoxynucleoside adducts for subsequent ^{1}H NMR and mass spectral analysis. If an appropriate solvent system can be found, the latter technique provides an elegant and rapid method for the isolation of pure phenyl glycidyl ether adducts. As a separation method elaborated on an analytical TLC plate can in most instances be easily transferred to the centrifugal circular TLC (Chromatotron) system without too large a decrease in efficiency, an analytical TLC system was first elaborated for both reaction mixtures. The results are summarized in Table III.

Some restrictions are imposed on the use of solvent systems in circular TLC. Therefore, mixtures of THF and dichloromethane were tested for preparative purposes.

The thymidine reaction mixture was easy to analyse as two well separated bands could be collected. NMR and MS, discussed below, identified the compound with R_F 0.80 as a monoalkylated thymidine adduct. The two 2′-deoxyadenosine adducts were characterized as monoalkylated material (AD-1) and a mixture of mono- and dialkylated material (AD-2). The fact that the second band contained a mixture of mono- and dialkylated material could be explained by the difficulty in the visual resolution of bands with a low R_F value in the Chromatotron system. Bands with a high R_F value are sharp, in contrast to bands with a low R_F value, which tend to be diffuse, rendering a complete separation difficult.

Thymidine adduct

The ^{1}H NMR data for the thymidine adduct in [$^2H_6$]dimethyl sulphoxide ([$^2H_6$]DMSO) and of the 2′-deoxyadenosine adduct in [$^2H_4$]methanol–water (1:1) are given in Table IV, together with the appropriate reference data. Compared with

thymidine, additional resonances in the region δ = 3.88–4.14 (six protons) and the aromatic region (five protons) indicated the presence of a phenyl glycidyl ether moiety on the pyrimidine ring.

In order to exclude possible alkylation at the sugar hydroxyl functions, the spectra of the phenyl glycidyl ether–thymidine adduct were recorded in [$^2H_6$]DMSO and [$^2H_6$]DMSO–trifluoroacetic acid (TFA). In the latter spectrum there is a narrowing of the H′-3 and H′-5 pattern, wich could be explained by the disappearance of the 3J(H,OH) coupling. This was proof of the presence of an intact 2′-deoxyribofuranosyl moiety. When we considered in more detail the OH resonances in the [$^2H_6$]DMSO spectrum, the doublet at δ = 4.2 ppm could be assigned to 3′-OH and the triplet at δ 4.95 to 5′-OH. Two triplets were found at 5.19 and 5.22 ppm, each integrating for one proton. The signal at δ = 5.22 ppm belongs together with a resonance at δ = 3.15 ppm (shown by a double irradiation experiment) to an impurity. The resonance signal at δ = 5.19 ppm was assumed, however, to be built up of two doublets originating from the phenyl glycidyl ether hydroxyl function. The latter observation was substantiated by the observation that the proton resonances of the phenyl glycidyl ether moiety were split, conistent with the occurrence of two different hydrogen bridges, as shown in Fig. 3.

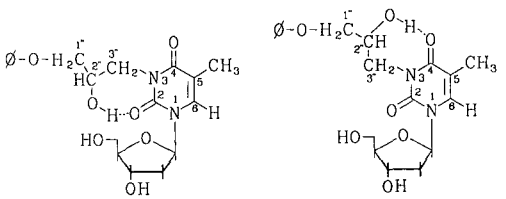

Fig. 3. Possible formation of hydrogen bridges of N-3-(2-hydroxy-3-phenoxypropyl)thymidine. ∅ = Phenyl.

This was an indication that the reaction between thymidine and phenyl glycidyl ether occurred at N-3 and at the less hindered position of the phenyl glycidyl ether. Because of degeneration of the spin system of H-1A″, H-1B″ and H-2″, their mutual coupling constants could not be measured. For H-2″, H-3A″ and H-3B″ we observe a downfield shift in the range of 0.37–0.62 ppm, caused by the change of linkage from an OH to the base and another indication that the reaction occurred at C-3″ of the glycidyl ether, which confirmed our finding from the OH resonances. The coupling constant 2J(3A″, 3B″) of 12 Hz in the adduct (Table V) could be attributed to the C-2″, C-3″ moiety of the glycidyl part by comparison with the coupling constants of phenyl glycidyl ether-diol in ^2H_2O solution. We must point to the collapse of the two protons of C-1″ for the two modifications, which is acceptable only if the phenoxy-CH2(1″) part does not belong to one of the supplementary rings caused by the hydrogen bridge.

Adenosine adduct

The 360-MHz ^{1}H NMR spectrum of the adenosine adduct was recorded in [$^2H_4$]methanol. Comparison of the chemical shifts of the glycidyl moiety in the adduct with those observed in phenoxypropane-1,2-diol showed an important downfield shift in the range of 0.6–0.7 ppm of the protons on C-3″, which indicates that the reaction occurred on the less hindered carbon atom. The assignments of the 1D ^{1}H NMR

TABLE IV

CHEMICAL SHIFTS OF THYMIDINE- AND 2'-DEOXYADENOSINE–PHENYL GLYCIDYL ETHER REACTION MIXTURES

Atom	*Thy*	*Phenyl glycidyl ether-diol in [$^2H_6$]DMSO–TFA*[a]		*Thy adduct*	*dAdo*		*Phenyl glycidyl ether-diol in [$^2H_4$]methanol*	*dAdo adduct*
H-1′	6.15			6.18 (Δ = 1.6 Hz)		6.42		6.44
H-2A′	2.07			2.09 (Δ = ?)[c]		2.78		2.77
H-2B′	2.04			2.03 (Δ = ?)[c]		2.41		2.54
H-3′	4.22			4.23 (Δ = 2.0 Hz)		4.58		~4.50
H-4′	3.76			3.77 (Δ = 1.0 Hz)		4.08		4.08
H-5A′	3.58			3.61 (Δ = 1.9 Hz)		3.85		3.82
H-5B′	3.53			3.55 (Δ = 1.0 Hz)		3.76		3.74
H-6	7.68			7.77	H-8	8.31		8.49
CH_3-5	1.86		*In ^2H_2O*[b]	1.80	H-2	8.16		8.42
H-1A″		3.97	4.16	3.88			3.96	4.14
H-1B″		3.82	4.05	3.88			3.96	4.14
H-2″		3.78	4.10	4.15 (Δ = ?)[c]			4.04	
H-3A″		3.43	3.78	4.05 (Δ = 7.1 Hz)			3.63	4.2/4.3
H-3B″		3.43	3.69	3.92 (Δ = 7.0 Hz)			3.66	
Aromatic		7.27 (int. 2)		6.80 (int. 3)			6.91 (int. 3)	6.95 (int. 3)
		6.91 (int. 3)		6.83 (int. 1)			7.25 (int. 2)	7.35 (int. 5)
				7.25 (int. 1)				

[a] In [$^2H_6$]DMSO a doublet at δ 4.10 ppm and triplets at δ 4.95, 5.19 and 5.22 ppm, each integrating for about one proton are found. The triplet at δ 5.22 ppm corresponds to a doublet at δ 3.15 ppm. They are assigned to an impurity.

[b] Ref. 35.

[c] Δ values were not determined because of overlap.

TABLE V

COUPLING CONSTANTS (Hz) OF THYMIDINE- AND 2'-DEOXYADENOSINE–PHENYL GLYCIDYL ETHER REACTION MIXTURES

J	*dThy*	*Phenyl glycidyl ether-diol*		*dThy adduct*	*dAdo*	*dAdo adduct*
^3J(1',2A')	6.5			6.4	6.1	6.1
^3J(1',2B')	7.0			6.5	5.9	5.9
^2J(2A',2B')	13.0				−13.5	−13.1
^3J(2A',3')	6.5				6.8/7.7	7.0
^3J(2B',3')	4				2.3	3.7
^3J(3',4')	2.7			2.5	3.0	
^3J(4',5A')	3.8			3.8	2.9	3.6
^3J(4',5B')	3.9			3.9	3.3	4.3
^2J(5A',5B')	−11.8		*In* ^2H_2O	−11.9	−12.3	−12.2
^3J(1A'',2'')		4.1	3.0			
^3J(1B'',2'')		6.1	6.0			
^2J(1A'',1B'')		−9.6	−9.2			
^2J(2'',3A'')		–	4.4	4.0		
^3J(2'',3B'')		–	5.6	6.0		
^2J(3A'',3B'')		–	−11.6	−12.0		

spectrum were confirmed by a spin-lock experiment, yielding both homonuclear Hartmann–Hahn[32] and rotating frame NOE(ROE)[31] cross-peaks.

In the 1D ^{1}H NMR spectrum, some resonance signals coincide with the water peak in [$^2H_4$]methanol, making some assignments difficult, but from the connectivities afforded by homonuclear Hartmann–Hahn cross-peaks in the spin-lock experiment, H-3' could be assigned from its connectivity with H-4'. From the phenyl glycidyl ether moiety, only the doublet of H-1A'' and H-1B'' at δ = 4.14 ppm can be seen. Likewise, with the help of the Hartmann–Hahn cross-peaks in the spin-lock experiment, the hidden resonances for H-2'' and H-3'' could be traced under the water peak. The assignment of the glycidyl protons was confirmed by an ROE cross-peak between one of the aromatic protons and the doublet of H-1A'' and H-1B''. We observed an ROE

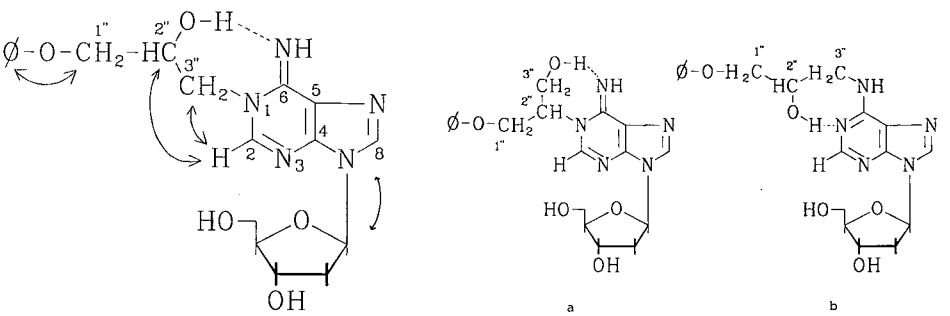

Fig. 4. Proposed structure of main 2'-deoxyadenosine–phenyl glycidyl ether adduct: N-1-(2-hydroxy-3-phenoxypropyl)-2'-deoxyadeosine. The arrows show the ROE effects measured.

Fig. 5. Unlikely 2'-deoxyadenosine–phenyl glycidyl ether adduct structures: N-6 alkylation products.

effect between one of the purine ring protons and H-1′ of the sugar moiety. When we took the H-1′–H-2 and H-1′–H-8 distances into consideration and took into account that only one cross-peak was observed, we may accept an ROE contact between H-1 and H-8. This hypothesis was substantiated by the observation of ROE cross-peaks between the protons on C-2″ and C-3″ with H-2 of the base. An ROE effect between H-8 and the protons on the phenyl glycidyl part is excluded.

The observations discussed above can only be explained if the reaction has occurred between N-1 and the less hindered epoxide carbon atom of the phenyl glycidyl moiety.

The ROE effects are show in Fig. 4. Indeed, if the reaction had occurred between N-1 and C-2″, an ROE effect between H-2 and H-3″ would have been impossible and an NOE effect between H-2 and H-1″ must be expected (Fig. 5a). The occurrence of an ROE contact between H-3″ and H-2″ with H-2 implies that the reaction did not occur at the NH on C-6. In this instance an ROE contact between H-2 and H-2″ and also between H-2 and the H-3″ resonances is unlikely (Fig. 5b). From the ROE data there is little doubt that the reaction occurred between N-1 and C-3″ (Fig. 4).

The DCI (ammonia) mass spectrum of the phenyl glycidyl ether adduct of thymidine was characterized by the presence of a protonated molecule $[MH]^+$ at m/z = 393 (100%). Fragment ions were detected at m/z = 277 (72%), m/z = 188 (84%), m/z = 116 (36%) and m/z = 134 (38%). The ion at m/z = 277 can be assigned to the base protonated ion $(BH_2)^+$ as a result of a rearrangement process involving the cleavage of the anomeric C-1′–N bond[36] and subsequent loss of a molecule of phenol results in the formation of m/z = 183. The fragment ions at m/z = 116 and 134 can be attributed to the sugar protonated ion, $[S-H]^+$ and $[S-H] \cdot NH_4^+$.

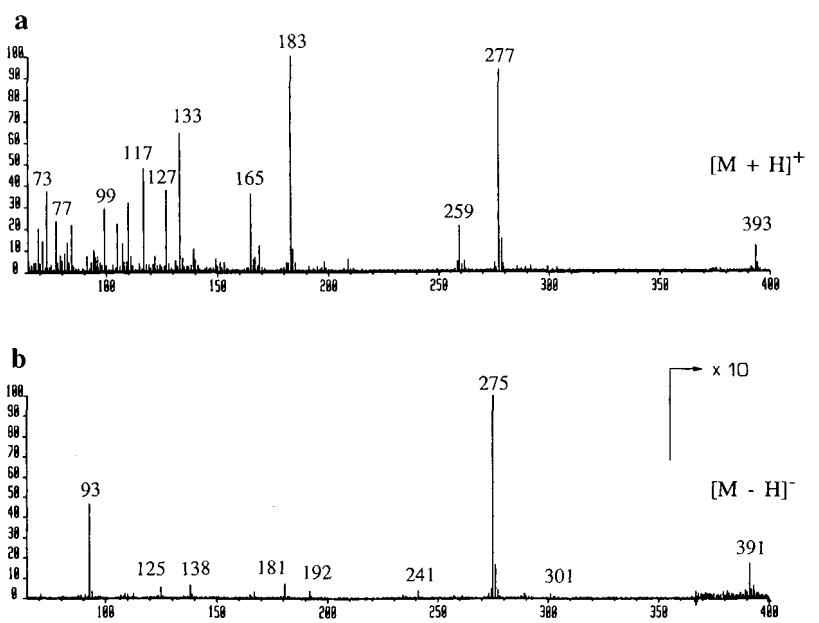

Fig. 6. FAB mass spectra of the tymidine–phenyl glycidyl ether adduct: (a) positive and (b) negative ion mode.

With the phenyl glycidyl ether adduct of 2′-deoxyadenosine, structurally analogous ions were observed, although $[MH]^+$ was less abundant. The following ions were detected: m/z = 402 ($[MH]^+$, 15%), m/z = 286 ($[BH_2]^+$, 100%), m/z = 192 ($[BH_2-\text{phenol}]^+$, 20%), m/z = 116 (35%) and m/z = 134 (48%). In both instances the typical rearrangement ions for 2′-deoxynucleosides, *i.e.*, $[B+30]^+$ and $[B+28]^+$ were absent.

Analysis of the phenyl glycidyl ether adduct formation for 2′-deoxyadenosine after a prolonged reaction time (48 h) revealed the presence of additional ions at m/z = 552 and 436. These are suggestive of a bisalkylated 2′-deoxyadenosine. This was unequivocally proved with the aid of FAB-MS–MS.

The FAB mass spectra (positive-ion mode) show a remarkable similarity with the DCI spectra. The positive FAB mass spectrum of the phenyl glycidyl ether adduct of thymidine yields a protonated molecule $[MH]^+$ at m/z = 393 (Fig. 6a). The intense fragment ions at m/z = 277 and 117 are formed by cleavage of the N-glycosidic bond and correspond to the chemically modified base $[BH_2]^+$ and the sugar moiety $[S]^+$, respectively. The $[BH_2]^+$ ion further decomposes by loss of even-electron species, giving rise to fragments at m/z = 259 (loss of H_2O), m/z = 183 (loss of phenol), m/z = 165 (combined loss of H_2O and phenol) and m/z = 127 (loss of phenyl glycidyl ether). Additional structural information is obtained from the fragmentation of the 2-hydroxy-3-phenoxypropyl group (R) (*e.g.*, R^+ at m/z = 151, $[R-H_2]$ at m/z = 149, $[R-H_2O]^+$ at m/z = 133 and $[R-C_2H_4O]^+$ at m/z = 107).

The FAB mass spectrum (negative ion mode) of the phenyl glycidyl ether adduct of thymidine shows an $[M-H]^+$ ion at m/z = 391 and a fragmentation pattern similar to that obtained in the positive ion mode (Fig. 6b). Only limited additional structural information is gained. The abundant ion at m/z = 93 corresponds to the phenolate anion. The ion at m/z = 192 can be rationalized by a retro-Diels–Alder (RDA) rearrangement with retention of the negative charge on the side-chain (Fig. 7). This fragmentation provides evidence that the alkylation takes place at the N-3 position.

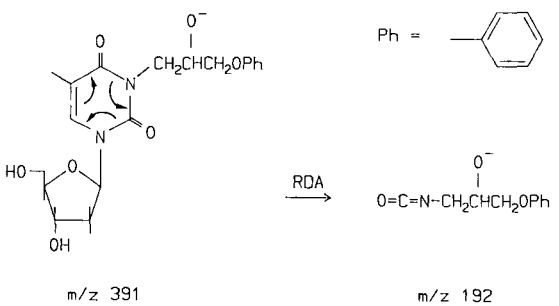

Fig. 7. Retro-Diels-Alder rearrangement of phenyl glycidyl ether adduct of thymidine.

With the phenyl glycidyl ether adducts of the 48-h reaction mixture of 2′-deoxyadenosine, the situation is more complex because the isolated fraction consists of a mixture of the mono- and bisalkylated 2′-deoxynucleosides. In the positive FAB mass spectrum, the $[MH]^+$ ions are detected at m/z = 402 and 552, respectively (Fig. 8a). Because a mixture is involved, it is impossible to distinguish which fragment ions are associated with which protonated molecules. An additional problem is that

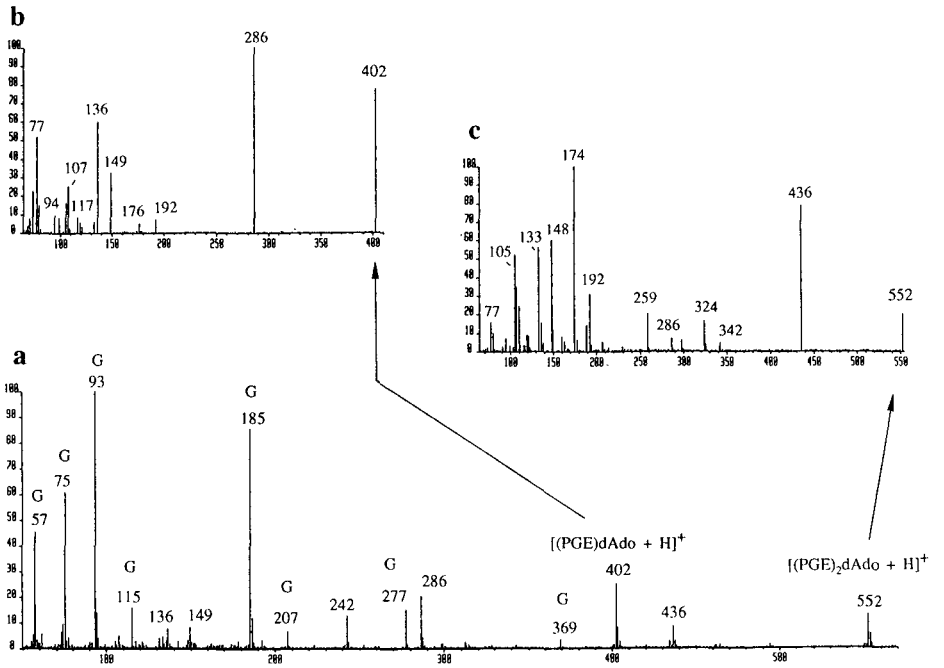

Fig. 8. (a) FAB mass spectrum (positive ion mode) of 2′-deoxyadenosine–phenyl glycidyl ether adducts of 48-h reaction mixture; ions originating from the glycerol matrix are labelled G; (b,c) daughter ion spectra (MS–MS) of the ions at (b) $m/z = 402$ and (c) $m/z = 552$ obtained by CAD at a collision energy of 30 eV and a gas pressure of 10^{-5} mbar.

low-abundance fragment ions are obscured by the chemical noise originating from the matrix (see glycerol peaks labelled G in the spectrum). To overcome these two often-encountered drawbacks of FAB-MS, we used collisionally activated decomposition in combination with tandem mass spectrometry. With the FAB-MS–CAD-MS techique an ion of interest is selected (MS-I), fragmented by collisionally activated decomposition and a daughter ion spectrum is taken of the fragments (MS-II). In this way, chemical noise is largely eliminated, stable fragment ions are induced to decompose and, with a mixture, parent–daughter relationships can be determined.

The daughter ion spectrum of the $[MH]^+$ ion ($m/z = 402$) of monoalkylated 2′-deoxyadenosine (Fig. 8b) is dominated by the BH_2^+ ion at $m/z = 286$, formed by loss of the sugar residue with concomitant proton transfer. The other fragments result from the combined loss of the sugar and phenol ($m/z = 192$), phenol and H_2O ($m/z = 174$) or phenyl glycidyl ether ($m/z = 136$). Abundant ions at $m/z = 149$, 133, 107, 105 and 77 originate from fragmentation of and charge retention on the 2-hydroxy-3-phenoxy-propyl group. In the CAD mass spectrum of the $[MH]^+$ ion ($m/z = 552$) of bisalkylated 2′-deoxyadenosine (Fig. 8c), a similar fragmentation behaviour is observed. The absence of the daughter ion at $m/z = 402$, corresponding to the $[MH]^+$ ion of the monoalkylated derivative, clearly demonstrates that the peak at $m/z = 402$ in the normal FAB mass spectrum (Fig. 8a) is due to the monoalkylated product

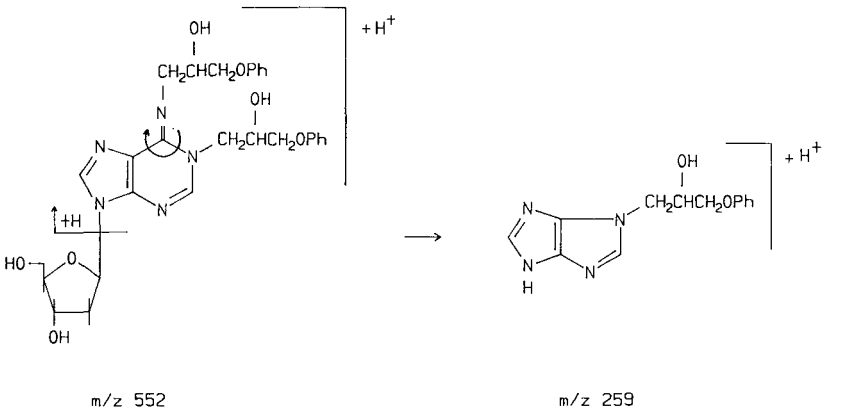

Fig. 9. CAD mass spectral fragmentation pattern of dialkylated 2′-deoxyadenosine.

occurring together with the bisalkylated derivative in the isolated fraction. Another point of interest is the presence of the ion at $m/z = 259$ in the CAD mass spectrum, which gives information about the position of phenyl glycidyl ether–base bonds, as outlined in Fig. 9.

From these results, it is clear that FAB in combination with MS–MS provides a valuable approach to the characterization of phenyl glycidyl ether–nucleoside adducts. In addition, FAB-MS–CAD-MS yields complementary structural information compared with FAB-MS alone. A more detailed discussion of the collisionally activated decomposition of gas-phase $[MH]^+$ and $[M-H]^-$ ions of phenyl glycidyl ether–nucleoside adducts will be reported elsewhere[37].

CONCLUSIONS

Circular preparative TLC proved to be a rapid separation method for the isolation of simple 2′-deoxynucleoside–phenyl glycidyl ether adduct mixtures such as thymidine–phenyl glycidyl ether. However, when the reaction mixtures are more complicated, such as in the 48-h deoxyadenosine–phenyl glycidyl ether mixture, resolution can be a problem. Preparative HPLC on an RP-18 reversed-phase column was efficient for the isolation of the main adducts of the thymidine– and deoxyadenosine–phenyl glycidyl ether mixtures. HPLC with photodiode-array detection proved to be an excellent method for the preliminary identification of the adducts. The structures already suggested by UV data for N-3(2-hydroxy-3-phenoxypropyl)thymidine and N-1-(2-hydroxy-3-phenoxypropyl)-2′-deoxyadenosine were confirmed by the additional NMR and mass spectral data. These adducts and the methods developed in this study will be used for the possible detection of DNA–phenyl glycidyl ether adducts.

ACKNOWLEDGEMENTS

J.E.S. acknowledges support by grant ROI ES 03345 from the National Institute of Environmental Health Sciences DHHS. The typing of the manuscript by C.

Rawoens is gratefully acknowledged. Professor Vandewalle is gratefully acknowledged for the use of the NMR facilities.

REFERENCES

1 H. Nishioka and H. Ohtani, *Mutat. Res.*, 54 (1978) 247–251.
2 E. J. Greene, M. A. Friedman, J. A. Sherrod and A. J. Salerno, *Mutat. Res.*, 67 (1979) 9–19.
3 M. J. Wade, J. W. Moyer and C. H. Hine, *Mutat. Res.*, 66 (1979) 367–371.
4 L. Fishbein, *Sci. Total Environ.*, 17 (1981) 97–110.
5 K. Hemminki, K. Falck and H. Vainio, *Arch. Toxicol.*, 46 (1980) 277–285.
6 E. D. Thompson, W. J. Coppinger, C. E. Piper, N. McCarroll, T. J. Oberly and D. Robinson, *Mutat. Res.*, 90 (1981) 213–231.
7 C. E. Voogd, J. J. Van der Stel and J. J. A. A. Jacobs, *Mutat. Res.*, 89 (1981) 169–282.
8 A. F. Frost ad M. S. Legator, *Mutat. Res.*, 102 (1982) 193–200.
9 K. Sugiura, M. Goto, *Chem. Biol. Interact.*, 45 (1983) 153–169.
10 J. P. Seiler, *Mutat. Res.*, 135 (1984) 159–167.
11 D. A. Canter, E. Zeiger, S. Haworth, T. Lawlor, K. Mortelman and W. Speck, *Mutat. Res.*, 172 (1986) 105–138.
12 S. H. Neau, B. H. Hooberman, S. W. Frantz and J. E. Sinsheimer, *Mutat. Res.*, 93 (1982) 297–304.
13 L. B. Rosman, P. K. Chakraborty, E. A. Messerly and J. E. Sinsheimer, *Mutat. Res.*, 206 (1988) 115–126.
14 J. B. Terrill, K. P. Lee, R. Culik and G. L. Kennedy, Jr., *Toxicol. Appl. Pharmcol.*, 64 (1982) 204–212.
15 E. B. Whorton, Jr., T. G. Pullin, A. F. Frost, A. Onofre, M. S. Legator and D. S. Folse, *Mutat. Res.*, 124 (1983) 225–233.
16 J. P. Seiler, *Chem. Biol. Interact.*, 51 (1984) 347–356.
17 J. B. Terrill and K. P. Lee, *Toxicol. Appl. Pharmacol.*, 42 (1977) 263–269.
18 J. Hopkins, *Food Chem. Toxicol.*, 22 (1984) 780–783.
19 NIOSH, *Criteria for a Recommended Standard, Occupational Exposure to Glycidyl Ethers,* U.S. Department of Health, Education and Welfare, Public Health Service, Center for Disease Control, National Institute for Occupational Safety and Healh, Cincinnati, OH, 1978.
20 H. P. Stein, N. A. Leidel, J. M. Lane, *Am. Ind. Assoc. J.*, 40 (1979) A36–A51.
21 D. R. Wade, S. A. Airy, J. E. Sinsheimer, *Mutat. Res.*, 58 (1978) 217–223.
22 S. W. Frantz and J. E. Sinsheimer, *Mutat. Res.*, 90 (1981) 67–78.
23 S. W. Frantz, E. Van en Eeckhout, J. E. Sinsheimer, M. Yashihare and M. Koreeda, *Toxicol. Lett.*, 25 (1985) 265–271.
24 L. B. Rosman, V. G. Beylin, V. Gaddami, B. H. Hooberman and J. E. Sinsheimer, *Mutat. Res.*, 171 (1986) 63–70.
25 L. B. Rosman, V. Gaddamidi and J. E. Sinsheimer, *Mutat. Res.*, 189 (1987) 189–204.
26 Z. Djuric and J. E. Sinsheimer, *Chem. Biol. Interact.*, 50 (1984) 219–231.
27 Z. Djuric and J. E. Sinsheimer, *Chem. Biol. Interact.*, 52 (1984) 243–253.
28 Z. Djuric, B. H. Hooberman, L. Rosman and J. E. Sinsheimer, *Environ. Mutat.*, 8 (1986) 369–383.
29 K. Hemminki and H. Vainio, in B. Holmstedt, R. Lauwereys, M. Mercier and M. Roberfroid (Editors), *Mechanism of Toxicity and Hazard Evaluation,* Elsevier/North-Holland, Amsterdam, 1980, pp. 241–243.
30 E. Van den Eeckhout, P. De Moerloose and J. E. Sinsheimer, *J. Chromatogr.*, 318 (1985) 343–349.
31 A. A. Bothner-By, R. L. Stephens, J. M. Lee, C. D. Warren and R. W. Jeanloz, *J. Am. Chem. Soc.*, 106 (1984) 811–813.
32 A. Bax, D. G. Davies, *J. Magn. Reson.*, 65 (1985) 355–360.
33 A. E. Derome, *Modern Techniques for Chemistry Research,* Pergamon, Oxford, 1987, p. 83.
34 B. Singer, in G. D. Fasman (Editor), *CRC Handbook of Biochemistry and Molecular Biology,* CRC Press, Cleveland, OH, 1975, pp. 409–447.
35 A. De Bruyn, D. De Keukeleire, E. Van den Eeckhout and W. Baeyens, *Bull. Soc. Chim. Belg.*, 92 (1983) 743–746.
36 J. A. McCloskey, *J. Am. Chem. Soc.*, 97 (1975) 3436–3444.
37 J. Claereboudt, E. Van den Eeckhout, E. Esmans, W. Baeten and M. Claeys, *Biomed. Environ. Mass Spectrom.*, in preparation.

Journal of Chromatography, 504 (1990) 129–138
Elsevier Science Publishers B.V., Amsterdam — Printed in The Netherlands

CHROM. 22 188

Automated amino acid analysis using precolumn derivatization with dansylchloride and reversed-phase high-performance liquid chromatography[a]

MAURIZIO SIMMACO, DANIELA DE BIASE, DONATELLA BARRA and FRANCESCO BOSSA*
Dipartimento di Scienze Biochimiche and Centro di Biologia Molecolare del Consiglio Nazionale delle Ricerche, Università La Sapienza, Piazzale A. Moro 5, 00185 Rome (Italy)
(First received June 26th, 1989; revised manuscript received December 4th, 1989)

SUMMARY

An automated procedure for the precolumn derivatization of amino acids with dansylchloride and a liquid chromatographic method for separation of the derivatives with fluorimetric detection in the picomole range are reported. The method involves a simple solvent preparation, which does not require the inclusion of non-volatile buffers of low ionic strength and delicate pH adjustments. The procedure was also utilized for the identification of COOH-amidated amino acids released from peptides after digestion with carboxypeptidase.

INTRODUCTION

Classical ion-exchange chromatography with subsequent post-column ninhydrin derivatization still remains the most reliable methodology for routine amino acid analysis in the nanomole range. For the detection of amino acids in the picomole range, a number of procedures have been described which require precolumn derivatization with reagents such as phenyl isothiocyanate (PITC), 4-dimethylaminoazobenzene-4-sulphonyl chloride (DABS-Cl), dimethylaminoazobenzene 4-isothiocyanate (DABITC), *o*-phthalaldehyde (OPA), 9-fluorenylmethyl chloroformate (FMOC-Cl) or dimethylaminonaphthalene-1-sulphonyl (dansyl) chloride[1–7], followed by separation and identification of the derivatives by reversed-phase high-performance liquid chromatography (RP-HPLC). The state-of-the art of these techniques, and in particular of amino acid analysis using phenylisothiocyanate derivatization, was recently reviewed[8]. The success of the different procedures reported in the literature depends on a multiplicity of factors, such as the possibility of finding reaction conditions adequate for all protein amino acids, the ease of automation of the procedure, the stability and spectroscopic properties of the derivatives and the effi-

[a] Dedicated to Professor G. B. Marini Bettolo on the occasion of his 75th birthday.

0021-9673/90/$03.50

ciency of the chromatographic method proposed for their separation and identification.

These methods often prescribe the inclusion of non-volatile buffers of low ionic strength and with pH values in the range 3.5–6.5 in the formula of at least one of the solvents to be used for the chromatographic separation. Slight alterations of these parameters can modify significantly the retention times of several amino acids. Further, salts adversely affect the maintenance of the hydraulic components of the apparatus and the lifetime of the column.

Using an automated version of the precolumn derivatization procedure with dansyl chloride, we developed an HPLC procedure capable of separating dansylamino acids and derivatives using a system of simply prepared volatile solvents. The entire procedure is flexible enough to permit both an adequately sensitive amino acid analysis of protein and peptide hydrolysates and the detection of some post-translationally modified forms of amino acids, *e.g.*, COOH-amidated residues.

EXPERIMENTAL

Acetonitrile and 2-propanol (HPLC grade) were obtained from Carlo Erba, trifluoroacetic acid, sodium hydrogencarbonate and sodium hydroxide from Merck, dansyl chloride from Fluka, amidated amino acids, dansylamino acid standards and N-[2-hydroxyethyl]piperazine-N′-[2-ethanesulphonic acid] (HEPES) from Sigma, L-[U-^{14}C]phenylalanine from New England Nuclear and carboxypeptidase Y (CPY) from Boehringer. A standard solution of amino acids (Pierce) was diluted in water (0.1 m*M*) and then stored at −20°C. Deionized water was first glass-distilled and then passed through a Sep-Pak C_{18} cartridge (Millipore).

Samples of peptides to be hydrolysed (25–250 pmol) were dried in recently pyrolysed glass microtubes (40 × 6 mm I.D.) after addition of 2 nmol of norleucine as internal standard, and then enclosed in a Pyrex container with a 1-ml layer of 5.7 *M* hydrochloric acid plus 0.1% phenol at the bottom. The container was evacuated, flushed with nitrogen, evacuated again and sealed. Hydrolysis was performed in the vapour phase for 20–24 h at 110°C. After the hydrolysis, the tubes were dried *in vacuo* at 40°C over sodium hydroxide pellets for 30 min. Automated dansylation of amino acid mixtures was achieved by using a Gilson auto-sampling injector consisting of two modules, a Model 231, sample injector equipped with a code 31 rack thermostated at 35°C and a 20-μl sample loop, and a Model 401 diluter, both controlled by the sample controller keypad. The rack positions 18/2, 18/4 and 18/6 were modified to accommodate glass vials (Pierce, 32 × 12 mm I.D.) containing the reagents. The tubes with dried samples were placed on the rack of the auto-sampling injector, which automatically dissolved the amino acid mixture in 10 μl of 0.1 *M* $NaHCO_3$–5 m*M* EDTA (pH 9.0), and then performed the derivatization by adding 10 μl of the dansylchloride solution (2.5 mg/ml in acetonitrile) followed by incubation for 30 min. One minute before loading onto the column, 10 μl of 0.4 *M* sodium hydroxide solution were added to the tubes to hydrolyse the excess of unreacted dansylchloride; 20 μl of this mixture were loaded onto the column.

For the chromatographic analysis, the apparatus consisted of two Waters Model 510 pumps (Millipore); gradient formation, quantification of chromatographic peaks and data treatment were effected by an IBM Model 286 PC XT computer using a Baseline 810 program (Millipore).

Separation of dansylamino acids was carried out on a Beckman Ultrasphere column (RP-18, 5 μm, 250 × 4.6 mm I.D.), thermostated at 48°C. The column was protected by a 2-μm stainless-steel filter (Rheodyne).

For the chromatographic separation a gradient was formed with two mobile phases: solvent A, 0.05% trifluoroacetic acid; and solvent B, acetonitrile–2-propanol (4:1, v/v). The flow-rate was 1.2 ml/min. The column effluent was mixed before the detector with 0.05 *M* sodium hydroxide in 20% acetonitrile using a Beckman Model 110A pump with the flow-rate set at 200 μl/min. This procedure permits the optimization of the fluorescence response of dansyl derivatives[9].

Dansylamino acids were detected using a Fluorichrom fluorescence detector for liquid chromatography (Varian), equipped with an excitation band filter at 280–340 nm and sharp emission cut-off filter at 430 nm.

Conventional amino acid analysis by ion-exchange chromatography (IEC) and post-column ninhydrin derivatization was performed using an LKB 2131 Alpha Plus instrument.

Digestion of peptides (1 nmol or less) with carboxypeptidase Y was performed at 35°C in 100 μl of 20 m*M* HEPES (pH 8.0) containing 2 nmol of norleucine as internal standard; the enzyme–substrate ratio was 1:50 (w/w). Aliquots of 20 μl, usually drawn at 1, 5, 10, 20 and 30 min, were immediately lyophilized and then derivatized with dansylchloride. Half of each sample was loaded onto the column for analysis; the remainder was dried, subjected to acid hydrolysis and then analysed.

RESULTS AND DISCUSSION

A simple program for the automated dansylation of amino acids and their derivatives was prepared for the Gilson auto sample injector and is reported in Table I.

The dansylation reaction yields stable, highly fluorescent derivatives with both primary and secondary amino acids[3]; no troublesome extraction of the products is required before analysis. According to the present version of the method, the samples are processed on-line under conditions which permit a complete dansylation also of the slowly reacting amino acids. The efficiency of dansylation and possible losses of the sample during automated derivatization were controlled by counting the radioactivity of an aliquot of a labelled phenylalanine solution before and after derivatization, and by counting the radioactivity of the dansylphenylalanine peak collected from the HPLC effluent, after automated injection of an aliquot of the labelled sample onto the column. The recovery was always $\geqslant 95\%$. The automated addition of dilute sodium hydroxide solution to the samples after the derivatization reaction effects the complete hydrolysis of unreacted dansyl chloride, with a consequent improvement of the baseline quality.

All dansyl derivatives of amino acids obtainable from protein hydrolysates can be separated in 30 min by using a system of volatile solvents of very simple preparation. The total running time, including column recycling, is about 34 min. The conditions for the chromatographic analysis are given in Table II and a typical chromatographic separation is shown in Fig. 1. The percentage of trifluoroacetic acid in solvent A is critical for the separation of Asp–Glu and Ala–Arg derivatives. Only slight adjustments of the gradient parameters are occasionally required to ensure prolonged

TABLE I

PROGRAM FOR AUTOMATED DANSYLATION WITH THE GILSON AUTO SAMPLER INJECTOR

```
1  RACK CODE 31
2  AUXIL 6/1
3  INPUT C/1
4  INPUT C0/41
5  INPUT C6/23
6  C1=0
7  FOR C2=1/10
8  FOR C3=1/6
9  C1=C1+1
10 PRINT/80
11 TUBE 18/4
12 HEIGHT
13 ASPIR 0/50/2
14 HEIGHT
15 ASPIR 0/12/0
16 HEIGHT
17 TUBE C2/C3
18 HEIGHT -1
19 DIS 0/18/0
20 TUBE 18/6
21 HEIGHT +7
22 ASPIR 0/12/0
23 TUBE C2/C3
24 HEIGHT -1
25 DIS 0/18/0
26 FOR C4=1/4
27 ASPIR 0/10/0
28 HEIGHT 0
29 DIS 0/11/0
30 HEIGHT -1
31 NEXT C4
32 HEIGHT
33 RINSE
34 DIS 0/1000/9
35 C5=0
36 FOR C5=1/C0
37 PRINT C5/25
38 WAIT 1
39 NEXT C5
40 PRINT/75
41 TUBE 18/2
42 HEIGHT
43 ASPIR 0/50/2
44 HEIGHT +8
45 ASPIR 0/10/1
46 TUBE C2/C3
47 HEIGHT -1
48 DIS 0/15/1
49 FOR C5=1/3
50 ASPIR 0/15/0
51 HEIGHT 0
52 DIS 0/17/0
53 HEIGHT -1
54 NEXT C5
55 HEIGTH
56 RINSE
57 DIS 0/1000/9
58 WAIT 30
59 PRINT C1/1
60 TUBE C2/C3
61 IF C6=0
62 GO TO 75
63 DIS 0/C6/0
64 HEIGHT
65 ASPIR 0/50/0
66 HEIGHT 0
67 FOR C5=1/3
68 ASPIR 0/20/0
69 HEIGHT 0
70 DIS 0/22/0
71 HEIGHT -1
72 NEXT C5
73 HEIGHT
74 WAIT 30
75 HEIGHT -1
76 ASPIR O/25/0
77 TUBE 0/0
78 DIS 0/27/0
79 WAIT 2
80 INJECT 1
81 AUXIL 7/2
82 WAIT /3/1
83 WAIT 100
84 INJECT 0
85 DIS 0/500/4
86 RINSE
87 DIS 0/1000/9
88 IF C1=>C
89 GO TO 92
90 NEXT C3
91 NEXT C2
92 WAIT C0
93 AUXIL 6/0
94 HOME
```

efficacy of the chromatographic performance. Under these conditions the column has a long lifetime (about 4000 analyses).

The reproducibility of the retention time of each derivative is shown in Table III. The coefficient of variation (C.V.) for each retention time was within 0.2% in six successive runs.

TABLE II

GRADIENT PARAMETERS

Time (min)	*Composition*[a]		*Curve*[b] *(type)*
	A (%)	*B (%)*	
0.0	93.0	7.0	
1.0	93.0	7.0	0
9.0	86.0	14.0	+1
24.0	57.0	43.0	+1
28.0	30.0	70.0	+7
28.2	0.0	100.0	+1
30.0	0.0	100.0	0
30.7	93.0	7.0	+1

[a] Solvents: A, 0.05% trifluoroacetic acid; B, acetonitrile–2-propanol (4:1, v/v).
[b] Waters gradient curve: 0 = isocratic; +1 = linear; +7 = convex.

For fluorescence detection we used a broad transmission band filter (280–340 nm) and an emission filter with a cut-off at 430 nm, as the nature of our solvent system affects both the fluorescence spectra and the intensity of the various dansyl-amino acids differently. The linearity of response of the method of derivatization was tested for amino acid standards at different concentration levels; the results are shown in Fig. 2. Peak area was proportional to the concentration of amino acid in the dansylation tubes from 0.3 to 50 μM. Inclusion of EDTA in the derivatization reaction mixture is essential in order to obtain good yields with those amino acids whose solubility is impaired by the formation of salts with cations extracted from glass during the hydrolysis[10].

All these features render this procedure an attractive alternative to other derivatization reactions for amino acid analysis at the picomole level. Moreover, the liquid

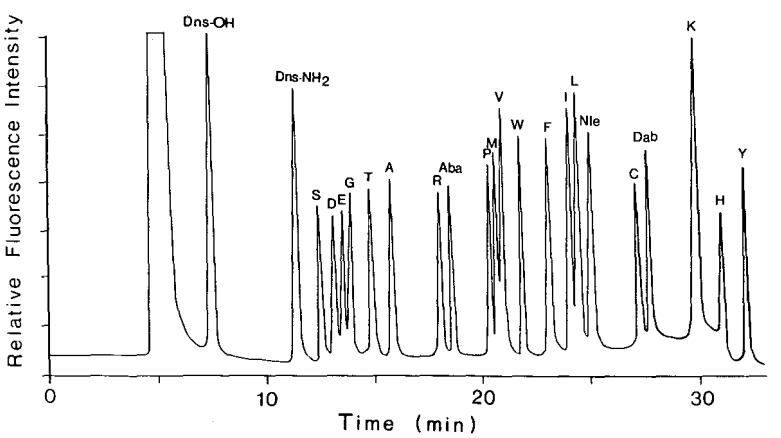

Fig. 1. Separation of an amino acid mixture after automated derivatization with dansylchloride. Sample size, 100 pmol of each amino acid. The peaks are labeled by one-letter abbreviations for the usual protein amino acids; Aba = α-aminobutyric acid, Nle = norleucine, Dab = 2,4-diaminobutyric acid, Dns-OH = 1-dimethylaminonaphthalene-5-sulphonic acid, Dns-NH_2 = 1-dimethylaminonaphthalene-5-sulphonamide.

TABLE III

REPRODUCIBILITY OF RETENTION TIMES OF DANSYLAMINO ACIDS

Compound	*Retention time (min)*	*C.V. (%)*
Dansyl-OH	7.21	0.18
Dansyl-NH_2	11.31	0.15
Dansyl-Ser	12.52	0.21
Dansyl-Asp	13.09	0.21
Dansyl-Glu	13.53	0.15
Dansyl-Gly	13.85	0.28
Dansyl-Thr	14.84	0.13
Dansyl-Ala	15.80	0.08
Dansyl-Arg	18.04	0.30
Dansyl-Aba	18.10	0.18
Dansyl-Pro	20.34	0.17
Dansyl-Met	20.70	0.08
Dansyl-Val	20.92	0.13
Dansyl-Phe	22.06	0.09
Dansyl-Ile	24.05	0.16
Dansyl-Leu	24.42	0.16
Dansyl-Nle	25.03	0.17
Di-dansyl-Cys	27.21	0.19
Di-dansyl-Dab	28.08	0.22
Di-dansyl-Lys	29.78	0.21
Di-dansyl-His	30.99	0.27
Di-dansyl-Tyr	32.09	0.20

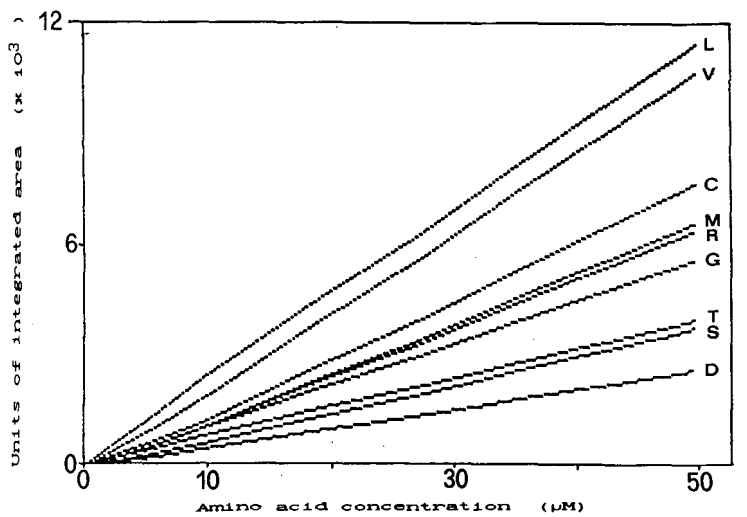

Fig. 2. Relationship between different concentrations (0.3, 1, 10, 50 μM) of amino acids and peak area of the corresponding derivatives after automated dansylation and chromatographic separation. For the sake of clarity only data related to some representative amino acids are reported.

chromatographic separation of dansyl derivatives can be used in the course of sequence determinations of peptides according to the manual dansyl–Edman procedure[11]. In fact, this procedure is still widely used not only because of its simplicity and low cost, but also because in some instances it gives more sequence information than expensive automated machines. The different scheme of the extraction steps may be very convenient for the analysis of hydrophobic peptides.

It should be noted that the vapour-phase hydrolysis of peptides, as described here, is both easy to perform and necessary in order to minimize contamination from various sources when analysing micro amounts of samples.

A comparison of the amino acid compositions of some bioactive peptides determined by the present method and by conventional IEC is reported in Table IV.

Finally, we adopted the automatic dansylation procedure for the analysis of amidated amino acid residues, which are often found at the C-terminus of biologically active peptides. The peptide of interest is digested with carboxypeptidase Y under conditions (see Experimental) that minimize the amidase activity. In fact, it has been shown that the salt composition and pH of the solvent affect to different extents the various enzymatic activities of carboxypeptidase Y, and in particular the amidase and the peptidyl amino acid amide hydrolase activities[12,13]. The time course of the release of amino acids from the C-terminus is monitored by analysing appropriate aliquots of the digestion mixture by the procedure described above. Under these conditions, at least a portion of the C-terminal amidated residue is released intact. It can be identified by direct HPLC analysis of its dansyl derivative. The identification can be confirmed by identifying in a second aliquot, after acid hydrolysis of the dansylamide, the corresponding dansylamino acid. Alternatively, the peptide can be subjected to the appropriate number of cycles of the Edman degradation; having subtracted the penultimate residue, the tube containing the putatively amidated C-terminal residue is

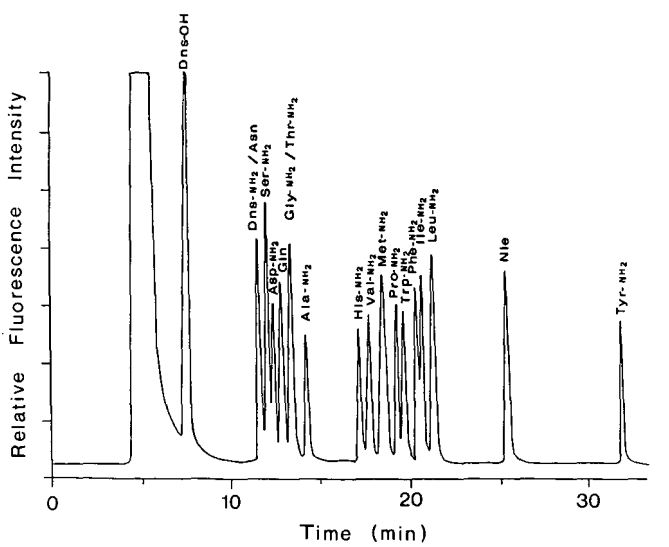

Fig. 3. Separation of an amidated amino acid mixture after automated derivatization with dansylchloride. Sample size, 200 pmol of each compound.

TABLE IV

AMINO ACID COMPOSITION OF BIOACTIVE PEPTIDES DETERMINED BY THE PRESENT METHOD[a] (Dns-Cl) AND BY CONVENTIONAL ION-EXCHANGE CHROMATOGRAPHY (IEC)

	HP1[b]			*HP2*[b]			*SP*[c]			*K*[c]		
Amino acid	*Dns-Cl*	*IEC*	*Sequence*[d]	*Dns-Cl*	*IEC*	*Sequence*[d]	*Dns-Cl*	*IEC*	*Sequence*[d]	*Dns-Cl*	*IEC*	*Sequence*[d]
Asp							1.8	1.7	2	0.9	0.9	1
Ser	1.0	1.1	1									
Glu	0.9	1.0	1				2.0	2.0	2	2.0	1.9	2
Pro	1.2	1.2	1	1.1	1.2	1	2.1	1.8	2	2.3	1.7	2
Gly	0.9	1.0	1	2.0	1.8	2	1.0	1.0	1	1.0	1.0	1
Ala	1.8	2.0	2	1.2	1.0	1						
Val										1.1	0.9	1
Met							1.1	0.9	1	1.0	1.0	1
Ile	1.9	2.1	2	1.1	1.0	1						
Leu	3.0	3.8	3	5.2	4.9	5	0.9	1.0	1	1.0	0.9	1
Phe	2.2	2.5	2	2.0	2.4	2	1.9	1.7	2	0.7	0.9	1
His										0.7	0.8	1
Lys				1.1	1.0	1						

[a] For hydrolysis and derivatization, see Experimental.
[b] Haemolytic peptides (HP) from the skin of *Rana esculenta*.
[c] Substance P-like (SP) and kassinin-like (K) peptides from the skin of *Pseudophryne güntheri*.
[d] Sequence was determined with a gas-phase sequencer (unpublished data from our laboratory).

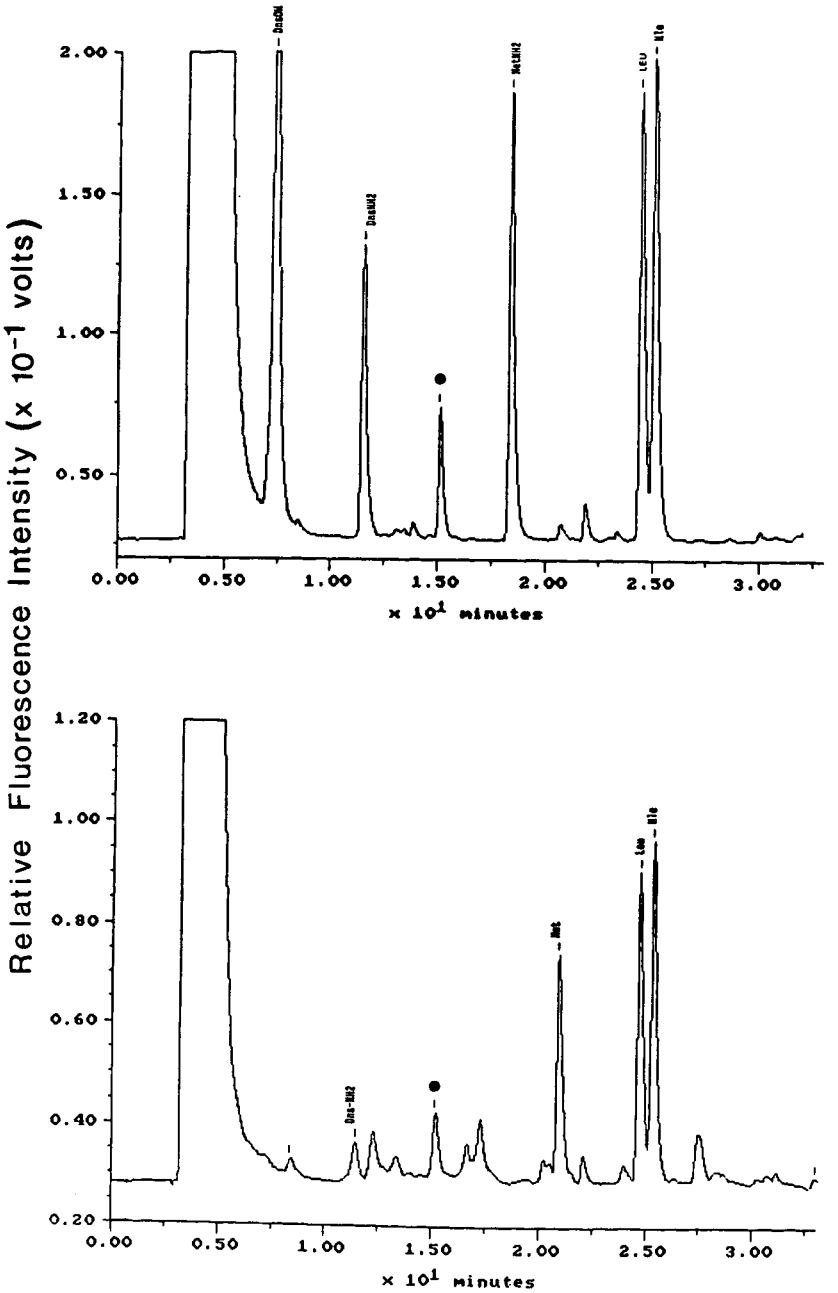

Fig. 4. Determination of the α-amide group on the carboxyl terminus of a kassinin-like peptide isolated from the skin of *Pseudophryne güntheri*, p-Glu–Pro–His–Pro–Asp–Glu–Phe–Val–Gly–Leu–$MetNH_2$ (unpublished data). Top, carboxypeptidase Y, 10 min; bottom, 6 *M* hydrochloric acid, 110°C, 2 h. ●, Buffer impurity.

reacted with dansylchloride and analysed as above. The separation of dansyl derivatives of amidated amino acids is shown in Fig. 3. In Fig. 4 the determination of the C-terminal amidated residue of a kassinin-like peptide isolated from the skin of *Pseudophryne güntheri* is shown. In conclusion, automated precolumn derivatization with dansylchloride is a convenient way to study amino acid compositions and to determine the COOH-terminal structure of peptides in the picomol range.

ACKNOWLEDGEMENTS

This work was supported in part by a grant from the Ministero Pubblica Istruzione and by CNR Special Project "Chimica Fine II" contract No. 89.00804.72. We thank Mr. Marco Federici for excellent technical coordination.

REFERENCES

1 J. P. Zanetta, G. Vincendon, P. Mandel and G. Gombos, *J. Chromatogr.*, 51 (1970) 441.
2 J. M. Wilkinson, *J. Chromatogr. Sci.*, 16 (1978) 547.
3 Y. Tapuhi, D. E. Schmidt, W. Lindner and B. L. Karger, *Anal. Biochem.*, 115 (1981) 123.
4 N. Kaneda, M. Sato and K. Yagi, *Anal. Biochem.*, 127 (1982) 49.
5 F. G. Marquez, A. R. Quesada, F,. Sanchez-Jimenes and I. Nunez de Castro, *J. Chromatogr.*, 380 (1986) 275.
6 A. Negro, S. Garbisa, L. Gotte and M. Spina, *Anal. Biochem.*, 160 (1987) 39.
7 S. Kochhar and P. Christen, *Anal. Biochem.*, 178 (1989) 17.
8 S. A. Cohen, and D. J. Strydoom, *Anal. Biochem.*, 174 (1988) 1.
9 B. S. Hartley, *Biochem. J.*, 119 (1970) 805.
10 R. More, K. D. Berndt, H. Tsai and S. C. Meredith, *Anal. Biochem.*, 172 (1988) 368.
11 W. R. Gray and B. S. Hartley, *Biochem. J.*, 89 (1963) 59.
12 K. Breddman, F. Widmer and J. T. Johansen, *Carlsberg Res. Commun.*, 45 (1980) 237.
13 K. Breddman, *Carlsberg Res. Commun.*, 49 (1984) 535.

Journal of Chromatography, 504 (1990) 139–149
Elsevier Science Publishers B.V., Amsterdam — Printed in The Netherlands

CHROM. 22 185

Utilizing column selectivity in developing a high-performance liquid chromatographic method for ginsenoside assay

TORBEN GULDAGER PETERSEN* and BENT PALMQVIST
Product Development Unit, Ferrosan Ltd., Sydmarken 1–5, DK-2860 Soeborg (Denmark)
(First received March 3rd, 1989; revised manuscript received November 13th, 1989)

SUMMARY

A method for the determination of ginsenosides using reversed-phase high-performance liquid chromatography is described. It is demonstrated that the column selectivity can be used as a parameter in developing new methods. A study of commercial columns all packed with octadecylsilane established that these columns differ in selectivity. The method can be used for assaying ginseng raw materials, capsules, tablets and multivitamin formulations. A validation of the method is described.

INTRODUCTION

The active constituents of ginseng (*Panax ginseng* C. A. Meyer) are a complex mixture of saponins often referred to as ginsenosides. More than 30 different ginsenosides are known, but this study included only six of the most thoroughly described (Fig. 1). In ginseng plants, the amount and the composition of ginsenosides present are highly dependent on whether it orginates from the main root, the root hairs or the leaves[1]. The composition may also vary with the species, the time of harvesting and the method of preparation[2,3]. These variations in raw materials are bound to be reflected in the products available on the market. It was concluded in an American study of ginseng products that about one third of the samples did not contain any detectable ginsenosides[4]. This emphasizes the need for a quality definition for the description of ginseng products. The situation today is that the consumers have no objective way of choosing a quality ginseng product. Most product labellings specify the content in milligram of extract or milligram of root, but this does not guarantee anything. However, the pharmacological effects of the pure ginsenosides have been studied on animals. The experiments revealed that ginsenoside Rg1 possessed CNS stimulation activity and showed an anti-fatigue effect. The ginsenoside Rb1 suppressed CNS activity and showed tranquillizing properties[5–7]. Consequently, a logical labelling would be the total amount of ginsenosides and, owing to the demonstrated pharmacological effects of Rg1 and Rb1, the ratio between Rg1 and Rb1 (Rg1/Rb1).

In the last 10 years, many attempts have been made to assay ginseng by high-performance liquid chromatography (HPLC) either in the normal-phase mode or

0021-9673/90/$03.50

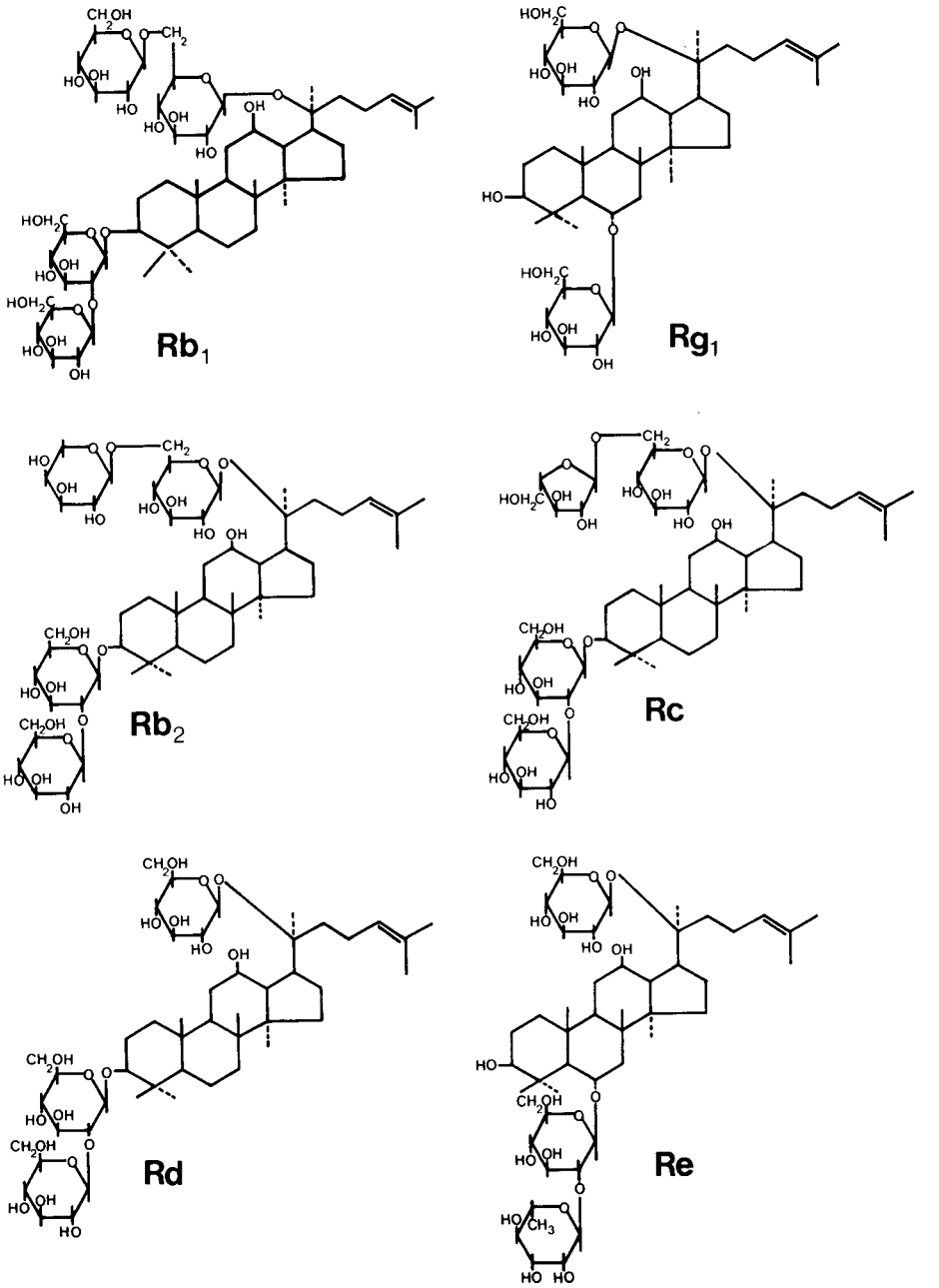

Fig. 1. The main ginsenosides, which according to their sapogenin (the aglycone part of the saponin), can be divided into two groups, the panaxatriols (Rg1 and Re) and the panaxadiols (Rb1, Rc, Rb2, Rd). The extra hydroxyl function at the panaxatriols makes them more polar than the panaxadiols. This is probably the explanation for the shorter retention times observed in reversed-phase systems for panaxatriols.

more recently in the reversed-phase mode. Previously methods such as spectrophotometry[8], gas chromatography (GC)[9] and thin-layer chromatography (TLC)[10] were employed, but with doubtful results. Spectrophotometric methods are insufficiently specific and often show large positive interferences, GC cannot be recommended for quantitative assays because of its poor reproducibility and TLC methods are too slow for routine analysis and must be regarded as antiquated. In one of the earliest HPLC methods, the saponins of ginseng were derivatized with benzoyl chloride in order to achieve greater UV sensitivity[11]. Another group of methods[12–16] uses two series of analyses, one mainly for separating Rg1 and Re and another for the remainder. More recently methods have appeared for determining all the ginsenosides using gradient elution[17–22]. However, most of them fail to separate Rg1 and Re, particularly in real samples.

Amino columns[23], ion-exchange columns[24] and columns packed with hydroxyapatite[19] have been tried, but to ensure the ruggedness of the method a C_{18} column seems to be the best choice.

In this paper we present a method in which ginsenosides are separated by a suitable reversed-phase C_{18} column and eluted with a two-step water–acetonitrile gradient with UV detection at 203 nm. The column selectivity was investigated by studying six different commericial columns under isocratic conditions.

EXPERIMENTAL

Materials

Acetonitrile was of HPLC grade (Merck, Darmstadt, F.R.G.). Water for use as a mobile phase constituent was prepared by passage through a Milli-Q water purification unit (Millipore, Bedford, MA, U.S.A.). Pure samples of ginsenosides (Rg1, Re, Rb1, Rc, Rb2 and Rd) were obtained from Sarsynthese (Merignac, France). Sep-Pak (C_{18}) cartridges were purchased from Waters Assoc. (Milford, MA, U.S.A.). The filters used were Minisart NML, pore size 0.8 μm (Sartorius, Göttingen, F.R.G.). Phosphate buffer was prepared by dissolving 3.532 g of potassium hydrogenphosphate (KH_2PO_4) (Merck) and 7.228 g of disodium hydrogenphosphate ($Na_2HPO_4 \cdot 2H_2O$) (Merck) in 1000 ml of water.

The liquid chromatograph consisted of two LC-6A pumps, a SIL-6A autoinjector, an SCL-6A system controller, an SPD-6A spectrophotometric detector and a C-R5A Chromatopac integrator, all purchased from Shimadzu (Kyoto, Japan). The detector was operated at 203 nm and its output signal was recorded by the integrator. The integrator was also used for chromatographic peak-area integration, peak-height measurement and calculations derived from those measurements.

Chromatographic conditions

The HPLC column was eluted at a constant flow-rate of 1.3 ml/min. The injection volume was set at 400 μl. The separations were obtained by gradient elution using the eluents (A) water and (B) acetonitrile according to the following profile: 0–20 min, 84–82% A, 16–18% B (curve 9); 20–55 min, 82–60% A, 18–40% B (curve 0).

The columns used were as follows: 1, μBondapak TM C_{18}, 10 μm (15.0 cm × 3.9 mm I.D.); 2, LiChrosorb RP-18, 5 μm (12.5 cm × 4.0 mm I.D.); 3, Nucleosil C_{18}, 5 μm (15.0 cm × 4.6 mm I.D.); 4, Spherisorb ODS, 5 μm (15.0 cm × 4.6 mm I.D.); 5,

Techopak C_{18}, 10 μm (15.0 cm × 3.9 mm I.D.); 6, Zorbax ODS, 7 μm (15.0 cm × 4.6 mm I.D.). Column 1 was purchased from Waters Assoc., 2 from Merck and 3–6 from HPLC Technology (Macclesfield, U.K.). In these experiments no guard columns were used to ensure that nothing but the column was creating the separations. In all other instances a suitable precolumn, LiChrosorb RP-18, 7 μm (3 cm × 4 mm I.D.), was used to protect the column. After each run a 10-min wash period consisting of 95% B at 2.7 ml/min and a 10-min stabilization period consisting of 16% B at 1.3 ml/min was introduced.

Sample preparation

Ginseng tablets. Accurately weigh tablet powder corresponding to 25 mg of ginsenosides into a 250-ml volumetric flask. Add 150 ml of phosphate buffer solution, shake at 35–40°C for 15 min, cool, dilute to volume with phosphate buffer solution and mix. Apply 10 ml of this solution to a Sep-Pak cartridge, prewashed with 5 ml of methanol and 5 ml of water. Wash the Sep-Pak cartridge with 10 ml of water followed by 15 ml of 30% methanol. Elute the ginsenosides into a 50-ml round-bottomed flask with 10 ml of methanol. Evaporate to dryness under vacuum at a maximum temperature of 50°C. Dissolve the residue in water to a final ginsenoside concentration of 0.1 mg/ml.

Capsules. Weigh into a centrifuge tube an accurate amount from capsules corresponding to 10 mg of ginsenosides. Rinse the substance by extraction with 3 × 10 ml of light petroleum. Dry the residue with nitrogen, suspend the residue in 50 ml of phosphate buffer and centrifuge. Use 5 ml in the Sep-Pak procedure described for tablets.

Fluids. Dilute a volume of sample corresponding to 100 mg of extract or 10 mg of ginsenosides to 50 ml with phosphate buffer and clean 5 ml of this solution by the Sep-Pak procedure.

Standard solution. Weigh an accurate amount of standard extract corresponding to 10 mg of ginsenosides in a 100-ml volumetric flask. Dissolve in phosphate buffer solution and dilute to volume. If necessary a short warming period of 5 min to a temperature of 40°C could be accomplished before dilution to volume. Apply 10 ml of this final solution in the Sep-Pak procedure.

The validity of the Sep-Pak procedure was checked by injecting the solution not applied in the Sep-Pak procedure and compared it with that cleaned by the Sep-Pak procedure. The standard extract was standardized by the use of the pure ginseng standards. Before injecting sample or standard solutions into the liquid chromatograph, all solutions were filtered through a 0.8-μm pore size filter.

RESULTS AND DISCUSSION

The results from testing the six types of columns are summarized in Tables I and II. From these tables and the chromatograms shown in Fig. 2 it can be seen that the columns differ in selectivity, efficiency and separation of impurities.

The selectivity α can be affected by the mobile phase and by the column packing material. The effects of the stationary and mobile phases on selectivity are not directly related, but we cannot expect to differentiate the column selectivity from the solvent

TABLE I

COLUMN SELECTIVITY UNDER ISOCRATIC CONDITIONS (21% ACETONITRILE, 1.3 ml/min)

t_0 = Time in minutes for unretained molecules to move from the point of injection to the detector; k'_{Rg1} = capacity factor for ginsenoside Rg1; k'_{Re} = capacity factor for ginsenoside Re; α = selectivity ($\alpha = k'_{Re}/k'_{Rg1}$).

Parameter	*μBondapak*	*LiChrosorb*	*Nucleosil*	*Spherisorb*	*Techopak*	*Zorbax*
t_0	0.793	0.628	0.935	0.880	0.896	0.818
k'_{Rg1}	16.18	21.68	21.06	21.25	15.09	13.51
k'_{Re}	18.79	24.46	23.48	24.67	17.17	14.38
α	1.16	1.13	1.11	1.16	1.14	1.06

selectivity in the described system. The solvent selectivity cannot be considered to be constant for several reasons. The concentration profile through the column will be a function of the column dimensions and the packing material. The packing material affects the mobile phase in a number of ways. Eddy diffusion is caused by velocity differences between various paths that the solvent will follow during passage through the porous bed. Film resistance close to the surfaces of the particles exists for laminar flow. In the pores of the particles, regions with stagnant solvent will be present. All this results in a certain degree of back-mixing. As a consequence of the different column dimensions and packing materials, none of the six columns tested were actually exposed to the same elution profile. A reasonable way to find an expression for the column selectivity is to test the columns under isocratic conditions. This will make the mobile phase composition constant and eliminate all solvent selectivity variations.

We chose to carry out an isocratic test with acetonitrile–water (21:79) as the mobile phase. The sample was a solution consisting of a mixture of Rg1 and Re standard. The column void time is an important factor in calculating the selectivity. The void time was carefully examined by injecting unretained molecules. For this

TABLE II

ESSENTIAL DATA FOR COLUMN PERFORMANCE

N = Number of theoretical plates calculated for Rg1 in the isocratic test by the equation $N = 5.54 (t_{Rg1}/W_{1/2})^2$; α = separation selectivity between Rg1 and Re in the isocratic test; R = resoluton between Rg1 and Re calculated assuming that the peaks in the gradient elution system were isosceles triangles.

Column	*N*	*α*	*R*	*Separation of impurity a (Fig. 2) from Rb1*	*Separation of impurity b (Fig. 2) from Rb2*
μBondapak	1500	1.16	0.9	Poor	Poor
LiChrosorb	3600	1.13	1.4	Usable	Good
Nucleosil	4800	1.11	1.0	Good	Good
Spherisorb	4100	1.16	1.1	Usable	Usable
Techopak	1700	1.14	1.0	Poor	Poor
Zorbax	3300	1.06	0.8	Poor	Good

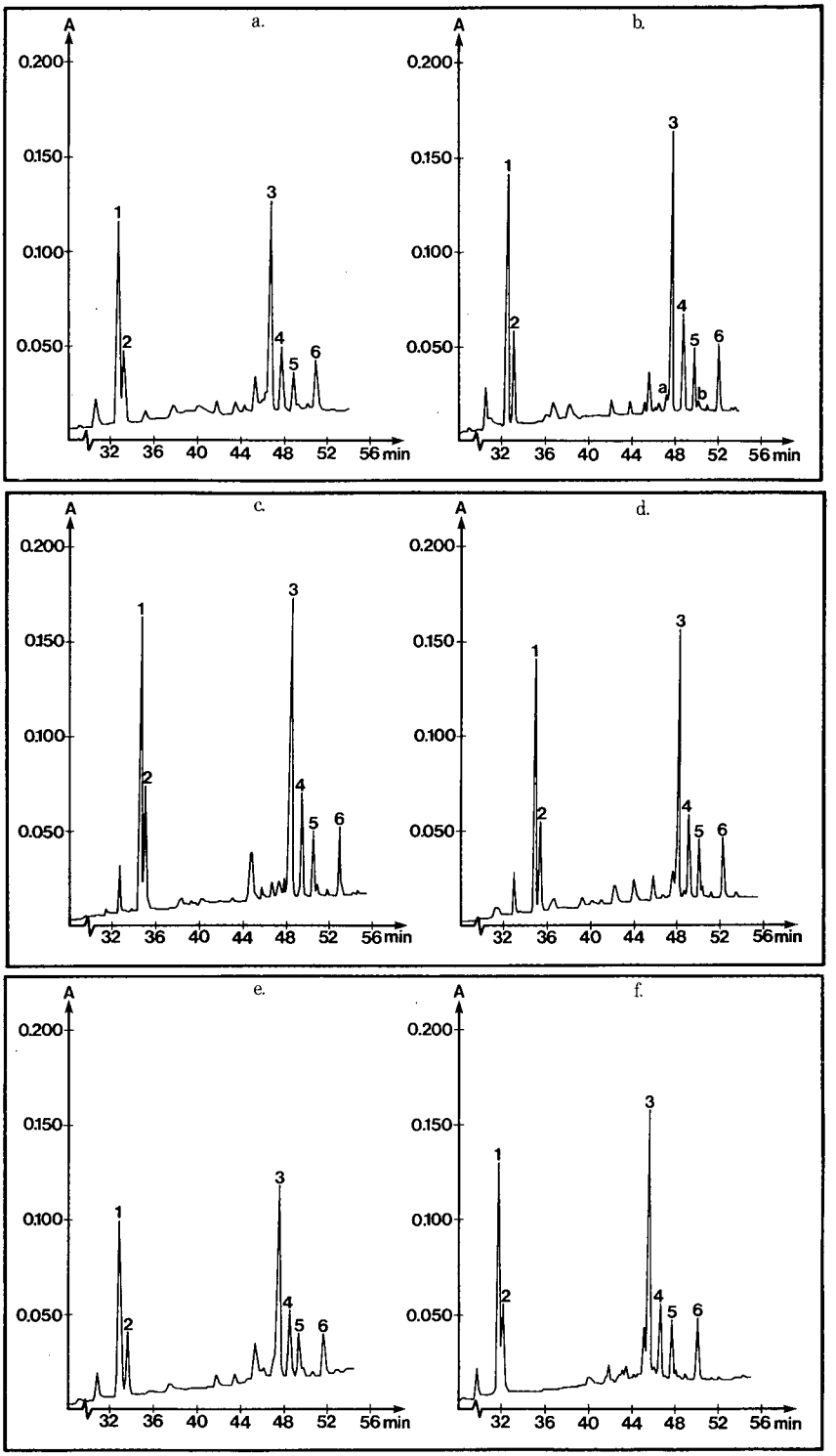

Fig. 2. Chromatograms for the performance of the columns in the gradient elution system. Peaks: 1 = Rg1; 2 = Re; 3 = Rb1; 4 = Rc; 5 = Rb2; 6 = Rd. The letters a and b in (b) refer to impurities often present close to Rb1 and Rb2, respectively. (a) μBondapak; (b) LiChrosorb; (c) Nucleosil; (d) Sperisorb; (e) Techopak; (f) Zorbax.

purpose, we used a sample of sodium nitrite as recommended[25]. The response was measured at both 355 and 260 nm. The peak-height ratio was then compared with that obtained for sodium nitrite solution measured at the same two wavelengths with an ordinary spectrophotometer. The results in Table I show pronounced differences in the values of the selectivity α. These differences must reflect the impact of the column on the selectivity.

To make it clear why the selectivity is so important, we can consider the approximate expression for the resolution:

$$R_s = 1/4[(\alpha - 1)/\alpha][k'/(1 + k')]\sqrt{N}$$

To improve the resolution, columns with better efficiency are not a very powerful tool, beause the resolution is a function of the square root of the number of theoretical plates. The resolution is far more sensitive to changes in selectivity, especially when α becomes close to unity. In Table II, the most important factors are summarized in order to judge which column should be used. The resolution between Rg1 and Re, actually obtained in the gradient elution system does not seem to fit perfectly with the data for efficiency and selectivity obtained in the isocratic column test. In the gradient elution system the selectivity is also affected by the solvent selectivity. Variations in solvent selectivity in the gradient elution test of the columns must be a result of different elution profiles. Changes in elution profiles can be caused either by different column dimensions or differences in the packing material. Columns 3 and 4 have the same dimensions and size of packing material, but the values for the resolution in Table II suggest that there is a difference in solvent selectivity. This change in solvent selectivity, which must be related to the nature of the packing material, also seems to occur if we compare columns 1 and 5. In gradient elution systems, changes in the elution profiles affect the solvent selectivity, and because the resolution is a function of the selectivity it is not possible to predict from an isocratic column selectivity test which column under the gradient elution conditions will give the best resolution. However, in general, the column with the best selectivity in an isocratic test is to be preferred.

From the values for the column selectivity and the number of theoretical plates in Table II, the best resolution should be achieved with column 4. Instead, we see that column 2 gives a better resolution. This means that for column 4 an even better resolution of Rg1 and Re should be possible by using another elution profile.

The resolution of Rg1 and Re is not the only aspect to be considered in judging the suitability of the columns for the ginsenoside assay. Often impurities near Rb1 and Rb2 can be observed in the chromatograms. These impurities might well be ginsenosides. Table II includes a qualitative grading of the ability of the columns to separate these impurities. Column 3 is the best for this purpose, but column 2 is almost as good.

Summarizing all this information, column 2 is the preferred choice, and this is also confirmed by the visual impression of the chromatograms in Fig. 2.

Method validation

Identification. The ginsenosides in the samples were identified by comparing the retention times of pure ginsenoside standards with the retention times obtained in the sample chromatograms. Further, the elution order of the ginsenosides was the same as reported with other reversed-phase methods.

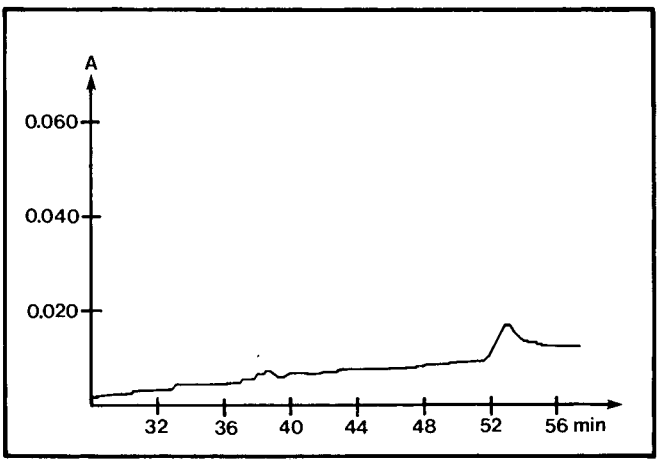

Fig. 3. Background chromatogram for the gradient elution system. The sample was a tablet containing vitamins and minerals, but no ginseng, degraded under accelerated conditions. Column: LiChrosorb RP-18, 5 μm (12.5 cm × 4.0 mm I.D.).

Specificity. Ginseng placebo tablets containing vitamins and minerals were checked for chromatographic background. The tests were performed on both fresh placebo and placebo degraded under accelerated conditions (6 months at 40°C and 75% relative humidity). No chromatographic interference was observed (Fig. 3).

Detection limit. At a 2:1 signal-to-noise ratio, the limit of detection was determined to be 20 ng/ml for all six ginsenosides. This is equivalent to 0.1% of the nominal concentration of 20 μg/ml. The low detection limit was a consequence of the large injection volume of 400 μl. A much smaller volume would not have ensured an adequate distance from the detection limit.

Precision. The values of the relative standard deviation for the six ginsenosides were found to be in the range 2.4–4.6%. For the total ginsenoside content the

TABLE III

DATA FOR LEAST-SQUARES REGRESSION ANALYSIS OF THE CALIBRATION GRAPH: $Y = SX + I$

Y = Response in mV s; X = concentration in μg/ml; S = slope; I = intercept; C = correlation coefficient; SDS = estimate of standard deviation of slope; SDI = estimate of standard deviation of intercept; SDM = estimate of standard deviation of single measurement.

Parameter	*Rg1*	*Re*	*Rb1*	*Rc*	*Rb2*	*Rd*
S	82.1	15.9	61.9	54.1	45.2	69.8
I	34.1	−5.9	−25.3	−10.4	−14.1	−56.3
C	0.9998	0.9994	0.9998	0.9998	0.9997	0.9994
SDS	0.72	0.25	0.57	0.53	0.47	1.07
SDI	30.5	9.6	23.1	21.6	18.7	43.6
SDM	53.9	16.9	40.8	38.2	32.9	77.0

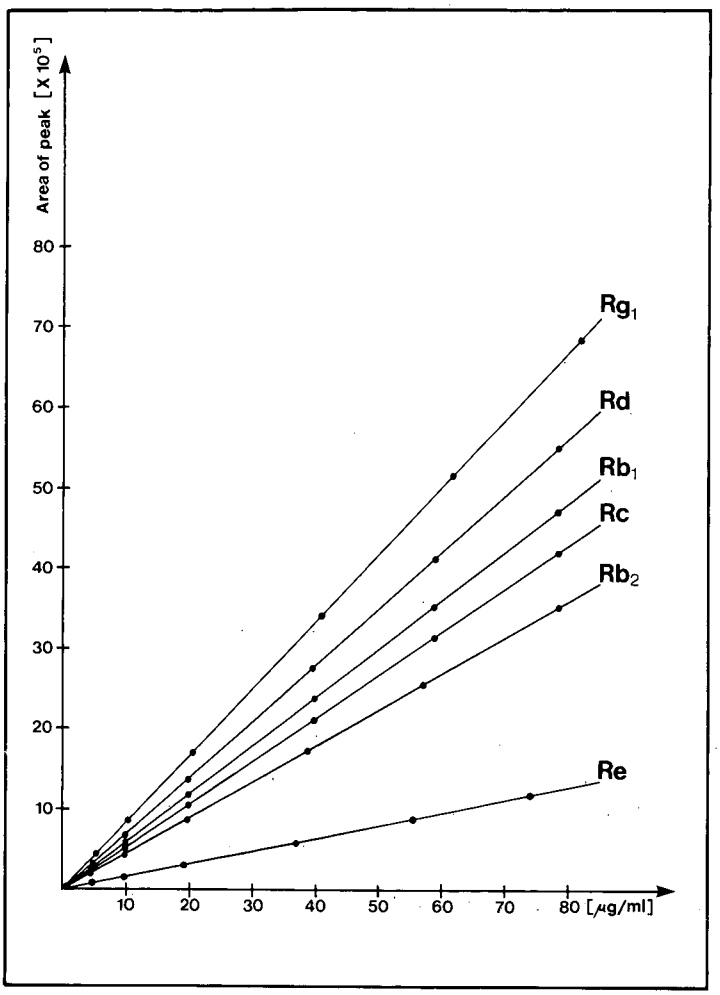

Fig. 4. Calibration graphs for the ginsenosides under gradient elution conditions. The units on the ordinate are $\mu V \cdot s$. Column as in Fig. 3.

reproducibility of the method was calculated by assaying eight replicates of the same batch. In this instance the relative standard deviation was estimated to be 2.7%.

Linearity. The linearity of the response *vs.* concentration curve for each of the six ginsenosides was investigated in the range 0–80 μg/ml. Regression analysis data are given in Table III and the calibration graphs for the ginsenosides are shown in Fig. 4. The calibration graphs had correlation coefficients very close to unity, and the intercepts were not statistically significantly different from zero at the 95% confidence level.

Accuracy. The accuracy of the Sep-Pak procedure was checked by comparing the results obtained from extract solutions applied in the Sep-Pak procedure with those from the same solutions not applied in the Sep-Pak procedure. Setting the result for

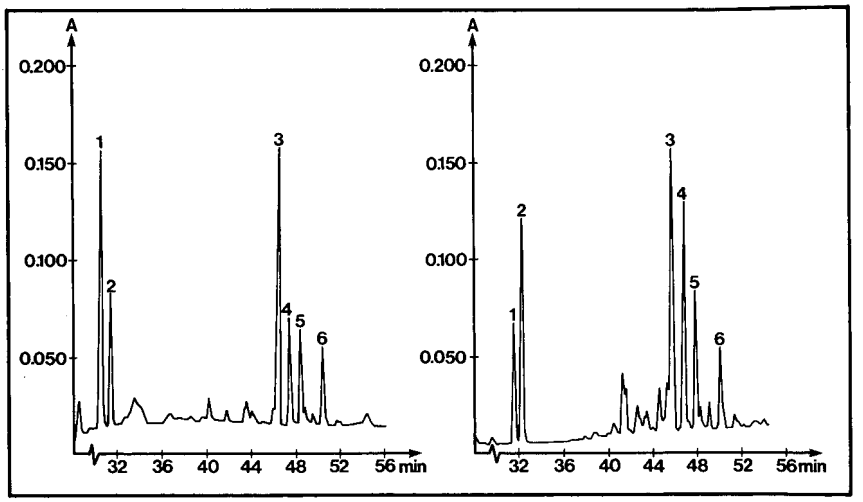

Fig. 5. Left: chromatogram obtained from a sample of Ginozin Combi (trade-name for a Ferrosan, Soeborg, Denmark, tablet containing 2 mg of ginsenosides, eleven vitamins and eight minerals). Right: chromatogram for a sample of Gericomplex (trade-name for a capsule produced by Pharmaton, Lugano, Switzerland, containing ginseng extract corresponding to 200 mg of root of *Panax ginseng* C. A. Meyer, ten vitamins and six minerals). The two chromatograms illustrate well that the profiles of ginsenosides in various products can be very different. Both analyses were performed with the gradient elution programme. Column as in Fig. 3. Peak numbers as in Fig. 2.

total ginsenosides for the extract solution not applied in the Sep-Pak procedure to 100%, the recovery for the Sep-Pak procedure was found to be 98.9% with calculated relative standard deviation of 4.2% (n = 41).

The accuracy of the method, including the Sep-Pak procedure, was substantiated by assaying production samples of ginseng tablets. The recovery was found to be 98.4% of theory for Ferrosan products, with a standard deviation of 5.0% (n = 7).

CONCLUSION

This method for assaying ginsenosides has the advantage of dealing with all the ginsenosides in question in a single run, with a good separation of all the compounds. Especially the resolution of Rg1 and Re, which has been a major drawback in many earlier methods, is acceptable (Fig. 5). The results emphasize that it is important which type of C_{18} column is chosen. The six columns tested here showed considerable differences in column selectivity. In developing new methods this fact can be utilized and should be thought of as a possible optimizing parameter together with the solvent selectivity and the number of theoretical plates.

REFERENCES

1 J. H. Lui and E. J. Staba, *J. Nat. Prod.*, 43 (1980) 340.
2 J. P. Hou, *Comp. Med. East West*, 5 (1977) 123.
3 S. K. Kim, I. Sakamoto, K. Morimoto, M. Sakata, K. Yamasaki and O. Tanaka, *Planta Med.*, 42 (1981) 181.

4 J. D. Phillipson and L. A. Anderson, *Pharm. J.*, 232 (1984) 161.
5 T. Kaku, T. Miyata, T. Uruno, I. Sako and A. Kinoshita, *Arzneiom.-Forsch.*, 25 (1975) 539.
6 H. Saito, Y. Yoshida and K. Takagi, *Jpn. J. Pharmacol.*, 24 (1974) 119.
7 T. Kita, T. Hata, Y. Kawashima, T. Kaku and E. Itoh, *J. Pharm. Dyn.*, 4 (1981) 381.
8 *Deutsches Arzneibuch 9*, Deutscher Apotheker Verlag, Stuttgart, 9th ed., 1986, p. 838.
9 E. Bombardelli, A. Bonati, B. Gabetta and E. M. Martinelli, *J. Chromatogr.*, 196 (1980) 121.
10 H. Wagner and A. Wurmböck, *Dtsch. Apoth.-Ztg.*, 33 (1978) 1209.
11 H. Besso, Y. Saruwatari, K. Futamura, K. Kunihiro, T. Fuwa and O. Tanaka, *Planta Med.*, 37 (1979) 226.
12 O. Sticher and F. Soldati, *Planta Med.*, 36 (1979) 30.
13 F. Soldati and O. Sticher, *Planta Med.*, 38 (1980) 348.
14 P. Pietta, P. Mauri and A. Rava, *J. Chromatogr.*, 356 (1986) 212.
15 W. Sye and P. Tsai, *J. Chin. Chem. Soc.*, 34 (1987) 1.
16 H. Kanazawa, Y. Nagata, Y. Matsushima, M. Tomoda and N. Takai, *Chromatographia*, 24 (1987) 517.
17 B. Meier, A. M. Bratschi, K. D. Tölke and O. Sticher, in H. M. Chang, H. W. Yeung, W.-W. Tso and A. Koo, *Advances in Chinese Medicinal Materials Research*, World Scientific Publ., Singapore, 1985, pp. 471–484.
18 B. Meier and O. Sticher, *Pharm. Ind.*, 48 (1986) 87.
19 R. Kasai, H. Yamaguchi and O. Tanaka, *J. Chromatogr.*, 407 (1987) 205.
20 P. Pietta and P. Mauri, *J. Chromatogr.*, 362 (1986) 291.
21 H. P. Nissen, H. Biltz and H. W. Kreysel, *GIT Fachz. Lab.*, 4 (1987) 293.
22 G. Sollorz, *Dtsch. Apoth.-Ztg.*, 41 (1985) 2052.
23 R. Bartomé, D. Masoliver, M. Soler and J. Vilagelie, *Alimentaria (Madrid)*, 24 (1987) 73.
24 H. Yamaguchi, H. Matsuura, R. Kasai, K. Mizutani, H. Fujino, K. Ohtani, T. Fuwa and O. Tanaka, *Chem. Pharm. Bull.*, 34 (1986) 2859.
25 K. Jinno, N. Ozaki and T. Sato, *Chromatographia*, 17 (1983) 341.

Journal of Chromatography, 504 (1990) 151–161
Elsevier Science Publishers B.V., Amsterdam — Printed in The Netherlands

CHROM. 22 224

Evaluation of high-performance liquid and capillary gas chromatography for analysis of sesquiterpene lactones of the Melampodiinae

JEFFREY D. WEIDENHAMER[a,*], ELIZABETH D. JORDAN and NIKOLAUS H. FISCHER
Department of Chemistry, Louisiana State University, Baton Rouge, LA 70803 (U.S.A.)
(First received August 9th, 1989; revised manuscript received December 12th, 1989)

SUMMARY

The capacity of reversed-phase high-performance liquid chromatography (HPLC) and capillary gas chromatography (GC) to separate 37 sesquiterpene lactones of the Melampodiinae has been investigated. The HPLC system employed a Hypersil ODS column and methanol–water as eluent for isocratic and gradient separations. The GC system utilized a RSL-150 bonded phase capillary column with flame ionization detection. The previously characterized melampolide melnerin B was determined by both HPLC and GC to be a mixture of two isomers, containing a 2-methylbutanoate (melnerin B) or a 3-methylbutanoate (melnerin B') substituent at C-8. The HPLC and GC methods developed have been applied to the analysis of a crude extract of *Melampodium cinereum*.

INTRODUCTION

Sesquiterpene lactones are a structurally diverse group of over 3000 natural products isolated primarily from plants of the Asteraceae. Many have important biocidal and pharmaceutical activities[1,2]. The leaves of feverfew, *Tanacetum parthenium*, have yielded several sesquiterpene lactones which inhibit prostaglandin synthesis and are used for the treatment of migraine headaches[3,4]. A highly potent molluscicide, 7α-hydroxy-3-desoxyzaluzanin C has been isolated from *Podachaenium eminens* (Asteraceae)[5]. Dihydroparthenolide, a constituent of common ragweed, *Ambrosia artemisiifolia*, stimulates germination of the devastating parasitic weed *Striga asiatica* at nanomolar levels[6].

Less work has been done on the ecological functions of these compounds[2,7]. However, because of their high alkylating power, which is due to the α-methylene-γ-lactone moiety which most possess, along with α,β-unsaturated carbonyl and epoxide moieties in certain compounds, it may be expected that these compounds will exhibit toxic effects against many organisms and play an important role in the chemical

[a] Present address: Department of Chemistry, Ashland University, Ashland, OH 44805 (U.S.A.)

0021-9673/90/$03.50

(a) **LEUCANTHOLIDES**

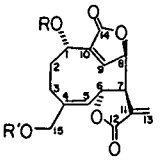

	R	R'
(1) Melampodin B	Ac	H
(2) Melampodin B Acetate	Ac	Ac
(3) Cinerenin	C_2H_5	H
(4) Cinerenin Acetate	C_2H_5	Ac
(5) Melampodin C	A	H
(6) Melampodin C Acetate	A	Ac
(7) Melampodin D	C	H

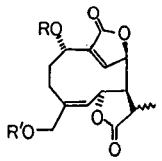

	R	R'
(8) 11,13-Dihydrocinerenin	C_2H_5	H

CIS.CIS-GERMACRANOLIDES

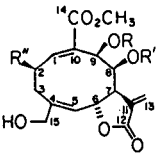

	R	R'	R''
(9) Melcanthin A	Ac	D	H
(10) Melcanthin B	Ac	D	OH
(11) Melrosin A	B	B	OH
(12) Longicornin B	A	A	H

REPANDOLIDES

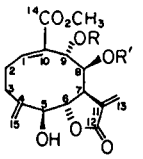

	R	R'
(13) Repandin A	E	A
(14) Repandin B	E	C

MELAMPOLIDES

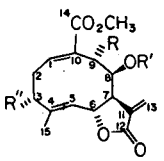

	R	R'	R''
(15) Melampolidin	H	I	H
(16) Leucanthinin	OAc	H	OH
(17) Desacetoxyleucanthinin	H	H	OH
(18) Leucanthinin Acetate	OAc	H	OAc

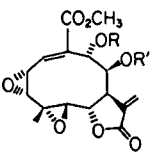

	R	R'
(19) Leucanthin B	Ac	H
(20) Desacetylleucanthin B	H	H

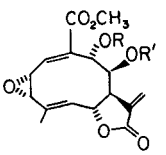

	R	R'
(21) Melampodin A	H	H
(22) Melampodinin A	Ac	I
(23) Melampodinin B	C	I

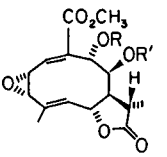

	R	R'
(24) 11,13-Dihydromelampodin A 9-α-[2-methylbutanoate]	C	H

Fig. 1.

(b)

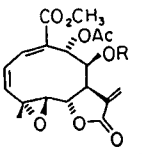

	R
(25) Leucanthin A	H

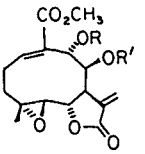

	R	R'
(26) Longipilin	H	D
(27) Enhydrin	Ac	H
(28) Desacetylenhydrin	H	H

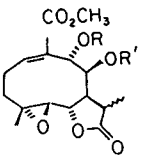

	R	R'
(29) 11,13-Dihydroenhydrin	Ac	H

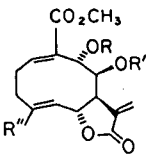

	R	R'	R''
(30) Longipin	H	H	CH_2OAC
(31) Tetrahelin C	C	I	CH_3
(32) Tetraludin C	F	G	CH_3

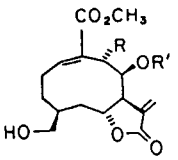

	R	R'
(33) Melnerin A	H	A
(34) 9-α-Acetoxymelnerin A	OAc	A
(35) Melnerin B	H	C
(36) Melnerin B'	H	J
(37) 9-α-Acetoxymelnerin B	OAc	C

ESTER SIDE CHAINS

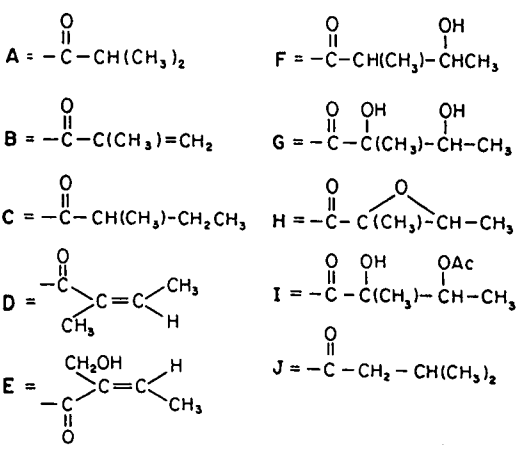

Fig. 1. Sesquiterpene lactones of the Melapodiinae. Ac = CH_3CO; OAc = CH_3COO.

defenses of plants which contain them. Evidence is accumulating that sesquiterpene lactones deter insect feeding[8,9], reduce the survival of insect larvae and adults[10,11], and inhibit germination and growth of other plants[12,13].

Melampolide-type sesquiterpene lactones (Fig. 1) are characteristic of plant species in the subtribe Melampodiinae of the Asteraceae[14]. The restricted distribution of many of these compounds has been used to clarify evolutionary relationships in this subtribe. There is evidence that melampodin A (**21**) and melampodinin A (**22**) deter insect feeding and inhibit insect growth[15].

The development of rapid, quantitative analytical methods for plant natural products is essential to studies of chemosystematics, chemical ecology and the monitoring of their production in cell and hairy root cultures[16]. Analytical high-performance liquid chromatography (HPLC) has been applied successfully to the separation of 33 pseudoguaianolides and xanthanolides of the genus *Parthenium*[17] and to the analysis of 21 pseudoguaianolides of *Arnica chamissonis*[18], as well as other compounds[19,20]. Acetonitrile–water[17] or methanol–water[18] gradients have been employed using reversed-phase columns, with detection at 210–225 nm to provide sensitivity. Successful separation of sesquiterpene lactones from *Helianthus* has been obtained with an isocratic methanol–water system[19]. Capillary gas chromatography (GC) has also been applied with success for certain underivatized sesquiterpene lactones[18,21]. Micro-sampling techniques developed by Spring *et al.*[20] have demonstrated that it is possible to directly sample the glandular trichomes of leaves and flower heads, where sesquiterpene lactones are sequestered.

The application of reversed-phase HPLC and capillary GC to sesquiterpene lactones of the Melampodiinae is reported in this paper. We have applied these methods to the analysis of a crude terpenoid extract of *Melampodium cinereum*.

EXPERIMENTAL

HPLC apparatus

HPLC analyses were performed on a Hewlett-Packard 1090 liquid chromatograph equipped with a diode array detector and auto-injector (25-μl syringe). Detection channels were set at 210, 220, 230 and 254 nm, with a bandwidth of 16 nm. Chromatograms were recorded and analyzed on a Hewlett-Packard HPLC Chemstation (Series 300 computer). The column was a 5-μm Hypersil ODS (150 × 4.6 mm I.D., Hewlett-Packard, Mt. View, CA, U.S.A.). Analyses were performed at ambient temperature with a flow-rate of 1.0 ml/min.

Elution

Two solvents were used: (A) HPLC-grade methanol and (B) distilled, deionized water. Compounds were eluted isocratically with 50% A. The gradient elution profile was 0–18 min, 20% A (isocratic); 18–36 min, 20–50% A (linear gradient); 36–46 min, 50–70% A (linear gradient); and 46–50 min, 70% A (isocratic).

GC equipment and experimental conditions

The GC system consisted of a Hewlett-Packard 5890 gas chromatograph equipped with a split/splitless injector system and a flame ionization detector. Nitrogen was the carrier gas and the carrier gas pressure was 20 p.s.i. Injections were

made in the split mode with a splitting ratio of 4:1. A 45 m × 0.25 mm I.D. fused-silica capillary column with a bonded polymethylsilicone stationary phase (RSL-150, Alltech, Deerfield, IL, U.S.A.) of 0.2-μm film thickness was used for the separations. Two temperature gradients were employed. For the first (G1), the initial temperature of 95°C was held for 2 min, increased to 285°C at 15°C/min and held at 285°C for 10 min. For the second (G2), the initial temperature of 125°C was held for 1 min, increased to 260°C at 15°C/min and held at 260°C for 15 min. The injection volume was 1 μl unless noted otherwise.

Samples

Compounds were obtained from the sample collection in our laboratory. A crude terpenoid extract of *Melampodium cinereum* var. *cinereum* was prepared by standard procedures[22] (Fischer No. 3792). Dried plant material was extracted with dichloromethane. After solvent removal by evaporation, the residue was taken up in 95% aqueous ethanol (100 ml/100 g plant material). To this solution an equal volume of 5% aqueous lead acetate was added and left overnight. The precipitated phenolics and chlorophyll were removed by filtration through Celite and the filtrate evaporated *in vacuo* to remove most of the ethanol. The residual material was extracted exhaustively with dichloromethane and this solvent evaporated to obtain the crude extract. Solutions of the sesquiterpene lactones and the extract were prepared in methanol to contain 1 mg/ml. Partial chemical change of a few compounds occurred over the several weeks they were kept in methanol solution. This was evidenced by the appearance of additional peaks and altered HPLC and GC retention times. These included melampodin B (**1**), melampodin C (**5**), longicorin B (**12**) and longipin (**30**).

RESULTS AND DISCUSSION

HPLC separations

HPLC (and GC) retention times of the 37 sesquiterpene lactones examined are listed in Table I. HPLC separations were performed both isocratically and using a gradient. Most compounds separated from one another with the isocratic system. The gradient developed increased the separation of the most polar compounds, allowing confirmation of their identities in plant extracts. Because of the presence of a restricted number of sesquiterpene lactones in any one species, there is only a slight likelihood of overlapping peaks in a given extract.

Of the various structural types of sesquiterpene lactones included in this study, the leucantholides were the least strongly retained, probably due to the added polarity given by the second lactone ring. The elution order of the eight individual leucantholides correlates well with the lipophilicity of the compounds. For example, elution of melampodin B (**1**, OR = acetate), cinerenin (**3**, OR = ethoxy), melampodin C (**5**, OR = 2-methylpropanoate) and melampodin D (**7**, OR = 2-methylbutanoate) was in the order **1** < **3** < **5** < **7**. One notable exception was 11,13-dihydrocinerenin (**8**), which eluted prior to cinerenin. Interestingly, Leven and Willuhn[18] also found that 11,13-dihydro compounds eluted before the homologous sesquiterpene lactones with an exocyclic methylene group.

The elution order of sesquiterpene lactones from the other structural classes examined also correlates well with the lipophilicity of the compounds. The presence of

TABLE I

HPLC AND GC RETENTION TIMES OF SESQUITERPENE LACTONES OF THE MELAMPODIINAE

t_R = Retention time; t_0 = dead time; na = data not available; I = injection volume 6 μl; T = severely tailed peak; X = decomposed.

No.	*Substance*	*Mol. wt.*	*HPLC isocratic* t_R *(min)*	*HPLC gradient* t_R *(min)*	*GC gradient 1* t_R *(min)*	*GC gradient 2* t_R *(min)*
			t_0 = 0.60	t_0 = 0.60	t_0 = 2.17	t_0 = 2.33
Leucantholides						
1	Melampodin B	334	1.30	6.96	15.84 TI	13.02 TI
2	Melampodin B acetate	376	1.94	27.98	16.51	14.02
3	Cinerenin	320	1.76	19.71	15.72 T	12.97 T
4	Cinerenin acetate	362	3.09	33.74	15.80	13.02
5	Melampodin C	362	2.06	27.29	15.70 TI	12.87 TI
6	Melampodin C acetate	404	4.02	36.50	16.97	14.97
7	Melampodin D	376	2.98	32.97	na	na
8	11,13-Dihydrocinerenin	322	1.48	9.99	15.17	12.32
cis,cis-Germacranolides						
9	Melcanthin A	448	5.44	39.38	16.81	14.65
10	Melcanthin B	464	3.38	35.91	17.76 X	15.89 X
11	Melrosin A	476	4.82	38.66	16.40 I	14.01 I
12	Longicornin B	464	12.89	43.14	16.58	14.26

Repandolides						
13	Repandin A	492	5.17	na	na	14.14 I
14	Repandin B	507	9.19	41.71	17.41	15.02 I
Melampolides						
15	Melampolidin	451	7.14	40.07	16.50	14.14
16	Leucanthinin	464	3.24	35.16	13.88 X	10.12 X
17	Desacetoxyleucanthinin	406	3.03	34.21	14.64	11.71
18	Leucanthinin acetate	522	6.46	39.86	16.65	14.36
19	Leucanthin B	478	5.30	38.37	– X	– X
20	Desacetylleucanthin B	436	1.75	20.23	17.42	15.62
21	Melampodin A	420	2.66	31.85	15.94	13.15
22	Melampodinin A	522	4.05	36.83	16.75 X	14.52 X
23	Melampodinin B	565	19.17	44.67	17.56 X	16.07 X
24	11,13-Dihydromelampodin A 9-α-[2-methylbutanoate]	507	24.72	45.75	16.72 X	15.00 X
25	Leucanthin A	462	3.92	36.46	– X	– X
26	Longipilin	406	3.86	35.68	16.02	13.40
27	Enhydrin	464	4.25	36.98	16.42	13.97
28	Desacetylenhydrin	422	3.86	35.69	16.03	13.42
29	11,13-Dihydroenhydrin	466	4.28	36.94	16.36	13.89
30	Longipin	464	2.85	33.68	17.16	15.21
31	Tetrahelin C	551	>30.00	47.31	17.83	16.62
32	Tetraludin C	525	7.06	40.38	16.78	14.53
33	Melnerin A	380	7.62	40.72	15.34	12.56
34	9-α-Acetoxymelnerin A	438	3.44	36.06	16.20	13.60
35	Melnerin B	394	13.63	43.38	15.80	13.12
36	Melnerin B′	394	12.52	42.96	16.05	13.42
37	9-α-Acetoxymelnerin B	452	3.45	36.01	16.17	13.62

hydroxyl substituents on a molecule decreased the HPLC retention times. Melcanthin B (**10**), with hydroxyl groups at C-2 and C-15, eluted before melcanthin A (**9**), wich lacks the C-2 hydroxyl. Compounds in which a hydroxyl group occurred in place of an acetate or other ester eluted before the corresponding ester; for example, melampodin B (**1**), cinerenin (**3**), melampodin C (**5**), leucanthinin (**16**), desacetylleucanthin B (**20**), and desacetylenhydrin (**28**) all eluted before their corresponding acetates. In some cases, the reasons for the magnitude of these differences in retention time are unclear. Replacement of the C-9 hydroxyl by acetate increases the isocratic retention time by 0.39 min for desacetylenhydrin (**28**), but 3.55 min for desacetylleucanthin B (**20**). A possible reason may be differences in the way these compounds are solvated in the mobile phase.

One surprising reversal of relative elution based on polarity considerations is leucanthin B (**19**), which elutes after leucanthin A (**25**). Leucanthin B contains an epoxide rather than a double bond at the C-2,3 position and behaves as the slightly more polar compound in normal-phase chromatography on silica gel. This anomaly may be due to interactions with underivatized silanol groups on the stationary phase.

Presence of the 2-methylbutanoate substituent (–OR; R = **C**) generally increased retention times markedly. Thus the isocratic retention times for melnerin B (**35**), which has the 2-methylbutanoate substituent, were 6 min longer than for melnerin A (**33**), which has an 2-methylpropanoate substituent in its place. The most strongly retained compounds, melampodinin B (**23**), 11,13-dihydromelampodin A 9-α-[2-methylbutanoate] (**24**) and tetrahelin C (**31**) all contain the 2-methylbutanoate ester side chain.

GC separations

With the non-polar methyl silicone chemically bonded column used for the GC separations, retention times normally increase with boiling point. Within groups of structurally similar compounds, it may be expected that this should be correlated with molecular weight. Although no general trend of this type is apparent, this behavior is observed when the compounds are grouped by structural types. The leucantholides exhibit this behavior, with the exception of melampodin C (**5**) and melampodin B (**1**), which both gave severely tailed peaks. The structurally similar melampolides longipilin (**26**), enhydrin (**27**), desacetylenhydrin (**28**) and 11,13-dihydroenhydrin (**29**), also eluted according to molecular weight.

Several of the sesquiterpene lactones under study decomposed, either in the injector port, which was at 270°C, or in the column itself. This was evidenced by multiple, poorly shaped peaks. The presence of a hydroxyl group at C-3, as in leucanthinin (**16**) and desacetoxyleucanthinin (**17**), or at C-2, as in melcanthin B (**10**) and melrosin A (**11**), made these compounds thermally unstable. However, if the acetate, rather than the alcohol, is present at C-3, such as in leucanthinin acetate (**18**), the compound did not decompose. Leucanthin A (**25**), leucanthin B (**19**), melampodinin A (**22**), melampodinin B (**23**) and 11,13-dihydromelampodinin A 9-α-[2-methylbutanoate] (**24**), all of which contain an epoxide in the 2,3- or the 4,5-position also decomposed. However, desacetylleucanthin B (**20**) and melampodin A (**21**) did not decompose, obscuring this correlation between structure and stability. In addition, within the leucantholides, the presence of a hydroxyl group at C-4 caused distorted peak shapes, such as tailing. This tailing was reduced in cinerenin (**3**) and 11,13-dihydrocinerenin (**8**), which both have an ethoxy substituent at C-1 rather than an ester group at this carbon. This trend does not hold for compounds of other structural types.

Comparison of HPLC and GC separations

For specific pairs of compounds, markedly better separation was often obtained by one of the two chromatographic methods. Cinerenin (**3**) and desacetylleucanthin B (**20**) co-eluted by HPLC but were easily separated by GC, with retention times of 15.72 and 17.42 min, respectively, on GC gradient 1. Cinerenin acetate (**4**) and melnerin B (**35**), on the other hand, did not separate by capillary GC under the conditions employed. These two compounds were easily distinguished by HPLC, with isocratic retention times of 3.09 and 13.63 min, respectively.

Several pairs of compounds were not resolved by either HPLC or capillary GC. These include enhydrin (**27**) and 11,13-dihydroenhydrin (**29**), longipilin (**26**) and desacetylenhydrin (**28**), and the 9-α-acetoxymelnerins A (**34**) and B (**37**). Use of ultraviolet spectra obtained with the diode array detector to confirm HPLC peak purity and/or positively identify these compounds is of limited utility. This is because of the high degree of similarity of the spectra of the sesquiterpene lactones in this study, most of which exhibit only end absorption. In cases where these compounds occur together in a given plant extract, optimization of gradient parameters or the use of longer HPLC columns should be possible. The initial separation of the 9-α-acetoxymelnerins A and B from a extract of *Melampodium leucanthum* was by preparative reversed-phase HPLC[23]. Marchand *et al.*[17] have also reported better resolution by preparative HPLC.

A sample of melnerin B (**35**), previously characterized and thought to be pure[23], was determined by both HPLC and GC to be a mixture of two isomers in approximately a 2:1 ratio. High field (400 MHz) NMR spectra of this sample clearly showed a mixture of melnerin B, which contains the 2-methylbutanoate substituent at C-8, and the corresponding compound with the 3-methylbutanoate ester (melnerin B′, **36**) in a 2:1 ratio, based on integration of the methyl signals. This information was used to assign the HPLC and GC retention times of the major (melnerin B) and minor (melnerin B′) components of the mixture.

Application to a crude plant extract

The joint application of HPLC and GC to analysis of an extract of *Melampodium cinereum* is illustrated in Figs. 2 and 3. HPLC indicated the presence of major amounts of cinerenin (**3**) or desacetylleucanthin B (**20**) (peak 1), along with 9-α-acetoxymelnerin A (**34**) or 9-α-acetoxymelnerin B (**37**) (peak 3). GC confirms the presence of 9-α-acetoxymelnerin A or B as a major constituent of the extract, while the presence of desacetylleucanthin B is ruled out. The absence of a major peak for cinerenin by GC is not unexpected because this compound gives small, tailed peaks. The presence of melcanthin A (**9**), melnerins A (**33**) and B (**35**), longicornin B (**12**) and leucanthinin acetate (**18**) is indicated as minor components of the extract. The presence of longipin (**30**) and enhydrin (**27**) or 11,13-dihydroenhydrin (**29**) in the extract, as indicated by HPLC peaks 2 and 4, was not confirmed by GC. Cinerenin, melcanthin A and the melnerins A and B have previously been reported from this species[14].

In conclusion, use of the GC and HPLC systems described here in conjunction with one another is a powerful technique for the rapid analysis of plant samples for these sesquiterpene lactones.

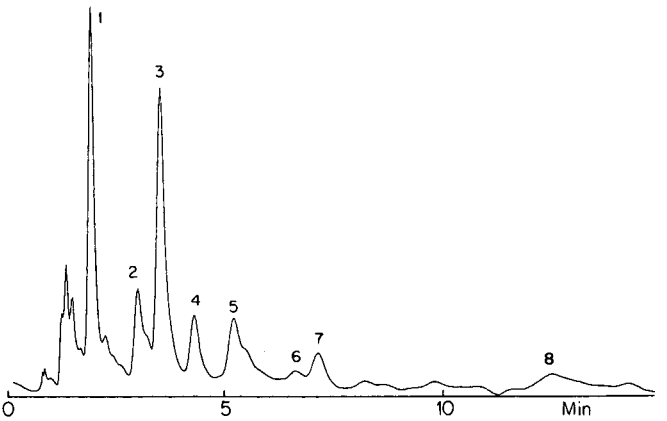

Fig. 2. HPLC (210 nm) of crude terpenoid extract of *Melampodium cinereum* var. *cinereum*. Peaks: 1 = cinerenin; 2 = unidentified; 3 = 9-α-acetoxymelnerin A or B; 4 = unidentified; 5 = melcanthin A; 6 = leucanthenin acetate; 7 = melnerin A; 8 = melnerin B and longicorin B.

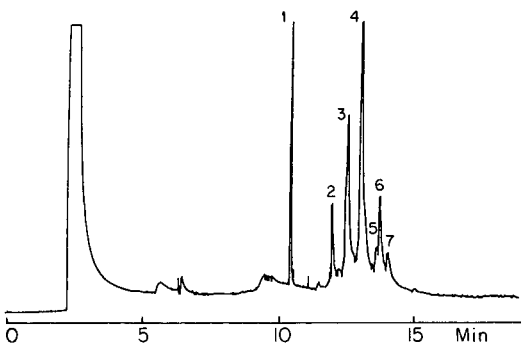

Fig. 3. GC of crude terpenoid extract of *M. cinereum* var. *cinereum*. Peaks: 1 = unidentified; 2 = melnerin A; 3 = melnerin B; 4 = 9-α-acetoxymelnerin A or B; 5 = longicorin B; 6 = leucanthenin acetate; 7 = melcanthin A.

ACKNOWLEDGEMENTS

This research was supported by the National Science Foundation Biotechnology Program (Project No. EET-8713078). Dr. J. Foley provided helpful comments on the manuscript.

REFERENCES

1 E. Rodriguez, G. H. N. Towers and J. C. Mitchell, *Phytochem.*, 15 (1976) 1573.
2 A. K. Picman, *Biochem. System. Ecol.*, 14 (1986) 255.
3 E. S. Johnson, N. Kadam, D. Hylands and P. Hylands, *Brit. Med. J.*, 291 (1985) 569.
4 D. M. Jessup, *Thesis*, University of London, London, 1982.
5 F. R. Fronczek, D. Vargas, N. H. Fischer and K. Hostettman, *J. Nat. Prod.*, 47 (1984) 1036.

6 N. H. Fischer, J. D. Weidenhamer and J. M. Bradow, *Phytochem.*, 28 (1989) 2315.
7 S. O. Duke, *Rev. Weed Sci.*, 2 (1986) 15.
8 W. C. Burnett, Jr., S. B. Jones, Jr., T. J. Mabry and W. G. Padolina, *Biochem. System. Ecol.*, 2 (1974) 25.
9 O. Spring, T. Priester, V. Klemt and J. Kruppa, *Proc. Nat. Sunflower Assoc.*, (1989) in press.
10 A. K. Picman, R. H. Elliot and G. H. N. Towers, *Can. J. Zool.*, 59 (1981) 285.
11 A. K. Picman and J. Picman, *Biochem. System. Ecol.*, 12 (1984) 89.
12 N. H. Fischer, in A. R. Putnam and C. Tang (Editor), *The Science of Allelopathy*, Wiley, New York, 1986, Ch. 12, p. 203.
13 N. H. Fischer, J. D. Weidenhamer and J. M. Bradow, *J. Chem. Ecol.*, 15 (1989) 1785.
14 F. C. Seaman, N. H. Fischer and T. F. Stuessy, *Biochem. System. Ecol.*, 8 (1980) 263.
15 C. M. Smith, K. M. Kester and N. H. Fischer, *Biochem. System. Ecol.*, 11 (1983) 377.
16 H. E. Flores, in H. LeBaron, R. Mumma, R. Honeycutt, J. Duesing, J. Phillips and M. Haas (Editors), *Biotechnology in Agricultural Chemistry*, (*ACS Symposium Series*, No. 334), American Chemical Society, Washington, DC, 1987, p. 66.
17 B. Marchand, H. M. Behl and E. Rodriguez, *J. Chromatogr.*, 265 (1983) 97.
18 W. Leven and G. Willuhn, *J. Chromatogr.*, 410 (1987) 329.
19 O. Spring, T. Priester, H. Stransky and A. Hager, *J. Plant Physiol.*, 120 (1985) 321.
20 O. Spring, U. Bienert and V. Klemt, *J. Plant Physiol.*, 130 (1987) 433.
21 K. Wilzer, *Ph. D. Dissertation*, Louisiana State University, Baton Rouge, LA, 1986.
22 N. Fischer, R. Wiley, H. Lin, K. Karimian and S. Politz. *Phytochem.*, 14 (1975) 2241.
23 E. J. Olivier, D. L. Perry and N. H. Fischer, *J. Org. Chem.*, 45 (1980) 4028.

Journal of Chromatography, 504 (1990) 163–178
Elsevier Science Publishers B.V., Amsterdam — Printed in The Netherlands

CHROM. 22 189

Lipophilic character of cardiac glycosides

R_M values as lipophilicity parameters

G. L. BIAGI*, A. M. BARBARO and M. C. GUERRA
Istituto di Farmacologia, Università di Bologna, Bologna (Italy)
P. A. BOREA
Istituto di Farmacologia, Università di Ferrara, Ferrara (Italy)
and
M. RECANATINI
Dipartimento di Scienze Farmaceutiche, Università di Bologna, Bologna (Italy)
(First received September 11th, 1989; revised manuscript received December 4th, 1989)

SUMMARY

Chromatographic R_M values were measured for a series of 41 cardiac glycosides and aglycones. By means of the ΔR_M values it was possible to calculate the R_M values for a further 19 compounds. An excellent correlation was found between the present R_M values and those measured or calculated with the Cohnen *et al.* system. In a similar way, the R_M values were shown to be well correlated with both high-performance liquid chromatographic data and octanol–water partition coefficients (log P). The additive contribution of each substituent group to the overall lipophilicity of the molecule seems to be constant in each subset of *Digitalis* derivatives.

INTRODUCTION

The cardiac steroids, despite their long history, are among the most important drugs in modern therapeutics. However, quantitative studies of the relationships between structure and activity (QSAR) of these compounds have received little attention[1–3]. Only in recent times has there been some increasing interest in QSAR studies of cardiac steroids[4–9]. As the lipophilic character is one of the most important physico-chemical factor determining the biological activity of drugs, several workers[4,6,7,10] have studied the determination of lipophilicity indices of cardiac steroids. Nevertheless, there is still a lack of data describing the lipophilic character of most of these compounds. The determination of the classical octanol–water partition coefficient is the main method for establishing the lipophilic character of drugs. However, the R_M and log k' values obtained by reversed-phase partition thin-layer (TLC) and high-performance liquid chromatography (HPLC) were shown to be well

0021-9673/90/$03.50

correlated with the partition coefficients of many chemicals and have been proposed as an alternative method[11,12]. The R_M values were calculated by means of the equation

$$R_M = \log\left(\frac{1}{R_F} - 1\right)$$

An earlier contribution to the study of the relationship between chemical structure and chromatographic behaviour was provided by Nover and co-workers[13,14] by means of adsorption paper and thin-layer chromatography. With regard to a QSAR study, the purpose of this work was to determine or calculate R_M and $\log k'$ values for a large series of cardiac steroids.

EXPERIMENTAL

Chemicals

Several cardiac glycosides and aglycones (compounds 4, 8, 41, 43, 44, 45, 46, 55, 57, 58 and 60) were a generous gift from Simes (Milan, Italy). Other compounds were obtained from commercial sources. All the drugs were used without further purification. All solvents were of analytical-reagent or HPLC grade.

Determination of R_M values

The TLC technique had been described previously[15]. Glass plates (20 × 20 cm) were coated with silica gel G (E. Merck, Darmstadt, F.R.G.). In order to control the pH of the stationary phase, a slurry of silica gel G was prepared with 0.09 *M* sodium hydroxide solution. A non-polar stationary phase was obtained by impregnating the silica gel G layer with silicone DC 200 (viscosity 350 cSt) (Applied Science Labs., State College, PA, U.S.A.). The impregnation was carried out by developing the plates in a 5% silicone solution in diethyl ether. Eight plates could be impregnated in a single chromatographic chamber containing 200 ml of the silicone solution. The plates were left in the chamber for 12 h, *i.e.*, for several hours after the silicone solution had reached the top of the plates. The chromatographic chamber was saturated with the vapour of the mobile phase.

A migration distance of 10 cm was obtained on all plates by cutting the layer at 12 cm and spotting the compounds on a line 2 cm from the lower edge of the plate. The mobile phase saturated with silicone oil was aqueous buffer (sodium acetate–Veronal buffer, 1/7 *M* at pH 7.2), alone or mixed with various amounts of acetone. Two plates were developed simultaneously in a chromatographic chamber containing 200 ml of mobile phase, at room temperature.

The cardioactive drugs were dissolved in methanol, acetone or water (1–2 mg/ml) and 1 μl of solution was spotted randomly on the plates in order to avoid any systematic error. The developed plates were dried and sprayed with an alkaline solution of potassium permanganate. After a few minutes at 120°C, yellow spots appeared on an intense pink background.

Determination of log P values

The *n*-octanol–water partition coefficients of six genins were measured by means of the shake-flask method[16], using distilled water as the polar phase and *n*-octanol as

the lipid phase; each phase was previously saturated with the other one and centrifuged if not clear.

A carefully weighed amount of compound was dissolved in the octanol phase, and an appropriate amount of water was added; the bottles were then shaken gently for *ca.* 5 min and centrifuged for 1.0 h at 2000 rpm (895 *g*). The ratio of the octanol and water volumes was chosen so as to give a reliable UV absorbance at the wavelength of maximum absorption.

The concentration in the aqueous phase was determined spectrophotometrically by means of a Varian DMS-90 UV–visible spectrophotometer; each reported log *P* value is the average of at least four determinations with $s \leqslant 0.03$.

Determination of log k′ values

HPLC was performed on a Waters Assoc. 820 chromatography workstation, using a μBondapak C_{18} column (300 × 3.9 mm I.D.) (Waters Assoc., Milford, MA, U.S.A.), packed with silica gel (particle size 10 μm) with a C_{18} chemically bonded non-polar stationary phase[17]. A Waters Assoc. UV detector at 220 nm and Hamilton 802 chromatographic syringes (25 μl) were used. The compounds were dissolved in methanol (1 mg/ml) and applied to the column in 5-μl volumes. All solutions and reagents were first filtered through Millipore filters (Type FH, pore size 0.5 μm). The separation was carried out using acetonitrile–water mixtures as the mobile phase at a flow-rate of 1 ml/min. The acetonitrile concentration ranged from 20–40 to 50–70%. The retention times were expressed as

$$\log k' = \log \left(\frac{t_x - t_0}{t_0} \right)$$

where t_x is the retention time of the compound and t_0 that of the solvent front.

RESULTS

R_M values and lipophilicity of cardioactive steroids

The reversed-phase TLC of the cardioactive compounds showed that most of them did not move from the starting line when the mobile phase was aqueous buffer alone. In order to obtain suitable R_M values it was necessary to add acetone to the mobile phase. Only with the six most hydrophilic compounds, ouabain, strophanthidol, k-strophanthidin, k-strophanthin β, k-strophanthoside and digoxigenin, could reliable R_M values be obtained even at 0% acetone in the mobile phase. However, as usual in TLC and HPLC, for all the compounds there was a linear relationship between R_M values and a range of acetone concentration.

The equations describing such a linear relationship allowed the calculation of extrapolated R_M values at 0% acetone in the mobile phase for the compounds that did not migrate with the aqueous buffer alone. The validity of the extrapolation technique is shown by the fact that the experimental R_M values of 0% acetone of the above six most hydrophilic compounds are very close to the extrapolated R_M values, calculated for the same compounds over a wider range of acetone concentrations. All the extrapolated R_M values are reported in Tables I and II.

The range of the linear relationship between R_M values and acetone concen-

TABLE I

R_M VALUES OF CARDIAC GLYCOSIDES AND AGLYCONES OF *DIGITALIS* SPP.

Compound		*Structure*		*Empirical formula*	*Molecular weight*	R_M[c]		
No.	*Generic name*	*Genin*	*Side-chain at C-3-β-OH*			*This work*	*Cohnen et al.*[10]	*Dzimiri et al.*[7]
1	Digoxigenin	Digoxigenin	–	$C_{23}H_{34}O_5$	390.53	0.98	0.49	−0.03
2	Digoxigenin monodigitoxoside	Digoxigenin	D-Digitoxose	$C_{29}H_{44}O_8$	520.67	1.24	0.98	−0.01
3	Digoxigenin bisdigitoxoside	Digoxigenin	2 D-Digitoxose	$C_{35}H_{54}O_{11}$	650.81	1.65	1.23	0.17
4	Digoxin	Digoxigenin	3 D-Digitoxose	$C_{41}H_{64}O_{14}$	780.92	2.01	1.78	0.23
5	α-Acetyldigoxin	Digoxigenin	3 D-Digitoxose + acetyl	$C_{43}H_{66}O_{15}$	822.91	2.27	2.05	0.49
6	β-Acetyldigoxin	Digoxigenin	3 D-Digitoxose + acetyl	$C_{43}H_{66}O_{15}$	822.91	2.38	2.10	0.70
7	Lanatoside C	Digoxigenin	3 D-Digitoxose + acetyl + D-glucose	$C_{49}H_{76}O_{20}$	985.10	2.19	1.84	–
8	Deslanoside C	Digoxigenin	3 D-Digitoxose + D-glucose	$C_{47}H_{74}O_{19}$	943.11	1.86	1.55[a]	–
9	α,β-Diacetyldigoxin	Digoxigenin	3 D-Digitoxose + 2 acetyl	$C_{45}H_{68}O_{16}$	864.95	2.89	2.37[a]	1.21
10	12-Acetyldigoxin	12-Acetyldigoxigenin	3 D-Digitoxose	$C_{43}H_{66}O_{15}$	822.96	2.96	–	0.89
11	12-Acetyl-β-methyldigoxin	12-Acetyldigoxigenin	3 D-Digitoxose + methyl	$C_{44}H_{68}O_{15}$	836.99	3.45	–	1.26
12	α-Methyldigoxin	Digoxigenin	3 D-Digitoxose + methyl	$C_{42}H_{66}O_{14}$	795.08	2.50	2.29[a]	0.54
13	β-Methyldigoxin	Digoxigenin	3 D-Digitoxose + methyl	$C_{42}H_{66}O_{14}$	795.08	2.48	2.29	0.60
14	α,β-Dimethyldigoxin	Digoxigenin	3 D-Digitoxose + 2 methyl	$C_{43}H_{68}O_{14}$	809.11	2.98[a]	2.80[a]	0.94
15	Digitoxigenin	Digitoxigenin	–	$C_{23}H_{34}O_4$	374.50	1.93	1.56	1.01
16	Digitoxigenin monodigitoxoside	Digitoxigenin	D-Digitoxose	$C_{29}H_{44}O_7$	504.67	2.23	2.34	1.05
17	Digitoxigenin bisdigitoxoside	Digitoxigenin	2 D-Digitoxose	$C_{35}H_{54}O_{10}$	634.81	2.65	2.44	1.28
18	Digitoxin	Digitoxigenin	3 D-Digitoxose	$C_{41}H_{64}O_{13}$	764.92	3.18	2.92	1.32
19	α-Acetyldigitoxin	Digitoxigenin	3 D-Digitoxose + acetyl	$C_{43}H_{66}O_{14}$	806.91	3.54	3.21[a]	–

20	β-Acetyldigitoxin	Digitoxigenin	3 D-Digitoxose + acetyl	$C_{43}H_{66}O_{14}$	806.91	3.53[a]	3.21[a]	–
21	Lanatoside A	Digitoxigenin	3 D-Digitoxose + acetyl + D-glucose	$C_{49}H_{76}O_{19}$	969.10	3.38	3.09	–
22	α,β-Diacetyldigitoxin	Digitoxigenin	3 D-Digitoxose + 2 acetyl	$C_{45}H_{68}O_{15}$	848.95	3.88[a]	3.50[a]	–
23	β-Methyldigitoxin	Digitoxigenin	3 D-Digitoxose + methyl	$C_{42}H_{66}O_{13}$	778.95	3.66[a]	3.43[a]	1.71
24	Evomonoside[b]	Digitoxigenin	L-Rhamnose	$C_{29}H_{44}O_8$	520.67	2.28[a]	1.83	–
25	Neriifolin[b]	Digitoxigenin	L-Thevetose	$C_{30}H_{46}O_8$	534.70	2.14	1.72	–
26	Gitoxigenin	Gitoxigenin	–	$C_{23}H_{34}O_5$	390.50	1.72	1.37	0.38
27	Gitoxigenin monodigitoxoside	Gitoxigenin	D-Digitoxose	$C_{29}H_{44}O_8$	520.67	2.15[a]	1.86[a]	0.46
28	Gitoxigenin bisdigitoxoside	Gitoxigenin	2 D-Digitoxose	$C_{35}H_{54}O_{11}$	650.81	2.58[a]	2.35[a]	–
29	Glucogitoroside	Gitoxigenin	D-Digitoxose + D-glucose	$C_{35}H_{54}O_{13}$	682.80	1.97[a]	1.63[a]	–
30	Gitoxin	Gitoxigenin	3 D-Digitoxose	$C_{41}H_{64}O_{14}$	780.92	3.00	2.83	0.68
31	α-Acetylgitoxin	Gitoxigenin	3 D-Digitoxose + acetyl	$C_{43}H_{66}O_{15}$	822.91	3.35[a]	3.12[a]	–
32	β-Acetylgitoxin	Gitoxigenin	3 D-Digitoxose + acetyl	$C_{43}H_{66}O_{15}$	822.91	3.35[a]	3.12[a]	–
33	Lanatoside B	Gitoxigenin	3 D-Digitoxose + acetyl + D-glucose	$C_{49}H_{76}O_{20}$	985.10	3.12	2.94[a]	–
34	α,β-Diacetylgitoxin	Gitoxigenin	3 D-Digitoxose + 2 acetyl	$C_{45}H_{68}O_{16}$	864.95	3.70[a]	3.41[a]	–
35	Pentaacetylgitoxin	16-Acetylgitoxigenin	3 D-Digitoxose + 4 acetyl	$C_{51}H_{74}O_{19}$	990.87	4.59	3.83[a]	1.86
36	16-Acetylgitoxin	16-Acetylgitoxigenin	3 D-Digitoxose	$C_{43}H_{66}O_{15}$	822.96	2.93	2.67[a]	0.88
37	16-Formylgitoxin	16-Formylgitoxigenin	3 D-Digitoxose	$C_{42}H_{64}O_{14}$	792.93	2.50	–	0.84
38	Oleandrigenin[b]	16-Acetylgitoxigenin	–	$C_{25}H_{36}O_6$	432.57	1.58	1.34	–
39	Oleandrin[b]	16-Acetylgitoxigenin	L-Oleandrose	$C_{32}H_{48}O_9$	576.70	2.34	2.26	–
40	16-Desacetyloleandrin[b]	Gitoxigenin	L-Oleandrose	$C_{30}H_{46}O_8$	534.66	2.44[a]	2.55	–

[a] Calculated R_M values (see text).
[b] Evomonoside, neriifolin, oleandrigenin, oleandrin and 16-desacetyloleandrin are listed in Table I as they are characterized by *Digitalis* aglycones.
[c] TLC system: see text.

TABLE II

R_M VALUES OF CARDIAC GLYCOSIDES AND AGLYCONES FROM OTHER BOTANICAL SOURCES

Compound		*Structure*		*Empirical formula*	*Molecular weight*	R_M[b]		
No.	*Generic name*	*Genin*	*Side-chain at C-3-β-OH*			*This work*	*Cohnen et al.*[10]	*Dzimiri et al.*[7]
41	k-Strophanthidin	Strophanthidin	–	$C_{23}H_{32}O_6$	404.49	0.94	0.65	−0.16
42	Strophanthidin-3-acetate	Strophanthidin	Acetyl	$C_{25}H_{34}O_7$	446.48	1.23	0.94[a]	–
43	Cymarin	Strophanthidin	D-Cymarose	$C_{30}H_{44}O_9$	548.65	1.34	1.23	−0.10
44	k-Strophanthin-β	Strophanthidin	D-Cymarose + D-glucose	$C_{36}H_{54}O_{14}$	710.84	1.02	1.00[a]	−0.50
45	k-Strophanthoside	Strophanthidin	D-Cymarose + 2 D-glucose	$C_{42}H_{64}O_{13}$	873.03	0.99	0.77[a]	−0.62
46	Convallatoxin	Strophanthidin	L-Rhamnose	$C_{29}H_{42}O_{10}$	550.63	1.29	1.26[a]	–
47	Desglucocheirotoxin	Strophanthidin	D-Gulomethylose	$C_{29}H_{42}O_{10}$	550.63	1.29[a]	0.92[a]	–
48	Olitoriside	Strophanthidin	D-Boivinose + D-glucose	$C_{35}H_{52}O_{14}$	696.79	1.10[a]	0.91[a]	–
49	Helveticoside	Strophanthidin	D-Digitoxose	$C_{29}H_{42}O_9$	534.63	1.21	1.14[a]	–
50	Erysimoside	Strophanthidin	D-Digitoxose + D-glucose	$C_{35}H_{52}O_{14}$	696.79	1.03[a]	0.91[a]	–
51	Strophanthidol	Strophanthidol	–	$C_{23}H_{34}O_6$	406.50	0.73	0.46[a]	–
52	Cymarol	Strophanthidol	D-Cymarose	$C_{30}H_{46}O_9$	550.65	1.19	1.04	–
53	Convallatoxol	Strophanthidol	L-Rhamnose	$C_{29}H_{44}O_{10}$	552.65	1.11[a]	1.07	–
54	Helveticosol	Strophanthidol	D-Digitoxose	$C_{29}H_{44}O_9$	536.65	1.03[a]	0.95[a]	–
55	Heptaacetyl-k-strophanthoside	Strophanthidin	D-Cymarose + 2 D-glucose + 7 acetyl	$C_{56}H_{78}O_{26}$	1166.9	3.41	2.80[a]	–
56	Ouabagenin	Ouabagenin	–	$C_{23}H_{24}O_8$	438.50	0.18[a]	−0.05[a]	–
57	Ouabain	Ouabagenin	L-Rhamnose	$C_{29}H_{44}O_{12}$	584.64	0.53	0.22	−0.70
58	Proscillaridin	Scillarenin	L-Rhamnose	$C_{30}H_{42}O_8$	530.64	2.15	1.92	–
59	Scillaren A	Scillarenin	L-Rhamnose + D-glucose	$C_{36}H_{52}O_{13}$	692.78	1.97[a]	1.69[a]	–
60	Peruvoside	Cannogenin	L-Thevetose	$C_{30}H_{44}O_9$	548.65	1.68	–	–

[a] Calculated R_M values (see text).
[b] TLC system: see text.

trations is limited by the fact that at lower and higher acetone concentrations all the compounds tend not to move from the starting line or to migrate with the solvent front, respectively, *i.e.*, to deviate from the linear relationship. Therefore, the extrapolated R_M values in Tables I and II were obtained from equations calculated by means of R_M

TABLE III

RANGES OF ACETONE CONCENTRATIONS USED FOR THE CALCULATION OF THE TLC EQUATIONS

Compound No.	*Acetone range (%)*	*TLC equation*		
		$a = R_M$	b	r
57	0–24	0.535 ± 0.019	−0.066 ± 0.001	0.996
51	0–24	0.732 ± 0.071	−0.033 ± 0.002	0.985
41	0–24	0.938 ± 0.098	−0.038 ± 0.038	0.967
1	0–32	0.980 ± 0.047	−0.048 ± 0.002	0.992
45	0–32	0.991 ± 0.162	−0.058 ± 0.007	0.961
44	0–36	1.022 ± 0.184	−0.063 ± 0.011	0.959
52	4–32	1.194 ± 0.043	−0.050 ± 0.002	0.995
49	4–36	1.213 ± 0.080	−0.045 ± 0.003	0.982
42	4–40	1.230 ± 0.100	−0.043 ± 0.003	0.987
2	4–24	1.240 ± 0.118	−0.063 ± 0.007	0.972
46	4–32	1.295 ± 0.090	−0.059 ± 0.004	0.983
43	4–24	1.343 ± 0.085	−0.065 ± 0.005	0.986
38	8–36	1.581 ± 0.070	−0.043 ± 0.002	0.991
3	8–32	1.650 ± 0.112	−0.063 ± 0.005	0.983
60	8–50	1.684 ± 0.117	−0.050 ± 0.004	0.976
26	8–50	1.719 ± 0.044	−0.050 ± 0.001	0.992
8	8–40	1.859 ± 0.131	−0.068 ± 0.005	0.981
15	16–50	1.932 ± 0.058	−0.050 ± 0.002	0.996
4	16–50	2.010 ± 0.094	−0.062 ± 0.003	0.989
25	16–50	2.141 ± 0.221	−0.055 ± 0.006	0.986
58	16–50	2.149 ± 0.120	−0.054 ± 0.003	0.985
7	16–50	2.187 ± 0.120	−0.066 ± 0.003	0.990
16	20–50	2.232 ± 0.122	−0.058 ± 0.004	0.990
5	20–50	2.268 ± 0.118	−0.063 ± 0.003	0.994
39	20–50	2.345 ± 0.139	−0.057 ± 0.004	0.989
6	24–50	2.377 ± 0.119	−0.067 ± 0.003	0.994
13	20–50	2.477 ± 0.057	−0.070 ± 0.002	0.985
12	20–50	2.503 ± 0.095	−0.071 ± 0.003	0.995
37	20–60	2.504 ± 0.124	−0.062 ± 0.003	0.991
17	28–55	2.653 ± 0.147	−0.065 ± 0.003	0.993
9	28–55	2.887 ± 0.122	−0.070 ± 0.003	0.994
36	28–50	2.933 ± 0.285	−0.068 ± 0.009	0.976
10	28–55	2.962 ± 0.209	−0.072 ± 0.005	0.988
30	32–40	3.000 ± 0.016	−0.076 ± 0.001	0.999
33	28–50	3.121 ± 0.113	−0.078 ± 0.003	0.996
18	28–60	3.183 ± 0.141	−0.070 ± 0.003	0.992
21	28–55	3.380 ± 0.120	−0.072 ± 0.003	0.996
55	28–50	3.406 ± 0.120	−0.066 ± 0.003	0.996
11	28–50	3.446 ± 0.303	−0.081 ± 0.008	0.985
19	36–50	3.540 ± 0.450	−0.074 ± 0.010	0.981
35	40–60	4.588 ± 0.800	−0.088 ± 0.017	0.966

values determined with acetone concentrations ranging from 0 to 24% or from 36–40 to 50–60% depending on the lipophilicity of the test compounds. The most hydrophilic compound, ouabain, shows a linear relationship between R_M values and acetone concentration in the range 0–24%. For the most lipophilic compound, penta-acetylgitoxin, acetone concentrations ranging from 40 to 60% were used.

The ranges of acetone concentrations and the TLC equations are reported in Table III, where a and b are the intercept and slope, with their standard errors, respectively, and r is the correlation coefficient. The intercepts ($a = R_M$) are also reported in Tables I and II. In Table III the compounds are listed in order of increasing lipophilicity to show the good correlation between extrapolated R_M values and ranges of acetone concentrations. The slopes in Table III show that the equations describe a series of almost parallel straight lines.

Cohnen *et al.*[10] measured the R_M values of a series of cardioactive steroids by means of a TLC technique which seems to be very similar to our own system. Their extrapolated R_M values at 0% acetone in the mobile phase are reported in Tables I and II. A very good correlation is shown by eqn. 1 between the present R_M values and those obtained by Cohnen *et al.* [10] for a series of 23 compounds for which the experimental R_M values were available in both TLC systems.

$$R_M = 0.361\ (\pm\ 0.063) + 0.937\ (\pm\ 0.033)\ R_{M\text{Cohnen}} \quad (1)$$
$$(n = 23;\ r = 0.987;\ s = 0.121;\ F = 784.7;\ P < 0.005)$$

In eqn. 1 and all subsequent equations, n is number of data points, r is the correlation coefficient, s is the standard error of the equation and F is the value of the F-test.

The experimental R_M values provide some understanding of the influence of substituent groups determining the lipophilicity of the whole molecule. The *Digitalis* glycosides can be grouped into three families on the basis of the aglycones (Table I). Cardiac glycosides and aglycones from different botanical sources are listed in Table II. The presence of digitoxosyl, acetyl or methyl group(s) in the sugar residue at C-3 increases the lipophilic character. The ΔR_M values reported in Table IV were used in the calculation of the R_M values of the mono- and bisdigitoxosides and also acetyl derivatives of trisdigitoxosides for which the experimental R_M values were not available. In the Cohnen *et al.* system the R_M value of helveticoside was obtained by adding the average ΔR_M value of the digitoxosyl group to the R_M value of strophanthidin.

The R_M values of desacetyllanatoside C, strophanthidin-3-acetate, pentaacetyl-gitoxin and heptaacetyl-k-strophanthoside in the Cohnen *et al.* system were calculated from the experimental R_M values for lanatoside C, strophanthidin, 16-acetylgitoxin and k-strophanthoside by subtracting or adding an average ΔR_M of 0.29 for each of the acetyl groups.

$$R_M\text{ (lanatoside B)} = R_M\text{ (gitoxin)} + [R_M\text{ (lanatoside A)} - R_M\text{ (digitoxin)}]$$
$$= 2.83 + (3.09 - 2.92) = 3.00$$
$$R_M\text{ (lanatoside B)} = R_M\text{ (gitoxin)} + [R_M\text{ (lanatoside C)} - R_M\text{ (digoxin)}]$$
$$= 2.83 + (1.84 - 1.78) = 2.89$$
$$\bar{x} = 2.94$$

TABLE IV

INFLUENCE OF SUBSTITUENT GROUPS ON THE LIPOPHILIC CHARACTER

Group	*Position*	*Compounds*	ΔR_M	ΔR_M *(Cohnen et al.*[10]*)*
OH	C-16	Gitoxin *vs.* digitoxin	−0.18	−0.09
		Gitoxigenin *vs.* digitoxigenin	−0.21	−0.19
			$\bar{x}=-0.19$	$\bar{x}=-0.14$
	C-12	Digoxin *vs.* digitoxin	−1.17	−1.14
		Digoxigenin monodigitoxoside *vs.* digitoxigenin monodigitoxoside	−0.99	−1.36
		Digoxigenin bisdigitoxoside *vs.* digitoxigenin bisdigitoxoside	−1.00	−1.21
		Digoxigenin *vs.* digitoxigenin	−0.95	−1.07
			$\bar{x}=-1.03$	$\bar{x}=-1.19$
$OCOCH_3$	C-16	Oleandrigenin *vs.* digitoxigenin	−0.35	−0.22
		16-Acetylgitoxin *vs.* digitoxin	−0.25	–
			$\bar{x}=-0.30$	
	C-12	12-Acetyldigoxin *vs.* digitoxin	−0.22	–
$OCOCH_3$ *vs.* OH	C-16	Oleandrin *vs.* 16-desacetyloleandrin	–	−0.29
		Oleandrigenin *vs.* gitoxigenin	−0.14	−0.03
		16-Acetylgitoxin *vs.* gitoxin	−0.07	–
			$\bar{x}=-0.10$	$\bar{x}=-0.16$
	C-12	12-Acetyldigoxin *vs.* digoxin	0.95	–
		12-Acetyl-β-methyldigoxin *vs.* β-methyldigoxin	0.97	–
			$\bar{x}=0.96$	
CH_2OH *vs.* CHO	C-10	Cymarol *vs.* cymarin	−0.15	−0.19
		Strophanthidol *vs.* strophanthidin	−0.21	–
			$\bar{x}=-0.18$	
CHO *vs.* OH	C-16	16-Formylgitoxin *vs.* gitoxin	−0.50	–
$OCOCH_3$ *vs.* OH	Side chain	α-Acetyldigitoxin *vs.* digitoxin	0.36	–
		α-Acetyldigoxin *vs.* digoxin	0.26	0.27
		β-Acetyldigoxin *vs.* digoxin	0.37	0.32
		α,β-Diacetyldigoxin *vs.* digoxin/2	0.44	–
		Pentaacetylgitoxin *vs.* 16-acetylgitoxin/4	0.41	–
		Heptaacetyl-k-strophanthoside *vs.* k-strophanthoside/7	0.34	–
			$\bar{x}=0.35$	$\bar{x}=0.29$
Glucosyl *vs.* OH	Side-chain	Deslanoside *vs.* digoxin	−0.15	–
		Lanatoside C *vs.* α-acetyldigoxin	−0.08	−0.21
		Lanatoside C *vs.* β-acetyldigoxin	−0.19	−0.26
		Lanatoside A *vs.* α-acetyldigitoxin	−0.16	–
		k-Strophanthin β *vs.* cymarin	−0.32	–
		k-Strophanthoside *vs.* cymarin/2	−0.17	–
			$\bar{x}=-0.18$	$\bar{x}=-0.23$

(Continued on p. 172)

TABLE IV *(continued)*

Group	*Position*	*Compounds*	ΔR_M	ΔR_M *(Cohnen et al.*[10]*)*
Rhamnosyl *vs.* OH	Side-chain	Convallatoxin *vs.* k-strophanthidin	0.35	–
		Evomonoside *vs.* digitoxigenin	–	0.27
Digitoxosyl *vs.* OH	Side-chain	Digoxigenin monodigitoxoside *vs.* digoxigenin	0.26	0.49
		Digoxigenin bisdigitoxoside *vs.* digoxigenin/2	0.33	0.37
		Digoxin *vs.* digoxigenin/3	0.34	0.43
		Digitoxigenin monodigitoxoside *vs.* digitoxigenin	0.30	0.78
		Digitoxigenin bisdigitoxoside *vs.* digitoxigenin/2	0.36	0.44
		Digitoxin *vs.* digitoxigenin/3	0.42	0.45
		Gitoxin *vs.* gitoxigenin/3	0.43	0.49
		Helveticoside *vs.* k-strophanthidin	0.27	–
		16-Acetylgitoxin *vs.* oleandrigenin/3	0.45	–
			$\bar{x}=$ 0.35	$\bar{x}=$ 0.49
Cymarosyl *vs.* OH	Side-chain	Cymarin *vs.* k-strophanthidin	0.40	0.58
		Cymarol *vs.* strophanthidol	0.46	–
			$\bar{x}=$ 0.43	
Oleandrosyl *vs.* OH	Side-chain	Oleandrin *vs.* oleandrigenin	0.76	0.92
Thevetosyl *vs.* OH	Side-chain	Neriifolin *vs.* digitoxigenin	0.21	0.16
OCH_3 *vs.* OH	Side-chain	α-Methyldigoxin *vs.* digoxin	0.49	–
		β-Methyldigoxin *vs.* digoxin	0.47	0.51
		12-Acetyl-β-methyldigoxin *vs.* 12-acetyldigoxin	0.49	–
			$\bar{x}=$ 0.48	

The ΔR_M value of the glucosyl group in the sugar residue was used for the calculation of the R_M values of glucogitoroside, erysimoside, scillaren A, k-strophanthin β and k-strophanthoside by adding it for one or two residues to the R_M values of gitoxigenin monodigitoxoside, helveticoside, proscillaridin and cymarin. The R_M values of evomonoside and ouabagenin were calculated from the R_M values of digitoxigenin and ouabain by adding or subtracting, respectively, the R_M value of the rhamnosyl group in the sugar residue.

The ΔR_M value of the acetoxyl group *vs.* OH at C-16 was used in the calculation of the R_M values of 16-acetylgitoxin and desacetyloleandrin by adding or subtracting it, respectively, from the R_M values of gitoxin and oleandrin.

The R_M values of helveticosol, convallatoxol, strophanthidol and convallatoxin were calculated by adding or subtracting the ΔR_M value for CH_2OH *vs.* CHO at C-10 from the R_M values of helveticoside, convallatoxin, strophanthidin and convallatoxol.

The R_M values of desglucocheirotoxin and olitoriside were calculated in both systems by adding the ΔR_M values of gulomethylose, or boivinose and glucose, respectively. As gulomethylose and boivinose are the isomeric forms of rhamnose and digitoxose, respectively, the ΔR_M values of the latter forms were used (Table IV). In fact, Davydov[6] had calculated the same retention values for both pairs of isomers. However, the results for another pair of isomers must be pointed out, *i.e.*, cymarose and oleandrose, whereas Davydov[6] had calculated the same retention values for these sugar residues, in the present and the Cohnen *et al.* system the ΔR_M values are different.

Finally, the R_M values of α-methyldigoxin, β-methyldigitoxin and α,β-dimethyldigoxin were calculated by means of the ΔR_M values for the α- and/or β-methyl groups in the side-chain.

The equation

$$R_M = 0.202\ (\pm 0.046) + 1.027\ (\pm 0.021)\ R_{M\ \text{Cohnen}} \quad (2)$$
$$(n=56;\ r=0.988;\ s=0.153;\ F=2265.3;\ P<0.005)$$

calculated by means of both experimental and calculated R_M values is very similar to eqn. 1 and shows that the calculated R_M values do not deviate from the relationship described by eqn. 1 for the experimental R_M values. The slopes in both eqns. 1 and 2 are very close to unity, which explains why the ΔR_M values in Table IV are fairly close in the two systems.

Hence any substituent group tends to induce the same variation of lipophilic character in both TLC systems. Intercepts higher than zero indicate a systematic difference between the two systems, probably due to the different kind of silicone oil used by Cohnen *et al.*[10]. Eqn. 2 holds over a wide range of R_M values, with a difference on a logarithmic scale of 4.65, which means a 44 668-fold difference in lipophilicity.

More recently, Dzimiri *et al.*[7] measured the R_M values of a series of cardiotonic steroids by means of a different TLC system, which had also been used by Cohnen *et al.*[10]. The stationary phase was characterized by the presence of octanol instead of silicone oil. The mobile phase was methanol–water (30:70), which yielded the experimental R_M values reported in Tables I and II. When a compound had been tested also by Cohnen *et al.*[10], an average R_M value is reported in Tables I and II.

The following equation describes the relationship between our R_M values and those measured by Dzimiri *et al.*[7]:

$$R_M = 1.477\ (\pm 0.092) + 1.331\ (\pm 0.105)\ R_{M\ \text{Dzimiri}} \quad (3)$$
$$(n=28;\ r=0.927;\ s=0.365;\ F=159.0;\ P<0.005)$$

The correlation coefficient is not as good as that for eqns. 1 and 2. A better equation was obtained when compounds 1, 15, 16, 30 and 35, which showed the largest deviations, were excluded from the analysis:

$$R_M = 1.532\ (\pm 0.064) + 1.286\ (\pm 0.078)\ R_{M\ \text{Dzimiri}} \quad (4)$$
$$(n=23;\ r=0.963;\ s=0.240;\ F=269.8;\ P<0.005)$$

A justification for excluding those compounds might be that they were the most deviant also when correlating the present R_M values with Dzimiri *et al.*'s log P values

TABLE V

OCTANOL–WATER PARTITION COEFFICIENTS AND HPLC RETENTION DATA FOR CARDIAC GLYCOSIDES

Compound No.	*Log P*	*Log P (Dzimiri et al.[7])*	*Log k'*	*ln V (Davydov et al.[4,6])*	*Log k' (Dzimiri et al.[7])*	*Compound No.*	*Log P*	*Log P (Dzimiri et al.[7])*	*Log k'*	*ln V (Davydov et al.[4,6])*	*Log k' (Dzimiri et al.[7])*
1	1.14	1.12	1.23	–	−0.44	31	–	–	–	–	–
2	–	1.09	1.29	–	−0.43	32	–	–	–	–	–
3	–	1.23	1.40	–	−0.36	33	–	–	2.01	3.94	–
4	–	1.26	1.59	3.36	−0.30	34	–	–	–	–	–
5	–	1.72	1.93	–	−0.01	35	–	3.46	2.75	–	1.69
6	–	1.98	1.95	–	0.10	36	–	2.15	1.95	–	0.36
7	–	–	1.60	3.25	–	37	–	2.04	2.10	–	0.26
8	–	–	1.72	2.75	–	38	2.09	–	1.63	–	–
9	–	2.52	1.87	–	0.63	39	–	–	1.85	4.01	–
10	–	2.29	2.25	–	0.20	40	–	–	–	–	–
11	–	2.87	2.29	–	0.61	41	0.64	0.61	1.12	2.18	−0.38
12	–	1.75	1.92	–	0.05	42	–	–	1.33	2.54	–
13	–	1.76	1.98	–	0.08	43	–	0.64	1.49	2.90	−0.10
14	–	2.14	2.28	–	0.44	44	–	−0.96	1.32	2.07	−0.66
15	2.64	2.41	1.70	–	0.26	45	–	−0.82	1.15	1.69	−0.68
16	–	2.49	1.79	–	0.28	46	–	–	1.65	1.91	–
17	–	2.45	1.74	–	0.38	47	–	–	–	2.11	–
18	–	2.83	2.04	4.89	0.52	48	–	–	–	1.95	–
19	–	–	2.37	5.47	–	49	–	–	1.57	2.45	–
20	–	–	–	–	–	50	–	–	–	1.86	–
21	–	–	2.30	4.78	–	51	–	–	1.12	–	–
22	–	–	–	–	–	52	–	–	1.13	–	–
23	–	3.11	–	–	0.92	53	–	–	–	–	–
24	–	–	–	–	–	54	–	–	–	–	–
25	–	–	1.72	–	–	55	–	–	2.07	–	–
26	1.76	1.64	1.46	–	−0.17	56	−0.02	–	0.83	–	–
27	–	1.78	–	–	−0.08	57	–	−1.85	0.75	0.62	−0.85
28	–	–	–	–	–	58	–	–	1.52	–	–
29	–	–	–	2.33	–	59	–	–	1.74	–	–
30	–	1.67	1.94	4.11	0.11	60	–	–	1.48	–	

(eqn. 5). In the correlation with the log k' values (see eqn. 8) they were not excluded, but again they were among the most deviant compounds.

The higher intercepts in eqns. 3 and 4 are due to the fact that Dzimiri *et al.*[7] used a stationary phase containing octanol instead of silicone oil. The higher slopes are due to the narrower range of Dzimiri *et al*'s R_M values. In eqns. 3 and 4 about 7–14% of the variance in our R_M values is not explained by the regression.

Relationship between R_M and log P or HPLC data

The log P and log k' values of the cardiac glycosides are reported in Table V, where most of the data available in the literature are also listed. Cohnen *et al.*[10] and Dzimiri *et al.*[7] measured the octanol–water partition coefficients of cardiac steroids. The best correlation between R_M and log P values was found by Dzimiri *et al.*[7]. Therefore, in Table V we report only the log P values of the compounds for which an R_M value in Dzimiri *et al.*'s system was available. For the compounds tested by both Cohnen *et al.*[10] and Dzimiri *et al.*[7] an average log P is reported in Table V. Eqn. 5, excluding compounds 1, 15, 16, 30 and 35, and eqn. 6, considering only the six genins, can be compared with eqn. 7, calculated with Dzimiri *et al.*'s R_M and log P values:

$$R_M = 1.248\ (\pm 0.118) + 0.634\ (\pm 0.061) \log P_{\text{Dzimiri}} \quad (5)$$
$$(n=23;\ r=0.914;\ s=0.362;\ F=107.0;\ P<0.005)$$

$$R_M = 0.345\ (\pm 0.145) + 0.637\ (\pm 0.088) \log P \quad (6)$$
$$(n=6;\ r=0.964;\ s=0.193;\ F=52.2;\ P<0.005)$$

$$R_{M\ \text{Dzimiri}} = -0.252\ (\pm 0.068) + 0.516\ (\pm 0.034) \log P_{\text{Dzimiri}} \quad (7)$$
$$(n=28;\ r=0.948;\ s=0.215;\ F=233.5;\ P<0.005)$$

The different intercepts in eqns. 5 and 6 compared with eqn. 7 are due to the use of octanol instead of silicone oil in the Dzimiri *et al.* TLC stationary phase. The difference between the intercepts in eqns. 5 and 6 is due simply to the high standard error in eqn. 5 and to the fact that the two equations share only two compounds (nos. 26 and 41). On the other hand, the slopes of the three equations are very close.

Obviously the results with eqns. 5 and 7 could have been expected on the basis of eqn. 4. The log k' values reported in Table V were extrapolated to 0% acetonitrile in the mobile phase from the linear relationship between log k' and acetonitrile concentration as already described[17]. In Table V the HPLC data measured by Davydov[6] and Dzimiri *et al.*[7] are also listed. The relationship between the R_M values and the HPLC retention data is described by the following equations:

$$R_M = -1.488\ (\pm 0.192) + 2.109\ (\pm 0.110) \log k' \quad (8)$$
$$(n=44;\ r=0.947;\ s=0.306;\ F=369.5;\ P<0.005)$$

$$R_M = -0.249\ (\pm 0.170) + 0.716\ (\pm 0.054) \ln V \quad (9)$$
$$(n=21;\ r=0.950;\ s=0.297;\ F=176.1;\ P<0.005)$$

$$R_M = 2.109\ (\pm 0.064) + 1.680\ (\pm 0.121) \log k'_{\text{Dzimiri}} \quad (10)$$
$$(n=28;\ r=0.938;\ s=0.336;\ F=192.0;\ P<0.005)$$

The ln V term in eqn. 9 is the retention index used by Davydov[6].

In eqns. 5 and 6 and 8–10, again about 7–17% of the variance in the R_M values is not explained by the regression. Nevertheless, the log P values and the HPLC data from two and three different laboratories, respectively, seem to agree with the R_M values as lipophilic indices of the cardiac steroids.

DISCUSSION

The ΔR_M values in Table IV can be used in order to describe the contribution of substituent groups to the lipophilicity of the whole molecule. As regards the Digitalis genins, the lipophilic character decreases in the order digitoxigenin > gitoxigenin > digoxigenin. In fact, attaching an OH group at C-12 (digoxigenin) or C-16 (gitoxigenin) decreases the lipophilic character of the parent compound, digitoxigenin. According to Dzimiri *et al.*[7], digoxigenin is more hydrophilic than gitoxigenin as the OH group at C-12 is more exposed to the complementary hydroxyl groups of the aqueous phase than the OH group at C-16. A similar conclusion can be drawn by considering the fragment values for the hydroxyl group at C-12 and C-16. In fact, the Δlog P values for the pairs digoxigenin–digitoxigenin and gitoxigenin–digitoxigenin are -1.50 and -0.88, respectively (Table V). Therefore, the Δlog P value for the OH at C-12 is much closer to the aliphatic fragment value of -1.64 for the OH group[18] than that for the OH at C-16. On the other hand, the acetyloxy group has the same hydrophilic character at both C-12 and C-16. Apparently the lactone ring is not able to mask the acetyloxy group at C-16. As a consequence, acetylation of the OH group has opposite effects at C-16 and C-12. k-Strophanthidin with an OH group at C-5 and a formyl group at C-10 is slightly more hydrophilic than digoxigenin. Ouabagenin (g-strophanthidin) is the most hydrophilic genin because of the addition of two other OH groups at C-1 and C-11 and the replacement of the formyl group with a more hydrophilic CH_2OH group at C-10. On the other hand, the replacement of the OH group at C-16 with a formyl group makes 16-formylgitoxin less lipophilic than gitoxin.

The sugar residues at C-3 examined in the present and Cohnen *et al.*'s system, *i.e.*, oleandrose, cymarose, digitoxose, rhamnose, thevetose and glucose, have polarities increasing in that order. As mentioned above, Davydov[6] obtained the same order of ranking except for oleandrose and cymarose, for which the same retention value was obtained. The introduction of an α- and/or β-methyl group and an acetyl group(s) into the sugar side-chain increases the lipophilicity. It may be noted that our experimental R_M values for heptaacetyl-k-strophanthoside and pentaacetylgitoxin, 3.41 and 4.59, respectively, are very close to those calculated in the present system from the R_M value of k-strophantoside and 16-acetylgitoxin, 3.44 and 4.33, respectively. The use of the average ΔR_M for the acetyl group in the side-chain in the calculation of the R_M value for strophantidin-3-acetate in the Cohnen *et al.* system may also be pointed out. This seems to be justified by the fact that in the present system the $OCOCH_3$ *vs.* OH group at C-3 has a ΔR_M value of 0.29 which is not far from the average ΔR_M of 0.35 reported in Table IV for any acetyl group in the side-chain.

The additivity of the lipophilic contribution of any substituent group at C-3 seems to rule out any significant kind of interaction between the steroid nucleus and the sugar side-chain. Fig. 1 shows histograms which illustrate the increments in lipophilicity due to the addition of the same sugar residue in each family of genins. It is shown that in each of the *Digitalis* derivatives families the lipophilicity increases in the

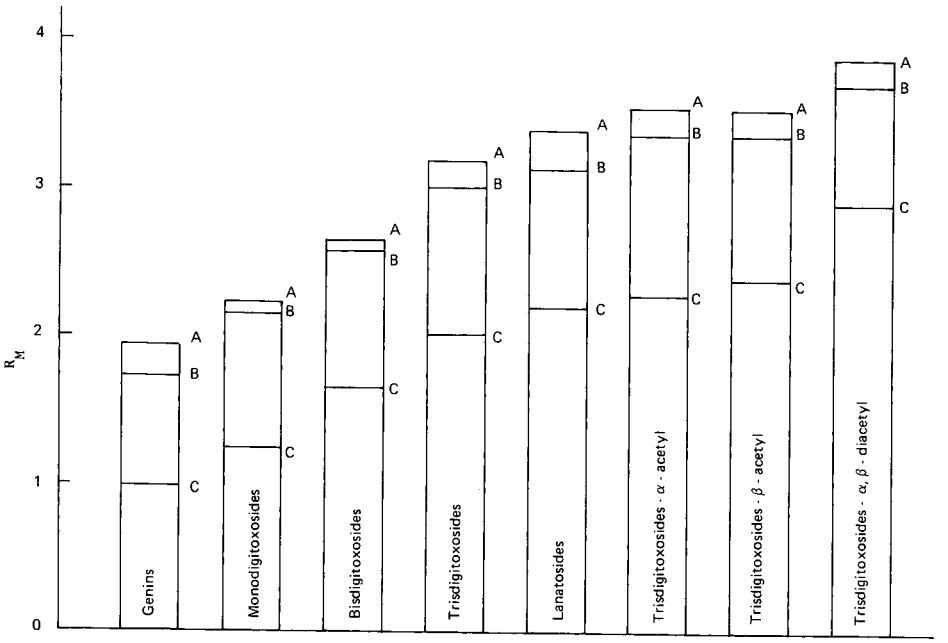

Fig. 1. Influence of side-chain composition on the overall lipophilicity of *Digitalis* cardiac glycosides. The different subsets are (A) digitoxigenin, (B) gitoxigenin and (C) digoxigenin.

order genin < monodigitoxoside < bisdigitoxside < trisdigitoxoside < α- or β-acetyl < α,β-diacetyl. Lanatoside A, B and C are less lipophilic than the α- or β-acetyl derivatives because of the presence of a glucosyl group in the side-chain.

A comment is deserved from a more general point of view. The present R_M values were obtained by extrapolation from the linear relationship between R_M values and acetone concentrations in the mobile phase. The extrapolation technique allows the calculation of a theoretical R_M value at 0% acetone in the mobile phase, *i.e.*, in a standard system where all the compounds could be compared.

Another great advantage over the determination of the R_M values at only one organic solvent concentration in the mobile phase is that in this way one can avoid the error that might arise because of different slopes of the straight lines describing the relationship between R_M values and organic solvent concentration in the mobile phase. Two compounds might have the same R_M value at a given organic solvent concentration and different extrapolated R_M values. Finally, the extrapolation procedure tends to yield a wider range of R_M values, which is reflected in the slopes of eqns. 3 and 4. In fact, the R_M values in the octanol system were measured at only one organic solvent concentration in the mobile phase.

CONCLUSION

The chromatographic data and the partition coefficients from the literature agree well with the present R_M values in describing the lipophilicity of cardiac steroids. The reliability of the ΔR_M values in Table IV is an important aspect. In fact, the

fragment values can be used in calculating the R_M values of other cardiac steroids. Finally, this work seems to have demonstrated some advantages of reversed-phase TLC or any other chromatographic system over the use of the classical partition coefficient[7,19]. The chromatographic method is simple and rapid; it requires little material, which is important with compounds that are expensive and/or difficult to synthesize, such as the cardiac steroids; the material does not need to be very pure; and the detection of spots by non-specific methods avoids the need for specific quantitative analytical methods.

REFERENCES

1 F. W. Hempelmann, N. Heinz and H. Flasch, *Arzneim.-Forsch.*, 28 (1978) 2182.
2 F. W. Hempelmann and N. Heinz, *Arzneim.-Forsch.*, 28 (1978) 2185.
3 F. J. Zeelen, *Quant. Struct.–Act. Relat.*, 5 (1986) 131.
4 V. Ya. Davydov, M. Elizalde Gonzales and A. V. Kiselev, *J. Chromatogr.*, 248 (1982) 49.
5 K. Jinno, *J. Chromatogr.*, 264 (1983) 485.
6 V. Ya. Davydov, *J. Chromatogr.*, 365 (1986) 123.
7 N. Dzimiri, U. Fricke and W. Klaus, *Br. J. Pharmacol.*, 91 (1987) 31.
8 N. Dzimiri and U. Fricke, *Br. J. Pharmacol.*, 93 (1988) 281.
9 W. Schonfeld and K. R. H. Repke, *Quant. Struct.–Act. Relat.*, 7 (1988) 160.
10 E. Cohnen, H. Flasch, N. Heinz and F. W. Hempelmann, *Arzneim.-Forsch.*, 28 (1978) 2179.
11 E. Tomlinson, *J. Chromatogr.*, 113 (1975) 1.
12 S. H. Unger, P. S. Cheung, G. H. Chiang and J. R. Cook, in W. J. Dunn, J. H. Block and R. S. Pearlman (Editors), *Partition Coefficient Determination and Estimation*, Pergamon Press, New York, 1986, pp. 69–81.
13 L. Nover, G. Juttner, S. Noack, G. Baumgarten and M. Luckner, *J. Chromatogr.*, 39 (1969) 419.
14 L. Nover, G. Baumgarten and M. Luckner, *J. Chromatogr.*, 39 (1969) 450.
15 G. L. Biagi, A. M. Barbaro, M. F. Gamba and M. C. Guerra, *J. Chromatogr.*, 41 (1969) 371.
16 T. Fujita, J. Iwasa and C. Hansch, *J. Am. Chem. Soc.*, 86 (1964) 5175.
17 M. C. Guerra, A. M. Barbaro, G. Cantelli Forti, M. C. Pietrogrande, P. A. Borea and G. L. Biagi, *J. Liq. Chromatogr.*, 7 (1984) 1495.
18 C. Hansch and A. J. Leo, *Substituent Constants for Correlation Analysis in Chemistry and Biology*, Wiley-Interscience, New York, 1979.
19 G. L. Biagi, A. M. Barbaro and M. C. Guerra, *Adv. Chem. Ser.*, 114 (1972) 61.

Journal of Chromatography, 504 (1990) 179–185
Elsevier Science Publishers B.V., Amsterdam — Printed in The Netherlands

CHROM. 22 186

High-performance thin-layer chromatography of rare earth tetraphenylporphine complexes

NOBUO SUZUKI*, KOICHI SAITOH and YOSHIHIKO SHIBATA
Department of Chemistry, Faculty of Science, Tohoku University, Sendai, Miyagi 980 (Japan)
(First received September 14th, 1989; revised manuscript received December 4th, 1989)

SUMMARY

The thin-layer chromatographic (TLC) behaviour of the metal complexes of tetraphenylporphine with twelve rare earths, *viz.*, Y(III), Nd(III), Sm(III), Eu(III), Gd(III), Tb(III), Dy(III), Ho(III), Er(III), Tm(III), Yb(III) and Lu(III), on TLC plates coated with octadecylsilica gel (C_{18}) and aminopropylsilica gel (NH_2) is described. Most of these metal complexes can be successfully developed without undesirable demetallation of the complexes in the migration process with a methanol–water mixture (90:10, v/v) containing both acetylacetone and diethylamine, typically at 5–10% and 0.5–1% for the C_{18} and NH_2 plates, respectively. On a C_{18} plate, the mobility (R_F) of the complexes of lanthanide metals tends to decrease in the order of the atomic numbers of the metals, whereas on an NH_2 plate the reverse order occurs. On both C_{18} and NH_2 plates the R_F value of the Y(III) complex lies between those of the Dy(III) and Ho(III) complexes.

INTRODUCTION

The convenience of thin-layer chromatography (TLC) has been applied to the isolation or identification of porphyrins and porphyrin esters by many investigators[1,2]. TLC studies on metalloporphyrins, however, have covered only a small number of compounds so far, *e.g.*, several metal complexes of protoporphyrin IX dimethyl ester on a cellulose thin layer[3] and those of tetraphenylporphine (TPP)[4,5] and octaethylporphyrin[6] on a silica gel thin layer.

High-performance TLC (HPTLC) gives a higher resolution and reprodicibility than conventional TLC, but few HPTLC studies dealing with metalloporphyrins have been published. In our laboratory, the HPTLC behaviour of the metal complexes of TPP[7], tetratolylporphine[8,9] and etioporphyrin[10] have been investigated using both normal and reversed-phase separation modes and those of porphine[11], hematoporphyrin IX[12], chlorophyll-a and -b[13] and pheophorbide-a and -b[14] only in the reversed-phase mode.

This paper deals with the HPTLC migration behaviour of the porphyrin complexes of rare earth (RE) metals. At most about 100 papers have dealt with RE

0021-9673/90/$03.50

complexes of porphyrin, mostly in the last 10 years. The chromatography of RE–porphyrin complexes has not yet been reported, except for alumina column chromatography briefly used in the preparation of RE–porphyrin complexes[15]. The complexes of porphyrin with trivalent REs are considerably less stable than those with other metals, such as Fe(II), Fe(III), Ni(II) and Cu(II), owing to the larger ionic radii of the RE ions (larger than 100 pm at coordination number >6) than the best fit (64 pm) for the hole in the N_4-moiety of porphyrin[16]. Accordingly, demetallation of an RE–porphyrin complex is a probable and undesirable phenomenon in chromatographic processes. Suppression of the the demetallation is the prime need for successful chromatography of these metal complexes.

This work was undertaken to find the mobile phase composition with which RE–porphyrin complexes can be chromatographed with sufficient stability and to examine how much the mobility of the complex varies with RE in spite of the chemical similarities among the REs. The HPTLC behaviour of twelve RE(III)–TPP complexes on octadecyl- and aminopropyl-bonded silica gel plates was investigated.

EXPERIMENTAL

Materials

The free acid form of TPP (H_2tpp; see Fig. 1) was synthesized by the method of Adler *et al.*[17] and purified by the procedure proposed by Barnett *et al.*[18]. Acetylacetonates of RE(III), RE(acac)$_3 \cdot n H_2O$, were prepared as described[19]. The complexes of TPP with RE(III) (RE = Y, Nd, Sm, Eu, Gd, Tb, Dy, Ho, Er, Tm, Yb and Lu) were synthesized by the reaction of H_2tpp with the acetylacetonate of the corresponding metal in refluxing 1,2,4-trichlorobenzene in a stream of nitrogen[15]. The reaction mixture, after preliminary concentration, was poured into a neutral alumina column. After complete elution of unreacted H_2tpp with toluene, the desired metal complex was eluted with a mixture of dimethyl sulphoxide and water (80:20, v/v), followed by extraction from the eluate with chloroform. After removal of the solvent, the final product was obtained as crystalline needles or an amorphous solid.

The UV–visible and infrared spectra of the final products agreed with those for mixed-ligand complexes, RE(tpp)(acac)[15,20]. Further, a significant peak appeared in the mass spectrum at an m/z value conistent with molecular ion $[RE(tpp)(acac)]^+$. The complexes thus prepared were reasonably identified as being in the form RE(tpp)-

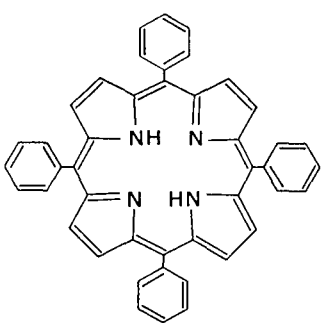

Fig. 1. Structural formula of H_2tpp.

(acac). The term RE–TPP complex is hereafter taken to mean RE(tpp)(acac), unless indicated otherwise.

Methanol was distilled. Benzene, dichloromethane (DCM), acetylacetone (Hacac) and diethylamine (DEA) were of analytical-reagent grade (Wako, Osaka, Japan). Water was doubly distilled in glass.

HPTLC

HPTLC plates (10 × 10 cm) coated with octadecyl-bonded silica gel (C_{18} plate; RP-18 F_{254S}, No. 13724) and aminopropyl-bonded silica gel (NH_2 plate; NH_2 F_{254S}, No. 15647) were obtained from Merck (Darmstadt, F.R.G.). The front portion of the thin-layer coating was scraped off every TLC plate so that the development would stop automatically when the solvent front had moved 75 mm from the origin.

A sample solution of each RE–TPP complex was prepared at a concentration about 0.1 m*M* in DCM–DEA (50:1, v/v). A 0.25-μl volume of sample solution was spotted at the sample origin, 5 mm from the rear edge of the TLC plate. The chromatogram was developed horizontally in a Camag (Muttenz, Switzerland) Model 28510 chamber in a room regulated at 25 ± 1°C. After the migration of the solvent front had automatically stopped at the expected distance from the sample origin (75 mm), the development procedure was allowed to continue for an additional 5 min so that the irregularity of the amount of solvent at the solvent front was reduced. The chromatogram was recorded photometrically at 420 nm with a Simadzu CS-920 densitometer (Kyoto, Japan).

RESULTS AND DISCUSSION

Sample solutions

Some RE–TPP complexes, particularly those of Nd(III), Sm(III) and Eu(III), were relatively unstable in common solvents such as benzene, chloroform, DCM, acetone, acetonitrile and methanol. The UV–visible spectra recorded for these complexes in such solvents changed to those corresponding to metal-free TPP (that is, H_2tpp) within 1 h after the preparation of the solutions (at about the 0.1 m*M* level). Such undesirable phenomena took place in solutions kept in containers made of both polyethylene and glass. It was found that the demetallation of these RE–TPP complexes could be suppressed by the addition of a small amount of an amine, such as DEA, to the solutions. In this work, the solution of an RE–TPP complex to be applied to HPTLC was prepared in DCM–DEA (50:1, v/v).

Chromatography on a C_{18} plate

According to some preliminary experiments, no RE–TPP complex could be moved from the origin on the plate with organic solvents such as methanol, ethanol, propanol, acetonitrile and acetone. It was found that Hacac and DEA were effective additives to the developing solvents. Unless indicated otherwise methanol–water (90:10, v/v) was used as the solvent, to which Hacac and DEA were added as modifiers.

The R_F values of RE–TPP complexes observed on C_{18} plates with different compositions of the developing solvents are given in Table I. None of the complexes moved from the origin. When the developing solvent contained either Hacac or DEA

TABLE I

R_F VALUES OF RE–TPP COMPLEXES ON A C_{18}-BONDED THIN LAYER

RP-18 F_{254S} HPTLC plate (Merck, No. 13724), 75 mm development at 25°C.

Developing solvent[a]		$R_F \times 100$											
No.	*CH_3OH:H_2O:Hacac:DEA*	*Y*	*Sm*	*Eu*	*Gd*	*Tb*	*Dy*	*Ho*	*Er*	*Tm*	*Yb*	*Lu*	*H_2tpp*
I	90:10:0:5	0	0	0	0	0	0	0	0	0	0	0	0
II	90:10:5:0	0	0	0	0	0	0	0	0	0	0	0	0
III	90:10:2.5:5	19	24	23	23	22	19	16	12	12	11	10	1
IV	90:10:5:5	23	30	28	29	28	24	20	17	16	14	14	2
V	90:10:10:10	40	42	42	42	42	40	38	33	30	28	25	4
VI	90:10:20:10	42	46	47	46	45	43	40	35	29	27	26	5
VII	90:10:0:5 (+ 0.05 *M* NaCl)	5	12	12	12	8	7	8	7	7	7	7	3
VIII	90:10:0:5 (+ 0.05 *M* $NaNO_3$)	7	7	8	8	9	8	8	8	7	7	7	6

[a] Volume ratio of components; CH_3OH = methanol; Hacac = acetylacetone; DEA = diethylamine.

(system I or II), still no migration of the complex occurred. The addition of both Hacac and DEA (systems III–VI) made it possible to move the complexes satisfactorily without undesirable demetallation. Exceptionally, the complex of Nd (III) showed continuous demetallation during the migration process. Accordingly, R_F values for the Nd(III) complex are not given in Table I.

The R_F value of each RE–TPP complex increased with increasing modifier (Hacac and DEA) content of the developing solvent. (Note: as Hacac and DEA have the same molar volume, 103 ml/mol at 25°C, both developing solvents IV and V contain equimolar mixtures of Hacac and DEA).

It has been reported[21] that the TPP complexes of trivalent metals, such as [Mn(tpp)Cl] and [Co(tpp)Cl], showed a large retention in reversed-phase HPLC using ethanol as an mobile phase, whereas the retention was reduced considerably on addition of a salt to the mobile phase. This phenomenon was explained in terms of the dissociation of Cl^- from the initial form of the complex, [M(tpp)Cl], followed by adsorption of the positively charged form $[M(tpp)]^+$ on an ion-exchangeable site (presumably a silanol group) present on the surface of the C_{18}-bonded material used.

The RE–TPP complexes were synthesized in the form [RE(tpp)(acac)]. When the dissociation of $[acac]^-$ from the complex took place on the thin layer, a reduction in the mobility of the complex was probable owing to adsorption of the dissociation product, $[RE(tpp)]^+$, on the thin layer. Enhancement of the concentration of the $[acac]^-$ anion in the developing solvent was a reasonable way to suppress the dissociation of RE–TPP complexes and to improve their mobilities. In practice, a developing solvent containing Hacac but not DEA (system II) was not effective in improving the mobilities of the RE–TPP complexes. One of the effective functions of DEA in the presence of Hacac (in solvent systems III–VI) is considered to be the base which promotes the dissociation of weakly acidic Hacac.

When sodium chloride (system VII) or sodium nitrate (system VIII) was used as the developing solvent additive in place of Hacac, every RE–TPP complex moved to

small extent relative to that observed with Hacac. It is considered that the exchange of the counter anion of $[RE(tpp)]^+$ from $acac^-$ to Cl^- or NO_3^- occurred at the origin.

The R_F values of RE–TPP complexes tend to decrease in the order of the atomic number (Z) within the lanthanide series. The R_F value of the complex of Y(III) was found to be between those of Dy(III) and Ho(III), whose ionic radii were close to that of Y(III). Two examples of the R_F *versus* Z plots are shown in Fig. 2.

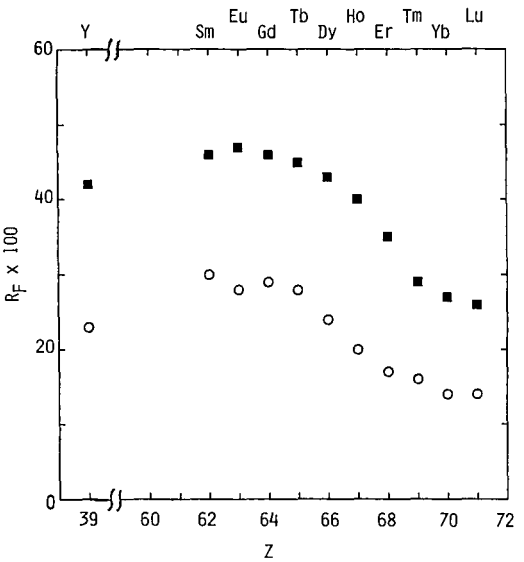

Fig. 2. R_F values of RE–TPP complexes plotted against the atomic number (Z) of the REs. HPTLC plate: C_{18}-bonded silica gel. Solvent systems: (○) IV and (●) VI in Table I.

Chromatography on an NH_2 plate

The developing solvents were prepared by addition of certain amounts of Hacac and DEA to methanol–water (90:10, v/v) used as the solvent. The R_F values of the RE–TPP complexes observed with different compositions of the developing solvents are given in Table II. When DEA was not present in the developing solvent (system I), demetallation of the TPP complexes of light lanthanides, such as Nd(III), Sm(III), Eu(III) and Gd(III), occurred during the migration. These undesirable chemical changes in the metal complexes were suppressed by adding DEA to the developing solvent (systems II–IV). It is notable that the Nd(III)–TPP complex, which could not be chromatographed successfully on the C_{18} plate owing to its low stability, moved on the NH_2 plate without demetallation when using a developing solvent containing at least 1% of DEA.

The R_F values of RE–TPP complexes observed on the NH_2 plate tend to increase in the order of the atomic number within the lanthanide series, as shown in Fig. 3, which is the reverse trend to that found on the C_{18} plate (see Fig. 2). The R_F value of Y(III)–TPP was found to be between those of the Dy(III) and Ho(III) complexes, which is similar to the result on the C_{18} plate.

TABLE II

R_F VALUES OF RE–TPP COMPLEXES ON AN NH_2-BONDED THIN LAYER

NH_2 F_{254S} HPTLC plate (Merck, No. 15647), 75 mm development at 25°C.

Developing solvent[a]		R_F × 100											
No.	*CH_3OH:H_2O:Hacac:DEA*	*Y*	*Nd*	*Sm*	*Eu*	*Gd*	*Tb*	*Dy*	*Ho*	*Er*	*Tm*	*Yb*	*Lu*
I	90:10:5:0	48	[b]	[b]	[b]	[b]	27	42	56	79	95	95	95
II	90:10:0.5:0.5	77	[b]	53	57	57	66	73	79	84	88	89	89
III	90:10:1:1	81	64	64	66	69	73	78	84	90	91	92	95
IV	90:10:1:5	92	91	92	92	93	93	93	94	95	97	97	97

[a] See Table I.
[b] Demetallation occurred.

It was observed on both the C_{18} and NH_2 plates that the R_F value of an RE–TPP complex increased with increase in the DEA content of the developing solvent. This suggests that certain kind(s) of interaction between DEA and the RE–TPP complex should be taken into consideration. The stronger the interaction between DEA and the RE complex, the more enhanced is the mobility (R_F value) on the C_{18} plate because of a preferential distribution of the complex into the developing solvent phase. According to the results in Fig. 2, the interaction between DEA and an RE–TPP complex apparently decreases in the order of the atomic number in the lanthanide series. The effect of DEA is complicated on NH_2 plates owing to an additional interaction between the complex and the amino group located on the

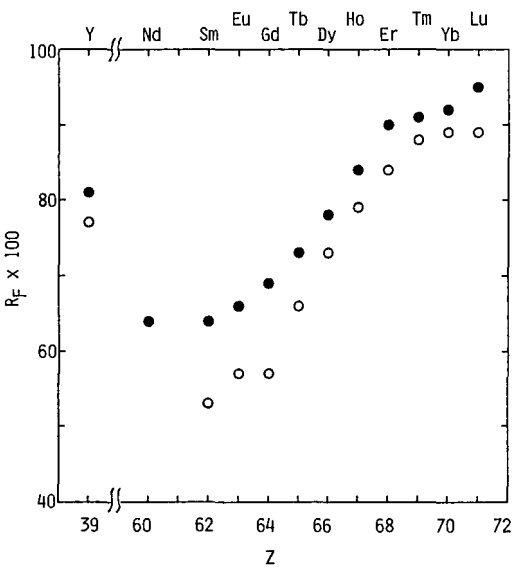

Fig. 3. R_F values of RE–TPP complexes plotted against the atomic number (Z) of the REs. HPTLC plate: NH_2-bonded silica gel. Solvent systems: (○) II and (●) III in Table II.

surface of the silica gel. The R_F values of the RE–TPP complexes tend to increase in the order of the atomic number on the NH_2 plates, as shown in Fig. 3, which is the reverse of the results on the C_{18} plate. It is considered that this reversed trend in mobility order resulted from the additional interaction between the complex and the amino group, and suggested that this interaction tends to decrease with increasing atomic number of the RE.

The effects of amines on the mobility of RE–TPP complexes cannot be clearly explained at this stage. More detailed mobility studies on these complexes will be carried out by a column method using various amines.

REFERENCES

1 J.-H. Fuhrhop and K. M. Smith, in K. M. Smith (Editor), *Porphyrins and Metalloporphyrins*, Elsevier, Amsterdam, 1975, p. 839.
2 W. I. White, R. C. Bachmann and B. F. Burnham, in D. Dolphin (Editor), *The Porphyrins*, Vol. I, Academic Press, New York, 1978, p. 553.
3 Y. Onoue, *Bull. Chem. Soc. Jpn.*, 54 (1981) 1972.
4 M. Sato and T. Kwan, *Chem. Pharm. Bull.*, 20 (1972) 840.
5 K. S. Hui, B. A. Davis and A. A. Boulton, *J. Chromatogr.*, 115 (1975) 581.
6 J. W. Buchler, L. Puppe, K. Rohbock and H. H. Schneehage, *Chem. Ber.*, 106 (1973) 21710.
7 K. Saitoh, M. Kobayashi and N. Suzuki, *Anal. Chem.*, 53 (1981) 2309.
8 M. Kobayashi, K. Saitoh and N. Suzuki, *Chromatographia*, 18 (1984) 441.
9 M. Kobayashi, K. Saitoh and N. Suzuki, *Chromatographia*, 20 (1985) 49.
10 S. Miyake, K. Saitoh and N. Suzuki, *Chromatographia*, 20 (1985) 417.
11 Y. Wakui, K. Saitoh and N. Suzuki, *Chromatographia*, 22 (1986) 160.
12 N. Suzuki, K. Saitoh and Y. Sugiyama, *Chromatographia*, 21 (1986) 509.
13 N. Suzuki, K. Saitoh and K. Adachi, *J. Chromatogr.*, 408 (1987) 181.
14 K. Adachi, K. Saitoh and N. Suzuki, *J. Chromatogr.*, 457 (1988) 99.
15 C. P. Wong, *Inorg. Synth.*, 22 (1983) 152.
16 J. W. Buchler, In K. M. Smith (Editor), *Porphyrins and Metalloporphyrins*, Elsevier, Amsterdam, 1975, p. 191.
17 A. D. Adler, F. R. Longo, J. D. Finavelli, J. Goldmacher, J. Assour and L. Korsakoff, *J. Org. Chem.*, 32 (1967) 476.
18 G. H. Barnett, M. F. Hudson and K. M. Smith, *J. Chem. Soc., Perkin Trans. 1*, 1975, 1401.
19 J. D. Stites, C. N. McCarthy and L. L. Quill, *J. Am. Chem. Soc.*, 70 (1948) 3142.
20 C. P. Wong and W. D. Horrocks, Jr., *Tetrahedron Lett.*, 31 (1975) 2637.
21 N. Suzuki, T, Takeda and K. Saitoh, *Chromatographia*, 22 (1986) 43.

Journal of Chromatography, 504 (1990) 186–190
Elsevier Science Publishers B.V., Amsterdam — Printed in The Netherlands

CHROM. 22 246

Note

Implications of solvent selectivity triangles in assessing stationary phases for gas chromatography

T. J. BETTS
School of Pharmacy, Curtin University of Technology, GPO Box U1987, Perth, W.A. 6001 (Australia)
(First received December 15th, 1989; revised manuscript received January 3rd, 1990)

Poole and Poole[1] have recently reviewed the characterization of solvent properties of gas chromatography (GC) liquid stationary phases. Referring to the use of Snyder's solvent selectivity triangle[2] which they note "has strong visual impact" they comment that this "original choice of (solvents for triangular) axes for proton-donor-acceptor and orientation interactions ... is quite reasonable". Snyder's probe solutes used for studies of GC stationary phases were ethanol, nitromethane (Y and U respectively as designated by Rohrschneider[3]) and dioxane (l′ by McReynolds[4]) and Kersten and Poole[5] in 1988 found that "the retention of ethanol and nitromethane on the non-polar GC phases is inadequate" even at their low temperature of 80.8°C. They also found that "dioxane is a rather insensitive probe for proton-donor interactions ... New probes should be selected". Poole thus ignores his own observations in the review[1] allowing him to reuse his previous triangular figures. The earlier paper[5] comments that "*n*-butanol, nitropropane, 2-pentanone and pyridine (McReynolds' y′, u′, z′ and s′, respectively) ... are better retained on most phases. These additional probes can be used to determine whether the choice of the test solute influences the position of a particular phase in the solvent selectivity triangle". As only three probes must be used to construct such a triangle, it seems self-evident that their choice must do so and I have examined this here. Kersten and Poole[5] noted that (Snyder's) nitromethane does not behave characteristically of the other nitroalkanes on most selective (GC) phases. "The use of higher molecular weight nitroalkanes in place of nitromethane will significantly change the relative position of a phase in the selectivity triangle". They further comment "that both pyridine and 2-pentanone have reasonably large dipole moments compared to dioxane and consequently their retention will be more influenced by orientation interactions"[5]. It seems desirable to use these two solutes in solvent triangles.

Poole and Poole note my work[6] using *n*-butanol, pyridine and 2-octyne (McReynolds' k′) for a selectivity triangle with the comment "it is not clear what advantage was gained by the change. 2-Octyne measures mainly dispersive interactions so that ... the triangle is changed"[1]. It was chosen because, of the McReynolds solute probes, it gave the best spread of results in the triangle —surely a good reason? This allowed me to perceive three groups of stationary phases: (1) fully methyl polysiloxanes such as OV-1, SE-30, SP-2100; and phenyl–methyl (nominally 50:50)

0021-9673/90/$03.50

polysiloxanes like OV-17 or SP-2250, with the sequence of probes being butanol–pyridine–*octyne*. (2) More polar polysiloxanes such as cyanopropyl–phenyl–methyl (25:25:50) like OV-225; and the trifluoropropyl–methyl (50:50) ones like OV-210, with the sequence of probes being butanol–octyne–*pyridine*. (3) Highly polar phases such as cyanopropyl–methyl (90:10) polysiloxanes like SP-2330; polyethylene glycols (PEG) (20M and 1500) and diethylene glycol succinate, with the sequence of probes being octyne–*butanol*–pyridine.

If such results can indicate that only three phases may be enough for most purposes —possibly three different polysiloxanes— surely this justifies the choice of solute probes?

Kersten and Poole[5] detected but did not enclose four selectivity groups in their Snyder triangle (using the undesirable ethanol, nitromethane and dioxane), given below in my sequence and labelling: (A) phenyl–methyl (50:50) such as OV-17; and trifluoropropyl–methyl (50:50) polysiloxanes (QF-1). (B) Cyanopropyl–methyl (25:75?) polysiloxanes like the unusual OV-105. (C) Cyanopropyl–phenyl–methyl (25:25:50) polysiloxanes like OV-225; and polyethylene glycols (20 M). (D) Thiocyanates —synthesised by them; not widely used.

Apart from the thiocyanates, the other groups all show the same probe sequence of ethanol–nitromethane–dioxane, suggesting these solutes are a poor combination.

Although for some reason they did not study fully methyl polysiloxanes, nor Apiezons, nor diethylene glycol succinate they still failed to note what I previously pointed out[6], that the most polar (thiocyanate) phases were nearest to the centre of the selectivity triangle, and the lower polarity groups A and B furthest from the centre. "A phase exhibiting minimum selectivity would be located at the centre of the triangle. The most selective phases are found towards the corners of the triangle"[5]. This can be achieved by applying bias to the triangle axes —Kersten and Poole use 0.2–0.7 for ethanol and nitromethane, but 0.1–0.6 for dioxane, these being not quite the same axis values as those of Snyder[2].

PROCEDURE

To check this possibility that strongly polar phases might be indicated triangularly to be less selective than those of low polarity, I plotted selectivity triangles using published McReynolds values[4] for different combinations of three of his first five solutes. The combination of benzene–butanol–nitropropane gave poor discrimination as every GC phase yielded the probes in this sequence. Other combinations gave different degrees of discrimination and butanol–nitropropane–pyridine was selected. It is interesting that two of these solutes were probes I selected previously in 1986[6].

Values for each of these probes were calculated by

$$x = (\overline{\mathrm{McR}}_{\mathrm{solute}})/\Sigma(\overline{\mathrm{McR}}_{\mathrm{three\ solutes}})$$

where $\overline{\mathrm{McR}}$ are the McReynolds values published[4] and these are given in Table I and plotted in a biased triangle in Fig. 1.

DISCUSSION

It is clear in Fig. 1 that strongly polar phases are clustered together near to the centre of the selectivity triangle, which can be included with them in a circle of radius

TABLE I

PROPORTIONS (x) OF THE SUM OF THREE RECORDED McREYNOLDS VALUES, OR FROM KERSTEN AND POOLE[5]

$\overline{McR}$ = McReynolds value published[4]; PSX = polysiloxane; PEG = polyethyleneglycol. x Values in italics are in the range 0.327–0.335 (around the "mid" value of 0.333). $\overline{K/P}$ = Values calculated according to McReynolds procedure from data[5]; bu = butanol; di = dioxane; et = ethanol; nim = nitromethane; nip = nitropropane; py = pyridine.

No.	*Stationary phase*	*n-Butanol*		*Nitropropane*		*Pyridine*		$\Sigma\overline{McR}$	*Probe solute sequence*
		$\overline{McR}$	x	$\overline{McR}$	x	$\overline{McR}$	x		
1	Apiezon L grease	22	0.229	32	*0.333*	42	0.438	96	bu-nip-PY
2	PSX-fully methyl (SE-30, OV-1, SP-2100)	53	*0.335*	64	0.405	41	0.260	158	py-BU-nip
3	PSX-phenyl-methyl (50:50) (OV-17, SP-2250)[a]	158	0.262	243	0.403	202	*0.335*	603	bu-py-NIP
4	PSX-phenyl-methyl (75:25) (OV-25)	204	0.258	305	0.387	280	0.355	789	bu-py-NIP
5	PSX-trifluoropropyl-methyl (50:50) (OV-210, QF-1)	233	0.233	463	0.463	305	0.305	1001	bu-py-NIP
6	PSX-cyanopropyl-phenyl-methyl (25:25:50) (OV-225)	369	0.296	492	0.394	386	0.309	1247	bu-py-NIP
7	PEG 20M	536	*0.331*	572	0.353	510	0.315	1618	py-BU-nip
8	PSX-cyanopropyl-phenyl (50:50) (SP-2300)	495	0.299	637	0.383	531	0.319	1663	bu-py-NIP
9	Free fatty acid phase	580	0.321	602	*0.333*	627	0.347	1809	bu-nip-PY
10	PEG 1500	607	*0.333*	626	0.344	589	0.323	1822	py-BU-nip
11	Diethylene glycol succinate	751	0.306	840	0.343	860	0.351	2451	bu-nip-PY
12	Tris-(cyano-ethoxy)propane	857	0.306	1028	0.367	915	*0.327*	2800	bu-py-NIP
13	Bis-(cyano-ethyl)formamide	991	0.320	1110	0.358	1000	0.322	3101	bu-py-NIP
		Ethanol		*Nitromethane*		*Dioxane*		$\Sigma\overline{K/P}$	
		$\overline{K/P}$	x	$\overline{K/P}$	x	$\overline{K/P}$	x		
3′	PSX-phenyl-methyl (50:50)	139	0.238	263	0.450	182	0.312	584	et-di-NIM
5′	PSX-trifluoropropyl-methyl (50:50)	263	0.230	427	0.484	253	0.286	883	et-di-NIM
6′	PSX-cyanopropyl-phenyl-methyl (25:25:50)	383	0.311	517	0.419	333	0.270	1233	di-ET-nim
7′	PEG 20M	581	*0.330*	727	0.413	450	0.256	1758	di-ET-nim

[a] Approximate side chain percentage is indicated.

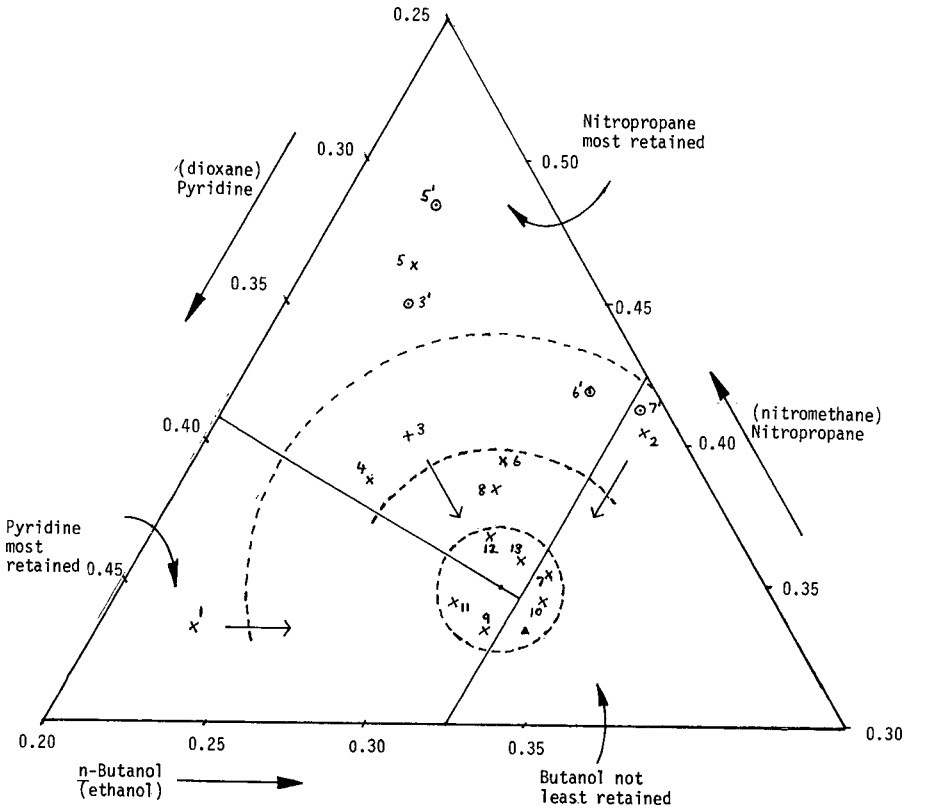

Fig. 1. Plot of McReynolds values on various gas chromatographic stationary phases (×) for the three solute probes *n*-butanol (from left side to lower right apex), nitropropane (top apex) and pyridine (lower left apex). Also shown are values from Kersten and Poole[5] for corrected I_R (retention index based on *n*-alkanes) on some of the phases (⊙) for the solutes ethanol (lower right apex), nitromethane (top apex) and dioxane (lower left apex). Numbers 1–13 refer to the phases listed in Table I. ▲ is the centre of the full triangle plot (0.333 for all three solutes).

about 0.02 drawn at about 0.318 butanol–0.333 pyridine. Phases of fairly high polarity (SP-2300 and OV-225) are outside this circle whilst lower polarity SE-30, OV-17 and OV-25 are more remote. The most distant phases are Apiezon L and OV-210, and these are directed towards the pyridine-retaining and nitropropane-retaining corners of the triangle, respectively. It is possible to draw a line at butanol 0.325 to include the phases SE-30 and polyethylene glycols for which butanol is not the least retained (probe sequence pyridine–*butanol*–nitropropane). Another line separates from the remaining phases three which retain pyridine most strongly (diethylene glycol succinate, free fatty acid phase and Apiezon L) with probe sequence butanol–nitropropane–*pyridine*. This leaves a large group with strong affinity for nitropropane and least retention of butanol (probe sequence butanol–pyridine–*nitropropane*). These solute sequence-defined groups are very like my 1986 ones[6], with nitropropane in place of octyne.

These divisions are quite odd, as each includes both low and high polarity phases. For example, fully methyl polysiloxane is grouped with the polyethylene

glycols, and Apiezon L is grouped with a polyester. What are the implications? It cannot be suggested sensibly that highly polar phases such as free fatty acid phase and PEG 1500 should be discarded as lacking solute discrimination because they plot near the 0.333 centre of the triangle. Nor is it reasonable to suggest that only phases near the apices of the triangle (Apiezon L and OV-210) should be used for their high discrimination. Perhaps phases should be selected for particular separations if they are virtually "neutral" to one of the solute probes (with a value close to 0.333) and hence preferentially retain one of the other two, so discriminating well, substances of this type retained? For example, Apiezon L (1 in Fig. 1) is neutral to nitroalkanes and selective for aromatics like pyridine, which it retains relatively strongly. It should not be chosen to resolve aliphatic alcohols. Free fatty acid phase (9) shows this to much lesser extent. Fully methyl polysiloxanes (2) are neutral to these alcohols, selective for nitroalkanes, and should not be chosen for aromatics; and this applies to PEG 1500 (10) to a lower degree. The commonly used phenyl–methyl (50:50) polysiloxanes (3) are surprisingly neutral to aromatics, selective for nitroalkanes, but not the phase of choice for aliphatic alcohols. Without exhibiting any fully "neutral" character tris-(cyano-ethoxy)propane (12) shows a reduced response of this type. Of course, this reduced discrimination response is due partly to the larger figures of McReynolds values given by the polar phases. Differences between the smaller values of the non-polar phases produce a relatively more severe displacement from the centre of the triangle.

Perhaps the best use for this plot is to indicate, for example, that Apiezon L is a low polarity alternative to diethylene glycol succinate. Similarly tris-(cyano-ethoxy)propane, OV-225, OV-17, OV-210 represent a decreasing polarity sequence of similar discriminatory potential. Corresponding results are obtained (with a somewhat different plot) using pentanone values with butanol and pyridine. Even using Kersten and Poole's results[5] for ethanol–nitromethane–dioxane and plotting them on my butanol–nitropropane–pyridine triangle gives points for the phases which remain in the same groupings (Fig. 1).

The British Pharmacopoeia 1988 (Vol. I)[7] includes over 60 examples of the use of GC on liquid phases and hence should provide a useful review of the selection of stationary phases for drug analysis. From my pyridine-retaining group, Apiezon L is only recommended twice, free fatty acid phase three times and polyester phases eight times. These phases thus form only about 22% of the GC uses. From my butanol-not-least-retained group, polyethylene glycols are recommended for twelve uses and fully methyl polysiloxanes for thirteen, giving 42% of the British Pharmacopoeia analyses and forming the main group. Most of the 36% remaining are from the butanol-pyridine-nitropropane group, although trifluoropropyl–methyl polysiloxanes such as OV-210 are not used at all. Perhaps these phases and Apiezon L, should be uitilised?

REFERENCES

1 C. F. Poole and S. K. Poole, *Chem. Rev.*, 89 (1989) 377.
2 L. R. Snyder, *J. Chromatogr.*, 92 (1974) 223.
3 L. Rohrschneider, *J. Chromatogr.*, 22 (1966) 6.
4 W. O. McReynolds, *J. Chromatogr. Sci.*, 8 (1970) 685.
5 B. R. Kersten and C. F. Poole, *J. Chromatogr.*, 452 (1988) 191.
6 T. J. Betts, *J. Chromatogr.*, 354 (1986) 1.
7 *The British Pharmacopoeia*, Vol. I, Her Majesty's Stationery Office, London, 1988.

Journal of Chromatography, 504 (1990) 191–196
Elsevier Science Publishers B.V., Amsterdam — Printed in The Netherlands

CHROM. 22 240

Note

Analysis of thymidine hydroperoxides by post-column reaction high-performance liquid chromatography

J. R. WAGNER

MRC Group in the Radiation Sciences, Faculty of Medicine, University of Sherbrooke, Sherbrooke, Quebec J1H 5N4 (Canada)

M. BERGER and J. CADET

Laboratoires de Chimie, Département de Recherche Fondamentale, Centre d'Etudes Nucléaire de Grenoble, 85X, 38041 Grenoble Cedex (France)

and

J. E. VAN LIER*

MRC Group in the Radiation Sciences, Faculty of Medicine, University of Sherbrooke, Sherbrooke, Quebec J1H 5N4 (Canada)

(First received September 6th, 1989; revised manuscript received December 11th, 1989)

Hydroperoxides are common products or intermediates of oxidative processes[1]. Thymidine hydroperoxides result from the action of hydroxyl radicals on DNA in oxygenated solutions[2,3]. In fact, initially formed hydroperoxides are estimated to make up about 70% of the total DNA base damage induced by the action of ionizing radiation on DNA in aqueous solution[4]. Since exposure of 2′-deoxycytidine, 2′-deoxyguanosine or 2′-deoxyadenosine to ionizing radiation in aqueous oxygenated solutions does not yield detectable amounts of hydroperoxides, the majority of DNA hydroperoxides is expected to be made up of thymidine hydroperoxides. Similar pathways involving hydroxyl radicals and the formation of thymidine hydroperoxides can also be implicated in the action of therapeutic drugs[5] and in the process of aging[6].

We report the complete separation of the eight possible 5(6)-hydroxy-6(5)-hydroperoxides of thymidine by reversed-phase high-performance liquid chromatography (HPLC). The hydroperoxides are selectively detected by mixing the HPLC eluent with Fe^{2+}–xylenol orange reagent. This system is easy to assemble, uses conventional HPLC equipment and reaches pmol levels of detection. Previously, this method was reported in a qualitative study of several hydroperoxides formed from $OH^{\cdot}$ induced oxidation and one-electron oxidation of thymidine[7]. In this article, emphasis has been placed on the methodology and quantitative aspects of the post-column reaction for the detection of hydroperoxides.

EXPERIMENTAL

Chemicals

Thymidine and the reagents for post-column reaction were purchased from Sigma and used as received. Solvents were of the highest purity available from

0021-9673/90/$03.50

Anachimia (Montreal, Canada). Water in all experiments was distilled twice in quartz. [^{14}C(2)]Thymidine was obtained from Amersham and was purified immediately before use by HPLC. Thymidine hydroperoxides were obtained by two methods. The four diastereomers of 5-hydroxy-6-hydroperoxy-5,6-dihydrothymidine were obtained from peroxidation of thymidine using trifluoroperacetic acid[8]. The four 6-hydroxy-5-hydroperoxy-5,6-dihydrothymidine diastereomers and 5-hydroperoxymethyl-2′-deoxyuridine were prepared by near-ultraviolet photolysis of thymidine solutions in the presence of 2-methyl-1,4-naphthoquinone[9]. The stereochemistry of each hydroperoxide was determined by comparing the corresponding 5,6-diol of thymidine, obtained after treatment of the hydroperoxide with zinc powder in 3% aqueous acetic acid, to authentic reference samples and assigned structures were confirmed by ^{1}H NMR and ^{13}C NMR[10].

Chromatography

Thin-layer chromatography (TLC) was carried out on SIL-G UV 0.25 mm thick silica plates (Machery-Nagel, Düren, FRG) by two-dimensional analysis, first the plates were developed in solvent I [chloroform–methanol–water (4:2:1, v/v/v); methanol was added (5%, v/v) to the organic phase] and then after drying, at right angles in solvent II [methyl propionate–2-propanol–water (75:16:9, v/v/v)][11]. Hydroperoxides were detected directly on the TLC plates by spraying with N,N-dimethyl-1,4-phenylenediamine in 50% aqueous methanol[12]. R_F values are reported relative to those of thymidine which migrates with an absolute R_F of 0.67 in both solvent systems. HPLC equipment consisted of a dual piston pump (Waters No. M6000; Mississauga, Canada), a fixed-volume injector (Rheodyne; Berkeley, CA, U.S.A.), a fixed-wavelength detector (Waters No. 441) and an analog–digital integrator (Varian No. 4270; Georgetown, Canada). Two C_{18} reversed-phase columns were used: a semi-preparative column, 25 cm × 7.5 mm I.D., packed with 5-μm Spherisorb (Chrom. Specialities, Brockville, Canada) and an analytical column, 25 cm × 4.6 mm I.D., packed with 5-μm Ultrasphere (Beckman; Berkeley, CA, U.S.A.). Water (pH $\simeq$ 6) was used as the mobile phase for both columns.

Post-column reaction

The basic flow system described above was also used in the post-column reaction HPLC system to detect thymidine hydroperoxides, except that a second pump was used to mix a peroxide reagent into the first HPLC line (Fig. 1). In order to assure a stable baseline, it was essential that the pumps were equiped with pulse dampeners. All compounds, including hydroperoxides, were detected prior to the post-column reaction by an UV absorption detector set at 229 nm. The eluent and reagent were mixed in a right angle tee before entering the reactor coil. The reactor coil consisted of 6 m × 0.52 mm I.D. stainless-steel tubing, shaped in 80 coils of 2 cm diameter submerged in a water bath thermostated at 60°C. An additional 2 m of tubing shaped in 20 coils was submerged in a water bath kept at room temperature. Absorbance of the eluent-reagent mixture was measured at 546 nm. The peroxide reagent consisted of $5.8 \cdot 10^{-4}$ *M* xylenol orange (tetrasodium salt) and $2.3 \cdot 10^{-4}$ *M* ammonium ferrous sulfate in 0.035 *M* H_2SO_4. The final concentration of the reactants after mixing with the HPLC eluent is identical to that used in the conventional colorimetric test for hydroperoxides[13]. The post-columns reactions are presented by eqns. 1 and 2.

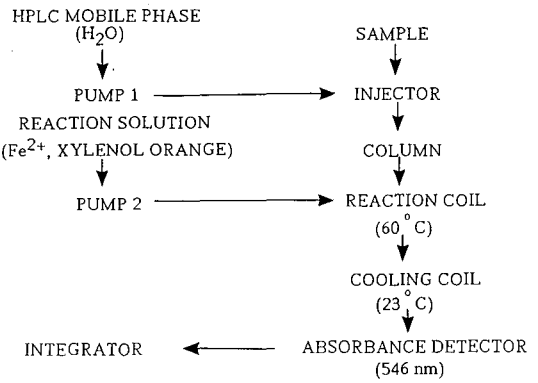

Fig. 1. Flow diagram of post-column reaction HPLC for the detection of thymidine hydroperoxides.

$$Fe^{2+} + ROOH \rightarrow Fe^{3+} + ROH \quad (1)$$

$$Fe^{3+} + \text{xylenol orange} \rightarrow Fe^{3+}\text{–xylenol orange} \quad (2)$$
$$(\varepsilon_{540nm} = 26\,800\ M^{-1}cm^{-1})$$

(where ROOH is hydroperoxide). Under our experimental conditions, the background absorption measured at 546 mm was 0.08 absorbance units with water as a reference. The flow-rates provided by the primary and reagent pumps were adjusted to 0.7 and 1.5 ml/min respectively which gave reasonable head pressures of 28 and 86 atm. This flow-rate combination gave the best response. Lowering the flow-rate of the reagent pump, while keeping the final concentration of reagent the same, resulted in greater baseline fluctuations likely due to poor mixing. At these flow-rates, the reagent and eluent are in contact for less than 1 min. The reaction was considered to be complete at this time since neither increasing the temperature of the bath nor diminishing the flow-rate gave higher signals for the hydroperoxides. The reaction time is considerable faster than the 10 min required in the standard colorimetric test at room temperature[14]. The response of the detector was found to be linear with the amount of hydroperoxide injected from 100 nmol, at which point the detector is saturated, down to 10 pmol. A signal representing 10 pmol is about 20 times greater than the background absorption. Comparison of the bandwidths of eluting compounds using the 229 nm UV detector *versus* the 546 nm post-column reaction detector indicates that the reaction coil introduces about 20% diffusion of the elution peaks. This diffusion was independent of the injection volume over the range of 20–100 μl.

ANALYSIS OF THYMIDINE HYDROPEROXIDES

There are eight possible isomers of 5(6)-hydroxy-6(5)-hydroperoxides of thymidine (Fig. 2). They are not completely resolved by two-dimensional TLC on silica gel (Table I) and the diastereomers **3** and **4** are indistinguishable under the conditions used. Furthermore, the quantitation of thymidine hydroperoxides by TLC is difficult because they tail and partly decompose under these conditions. The R_F values were

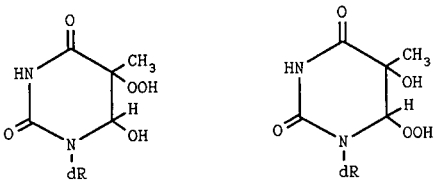

(1) *trans*(5S,6S)
(2) *trans*(5R,6R)
(7) *cis*(5R,6S)
(8) *cis*(5S,6R)

(3) *trans*(5R,6R)
(4) *trans*(5S,6S)
(5) *cis*(5S,6R)
(6) *cis*(5R,6S)

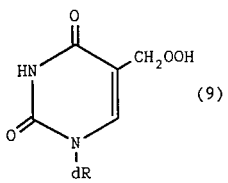

(9)

Fig. 2. Structures of thymidine hydroperoxides. dR = 2-β-D-*erythro*-Pentofuranosyl moiety.

obtained from analysis of pure hydroperoxides and agree with previous analysis of these compounds from complex mixtures of the hydroxyl radical-induced thymidine oxidation products[2,10]. All eight isomeric 5(6)-hydroxy-6(5)-hydroperoxides of thymidine are resolved by reversed-phase HPLC (Table I and Fig. 3). Unlike TLC

TABLE I

CHROMATOGRAPHIC PROPERTIES OF THE NINE HYDROPEROXIDES OF THYMIDINE

Thymidine Hydroperoxide	R_F *TLC*[a]		*HPLC*[b] *retention volume (ml)*	*Ratio*[c] *of absorbance 546 nm/229 nm*	*Ratio*[d] *of pmol of hydroperoxide to absorbance at 546 nm*
	solvent I	*II*			
1	0.46	1.15	6.7	3.4	4.5
2	0.50	1.30	8.0	3.1	3.9
3	0.48	1.12	8.8	4.3	–
4	0.48	1.12	9.0	4.3	–
5	0.43	0.77	9.9	7.1	3.7
6	0.43	0.90	13.1	7.7	2.9
7	0.41	0.73	16.1	6.3	3.6
8	0.48	0.78	16.9	5.6	3.8
9	0.56	0.99	10.7[e]	2.9	–

[a] Two dimensional TLC in system I (organic phase of chloroform–methanol–water (4:2:1, v/v/v), to which was added 5% methanol (v/v) and system II methyl propionate–2-propanol–water (75:16:9, v/v/v). R_F values are relative to thymidine.
[b] Analytical reversed-phase column (void volume, 2.2 ml) with water as the mobile phase.
[c] UV detection of hydroperoxides was made before the post-column reaction.
[d] Factor used to convert the integrated 546 nm signal to the quantity of hydroperoxide injected on the HPLC column; 1 corresponds to an absorbance of 0.0002 at the peak maximum at 546 nm.
[e] Mobile phase: 5% aqueous methanol.

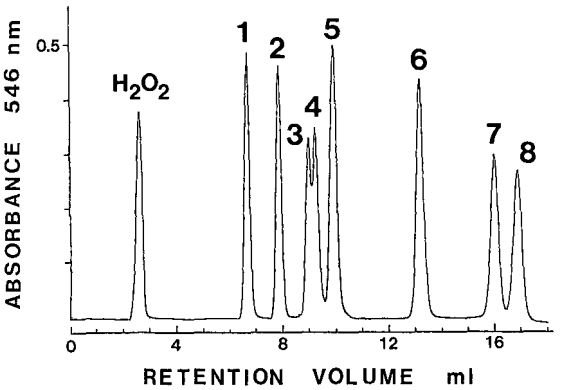

Fig. 3. Analysis of a mixture consisting of 500 pmol each of the eight 5(6)-hydroxy-6(5)-hydroperoxides of thymidine by reversed-phase post-column reaction HPLC. The hydroperoxides were separated on a 5-μm C_{18} column operated with water as the mobile phase. The post-column reaction consisted of mixing the eluent with $5.8 \cdot 10^{-4}$ *M* xylenol orange and $2.3 \cdot 10^{-4}$ *M* NH_4FeSO_4 in 0.035 *M* H_2SO_4 and monitoring the absorption of the Fe^{3+}–xylenol orange complex at 546 nm.

analysis, there is very little tailing of the peaks or decomposition during HPLC analysis and baseline resolution is observed for all hydroperoxides except for **3** and **4**. The isomeric *cis*-hydroperoxides are longer retained on reversed-phase chromatographic columns than the corresponding *trans*-hydroperoxides. This likely reflects intramolecular H-bonding between the vicinal polar hydroxy and hydroperoxy groups of the *cis* isomers. A similar effect has been observed between *cis*- and *trans*-thymidine 5,6-diols[15]. Also, the **6***R* elute faster than the **6***S* diastereomers of 5-hydroxy-6-hydroperoxides whereas the reverse is true for 6-hydroxy-5-hydroperoxides. These differences are likewise attributed to the different orientation of the hydroxy and hydroperoxy groups and to their ability to form intramolecular bonds. In contrast to the 5,6-saturated thymidine hydroperoxides (**1**–**8**), hydroperoxymethyl-2'-deoxyuridine (**9**) is retained much longer during reversed-phase chromatography.

The ratio of absorption at 546 nm (peroxide reagent) to that at 229 nm (direct absorption) varies from 3–8 for the different hydroperoxides (Table I). These variations do not reflect differences in the absorbance at 546 nm induced per mole of hydroperoxide, which appears to be constant for all the hydroperoxides. Instead, this results from variations in absorption by the hydroperoxides at 229 nm, which is an inherent property of these compounds. Thus, *trans*-isomers absorb about twice as much light at 229 nm as *cis*-isomers.

Post-column reaction HPLC using xylenol orange–Fe^{2+} as a colorimetric reagent for hydroperoxides provides a simple and reliable method to selectively detect and quantitate thymidine hydroperoxides in the rang of 1–10 pmol. The sensitivity of this method is comparable to that involving an enzyme-mediated chemiluminescence assay used for the detection of lipid hydroperoxides[16].

ACKNOWLEDGEMENTS

The authors are grateful to the France-Québec Exchange programme and to the Medical Research Council of Canada for generous financial support.

REFERENCES

1 S. Patai (Editor), *The Chemistry of Functional Groups, Peroxides,* Wiley, New York, 1983.
2 J. Cadet and R. Téoule, *Tetrahedron Lett.*, 31 (1972) 3225.
3 H. B. Michaels and J. W. Hunt, *Anal. Biochem.*, 87 (1978) 135.
4 M. C. Schweibert and M. Daniels, *Int. J. Rad. Phys. Chem.*, 3 (1971) 353.
5 P. Powis, *Free Rad. Biol. & Med.*, 6 (1989) 63.
6 R. Aldelman, R. L. Saul and B. N. Ames, *Proc. Natl. Acad. Sci.*, 85 (1988) 2706.
7 J. R. Wagner, J. E. van Lier, C. Decarroz and J. Cadet, *Bioelectrochem. Bioenergetics*, 18 (1987) 155.
8 D. Swern, G. Billen and J. T. Scanlan, *J. Am. Chem. Soc.*, 68 (1946) 1504.
9 J. R. Wagner, J. E. van Lier, C. Decarroz, M. Berger and J. Cadet, *Methods Enzymol.*, (1990) in press.
10 J. R. Wagner, *Ph.D. Thesis*, University of Sherbrooke, Sherbrooke, 1988.
11 J. Cadet and R. Téoule, *J. Chromatogr.*, 70 (1973) 407.
12 L. L. Smith and F. L. Hill, *J. Chromatogr.*, 66 (1972) 101.
13 B. L. Gupta, *Michrochem. J.*, 18 (1973) 363.
14 R. S. Deelder, M. G. F. Kroll and A. J. B. Beeren, *J. Chromatogr.*, 149 (1978) 669.
15 J. Cadet, M. Berger and L. Voituriez, *J. Chromatogr.*, 238 (1982) 488.
16 Y. Yamamoto, M. H. Brodsky, J. C. Baker and B. N. Ames, *Anal.Biochem.*, 160 (1987) 7.

Journal of Chromatography, 504 (1990) 197–201
Elsevier Science Publishers B.V., Amsterdam — Printed in The Netherlands

CHROM. 22 270

Note

Determination of zeatin and zeatin riboside in plant tissue by solid-phase extraction and ion-exchange chromatography

P. E. CAPPIELLO[a,*] and G. J. KLING
Department of Horticulture, University of Illinois, Urbana, IL 61801 (U.S.A.)
(First received July 18th, 1989; revised manuscript received December 1st, 1989)

Kling *et al.*[1] recently reported on a high-performance liquid chromatographic (HPLC) system for analysis of indoleacetic acid (IAA) in plant tissue. One of the benefits of the reported system is that the initial preparative HPLC procedure yields three partially purified fractions; one containing IAA, another containing abscisic acid (ABA) and the third fraction containing the cytokinins zeatin and zeatin riboside. Final quantitative HPLC procedures for analysis of IAA[1] and ABA[2] have been reported. This paper describes a rapid and reproducible system for quantitative analysis of zeatin and zeatin riboside in the above mentioned fraction.

Many systems have been reported for final separation and quantitation of cytokinins. These systems include bioassay[3–8], radioimmunoassay[9,10], ion-exchange chromatography[11], reversed-phase chromatography[12–16], reversed-phase ion-pair chromatography[13] and chromatography on polyvinylpolypyrrolidone (PVPP) columns. Bioassay was not used as a quantitative procedure due to the inherent problems with reproducibility and interfering compounds present in plant extracts[17]. None of the above chromatography systems were effective at separating the cytokinins from interfering compounds present in the partially purified fraction. Insoluble PVPP has been used in open columns for sample purification and final separation in several hormone analysis systems[13,18,19]. PVPP exhibits strong retention of cytokinins at neutral pH, and rapid elution is possible using methanol[18]. The present study reports on the use of PVPP solid phase extraction followed by analytical cation-exchange HPLC to accomplish rapid analysis of zeatin and zeatin riboside, previously purified on our preparative system.

There are many reports of systems for purification and quantitation of the cytokinins however few of these contain information on recovery and variability[3,4,6,10,20,21]. The coefficient of variation (C.V.)[22] indicates the variability of a system and is useful for evaluation of analytical procedures; however, it is seldom included in descriptions of analysis systems. The C.V. can be calculated or estimated from the data presented in some reports. The system reported here has been evaluated for recovery and reproducibility using a radiolabelled internal standard.

[a] Present address: Department of Plant and Soil Sciences, University of Maine, Orono, ME 04469, U.S.A.

0021-9673/90/$03.50

MATERIALS AND METHODS

The entire system for analysis of zeatin and zeatin riboside in plant tissue consists of four steps; extraction, preparative HPLC, solid-phase extraction using PVPP cartridges and ion-exchange chromatography. The extraction and preparative HPLC procedures have been described previously[1]. The following is a description of the PVPP and ion-exchange procedures.

Solid-phase extraction

Dry, methanol-washed PVPP (GAF, New York, NY, U.S.A.) was loaded into 4-ml plastic syringe barrels (PGC Scientifics, Gaithersburg, MD, U.S.A.) (0.25 g PVPP/syringe) with two glass microfibre filters (1.0 cm GF/D, Whatman, Maidstone, U.K.) to hold the packing material in place. The PVPP was packed loosely in the syringe barrel and settled with a 4-ml methanol wash. Before use, the cartridge was washed with an additional 4-ml volume of methanol followed by 4 ml of water. The cytokinin fraction resulting from preparative HPLC[1] was concentrated to approximately 1 ml and was loaded onto the cartridge and drawn through under vacuum. The cartridge was washed with 4 ml of water and the cytokinins were then eluted with a 4-ml methanol wash. The resultant methanol fraction was reduced to dryness *in vacuo* at 35°C and the remaining sample was dissolved in 1.0 ml of water.

Ion-exchange HPLC

A 400-μl aliquot of the above sample was analyzed for zeatin on a Vydac 401TP SCX column (5-μm particle diameter, 150 × 4.6 mm I.D., Alltech, Deerfield, IL, U.S.A.) with an isocratic delivery of 0.05 *M* $NH_4C_2H_3O_2$ (pH 4.1) at a flow-rate of 2.0 ml/min at 40°C. A second 400-μl aliquot was used for zeatin riboside analysis. The same buffer was used at a concentration of 0.01 *M* and a pH of 3.6 with all other parameters the same as for zeatin analysis. The solvent delivery system was composed of a Hewlett-Packard 1082b HPLC system (Avondale, PA, U.S.A.) equipped with a Hewlett-Packard (Model 79870A) 254 nm UV absorbance detector.

Determination of recovery and reproducibility

An internal standard of [8-^{3}H]adenine (27 Ci/mmol) was used for determination of recovery of cytokinins from each sample. In the preparative HPLC system the cytokinins coelute, approximately 1.5 min following the adenine. Rather than collect a wider fraction to include the cytokinins and the adenine (and additional interfering substances) the radiolabelled adenine was added separately to samples before extraction–preparative HPLC, and before the solid-phase extraction–analytical HPLC, to determine recovery from both procedures.

Recovery of adenine from the extraction and preparative HPLC system was determined in three sets of eight plant samples. Samples (2 g) of *Pseudotsuga menziesii* root tissue were enriched with [^{3}H]adenine (approximately 3000 dpm/g tissue) and processed through the extraction and preparative HPLC procedures as described[1]. Aquasol-2 (15 ml) (NEN Research Products, Boston, MA, U.S.A.) was added to each adenine fraction and ^{3}H determined in a Beckman LS 3800 liquid scintillation counter. Recovery was calculated by comparison with [^{3}H]adenine standards not processed through the extraction and preparative HPLC procedures.

Performance of the entire system for analysis of zeatin and zeatin riboside, extraction through final quantitation, was tested with extracts made from roots and shoot apices of dormant and actively growing *Cornus sericea* plants. Samples (1 g, fresh weight) from roots (2–4 mm diameter) and 2-cm shoot tips of eight dormant *Cornus sericea* plants were harvested and processed according to the method described by Kling *et al.*[1]. Additional plants were placed in hydroponic culture (one half strength Hoagland's solution No. 1, pH 6.5, with aeration) in a growth chamber (Conviron E-15, Pembina, ND, U.S.A.) at 24°C with a 15-h photoperiod. When plants were in an active vegetative state of growth, roots and the terminal 1-g portion of the newly expanding shoots were harvested and processed as above. The experiment was a completely randomized design with eight replications.

Identity of the zeatin and zeatin riboside peaks was verified with coupled gas chromatography–mass spectrometry (GC–MS). The two fractions containing the cytokinins from the ion-exchange HPLC procedure were collected, derivatized with tetramethylsilane (TMS) (Pierce, Rockford, IL, U.S.A.) and separated on a Hewlett-Packard 5985 GC–MS system.

RESULTS

The mean recoveries and C.V. values[22] for the three sets of [^{3}H]adenine-enriched plant extracts processed through the extraction and preparative systems combined were 89.7 (C.V. 1.9%), 88.2 (C.V. 1.8%) and 90.6 (C.V. 2.1%). The C.V. of [^{3}H]adenine recovery for the 24 samples grouped together was 2.1%.

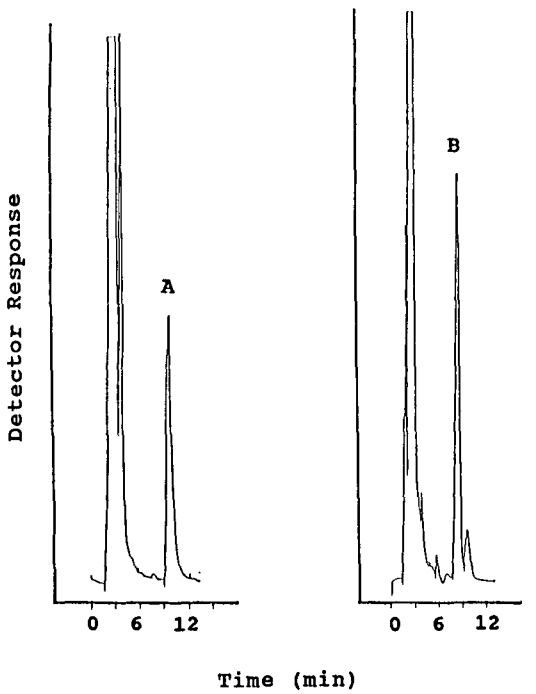

Fig. 1. Chromatograms of zeatin (A) and zeatin riboside (B) separated from *Cornus sericea* plant extracts using cation-exchange HPLC. See text for chromatographic conditions.

Adenine was separated sufficiently from zeatin and zeatin riboside in the cation-exchange analytical system and did not interfere with quantitation (Fig. 1). The retention times for adenine in the zeatin and zeatin riboside systems were 13.8 and 12.0 min, respectively.

The procedures for final separation and quantitation of the cytokinins proved to be reproducible enough to allow for routine analysis of zeatin and zeatin riboside. This system was able to detect differences in the levels of these hormones in both root and shoot tissue of dormant and actively growing *Cornus sericea* (Table I). Mean recovery of [^{3}H]adenine from the PVPP and ion-exchange procedures was 86.3% with a C.V. of 7.0%. The individual C.V.s for each set of samples are presented in Table I.

TABLE I

LEVELS OF ZEATIN AND ZEATIN RIBOSIDE IN ROOTS AND SHOOT TIPS OF DORMANT AND ACTIVELY GROWING *CORNUS SERICEA* PLANTS

	Dormant		*Growing*[a]	
	Root	*Shoot*	*Root*	*Shoot*
Zeatin (ng/g fresh weight)	45.98 c[b]	36.45 d	127.38 b	163.49 a
C.V. (%)	6.9	7.1	5.8	6.6
Z. riboside (ng/g fresh weight)	40.91 d	65.94 c	153.73 b	171.82 a
C.V. (%)	5.8	7.0	7.4	6.9

[a] See text for growth chamber conditions.

[b] Values followed by different letters are significant at the 5% level (least significant difference).

DISCUSSION

A system described by Dixon *et al.*[12] consisted of solvent partitioning, Dowex 50 cation-exchange chromatography and reversed-phase HPLC. They did not report percent recovery; however, a C.V. of 25% can be estimated from the data presented. Doumas and Zaerr[9] employed DEAE-cellulose chromatography and immunoaffinity chromatography followed by reversed-phase HPLC. They reported 65% recovery and C.V.s ranging from approximately 6% to 60% can be estimated from their data. A system described by Smith and Schwabe[5] consisted of solvent partitioning and thin-layer chromatography, followed by bioassay. The C.V. calculated from their data is approximately 25%. Mousdale and Knee[18] reported 97% recovery from a PVPP column, however they did not publish recovery or variation information for the entire system. Purse *et al.*[7] reported 100% recovery of radiolabelled cytokinins from a column of Sephadex, and recovery from TLC of 65% and 25% for zeatin and zeatin riboside, respectively. Stevens and Berry[16] indicate a C.V. of approximately 9.0% for cytokinins in culture filtrate using reversed-phase HPLC followed by GC–MS. They were able to by-pass much of the usual sample purification because they were working with culture medium filtrate, a relatively clean sample compared with crude plant tissue extracts.

The results from our experiments show lower coefficients of variation than

previous systems with comparable recovery rates. Total recovery of [^{3}H]adenine, extraction through analytical determination, was calculated to be 77.2%. The low variability of the system allowed for significant differences to be found in the levels of cytokinins in several plant tissues in different stages of development (Table I).

The identity of the presumed zeatin and zeatin riboside peaks from plant extracts were confirmed by GC–MS. Comparison of the mass spectra of the TMS-derivative of the plant zeatin, with that of authentic TMS-zeatin, showed both with characteristic ions at 261 (molecular ion, M^+), 230, 216, 188, 162, 135, 133 and a base peak at 73 (TMS). Mass spectra of TMS-derivatized plant sample and authentic zeatin riboside both contained ions of m/z 639 (M^+), 624, 550, 536, 319, 230, 202 and a base peak of 73 (TMS). Similar results were reported by Dixon *et al.*[12].

With the addition of the described cytokinin analysis procedures, we are now able to quantitate four major plant hormones from a single 1-g tissue sample. These methods will greatly facilitate studies of the interactive nature of plant hormones.

REFERENCES

1 G. Kling, L. M. Perkins, P. E. Cappiello and B. A. Eisenberg, *J. Chromatogr.*, 407 (1987) 377.
2 M. B. Hein, M. L. Brenner and W. A. Brun, *Plant Physiol.*, 76 (1984) 951.
3 N. A. C. Brown and J. vanStaden, *Physiol. Plant.*, 28 (1973) 388.
4 E. W. Hewett and P. F. Wareing, *Physiol. Plant.*, 28 (1973) 393.
5 D. J. Smith and W. W. Schwabe, *Physiol. Plant.*, 48 (1980) 27.
6 B. W. Wood, *J. Amer. Soc. Hort. Sci.*, 108 (1983) 333.
7 J. G. Purse, R. Horgan, J. Horgan and P. F. Wareing, *Planta*, 132 (1976).
8 P. Lejeune, J. M. Kinet and G. Bernier, *Plant Physiol.*, 86 (1988) 1095.
9 P. Doumas and J. B. Zaerr, *Tree Physiol.*, 4 (1988) 1.
10 E. M. S. MacDonald, D. E. Akiyoshi and R. O. Morris, *J. Chromatogr.*, 214 (1981) 101.
11 M. G. Carnes, M. L. Brenner and G. R. Andersen, *Plant Growth Substances 1973, Proc. 8th Int. Conf. on Plant Growth Subst.*, Hirokawa, Tokyo, 1974, p. 99.
12 R. K. Dixon, H. E. Garrett and G. S. Cox, *Tree Physiology*, 4 (1988) 9.
13 M. A. Walker and E. B. Dumbroff, *J. Chromatogr.*, 237 (1982) 316.
14 R. A. Anderson and T. R. Kemp, *J. Chromatogr.*, 172 (1979) 509.
15 R. Horgan and M. R. Kramers, *J. Chromatogr.*, 173 (1979) 263.
16 G. A. Stevens and A. M. Berry, *Plant Physiol.*, 87 (1988) 15.
17 M. L. Brenner, *Ann. Rev. Plant Physiol.*, 32 (1981) 511.
18 D. M. A. Mousdale and M. Knee, *J. Chromatogr.*, 177 (1979) 398.
19 N. L. Biddington and T. H. Thomas, *J. Chromatogr.*, 7 (1973) 122.
20 R. Alvim, E. W. Hewett and P. F. Saunders, *Plant Physiol.*, 57 (1976) 474.
21 J. S. Taylor, M. Koshioka, R. P. Pharis and G. B. Sweet, *Plant Physiol.*, 74 (1984) 626.
22 R. G. Steele and J. H. Torrie, *Principles and Procedures of Statistics, a Biometrical Approach*, McGraw-Hill, New York, 1980, p. 27.

Journal of Chromatography, 504 (1990) 202–206
Elsevier Science Publishers B.V., Amsterdam — Printed in The Netherlands

CHROM. 22 226

Note

Argentation chromatography of fatty acid methyl esters using silver-loaded solid-phase extraction columns

FRANZ ULBERTH* and ELISABETH ACHS
Department of Dairy Research and Bacteriology, Agricultural University, Gregor Mendel Str. 33, A-1180 Vienna (Austria)
(First received August 24th, 1989; revised manuscript received December 19th, 1989)

Argentation chromatography, either on thin layers (TLC)[1] or on conventional columns[2], has proved to be of great value for the separation of unsaturated fatty acid methyl esters (FAMEs) according to the degree of unsaturation and geometry of the double bond(s)[3]. Recently, these established methods were adapted to high-performance liquid chromatographic (HPLC) techniques[4]. For this type of fractionation, custom-prepared silica gel impregnated with silver ions is used as the stationary phase by most workers[5,6]. One disadvantage of HPLC with silver-loaded silica phases is the relative short column life, due to the leaching of silver ions from the column by polar solvents[6]. In order to circumvent this problem, ion-exchange resins[7] and later benzenesulphonic acid, chemically bonded to silica gel[8–10], were successfully introduced as alternatives. With ion-exchange materials, the feasability of *in situ* impregnation of prepacked columns with silver ions by simply injecting an aequous silver solution into the column offers an additional benefit to the analyst[9–11].

As HPLC is expensive for sample pretreatment, it would be advantageous to separate FAMEs according to the number of double bonds by means of commercially available solid-phase extraction (SPE) tubes packed with cation-exchange material. This paper deals with the development of such a technique for the fractionation of milk fat FAMEs for subsequent gas–liquid chromatographic (GLC) analysis.

EXPERIMENTAL

Materials

Reagents and solvents were of analytical-reagent grade and used as received (E. Merck, Darmstadt, F.R.G.). The solid-phase extraction (SPE) columns, CHROMABOND SA (64 mm × 9 mm I.D., packed with 500 mg of benzenesulphonic acid, solvent volume 3 ml), were obtained from Macherey, Nagel & Co. (Düren, F.R.G.), Cat. No. 730 077. Reference FAMEs were purchased from E. Merck and Sigma (St. Louis, MO, U.S.A.).

0021-9673/90/$03.50

Argentation chromatography (Ag^+/SPE)

SPE columns were converted to the NH_4^+ form by flushing with 1% (w/v) ammonium acetate solution (10 ml), followed by distilled water (10 ml). A 2-ml volume of 1% (w/v) silver nitrate solution was allowed to drain by gravity flow through the column to impregnate the solid phase with silver ions. Excess silver ions were removed with methanol (10 ml), followed by 10 ml of dichloromethane (DCM) and *n*-hexane (10 ml) in order to re-equilibrate the column for apolar solvents. Typically, 1 ml of standard or sample solution was applied to the prepared column. After washing the column with 2 ml of *n*-hexane, FAMEs were eluted stepwise with various solvent mixtures at ambient temperature (20–25°C). The separated FAMEs were determined by drying the relevant fractions at 40°C in a stream of nitrogen and adding 1 ml of *n*-hexane containing methyl heptadecanoate as an internal standard for subsequent GLC analysis. Further details of the Ag^+/SPE procedure are outlined under Results and Discussion.

A standard FAME mixture (FAME standard) consisting of methyl esters of stearic acid (18:0), elaidic acid (18:1t), oleic acid (18:0c), linoleic acid (18:2), linolenic acid (18:3) and arachidonic acid (20:4) was prepared by dissolving approximately equal amounts (1 mg/ml) of each in *n*-hexane.

Milk fat was transesterified with methanolic potassium hydroxide as described by Christopherson and Glass[12], and finally diluted with *n*-hexane to give a FAME content of 2 mg/ml. Identification of major FAMEs in milk fat was performed by comparing the retention times obtained with those for a FAME standard resembling the approximate composition of milk fat (MF-FAME standard).

Gas–liquid chromatography

A Carlo Erba Mega 5300 high-resolution gas chromatograph, fitted with a dual injection system (on-column and split/splitless) and a flame ionization detector connected to a Spectra-Physics 4270 integrator, was used. The column installed was a 25 m × 0.32 mm I.D. fused-silica capillary column, coated with CP-Sil-88, d_f = 0.2 μm (Chrompack, Middelburg, The Netherlands). The carrier gas was hydrogen and the make-up gas was nitrogen. For split injection the column was operated isothermally at 150°C, whereas for on-column injection the temperature was programmed from 50°C (1 min isothermal) at 7°C/min to 220°C. Usually the FAME standard was split injected and the MF-FAME standard or milk fat FAMEs (MF-FAMEs) injected on-column.

RESULTS AND DISCUSSION

Method development

In principle, the procedure for preconditioning the CHROMABOND SA column with silver ions resembles the method described by Christie[9] for the preparation of a silver-loaded HPLC column. However, the solvent volumes used were adapted according to the reduced column size (500 mg of sorbent in the SPE column). For proper column impregnation, the silver solution must be allowed to pass through the SPE column by gravity flow, whereas the other solvents could be forced through the sorbent bed at a flow-rate of *ca.* 1 ml/min.

In a first attempt to separate the FAME standard, various solvent mixtures with

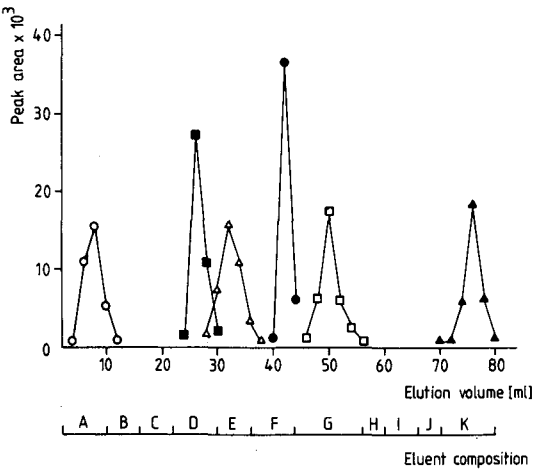

Fig. 1. Separation of FAMEs according to the geometry and number of double bonds. The Ag^+/SPE column was eluted batchwise (2-ml portions) with the eluents listed below. The amount (peak area) and identity of FAMEs (○ = 18:0; ■ = 18:1-*trans*; △ = 18:1-*cis*; ● = 18:2; □ = 18:3; ▲ = 20:4) present in each fraction was determined by GLC. Eluent composition (v/v): (A) 1% DCM in *n*-hexane; (B) 5% DCM in *n*-hexane; (C) 10% DCM in *n*-hexane; (D) 50% DCM in *n*-hexane; (E) 100% DCM; (F) 3% methanol in *n*-hexane; (G) 10% methanol in *n*-hexane; (H) 50% methanol in *n*-hexane; (I) 100% methanol; (J) 1% acetonitrile in methanol; (K) 10% acetonitrile in methanol.

increasing polarity were applied batchwise in 2-ml portions and the column effluents were analysed by GLC. In Fig. 1 the detector response (peak area) of the separated FAMEs is plotted against the elution volume and the eluent composition. The major proportion of 18:0 was eluted with 10 ml of 1% DCM in *n*-hexane. Unsaturated FAMEs were retained on the column unless the DCM concentration reached 50%. With this DCM–*n*-hexane mixture, 18:1t eluted as a relative sharp peak, but was not completely separated from 18:1c, which was recovered from the column with pure DCM. In order to elute the more unsaturated FAMEs, the polarity of the eluent had to be further increased by adding methanol to DCM. As is evident from Fig. 1, the dienoic and trienoic FAMEs were well resolved with DCM containing 3% and 10% methanol, respectively. Even with pure methanol, 20:4 did not elute. Thus acetonitrile, which is able to displace polyolefins from silver-loaded resin columns[13], was incorporated in the solvent. A concentration of 10% acetonitrile in methanol was necessary to speed up the elution of 20:4 and to recover this polyunsaturated FAME entirely. With a silver-loaded Nucleosil 5SA HPLC column and a linear gradient from methanol to methanol–acetonitrile (9:1), an excellent separation of bovine testis FAMEs according to the number of double bonds was obtained by Christie[9]. Although the SPE sorbent bed consisted of the same type of packing material, eluents with a lower polarity had to be used for the fractionation of the FAMEs in this study. Starting the procedure with methanol resulted in almost complete elution of the FAMEs without separation taking place.

Another series of experiments was carried out to optimize the elution strength and the amount of solvents needed to separate the FAME standard into pure components. Fractions of high purity and also excellent recoveries of the standard

compounds (usually $\geq 95\%$) were obtained with the selected solvent mixtures. Stearic acid was eluted with 5 ml of 10% DCM in *n*-hexane, 18:1t with 5 ml of 40% DCM in *n*-hexane, 18:1c with 5 ml of 0.5% methanol in DCM, 18:2 with 5 ml of 3% methanol in DCM, 18:3 with 5 ml of 1% acetonitrile in methanol and 20:4 with 10% acetonitrile in methanol. Only the geometric 18:1 isomers were not as well resolved as the remaining FAMEs; 2.3% of the applied 18:1t coeluted with the 18:1c fraction and 8.5% of the 18:1c with the 18:1t fraction. Complete resolution of a standard mixture containing geometric and positional 18:1 isomers was achieved by the aforementioned HPLC system, employing dichloromethane–1,2-dichloroethane (1:1) instead of the methanol–acetonitrile gradient as the elution solvent[10]. However, the separation efficiency of an analytical HPLC column is obviously not comparable to that of an SPE column commonly intended for sample pretreatment.

Application of the Ag^+/SPE method to milk fat FAMEs

When the optimized Ag^+/SPE method was applied to the separation of an MF-FAME standard, results in agreement with the standard mixture used during method development were obtained, except for the impaired resolution of 18:1t and 18:1c. With this test mixture, about one third of the 18:1t coeluted with the *cis*-monoenoic fraction. Saturated FAMEs eluted with 5 ml of 10% DCM in *n*-hexane as one fraction, independent of the chain length. Short-chain FAMEs were not recovered completely, because of their partial evaporation during the nitrogen drying step involved in sample preparation. Modifications of the solvent systems applied did not lead to any significant improvement in the *cis*/*trans*-monoene separation. Thus

TABLE I

APPLICATION OF THE Ag^+/SPE PROCEDURE TO THE FRACTIONATION OF MILK FAT FAMEs

Eluent	*FAME*	*Recovery (%)*[a]	
		Milk fat I[b]	*Milk fat II*[c]
10% DCM in *n*-hexane (5 ml)	8:0	51.0 ± 4.0	35.9 ± 4.8
	10:0	82.3 ± 0.6	72.8 ± 1.9
	12:0	93.8 ± 1.2	92.9 ± 2.6
	14:0	97.0 ± 1.3	98.1 ± 0.3
	15:0	97.4 ± 1.1	98.0 ± 0.9
	16:0	99.1 ± 0.8	94.6 ± 3.7
	18:0	99.5 ± 0.9	97.9 ± 5.2
0.5% methanol in DCM (5 ml)	10:1	90.7 ± 1.8	96.3 ± 1.4
	14:1	94.9 ± 1.3	101.5 ± 0.8
	16:1	97.9 ± 1.1	98.0 ± 1.7
	18:1	101.5 ± 0.4	102.7 ± 0.7
	18:2conj[d]	100.5 ± 0.7	99.6 ± 0.9
3% methanol in DCM (5 ml)	18:2	95.1 ± 0.6	103.3 ± 0.6
1% acetonitrile in methanol	18:3	93.3 ± 0.7	99.1 ± 3.9

[a] Mean ± standard deviation of four determinations.
[b] Iodine value 31.4.
[c] Iodine value 40.0.
[d] 18:2 conj = 9-*cis*,11-*trans*-octadecadienoic FAME.

MF-FAMEs, serving as a real sample, were separated into saturated and mono-, di- and triunsaturated FAME fractions, according to the elution scheme given in Table I. As in conventional argentation chromatography, the conjugated 18:2 (*cis*-9,*trans*-11-octadecadienoic FAME) eluted with the monoenoic fraction. The recoveries of the separated FAMEs from two different milk fat samples (iodine values 31.4 and 40.0, respectively) were in accordance with the values obtained in the preliminary experiments.

CONCLUSION

A silver-loaded solid-phase extraction column (Ag^+/SPE) provides a simple and rapid means for the fractionation of FAMEs according to the degree of unsaturation for subsequent GLC analysis. Relevant fractions of high purity and good recoveries are obtained with the procedure described. Compared with the commonly used argentation TLC, the Ag^+/SPE method offers the opportunity to separate and recover FAMEs in a single step, requiring only small solvent volumes.

REFERENCES

1 L. J. Morris, *Lab. Pract.*, 13 (1964) 284.
2 B. de Vries, *Chem. Ind. (London)*, 16 (1962) 1049.
3 L. J. Morris, *J. Lipid Res.*, 7 (1966) 717.
4 W. W. Christie, *High-Performance Liquid Chromatography and Lipids*, Pergamon Press, Oxford, 1987, p. 137.
5 C. R. Scholfield, *J. Am. Oil Chem. Soc.*, 56 (1979) 510.
6 M. Ozcimder and W. E. Hammers, *J. Chromatogr.*, 187 (1980) 307.
7 E. A. Emken, J. C. Hartman and C. R. Turner, *J. Am. Oil Chem. Soc.*, 55 (1978) 561.
8 W. S. Powell, *Anal. Biochem.*, 115 (1981) 267.
9 W. W. Christie, *J. High Resolut. Chromatogr. Chromatogr. Commun.*, 10 (1987) 148.
10 W. W. Christie and G. H. McG. Breckenridge, *J. Chromatogr.*, 469 (1989) 269.
11 W. W. Christie, *J. Chromatogr.*, 454 (1988) 273.
12 S. W. Christopherson and R. L. Glass, *J. Dairy Sci.*, 52 (1969) 1289.
13 W. J. DeJarlais, R. O. Adolf and E. A. Emken, *J. Am. Oil Chem. Soc.*, 60 (1983) 975.

Journal of Chromatography, 504 (1990) 207–209
Elsevier Science Publishers B.V., Amsterdam — Printed in The Netherlands

CHROM. 22 225

Letter to the Editor

Analysis of anthocyanins in red wines by high-performance liquid chromatography using butylamines in the mobile phase

Sir,

We are studying the optimization of the separation of anthocyanins in red wine by high-performance liquid chromatography (HPLC) by using alkylamines in the mobile phase with gradient elution. In the present experiments we used a Varian 8500 chromatograph, a Variscan 634 D UV–VIS spectrophotometric detector, an A-25 recorder and a high-pressure stop-flow injection system. The column (15 cm × 0.32 cm I.D.) was packed with CGX C_{18} silica gel chemically modified with octadecyl groups (particle 5 μm) (Tessek, Prague, Czechoslovakia). The wavelength of detection was 520 nm; the pressure was 14 MPa[1,2].

The wine sample selected was Alibernet (Komplexný Výskumný Ústav Vinohradnický a Vinársky, Bratislava, Czechoslavakia) as it was found to exhibit the most uniform content of anthocyanins among those investigated, the other wines being Svätovavrinecké, Frankovka Modrá, Cabernet Sauvignon and André).

Butylamine, diethylamine, triethylamine, hexylamine and octylamine were examined as mobile phase additives and the best results were obtained with butylamine. We then optimized the gradient elution by means of solution A containing 10% (v/v) of methanol, perchloric acid (0.16 mol dm^{-3}) and butylamine (0.122 mol dm^{-3}) and solution B containing 90% (v/v) of methanol, perchloric acid (0.16 mol dm^{-3}) and butylamine (0.122 mol dm^{-3}). The pH of the solutions was 1.45. Similar pH conditions have been used by other workers[3–5].

The gradient was optimized in two steps involving the initial composition of the mobile phase and the form and slope of the gradient. As the optimization of gradient elution has not yet been mathematically processed, we tried to find out the most convenient gradient by experiment. The following gradient proved to be the best: start 25% B, finish 51% B, 0–8 min 25% B isocratic, 8–12 min from 25 to 41% B at 4% B min^{-1}, 12–22 min from 41 to 51% B at 1% B min^{-1} and 22–34 min 51% B isocratic.

The chromatographic separation of the anthocyanin pigments from Alibernet wine using the above gradient is shown in Fig. 1. The following peaks of anthocyanins were identified: (1) delfidin-3-glucoside, (2) cyanidin-3-glucoside, (3) petunidin-3-glucoside, (4) peonidin-3-glucoside, (5) malvidin-3-glucoside, (6) unidentified, (7) delfidin-3-glucoside acetate, (8) cyanidin-3-glucoside acetate, (9) petunidin-3-glucoside acetate, (10) peonidin-3-glucoside acetate, (11) malvidin-3-glucoside acetate, (12) delfidin-3-glucoside *p*-coumarate, (13) peonidin-3-glucoside *p*-coumarate and (14) malvidin-3-glucoside *p*-coumarate.

For comparison of gradient programmes with and without butylamine in the mobile phase, the time of analysis, separation efficiency and gradient reproducibility

0021-9673/90/$03.50

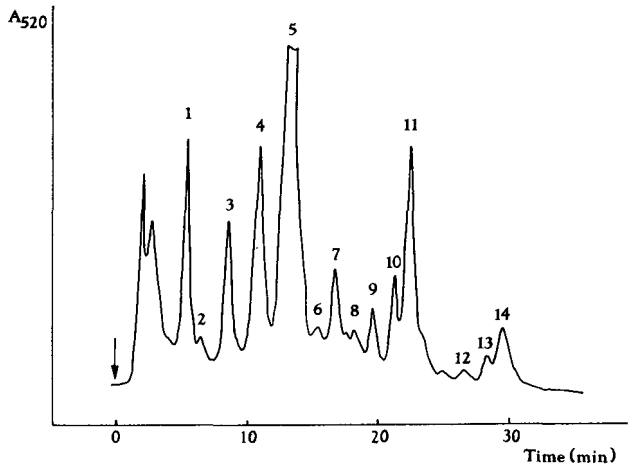

Fig. 1. Chromatogram for an Alibernet wine sample. Injection volume, 8 μl; sensitivity, 20 mV. For chromatographic conditions and peak identification, see text.

were considered. The gradient with butylamine requires 6 min less than that without butylamine. Also, the peaks are much more regularly located when butylamine is present. The gradients were compared with respect to selectivity (α), resolving power (R_S) and capacity factors (k'). In calculating the capacity factors given in Table I, the elution dead time $t_0 = 120$ s was taken into account. Table I demonstrates that better results and better resolution of peaks 4,5 and 10,11 in particular were obtained by using the gradient with butylamine. To evaluate the reproducibility of measurements

TABLE I

COMPARISON OF GRADIENTS FROM THE VIEWPOINT OF SELECTIVITY

Peak No.	*Gradient without butylamine*			*Gradient with butylamine*		
	k'	α	R_S	k'	α	R_S
1	3.37	1.33	16.33	1.71	1.43	17.29
2	4.48	1.20	11.26	2.45	1.39	17.41
3	5.37	1.22	12.78	3.40	1.35	17.05
4	6.57	1.10	6.37	4.58	1.24	13.18
5	7.22	1.41	21.35	5.67	1.19	11.06
6	–	–	–	6.73	1.10	6.61
7	10.18	1.14	9.14	7.42	1.11	6.83
8	11.61	1.08	5.26	8.20	1.08	5.55
9	12.49	1.10	6.79	8.88	1.09	5.97
10	13.73	1.02	1.82	9.67	1.05	3.68
11	14.07	1.05	3.58	10.18	1.14	9.26
12	14.77	1.05	3.57	11.63	1.06	4.35
13	15.50	1.04	2.60	12.35	1.07	5.09
14	16.05	1.05	3.57	13.25	1.05	3.52

[a] See text for identification of peaks.

we performed repeated analyses on nine different samples of Frankovka wine and calculated the mean capacity factor, standard deviation and scatter. The results showed that the reproducibility of the measurements made with the gradient in the presence of butylamine is much better and the system fulfils the high criteria demanded for the separation of anthocyanins by HPLC.

Department of Chemistry and Technology of Saccharides and Foods, Faculty of Chemical Technology, Slovak Technical University, CS-812 37 Bratislava (Czechoslovakia)

MILAN DRDÁK*
PAVOL DAUČÍK
JOZEF KUBASKÝ

1 M. Williams and G. Hrazdina, *J. Chromatogr.*, 155 (1978) 389–398.
2 K. Vande Casteele, H. Geiger, R. De Loose and Ch. F. Van Sumere, *J. Chromatogr.*, 259 (1983) 291–300.
3 J. Bakker and C. F. Timberlake, *J. Sci. Food Agric.*, 36 (1985) 1325–1333.
4 J. Bakker, N. W. Preston and C. F. Timberlake, *Am. J. Enol. Vitic.*, 37 (1986) 121–126.
5 J. Bakker, *Vitis*, 25 (1986) 203–214.

(First received July 3rd, 1989; revised manuscript received December 14th, 1989)

PUBLICATION SCHEDULE FOR 1990

Journal of Chromatography and Journal of Chromatography, Biomedical Applications

MONTH	J	F	M	A	M	
Journal of Chromatography	498/1 498/2 499	500 502/1	502/2 503/1 503/2 504/1	504/2 505/1	505/2 506 507	The publication schedule for further issues will be published later
Cumulative Indexes, Vols. 451–500		501				
Bibliography Section		524/1		524/2		
Biomedical Applications	525/1	525/2	526/1	526/2 527/1	527/2	

INFORMATION FOR AUTHORS

(Detailed *Instructions to Authors* were published in Vol. 478, pp. 453–456. A free reprint can be obtained by application to the publisher, Elsevier Science Publishers B.V., P.O. Box 330, 1000 AH Amsterdam, The Netherlands.)

Types of Contributions. The following types of papers are published in the *Journal of Chromatography* and the section on *Biomedical Applications:* Regular research papers (Full-length papers), Notes, Review articles and Letters to the Editor. Notes are usually descriptions of short investigations and reflect the same quality of research as Full-length papers, but should preferably not exceed six printed pages. Letters to the Editor can comment on (parts of) previously published articles, or they can report minor technical improvements of previously published procedures; they should preferably not exceed two printed pages. For review articles, see inside front cover under Submission of Papers.

Submission. Every paper must be accompanied by a letter from the senior author, stating that he is submitting the paper for publication in the *Journal of Chromatography*. Please do not send a letter signed by the director of the institute or the professor unless he is one of the authors.

Manuscripts. Manuscripts should be typed in double spacing on consecutively numbered pages of uniform size. The manuscript should be preceded by a sheet of manuscript paper carrying the title of the paper and the name and full postal address of the person to whom the proofs are to be sent. Authors of papers in French or German are requested to supply an English translation of the title of the paper. As a rule, papers should be divided into sections, headed by a caption (*e.g.*, Summary, Introduction, Experimental, Results, Discussion, etc.). All illustrations, photographs, tables, etc., should be on separate sheets.

Introduction. Every paper must have a concise introduction mentioning what has been done before on the topic described, and stating clearly what is new in the paper now submitted.

Summary. Full-length papers and Review articles should have a summary of 50–100 words which clearly and briefly indicates what is new, different and significant. In the case of French or German articles an additional summary in English, headed by an English translation of the title, should also be provided. (Notes and Letters to the Editor are published without a summary.)

Illustrations. The figures should be submitted in a form suitable for reproduction, drawn in Indian ink on drawing or tracing paper. Each illustration should have a legend, all the *legends* being typed (with double spacing) together on a *separate sheet*. If structures are given in the text, the original drawings should be supplied. Coloured illustrations are reproduced at the author's expense, the cost being determined by the number of pages and by the number of colours needed. The written permission of the author and publisher must be obtained for the use of any figure already published. Its source must be indicated in the legend.

References. References should be numbered in the order in which they are cited in the text, and listed in numerical sequence on a separate sheet at the end of the article. Please check a recent issue for the layout of the reference list. Abbreviations for the titles of journals should follow the system used by *Chemical Abstracts*. Articles not yet published should be given as "in press" (journal should be specified), "submitted for publication" (journal should be specified), "in preparation" or "personal communication".

Dispatch. Before sending the manuscript to the Editor please check that the envelope contains three copies of the paper complete with references, legends and figures. One of the sets of figures must be the originals suitable for direct reproduction. Please also ensure that permission to publish has been obtained from your institute.

Proofs. One set of proofs will be sent to the author to be carefully checked for printer's errors. Corrections must be restricted to instances in which the proof is at variance with the manuscript. "Extra corrections" will be inserted at the author's expense.

Reprints. Fifty reprints of Full-length papers, Notes and Letters to the Editor will be supplied free of charge. Additional reprints can be ordered by the authors. An order form containing price quotations will be sent to the authors together with the proofs of their article.

Advertisements. Advertisement rates are available from the publisher on request. The Editors of the journal accept no responsibility for the contents of the advertisements.